The Use of Image Analysis for the Characterisation of Filamentous Microorganisms

by

Helen Lyn Packer

1991

Submitted for the degree of Doctor of Philosophy
at The University of London

SERC Centre for Biochemical Engineering
Department of Chemical and Biochemical Engineering
University College London

Abstract

Characterisation of mycelial morphology is important for physiological and engineering studies of filamentous fermentations, and in the design and operation of such fermentations. Image analysis has been developed as a method for this characterisation and has been shown to be faster and generally more accurate than previous methods. A fully automatic system has been developed, in which speed has been gained, but with loss of accuracy in some cases. The method has been tested on *Streptomyces clavuligerus* and two strains of *Penicillium chrysogenum*, one of which was in a medium containing undissolved solids.

Additionally a method for the estimation of biomass for the penicillin fermentation using image analysis is presented. Two regions of hyphae are defined to describe the growth of mycelia during fermentation 1) the cytoplasmic region and 2) the degenerated region including large vacuoles. The volume occupied by each of these regions in a fixed volume of sample is estimated from area measurements using image analysis. Areas are converted to volumes by treating the hyphae as solid cylinders with the hyphal diameter as the cylinder diameter. The volumes of the cytoplasmic and degenerated regions are converted into dry weight estimations using hyphal density values available in the literature. The image analysis method for biomass and cell volume estimation is shown to estimate successfully concentrations of mycelia from 0.03 to 38g/L for a number of fermentations of *Penicillium chrysogenum*. The image analysis method has also estimated cell volume and biomass even in the presence of 30g/L of undissolved solids in the medium. The image analysis estimation of biomass is shown to agree with the conventional method of measurement using filtration.

Both image analysis methodologies are powerful tools for the quantification and characterisation of filamentous microorganisms and will allow greater understanding of engineering and physiological processes occurring during fermentation.

Preface

I would like to express my special thanks to my supervisors, Dr Colin Thomas and Professor Malcolm Lilly, for their guidance and encouragement throughout the course of this work.

I would also like to thank Paul McDonnell for programming support and the debugging of Bones. Also I am grateful to H.Makagiansar, K.Stone and F.Roche for the provision of samples and to them and the rest of the research group for their support.

Contents

Figures

Tables

1.0 Introduction

Filamentous microorganisms such as fungi and actinomycetes are commercially important for the production of secondary metabolites, in particular antibiotics. In submerged culture they exhibit two distinct morphologies: pelleted and free filamentous. In the free filamentous form the microorganisms grow as free, branched threads of mycelia that easily become entangled to form loose aggregates sometimes referred to as "clumps". When cultured under unrestricted conditions the growth is exponential (Caldwell and Trinci, 1973). Free filamentous growth is very common in industrial fermentations, but the mycelia entanglement can lead to high broth viscosities and pseudoplastic behaviour particularly when the biomass concentration is high, with consequential poor mixing and mass transfer.

Mycelial growth in the pelleted form is not exponential (Oliver and Trinci, 1985). The growth rate is not constant throughout the pellet as the diffusion of nutrients from the periphery of the pellet to the centre is not efficient enough to maintain unlimited growth. The cells in the centre of the pellet become differentiated and eventually autolyse. The mechanisms of pellet formation by filamentous microorganisms and metabolite production in the pelleted form has been recently reviewed by Braun and Vecht-Lifshitz (1991).

In this work quantitative methodologies for characterising the morphology of free filamentous microorganisms were devised. The methodologies will enable the study of the effects of fermentation variables, such as stirrer speed and dissolved carbon dioxide concentration, on growth, product formation and morphology. This will lead to an improved understanding of their interrelationships, leading to better design and operation of fermentation processes.

A general review of the physiology and vegetative growth of filamentous fungi is presented in order to describe the complex morphology of these microorganisms which had to be considered during the establishment of methodologies for their quantitative characterisation. Also discussed are the problems of measuring mycelia from submerged culture and a review of current methodologies to evaluate their growth.

1.1 Fungal Structure

Fungi are diverse in their gross morphology appearing in a wide variety of morphological forms ranging from macroscopic, multicellular mushrooms to microscopic, single cellular yeasts. The filamentous fungi are composed of long branching filaments called hyphae or hyphal strands, and a mass of hyphae comprise a mycelium. Growth in this filamentous form would enable the organism to increase in size indefinitely without altering the ratio between the protoplasmic

volume and the surface area. Consequently, transport between the mycelium and the medium is accomplished over short distances and as the hyphae grow branches are formed, enabling the filament to cover solid substrates effectively.

Hyphae of fungi are likely to have a diameter of 3-10μm though some may have a diameter of up to 100μm, for example *Saprolegnia*. A hypha can be considered as effectively an elongated tubular cell. In some species such as the Basidiomycotina the hyphae are partitioned by cross-walls called septa. Nevertheless, in many fungi septa are interrupted by one or more pores so they are not an appreciable barrier to the passage of cellular materials and are thought to aid mechanical strengthening of the tubular filament. Septa often have a single central pore (50-500μm) which allows the passage of cellular materials including organelles such as nuclei and mitochondria. However these single central pores are bordered by a number of spherical Woronin bodies or hexagonal crystals (Gull, 1978) and during hyphal differentiation and following hyphal damage these bodies may plug the septal pores (Trinci and Collinge, 1973; Collinge and Markham, 1985). The presence of septa and their structure have a considerable influence on hyphal extension and branch formation (Trinci, 1979).

The hypha owes its shape to the turgor pressure of the protoplasm and particularly to the rigidity of its wall. This has been demonstrated by treating mycelia with enzymes which hydrolyse their walls (Villanueva, 1966). As the digestion of the wall proceeds the membrane bursts or, with osmotic protection, spherical protoplasts are formed. Chemical analyses of cell walls cleaned of cytoplasm show that they contain 80 to 90% polysaccharides with most of the remainder consisting of proteins and lipids (Aronson, 1965; Bartnicki-Garcia, 1968).

The wall contains a mixture of fibrillar components and amorphous or matrix components. The main fibrillar components are spirally orientated fibrils of chitin (a polymer of β(1-4) linked N-acetyl glucosamine) or cellulose (a polymer of D-glucose) and sometimes other glucans (Bartnicki-Garcia, 1968). The main matrix components include various glucans, proteins, polymers of galactosamines and mannans.

Even though information was available on the gross chemical composition of cell walls it was not until 1970 when Hunsley and Burnett published the results of their experiments on enzyme dissection of the wall (Hunsley and Burnett, 1970) that the architecture of the wall was elucidated.

For *Neurospora crassa*, which has probably an unusually complex cell wall, the cell wall was found to consist of four regions which grade into each other. The outermost layer consists of amorphous glucans and beneath this is a network of glycoprotein embedded in protein. Then, inside this is a layer of discrete protein and the innermost layer is the layer of chitin microfibrils

embedded in protein. It is now known that a common feature of fungi is that the innermost part of a mature wall contains fibrillar material embedded in matrix components and that these are overlaid in the outer part of the wall by further matrix materials(Figure 1 on page 14).
The plasma membrane is located inside the cell wall. Structurally it is a lipid bilayer with proteins interspersed within it. The "fluid mosaic" model of membrane structure (Singer and Nicholson, 1972) is the accepted model for the structure of the fungal membrane.

The cytoplasm, found immediately inside the plasma membrane, is a watery mass of dissolved solutes in which highly organised, membranous organelles such as mitochondria, Golgi apparatus and microbodies, as well as non-membranous structures such as ribosomes, microtubules and microfilaments are embedded. Also located in the cytoplasm is the fungal nucleus, which varies in shape, size and number. Fungal nuclei are quite elastic and have been observed squeezing through septal pores.

In some species of fungi the protoplasm continually moves forward as the hyphae extend occupying the newly formed areas and ultimately leaving behind an empty outer casing. This has lead to filamentous fungi being described as "plasmodia which creep about in tubes" (Smith, 1975). In other fungi the protoplasm becomes progressively more vacuolated with distance from the tip. Vacuoles are formed from the plasma membrane and also from the smooth endoplasmic reticulum or a dictyosome. These often increase in size by fusing with other vacuoles in the cytoplasm. Vacuoles, as well as their involvement in phagocytosis and pinocytosis, are used as storage areas for certain nutrients and are also used for storing water for the maintenance of turgor. In some filamentous fungi, vacuoles accumulate in older sections of the hyphal strand, leaving space for only a thin film of cytoplasm. Therefore as the vacuoles take up such a large proportion of the cell the bulk of the cytoplasm remains at the growing tip of the filament. The vacuoles thus allow the fungi to utilise a relatively small amount of cytoplasm to maintain a substantial volume of hyphae. This is obviously important for the survival of the organism.

1.2 Fungal Growth

1.2.1 Growth of Individual Hypha

Hyphae can extend by tip growth or intercalary growth. Intercalary growth only occurs in aerial structures such as conidiophores (Prosser and Tough, 1991) when wall material is deposited in subapical regions. Elongation of vegative hyphae occurs by tip growth.

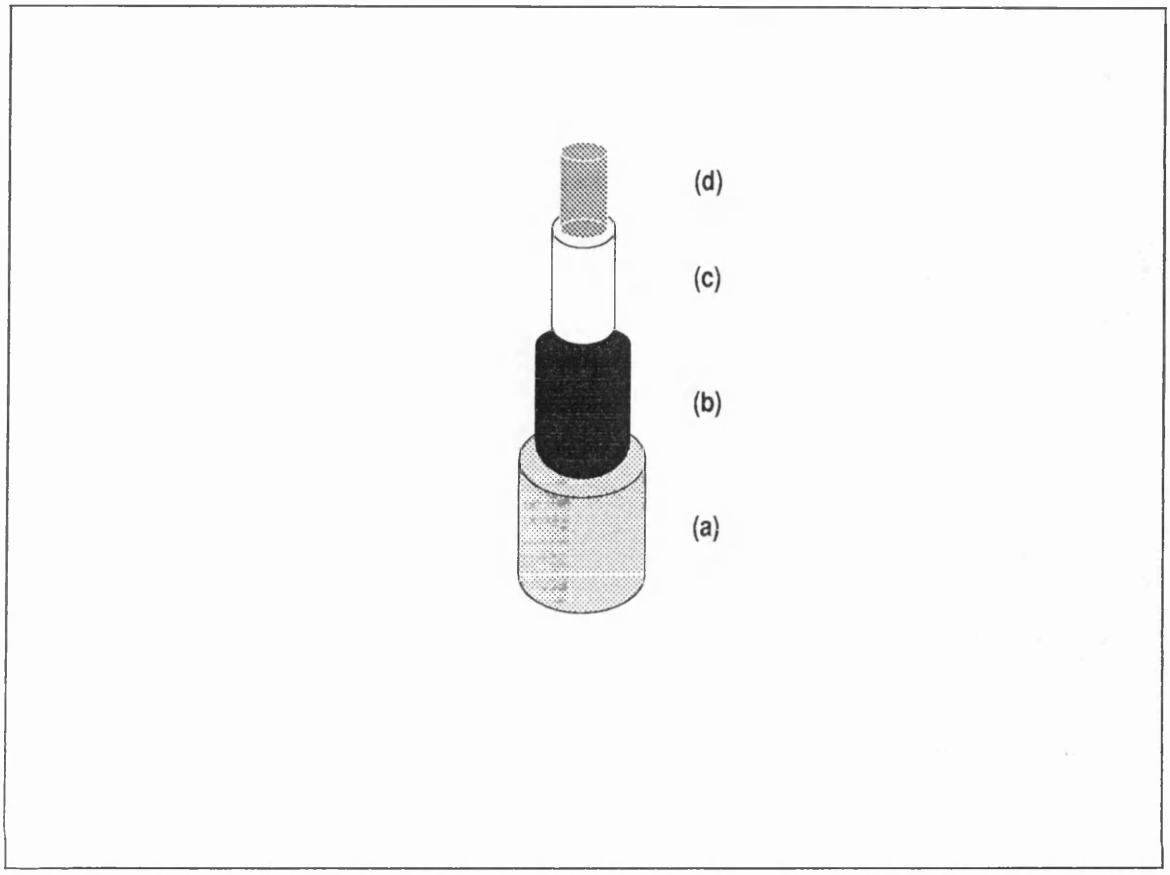

Figure 1. Diagram to illustrate wall architecture. Schematic structure of the cell wall of N.crassa. (a), outer mixed α- and β-glucans; (b), glycoprotein reticulum; (c), proteinaceous material; (d), inner chitinous region. Redrawn from Burnett (1979).

1.2.1.1 The Cytology of the Hyphal Tip

Substantial evidence exists that growth in length of filamentous fungi occurs at the hyphal tip (the extension zone). For example, autoradiographic studies have shown that labelled cell wall precursors such as ^{3}H-N-acetylglucosamine and ^{3}H-glucose are incorporated at the apex (Gooday, 1971). The length of the extension zone varies from approximately 2 to 35μm. When the hypha is growing at a linear rate, the length and shape of the hypha are constant and a linear relationship exists between the extension zone length and the rate of hyphal extension (Steele and Trinci, 1975). The extension zone has a distinctive ultrastructure.

Early microscopists observed an apical ironhaemotoxylin positive region designated the Spitzenkorper. The Spitzenkorper appears as a refractive, roughly spherical body with a diffuse outline and is located in close proximity to the apical pole. Its presence was linked to growth as it vanished when growth was experimentally arrested and reformed just as growth resumed (Girbardt, 1955). As well as the observation of the Spitzenkorper, which is now widely held to

be associated with apical growth in the septate fungi, vesicles were seen first by light microscopy and then by electron microscopy. The vesicles were observed accumulating in the apex and migrating there from the subapical zone (Grove and Bracker, 1970). High voltage electron microscopy of the apex of *Fusarium acuminatum* has indicated that the Spitzenkorper is composed of a cluster of vesicles surrounding a network of microfilaments, which may control the movement of the Spitzenkorper into the apical region (Howard and Aist, 1980; Howard, 1981).

The protoplasm in the tips is divided into a 1 to 2µm apical zone, excluding all organelles except the cytoplasmic vesicles and the subapical zone containing the other organelles (though never nuclei and storage vacuoles) as well as the vesicles. The vesicles are known to migrate from a generator of vesicles such as the Golgi apparatus to the apex where they eventually coalesce with the apical plasmalemma. And, in doing so, they simultaneously accomplish two essential functions: they extend the plasmalemma surface and discharge enzymes and/or material for cell wall formation (Grove and Bracker, 1970). The means by which the vesicles migrate is not known, though mechanisms involving cytoplasmic streaming, microtubules and electrochemical gradients have all been proposed. The contents of the cytoplasmic vesicles have been shown to be items such as cell wall and plasma membrane precursors, lytic enzymes and polysaccharide synthetases (Gooday and Trinci, 1980). Also, chitosomes have been isolated: these contain inactive chitin synthetase, are spherical (40-70nm in diameter), have a membrane like shell surrounding a granulated interior and can synthesise chitin microfibrils in vitro when activated (Bartnicki-Garcia, 1978). The activated form of chitin synthetase has been found to be located preferentially in the hyphal apex (Archer, 1977; Issac et al., 1978) and is believed to be located in the protoplasmic membrane.

The tip is therefore a specialised region in the hyphae designed for the incorporation of large number of vesicles, and consequent wall and hyphal extension. The role of subapical regions is to synthesise, package and transport the material required for extension. The rate of hyphal extension depends on the amount of material supplied to the extension zone, and it's ability to incorporate this material. The capacity to absorb material is determined by the size of the extension zone, such as diameter and length (Prosser and Trough, 1991). The precise shape of the extension zone has been studied.

Trinci and Saunders (1977) proposed a model of tip growth, based on a model proposed by Green (1969) and experimental measurements, which predicts that wall growth is maximal at the tip and decreases to zero at the base of the extension zone. As the extension zone wall does not vary appreciably in thickness the specific rate of wall synthesis at any point must be equal to the specific rate of area expansion. This model is the Cotangent model:- the shape of the extension zone is a half ellipsoid of revolution and therefore the expansion of its surface

area at a point (P) is related to the cotangent of the angle at the base of the extension zone between P and its longitudinal axis. A process of wall rigidification is also carried out but little is known about this process except that it must move forward along a hypha at exactly the same rate as hyphal extension (Robertson, 1965). In *Schizophyllum commune* it has been suggested that the plastic wall at the hyphal tip is rigidified at the base of the extension zone by cross-linking between chitin microfibrils (Wessels and Sietsma, 1981).

Trinci and Saunders have developed their model of tip extension further (1979). The extension zone of a hypha growing at a constant rate is considered to be in equilibrium. New wall material is added in an elastic state, which then sets gradually as the tip moves forward and rigidifies at the base of the extension zone where the hyphal diameter becomes constant. The wall is considered to be elastic and the shape is due to the wall adjusting itself in response to turgor pressure so as to adopt a shape that minimises the surface energy. The rate of supply of material was also shown to determine the ratio of the specific growth rate in the longitudinal and circumferential directions. Koch (1982) also suggested that tip shape is determined by surface tension effects.

1.2.1.2 The Peripheral Growth Zone

The peripheral growth zone is a region of the hypha which supports the tip extension. It is effectively a volume of protoplasm which remains constant as the hypha moves forward. The linear growth (K_r) of a hypha is a function of the length of this zone (w) and the organism's specific growth rate (u). Thus

$K_r=uw$

1.2.2 Growth of Mycelia

The germinating fungal spore absorbs water , swells and develops one or more germination tubes, from which the mycelium develops. Under suitable growth conditions (unrestricted) the total hyphal length and the number of branches increase exponentially at a specific rate determined by the species and the conditions of growth (Trinci, 1974; Oliver and Trinci, 1985). The mean length of hypha associated with each tip has been called the hyphal growth unit (Trinci, 1974). Shortly after spore germination, when the first branch is produced the hyphal growth unit length is halved. The amplitude of the oscillations in the length of the hyphal growth unit decrease progressively as the undifferentiated mycelium increases in size. Eventually the hyphal growth unit attains a more or less constant value. The mean rate of hyphal extension (E) may be calculated also as:-

$E=Gu$

where: G is the mean length of the hyphal growth unit of the mycelium and u is the organisms specific growth rate (Steele and Trinci, 1975)

The fact that there is an exponential increase in tip number reconciles the observations that the biomass of a mould grown in batch culture increases at an exponential rate whilst individual hyphae extend at a linear rate (Caldwell and Trinci, 1973). The growth of an undifferentiated hyphae may be thought of in the terms of a hypothetical growth unit which consists of a tip and specific length of hypha.

Usually two types of branches are distinguished in the filamentous fungi (Trinci 1970): lateral branching and sub-apical branching. In lateral branching (considered as normal branching) the new branch is formed some distance away from the tip in an older cell. The distance between the growing tip and the point of branch formation is constant under constant growth conditions. Carter and Bull (1971) have used this distance, designated the "mean hyphal segment length", to measure morphology. In sub-apical branching the new branch is formed directly behind the apical dome.

Trinci (1974, 1978) has advanced a general hypothesis to account for the regulation of branch initiation in moulds. It is proposed that the cytoplasmic components needed for cell wall extension are produced at a constant rate throughout the mycelium (Katz and Rosenberger, 1971). The components are then transported in vesicles towards the apices of the hyphae. Potentially a branch may be initiated from any part of the mycelium, though they actually occur where the cytoplasmic components involved in wall extension happen to accumulate and to fuse with the rigidified wall of the hypha instead of being transported to the tips. Trinci (1974) relates the branch formation to the equilibrium between vesicle formation and the rate of tip expansion and hypothesises that vesicles will accumulate whenever the rate of vesicle production exceeds the rate of their incorporation in the apex. That is, once the volume of cytoplasm associated with each tip, the hyphal growth unit, exceeds a critical size excess vesicles will cause a new branch to form somewhere in the mycelium (Trinci, 1978). Also an event which stops or reduces the transport of the protoplasm in a mycelium (such as the formation of a septum) will cause accumulation of the vesicles and is likely to initiate a branch.

The period of exponential growth in a submerged batch culture is usually quite short and is followed by a period of progressive deceleration in growth rate. Hyphae become differentiated with the appearance of vacuoles, empty cell walls, autolysis and also in submerged culture fragmentation may occur. Fencl (1978) has reviewed the process of cell ageing and autolysis.

Very little is known of the mechanisms which cause hyphae to fragment. To obtain stable prolonged batch cultures or continuous cultures new hyphal fragments must be formed from existing flocs. Fragmentation of filamentously growing mycelia occurs in submerged culture and produces mycelia with a wide spread both of length and hyphal growth unit length (Metz, 1976). It has been suggested that it is due to shear forces imparted by the impeller (e.g.Caldwell and

Trinci 1973). However though shear forces may be involved it is unlikely that they are sufficient to account for the observed breaking of hyphae. Similar mycelial lengths have been observed in shake flasks and stirred tanks, although the shear rates should be smaller in the former. Fragmentation may be the result of autolysis of some hyphal compartments and degradation of the wall of the lysed compartment. Occasional compartments showing advanced signs of autolysis have been observed in the middle of intact apparently growing hyphae of *Penicillium chrysogenum* (Righelato et al., 1968; Trinci and Righelato, 1970).

1.3 The Streptomycetes

Mycelial hyphae of streptomycetes are septate and are 0.5 to 1.5μm in diameter (Schuhmann and Bergter, 1976). These prokaryotic mycelia bear a remarkable similarity in morphology to the filamentous fungi and their growth has been reviewed in Oliver and Trinci (1985) and Prosser and Trough (1991). The growth is confined to the tips (Kalakoutskii and Agre, 1976; Schuhmann and Bergter, 1976). The lengths of individual hypha increase linearly with time,but the total mycelium length and the number of branches increases exponentially at the same specific growth rate (Kalakoutskii and Agre, 1976; Schuhmann and Bergter, 1976; Reisenberg and Bergter, 1979; Allan and Prosser, 1985).

1.4 Effect of the Environment on Morphology

Many microorganisms undergo morphological changes in response to environmental changes. Filamentous fungi demonstrate a great variety of morphological adaptations in response to appropriate stimuli when growing in submerged culture, such as spore formation, pellet formation and formation of yeast-like cells. Morphological changes usually occur gradually and take several hours or longer to complete. Forage et al (1985) have reviewed the effect of environment on microbial activity which discusses the underlying effects of environmental influences on microbial physiology.

Many studies have been made on a wide range of filamentous microorganisms (mainly filamentous fungi) to study the effects of various fermentation parameters on morphology and metabolite production (Van Suijdam and Metz, 1981). However the relationship between the morphology of a filamentous microorganism and its environment is complex. It is also difficult to identify the response of an organism to a change in one single environmental parameter as one can only rarely alter one aspect of the environment independently. For example, a simple change in pH may also affect the osmolarity of the solution, the CO_2 partial pressure and perhaps O_2 solubility (Forage et al, 1985). Additionally there have been limited examples of quantitative results due to the problems associated with measurement of morphological parame-

ters by manual means (1.5.2, Methods for Morphological Characterisation). Table 1 lists some of the morphological characteristics that have been effected by altering the fermentation variable shown. This list is not comprehensive but provides an insight into the responses of filamentous microorganisms to their environment that have been reported.

Table 1. Effects of the environment on morphology

Variable	parameter effected	Examples from the literature
Agitation	hyphal fragmentation	Van Suijdam and Metz (1981), Pitt and Bull (1982), Smith (1983), Belmar Campero and Thomas (1988)
	integrity of hypha	Tanaka et al. (1975)
	branching frequency	Dion and Kaushal (1954), Dion et al. (1954), Van Suijdam and Metz (1981) Metz et al. (1981), Ujcova et al. (1980), Smith (1985)
	pellet formation	Dion and Kaushal (1954)
	spore formation	Dion and Kaushal (1954)
	hyphal diameter	Dion et al. (1954), Ujcova et al. (1980)
	biomass concentration	Dion and Kaushal (1954), Konig et al. (1981)
	hyphal growth unit	Morrison and Righelato (1971), Katz et al. (1972), Robinson and Smith (1979), Rosenberg and Bergter (1979), Van Suijdam and Metz (1981), Miles and Trinci (1983)

Table 1. Effects of the environment on morphology

Variable	parameter effected	Examples from the literature
	hyphal length	Dion and Kaushal (1954), Dion et al. (1954), Robinson and Smith (1976, 1979), Van Suijdam and Metz (1981)
dissolved CO_2 concentration	biomass concentration	Graafsman (1973), Ho and Smith (1985,1986a,b)
	branching frequency	Ho and Smith (1986)
	hyphal diameter	Ho and Smith (1986)
	formation of yeast-like cells	Ho and Smith (1986)
Dissolved oxygen tension	sporulation, hyphal length, branching frequency	Dion et al. (1954), Zetalaki and Vas (1968)
pH	branch length, hyphal diameter, pellet formation, yeast-like cells	Pirt and Callow (1959)
	hyphal growth unit length, wall thickness	Miles and Trinci (1983)
Dilution rate	hyphal diameter	Robinson and Smith (1979), Rosenberg and Bergter (1979)
	hyphal growth unit	Miles and Trinci (1983)

1.5 Evaluation of Mycelial Growth

1.5.1 Measurement of Biomass

Difficulties in the evaluation of mycelial growth arise from the very nature of the mycelium itself. Fungi grow relatively slowly with mycelia extending and changing in composition as they age. At any given time, perhaps apart from the very early stages, parts of the culture are growing whilst other parts are ageing and dying. Also the composition of a mycelium is changing, for example at various times it may be storing reserve substances giving an increase in weight without formation of new cells. Additionally mycelia are usually grown in complex medium generally containing solids which present problems with simple evaluation methods. Calam (1969) has assessed the problems of measuring mycelial growth arising from the presence of complex media and the morphological variation of the culture.

Due to these problems there is an almost complete absence of any commercially available bioreactor instrumentation to monitor directly and reliably changes in microbial biomass (Clarke et al., 1985). Fermentations are notoriously variable in composition and properties may vary within and between fermentations.

It is generally considered that growth and division constitute the key criteria of microbial viability and therefore distinguishes metabolising cells from non-metabolising cells. Such an analysis has as yet been unattainable due to the time it would take for analysis. The basic approaches to biomass models have fundamental distinctions. The majority of measurements model the culture as two compartments, biomass and growth medium where the parameters measured, in effect, are averaged across the population. Usually microbial content is expressed in the terms of the following:-

1. The number of viable cells present. This is not generally applicable to filamentous fungi due to differentiation and also that the biomass changes independently of the cell number.
2. The total microbial biomass. This is generally the measure used especially in media without solids present.
3. The enclosed volume (fraction). This measure is the volume enclosed within the cytoplasmic membrane which may be used to describe the microbial biomass content (Nestaas and Wang, 1981; Harris et al., 1987).

Numerous measures of biomass have been used for example, optical density, fluorescence, ultrasound ,ATP concentration and dry weight. Often biomass measurement techniques are customised for a specific fermentation i.e. organism and medium, and are not readily transferable between fermentations. The technology that has been used is diverse and originates from different historical backgrounds. However there appears to be two mainstream

approaches to the problem of monitoring growth: the first is to measure substrate and product concentrations and use these to estimate the cell concentration or activity, and the second is to directly measure the cell mass. The boundaries between these two approaches are often unclear. A vast array of powerful technology exists for the measurement of substrate and product concentrations. Included amongst these techniques is quantitative on-line gas analysis which enables indirect mass balancing for estimating bioreactor state. Also instrumentation exists for monitoring liquid phase concentrations which includes the use of ion-selective electrodes, spectral analysis (particularly of infrared spectroscopy), biosensors and analytical HPLC. These techniques are reviewed by Phillips (1990) and Clarke et al. (1985)

For the measurement of cell mass even though many techniques are available their applicability to mycelial fermentations is limited and the presence of undissolved solids reduces this further. Optical techniques using measures of turbidity cannot be applied to complex mycelial morphologies as the application of Beer-Lambert law to model the turbidity concentration response is limited to dilute bacterial and yeast suspensions. Nepholometry which measures the scatter of light is even more limited to small particles. Techniques for the direct enumeration of cells such as the use of a Coulter Counter are also inapplicable for measurement of mycelia. An approach that has often been used is the assaying of cell constituents such as ATP, DNA, RNA, chitin and protein. These methods are all off-line and require the destruction of the sample.

Determination of intracellular adenosine triphosphate (ATP) concentration has been used to detect contamination in food (Hysert et al., 1976). Hendy and Gray (1979) have reported the detection of fungal biomass in a synthetic medium at a laboratory scale. Cochet et al. (1984) have investigated the feasibility of this potentially rapid method for estimating fungal growth and consequently cellulose consumption during cellulase production. The ATP content of the cells was determined by the luciferin-luciferase reaction (Strehler and McElroy, 1957).

$$ATP + luciferin + O_2 = oxyluciferin + AMP + PP_i + CO_2 + light$$

In the early phases of growth it was found that the biomass and ATP concentrations had similar profiles. However, there was no correlation throughout the fermentation between biomass and ATP concentration. Therefore it was concluded that a quantitative determination of biomass from ATP was impossible. Also the values of the ratio of ATP/biomass varied not only during one batch but also from batch to batch. Cochet et al. (1984) did find that even though no quantitative measurement of biomass was obtained, the method allowed the determination of: the end of the growth phase; the lowest values of the specific rate of cellulose consumption; the beginning of the cellulase excretion phase.

A variety of cellular components have been used as indicators of biomass. Commonly used assays for fungal fermentations include assays for: DNA, RNA, intracellular protein and chitin. The changes in concentration of chitin and glucosamine are good indicators of fungal growth. A rapid method for the estimation of chitin was developed by Ride and Drysdale (1972) which can be used for samples in complex solid-containing media. However the chitin content of the cell varies with age and composition, for as the cell ages vacuolisation occurs but the cell walls remain intact for a longer period. Ghost cells of hyphae i.e. cell walls without protoplasm, are a very common sight during the stationary phase. Therefore the concentration of chitin correlates well with growth of cells in the exponential phase, though in the stationary phase when the growth curve levels out the level of chitin continues to increase, though at a slower rate than previously. Also some degraded chitin is usually found in the medium. Using the chitin assay in combination with other assays, e.g. protein assay (Herbert et al., 1971) gives a good estimation of biomass.

Studies on changes of RNA concentration in *A. niger* have been made (Fencl, 1970; Machek and Fencl, 1973). During the first exponential phase RNA concentration was constant along the length of the hyphae, then later on as growth proceeded it decreased in parts distant from the tip and finally during the stationary phase some parts of the fungi lost their ability to synthesise RNA altogether and these began to autolyse. DNA concentration is also often assayed and once again the amount of DNA and rate of synthesis was found to vary across the hyphae (Rosenberg and Kessel, 1967, 1968) with the fastest rate being at the tip. DNA is degraded during autolysis so its concentration drops with age. As the concentrations of DNA and RNA vary along the hypha it is not possible to correlate them with dry weight, however they are useful measures of cellular activity in conjunction with other assays, and are often one of the few measures available during the use of complex media.

There are a number of reviews which extensively cover biomass measurement for microbial cultures (Harris and Kell, 1985; Agar, 1985; Clarke et al., 1986; Phillips, 1990). A selection of techniques are discussed below. These techniques are applicable or are potentially applicable to mycelial fermentations, are of current interest or are in use or development at present.

1.5.1.1 Measurement of Fluorescence

Considerable interest has arisen over a number of years in the measurement of culture fluorescence to monitor cellular activity and growth (Phillips, 1990). Many molecules of biological significance, such as DNA, proteins and amino acids, demonstrate intrinsic fluorescence when excited with UV or visible light of the proper wave length. One very useful fluorescent response is that of intracellular reduced nicotinamide adenine dinucleotide (NADH) and also reduced nicotinamide adenine dinucleotide phosphate (NADPH) which produce a characteristic fluorescent response detectable at 460nm when cells are irradiated with light at 366nm. The

oxidised forms of these nucleotides, such as NAD and NADP, do not fluoresce. In 1970, Harris and Chance built a device specifically to monitor changes in the NADH levels in microbial cultures. This device has since been adapted for on-line use and was the prototype for two commercially available systems marketed by Ingold and BioChem Technology as on-line probes for the continuous measurement of culture fluorescence.

Zabriskie and Humphrey (1978) conducted an extensive study of the applicability of fluorescence to estimate fermentation biomass. The measurements were made on batch cultures of *Saccharomyces cerevisiae* and a species of *Streptomyces*. They showed that the log of the fluorescent signal could be linearly related to the biomass concentration under strictly controlled operating conditions. Their data showed that the fluorescence signal from a microbial culture was interfered with, for as much as 85% of the signal could come from background fluorescence resulting from the presence of of other cellular material and media components. Also the signal was quenched exponentially by the presence of cellular material so that at high concentrations of cells there is little change in signal for large changes in cell concentration. Also Zabriskie and Humphrey (1978) found that many environmental conditions which vary in batch such as pH, temperature,dissolved oxygen concentration, influence the metabolic activity of the culture giving changes in the NADH pool which would prevent direct correlation with cell mass.

Scheper et al. (1986) studied the potential of on-line monitoring of NADH-dependent culture fluorescence. Two types of microfluorimeter probes were used, one was a prototype developed by Dr.W Ingold AG. and the other was a probe specially developed with a special fibre optic for detection of two different wavelengths (Scheper, 1985) and the organisms used were *Penicillium chrysogenum* and *Zymomonas mobilis*. For *Penicillium chrysogenum* the probe was used successfully over a period of 300h. The signal was not corrected regarding changes in light intensity but the light intensity was monitored simultaneously.

During monitoring it was found that several environmental factors influence the fluorescence signal such as the addition of oil, changes in the partial pressure of O_2 and CO_2. The signal was also influenced by biological parameters of the cells and the fluorescence was correlated with the ratio of living to dead cells. For the *Penicillium chrysogenum* fermentation a medium containing solids was used and therefore it was not possible to obtain accurate biomass measurements to correlate the fluorescence signal. For *Z. mobilis* however a synthetic medium was used and the biomass and the fluorescence data were found to strictly follow the same course. Therefore it was possible to measure NADH dependent culture fluorescence on-line during the cultivation of *Penicillium chrysogenum* and *Zymomonas mobilis*. It was also possible to estimate the biomass concentration and to study the metabolic effect of different substrates.

The fluorescence of a number of other fermentations has been monitored and it has been found that the fluorescent responses reflected the metabolic complexities of the fermentations. Also the fluorescent measurement proved to be a rapid indicator of shifts in metabolic activity. The fluorescent signal is therefore very complex as it is complicated by the multiplicity of responses of an active culture however if the signal were to be properly understood and interpreted, it could provide a sophisticated, high level monitor of the metabolic state of a culture and thus a tool for control and optimisation. At present, though, the use of fluorescence to monitor cell growth has limited use as it is necessary to strictly control cell metabolism and the environment of the culture to make use of the fluorescence reading.

1.5.1.2 Microscopy

Techniques using microscopical methods to measure growth are simple, direct, rapid and often inexpensive. The most common technique used is a direct count of the number of unicellular microorganisms present in a known volume of sample which is often refined to give viable counts. The use of microscopy was until recently very limited for the estimation of biomass and the growth of filamentous microorganisms. The commonly used microscopic assays, direct and viable cell counts, are not useful for measuring filamentous microorganisms as they grow by extension to form large branched organisms. Fluorochromes have been developed to stain for various parts of the cell, e.g. acridine orange for nucleic acids which may be used as a viable cell stain. They have been used in epifluorescence microscopy to detect organisms in environmental samples though not in fermentation samples. The potential for the use of microscopy to enumerate and detect whole and parts of microorganisms is only just being exploited using computerised image analysis techniques for direct quantification.

Using image analysis it is now possible relatively rapidly to detect parts of or whole cells and measure these to quantify their appearance. Most of the biological applications of image analysis have been carried out in the medical field using various stains, Fluorochromes and fluorescence microscopic techniques to study cells. Smith and Spomer (1987) have used image analysis to measure in-vitro cell growth of a cell line of tobacco grown in petri dishes on a solid medium They obtained good growth curves and showed that they had detected the cell walls accurately. Frame and Hu (1990) have also used image analysis techniques to measure the diameters of mammalian cells and used this to calculate the cell volume assuming spherical cells. The estimations of the cell volumes compared with values obtained using a Coulter counter and although the numerical values differed, the comparison indicated that the measurements both agreed as to the qualitative features of the cell distribution.

Hiraoka et al. (1986) have developed an image analysis system to quantify filamentous microorganisms. The system was developed for the detection and quantification of filamentous microorganisms in activated sludge during the sewage treatment process, and the control of the

treatment process. A sample was taken and placed under an optical microscope using bright field microscopy so that the object of interest, the filamentous microorganisms, appeared black and the background white. Then the image was captured and displayed as an image of 256 by 256 pixels of various values of greyness. The image was scanned with the filamentous microorganisms being detected as black objects. The image was then thresholded to detect the the object and the number of thresholded pixels was found. This gave a direct estimate of the quantity of filamentous microorganisms present in the sample. From this estimate it was possible to manipulate the conditions in the treatment process to maintain an optimum number of filamentous microorganisms. This method appears to be a crude measurement of the quantity of filamentous organisms present in the sample. However the method enabled the control of the sludge treatment process and as it is in the presence of solids would provide a fast, relatively accurate measure, as long as the amount of flocculation did not vary considerably.

1.5.1.3 Dry Weight

The measurement of dry cell weight is a direct technique for the determination of biomass and novel alternative techniques tend to be judged against it. However this technique is slow, is not very sensitive and also is not generally applicable to situations where undissolved solids are present in the medium. (Sometimes it may be possible to eliminate such non-dissolved solids during the biomass measurement procedure e.g. by dissolving calcium carbonate using mineral acids.) The first step in the procedure is the removal of the cells from the medium which is achieved by filtration or sometimes centrifugation. Both of these processes could result in inaccuracies therefore it is essential to select and examine the specific techniques carefully.

For filtration a sample of culture is filtered on a pre-dried, pre-weighed filter and washed to remove any traces of the medium. The washing should not be too severe resulting in lysis or leaching of the biomass but should be enough to remove the medium present. The washed sample and filter can then be dried to remove the water but the drying conditions should not result in the loss of biomass through oxidation or volatisation. Generally an oven at 110°C, or a high vacuum over P_2O_5 is used. The sample is dried to constant weight.

'O' Toole (1983) investigated the effect of the hygroscopic nature of microbial cells on dry weight measurements. It was found that dry cells absorb moisture during weighing, resulting in an error of 0.6%. This may be eliminated by taking readings over a few minutes and extrapolating back to zero time. Though when the poor sensitivity of the biomass measurement technique is considered such accuracy would not be required for most applications. Dry weight measurements are widely used throughout fermentation studies especially where solids are absent from the media.

1.5.1.4 Wet Weight and Cell Volume

This technique is faster but less accurate than dry weight as the sample is not dried and variable amounts of water are retained in and between the microorganism. A typical example of this method is a 20-50g sample of culture is weighed in its sample bottle. Next it is filtered and washed with water. The empty container is reweighed and the weight of the sample is noted. The filtered sample is squeezed dry by pressing it firmly between two sheets of filter paper and reweighed. The weight of the filter paper is found by weighing similarly damp identical filter paper and this is deducted to give the weight of the sample. The wet weight is useful in providing a rapid estimate of cell growth. It also gives a measure of the actual amount of the mycelia in the suspension in its original form. The wet weight is usually 2.5 - 5 times the dry weight (Calam, 1969).

A similar technique is the packed cell volume (PCV) in which instead of the mass the volume of the cellular material is measured in calibrated centrifuge tubes. However the volume is influenced by the conditions of the centrifugation, and the morphology of the mycelium. The presence of solids in the medium would also make this method inapplicable though sometimes it may be possible to eliminate a large proportion of the solids present using an initial centrifuging stage. Wet weight and PCV can be useful for following the growth of mycelial cultures as the results are rapid even though they are inaccurate. It is possible to assess the interstitial volume of water or medium in the PCV using the space technique proposed by Conway and Downey (1950) and use this to determine the cell volume.

Nestaas and Wang (1981) have described a related technique, the filtration probe, for monitoring mycelial growth during the penicillin fermentation. Filtration is used to separate the biomass and the volume of the filter cake is relatively independent of mycelial morphology. The filtration properties of the broth have been correlated with the cell mass concentration (Nestaas and Wang, 1981 and Nestaas et al. 1981). Furthermore cell respiratory activity, protein content and antibiotic production were related to the filtration properties (Nestaas and Wang 1981,and Nestaas et al, 1981). The broth samples (50-70cm^3) were filtered under a constant pressure onto a filter area of 2cm^2 and the filtrate volume was measured as a function of time, either gravimetrically (load cell) or volumetrically. The cake volume corresponding to a given filtrate volume was then determined using a photocell or manually. Nestaas and Wang (1981) showed that the filtration data could be interpreted to yield information about the cell morphology as the filtration time, the cake volume and the filtrate volume were shown to be related to the product of the hyphal density and the specific cake volume (cm^3 cake/g dry cake). This relationship is shown in equation 1 (Figure 2).

$$\tau = \frac{t_F}{V_c V_F} = \frac{K' \mu_F}{32 A^2 \Delta P} \frac{\rho_h \nu}{(\rho_h \nu - 1)^3 d_h^2} \quad (1)$$

$$X = 1000 \frac{V_c}{V_F + V_C} \frac{1}{\nu} \quad (2)$$

$$\nu = a + b\left[\frac{1}{\tau}\right] \quad (3)$$

$$\nu = \frac{\nu_{mp}}{K^3} \quad (4)$$

τ	specific filtration time
t_F	filtration time (s)
V_c	cake volume (cm^3)
V_F	filtrate volume (cm^3)
ρ_h	hyphae density (g (dry) hyphae/cm^3 (wet) hyphae)
ν	specific cake volume (cm^3 wet cake/g dry cake hyphae
K'	shape factor dimensionless
μ_F	filtrate viscosity (g/cm s)
A	filter area (cm^2)
ΔP	filtraton pressure (g/cm^3 s^2)
a+b	empirical constants
V_{mp}	specific volume of the particle (cm^3/g)
K	linear compression factor (proportion to the reduction in the effective particle diameter)
X	dry cell weight concentration (g (dry) cells/L broth)

Figure 2. The relationships established for the filtration probe. The relationships between measurements determined from the filtration probe and biomass or cell morphology (Nestaas et al. 1981)

Once the dry weight of the filter cake was evaluated then the specific cake volume (cm^3 cake/g dry cake) could be evaluated and the hyphal density predicted. Also the dry cell weight concentration could be evaluated using the following relationship shown in equation 2 (Figure 2).

Nestaas et al. (1981) have made use of this approach and have presented interesting results on the relationship between hyphae density and specific rate of penicillin production. This method, however, is not suitable for on-line applications because of the time delay of the dry weight measurements of the cake. Even though the experimental data presented by Nestaas et al. (1981) showed that the specific cake volume was reasonably constant for most of the fermentation changes did occur so the evaluation of the specific cake volume would be required for measurement of the hyphal density and the cell concentration. To overcome these difficulties Nestaas et al. (1981) as well as Thomas et al. (1985) recommended an empirical relationship between the specific cake volume and the specific filtration time (which is independent of cell concentration). The proposed correlation is shown in equation 3 (Figure 2). The calculation of the specific cake volume in this manner enabled the prediction of the unknown biomass concentration using the empirical relationship in combination with equation 1. Using this, Nestaas et al. (1981) found good agreement between cell mass estimated during fermentation from filtration data and measured cell dry weight during the production phase.

Reuss (1990), however, has shown that the validity of the empirical correlation critically depends upon the actual time course of the hyphal density. Nestaas et al. (1981a, b) reported that the cell degeneration and the corresponding decrease of hyphal density during the production phase of the penicillin fermentation can be prevented if the specific growth rate is beyond a critical value. Reuss showed that under these conditions of constant hyphal density significant discrepancies in the predicted value of the specific cake volume would be expected according to the comparison of the theoretical and empirical calculations.

In an analysis of the rapid growth phase of the penicillin fermentation Nestaas et al. (1981) also related the specific cake volume to the specific volume of a mycelial particle (equation 4 in Figure 2). The specific mycelial particle volume was calculated using microscopically measured main hyphal lengths, a fixed hyphal diameter of 5μm ,constant hyphal density (0.3g/cm^3) and assuming that the particle branched at every 37.5μm. A good fit was obtained for the relationship between the specific volume of the mycelial particle and that of the cake for the rapid growth phase after which the model no longer applied. Also the average mycelial particle dry weight was calculated and compared to the total mycelia weight and there was found to be good agreement between the mass of the average mycelial particle and the total biomass for the rapid growth phase. During exponential growth the ratio total dry weight/particle dry weight which produces the number of particles in the broth was in excellent agreement with the viable spore concentration of the inoculum. Therefore Nestaas et al. (1981) envisaged that if the size of the inoculum is known then the filtration data could reasonably accurately predict biomass during the first stage of the fermentation using the calculation of the mass of a particle.

Nestaas and Wang (1983) automated the filtration probe to monitor the penicillin broth semi-continuously. Using the experimental finding that the specific cake volume remained nearly constant during the production phase (Nestaas et al. 1981), the biomass was assumed to be almost proportional to the ratio filter cake volume/broth volume. This simple relationship was then used to determine the cell concentration using the automated probe on-line. The probe operates asceptically and returns the broth sample back to the fermenter after each filtration. The "Filtration Probe" has since been redesigned for measurement in situ (Thomas et al. 1985) and Reuss (1990) has redesigned the probe for use in pilot and industrial plants, the "Bio-Filtrator". The device developed by Thomas et al. (1985) was placed directly into the fermenter and measured the filtration characteristics of the broth, using fibre optic light guides in combination with a pair of light sources to detect the depth of the filter cake. The system is connected up to a computer system which allows the on-line estimation of biomass. The estimates obtained were in excellent agreement with the measured dry weights over a large range of *Penicillium* concentrations from circa 2g\l to 40g\l. This system appears to have the potential to be applied to other fermentations, such as yeast or prokaryotic, besides the penicillin fermentation to give estimates of cell concentration.

Notably all of the studies using the fermentation probe have been carried out in complex medium with corn steep liquor solids initially present in low concentration. The workers have assumed the concentrations of solids to be negligible which would probably have been a correct assumption for the production phase. The presence of solids in considerable quantities would significantly affect the filtration characteristics of the broth and prevent the measurement of the cake dry weight and the mycelial volume in the cake.

1.5.1.5 Ultrasound

Fermentation cultures can be considered essentially as a two- phase composite mass, composed principally of convertible substances in aqueous media and viable biomass, with the mass transfer from medium to biomass causing a change in the relative mass ratios with time. The degree of proportionality may be tested with a view to estimating biomass and this can be accomplished by measuring changes in the specific gravity. A technique used for this is acoustic resonance density (ARD). In most ARD instruments the sample is injected into a suitable chamber for this purpose. Then resonance is initially excited and sustained. Once the self-excitation has started oscillation continues so long as the system can supply sufficient energy to sustain the resonance for any given mass. A direct relationship exists between the density, D, and the square of the oscillation period, t:

$D = A (t^2 - B)$

where A and B are calibration constants. Temperature affects the sample density so this must be controlled. The biomass is determined by measuring the density of the culture and subtracting the density of the cell free culture filtrate. Blake-Coleman et al. (1985) have used this system to investigate cultures of *E. coli* and *E. chrysanthemi* in 400L bioreactors. They found a high linear correlation between ARD and growth curves using optical density. The data acquisition was rapid with a low error and wide range, and operation was apparently simple. Also the technique has been used on-line by Kilburn et al. (1989) for the measurement of the biomass of mammalian cells. However the cell mass has to be separated from media solids for accurate analysis. This system could be applied to mycelial fermentations and the system has the potential of being rapid although solids would need to be separated from the cell mass which would generally not be feasible and would limit this application to fermentations without large amounts of solids.

Ishimori et al. (1981) have proposed a method for the determination of microbial concentration utilising an ultrasonic device. This sensor system consisted of two piezoelectric membranes, 2.5mm apart. It was immersed in a medium containing cells and then ultrasonic waves were generated on one of the piezoelectric membranes and transmitted through the contained sample to the other membrane surface causing it to vibrate. The vibration was then read as an output voltage. The sensor was tested on *Saccharomyces cerevisiae, B. subtilis and Klebsiella sp.* by immersing the membrane block directly into cellular suspensions. The output voltage was shown to be affected by a number of factors such as temperature, pH, medium compressibility, medium conductivity and the presence of glycerol. The changes in output voltage correlated with changes in medium compressibility, not medium density. A linear calibration over the range from 10^6 to 10^8 cells per mL was obtained but this was species specific and had a mean error of 6%. Ishimori et al. (1981) found that the piezoelectric membrane was fragile and had poor directional transmission so a new system the piezoelectric gum sensor has been developed (Endo et al., 1989)

The piezoelectric gum sensor is steam sterilisable and was used to monitor growth of *E. coli* and *Saccharomyces cerevisiae* in situ. With this sensor the output voltage was not affected significantly by pH, conductivity and viscosity although temperature caused changes. Calibration curves for *E. coli* and *S. cerevisiae* were linear in the range of 1.0 to 3.8g/L and 0.5 to 9.8g/L respectively which is below the level of biomass normally attained in fermentation particularly of yeast. Also the calibration was species specific which indicated that the output voltage was also dependent on the cell properties such as size, surface area and volume as well as the cell concentration. However bubbles affected the output voltage so it was necessary to switch off aeration during measuring. The presence of non-dissolved solids would also affect the measurement as they would absorb sound waves so this method would not be applicable to fermentations with significant quantities of solids. Endo et al.(1989) intend to investigate the

applicability of this technique to mycelial cultures and to solve the problem of interference by aeration.

1.5.1.6 Calorimetry

One interesting parameter of fermentations is heat evolution. Heat evolution is closely related to the catabolic activity of the cell and is valuable as a measure of the efficiency with which available chemical energy is utilised. Because heat evolution during growth and metabolism is a universal characteristic of living organisms it can potentially be used to monitor all kinds of microbial systems even in complex media. Mou and Cooney (1976) measured the rate of heat production during mycelial fermentations accompanied by product formation and in the presence of non-cellular solids. One system was the production of novobiocin by *Streptomyces niveus* in a complex distillers solids based medium. The second system only reached low levels of biomass and was not very useful in interpretation of the results. Though the organisms used were not filamentous fungi, the same type of problems tend to apply.

A dynamic calorimetric technique was used to measure the rate of heat production during the course of the fermentation. This procedure utilised the heat released during metabolism to raise the temperature of the fermentation broth when the temperature control system was switched off. A sensitive thermistor circuit was constructed to record the rise in temperature as a function of time. The outside of the fermenter was insulated with air-craft fibre-glass to minimise heat loss to the outside environment. The heat loss due to evaporation of water into the air stream and the heat loss to the air stream were made negligible by saturating the inlet air with water at the operating temperature before it was introduced. Therefore:

$$\begin{matrix}\text{Heat of} \\ \text{fermentation}\end{matrix} = \begin{matrix}\text{Rate of} \\ \text{heat accumulation}\end{matrix} - \left(\begin{matrix}\text{heat of} \\ \text{agitation}\end{matrix} + \begin{matrix}\text{heat lost to} \\ \text{environment}\end{matrix}\right)$$

Since the impeller speed and aeration rates were kept constant the heat of agitation and the heat loss to the environment were calibrated before the fermentation. Therefore it was possible to calculate the heat of fermentation. Due to the lack of precise dry cell weight data it was not possible to make an exact correlation between total heat evolved and the cell mass formed. However a close relationship between the total heat evolved, the packed cell volume and the total solids concentration existed. From the data a value for the thermal yield over the first 38h was estimated to be 0.3g cell synthesised per kcal of heat evolved. After the initial growth phase, growth is slow, and the energy for maintenance and product formation become the dominant term in heat evolution therefore the integrated heat curve deviated from the cell growth curve.

Mou and Cooney (1976) found some technical problems with this technique. If the fluid properties change this can alter the power drawn into the fermentation broth, therefore this would be a problem with most filamentous fungi fermentations as broths tend to be very viscous and are frequently non-Newtonian at high cell concentrations. Also surface-acting agents can change the gas hold-up in the vicinity of the impeller and thus change the fluid density.

For large scale production the use of an insulated fermenter to measure heat evolution would be impractical therefore microcalorimetry is usually considered using flow-sampling techniques which with mycelia produce their own problems due to entanglement and fouling. Another problem is the complexity of the enthalpy profiles obtained for there are many factors producing heat in during fermentation and the microorganisms themselves are in diverse physiological and metabolic states so relating the enthalpy profile to biomass and cellular activity can be a difficult problem.

1.5.1.7 Dielectric Measurements

Monitoring impedance of microbial cultures is an accepted practice for the early detection of microbial growth in laboratories (Harris and Kell 1985). However these methods depend upon the changes in potential caused by the growth of microorganisms and the production of electroactive metabolites, therefore the detection time is relatively long and additions of ionic solutes for control during the course of a fermentation would seriously affect the value of the data obtained. An alternative method is to measure the dielectric properties of the cellular suspensions themselves rather than that of the suspending medium or the electrodes themselves. There has been considerable interest in the development of impedance measurements for the monitoring of culture growth which is reviewed extensively (Harris and Kell 1985, Phillips 1990). One important development is the use of admittance spectroscopy to provide dielectric dispersion data for microbial cultures which can be used to give values for the biomass volume fraction (Harris et al. (1987). Harris et al. (1987) have described the performance of a (steam sterilisable) probe consisting of four gold electrodes in an insulating housing. This probe operates at frequencies, centred in the radio frequency range of the electromagnetic spectrum, where the dielectric properties of the microbial suspension differ significantly from those of particulate and gaseous species in solution. The dielectric properties of the microbial suspension are caused by the charging of the membrane capacitance displayed by all intact cells which is due to the possession by cells of non-micellar phospholipid membranes of molecular thickness. Using the measurement of the dielectric permittivity of cell suspensions Harris et al. (1987) have shown that the probe can be used to estimate the volume fraction specifically enclosed within the cytoplasmic or plasma membrane of the cells of interest. They have also shown that the radiofrequency dielectric properties of microbial cell suspensions are a direct and monotonic function of the volume fraction so defined (and differ significantly from those of

particulate matter, gas bubbles and aqueous solutions). Therefore the probe is specific for viable cells (Kell et al. 1990).

The system was demonstrated on suspensions of *Saccharomyces cerevisiae* grown on a complex medium in an air lift fermenter. The system response was shown to be linear with yeast concentration up to at least 100g/L. Harris et al. (1987) added calcium carbonate, up to concentrations of 30g/L, to yeast suspensions and found no interference to the probe response. The performance of the probe has not yet been reported on a variety of complex medium formulations and the applicability of the system to a typical stirred tank reactor. However in growth media of high conductivity the dielectric properties of the cell volume fraction becomes difficult to detect (Clarke et al. 1986) so the probes function have limited on-line applicability and off-line sampling and dilution may be required for certain media. The probe appears to be a rapid and promising technique though it has not yet been shown to work with mycelial microorganisms. One would expect the probe to correlate well with biomass through the initial growth phase when virtually all of the cells are intact. However once hyphal differentiation starts then the probe would no longer be able to follow the biomass curve as it only measures cells with intact membranes so it would not be able to measure the necromass. This would not be problematic as the necromass is not related to the metabolic activity of the cell. There are also cells which have intact cell membranes but which are in various stages of degeneration with large vacuoles present, these would be measured as typical viable cells but would actually only have a small contribution to the metabolic activity of the hypha. Therefore the response of the probe would be linear only for a given cell morphology and it would also probably be very difficult to correlate the measurements from the probe with cellular activity in the production phase of growth.

1.5.2 Methods for Morphological Characterisation

Although morphological parameters have been widely reported in the literature over many years, generally only qualitative descriptions have been used such as short fragmented hyphae or long slender hyphae. A number of detailed studies of the morphology of filamentous microorganisms have been made some of which have developed a qualitative scoring system for morphology in an attempt to standardise the results (Duckworth and Harris, 1949; Hockenhull, 1963; Butler and Harris, 1949; Doskocil et al., 1958). Where work has actually measured morphology such as the hyphal growth unit length then methods of photomicrography have been used and the measurements have been made on an enlarged photograph or even in some cases measurement during microscopy using an eyepiece graticule. These methods are extremely time consuming so that only a few organisms were usually measured. Therefore in order to allow quantification of the morphology an easier, rapid, more transferable, less subjective method was required.

Metz et al. (1981) have developed a semi-automatic method to characterise a number of morphological parameters quantitatively:. The parameters that were chosen were

1. the length of the main hypha or effective length
2. the total length of all hyphae of a particle
3. the mean length of the branches
4. the mean length of the segments
5. the number of branches
6. the hyphal growth unit: the length of hyphae per growth tip
7. the hyphal diameter (estimated mean)
8. the dimensionless effective length (the length of main hypha divided by the hyphal diameter)

The actual measurements made to determine the above parameters were the main hyphal length, the length of the segments, the length and number of the branches and the hyphal diameter. All of the other morphology parameters were computed from these.

The method of quantification used an electronic digitiser. First photographs of the mycelial particles were made essentially randomly. The photographs were projected by means of an adapted microfilm reader onto an electronic digitising table linked up to a suitable computer. The digitising table determined the X and Y coordinates of a point touched on the image of an organism by a special pen, so that touching a mycelium at points along its length gave coordinates from which the computer could calculate the length of the mycelia. To do this software was used to calculate chord lengths which additionally allowed each of the parameters to be identified for later analysis. Metz et al. (1981) used this method to determine the hyphal morphology for at least 10 to 20 microorganisms for every sample from each fermentation.

Metz et al.(1981) found very large deviation of the observations around the mean due to the range of morphologies in a single sample rather than experimental error. Overall this method of quantitative representation of hyphal morphology was very effective. However the measurement of hyphal diameter was not useful as it showed relatively large variation. The most useful morphological indices were the main and total hyphal lengths, and the hyphal growth unit. However the reproducibility of the morphology data of batch cultures was found to be poor although for continuous culture data it was better.

Digitising by this method has the disadvantage of being labour intensive and time consuming. The values obtained would be influenced by the operators skill at using the pen. Therefore a

semi-automatic image analysis method was proposed (Adams and Thomas 1988) and this was compared with the digitising table method. For image analysis a TV camera was mounted on a microscope, and the video signal was passed to a computer capable of image processing and analysis. The image was digitised and captured, making it available for analysis. The method used captured a image of a single organism the quality of which was then improved. The enhanced image was segmented and skeletonised after which the resulting binary image was edited manually to remove any objects other than the skeletons of microorganisms. After breaking the skeletons into segments (breakage at the nodes), manual editing was used to isolate the length of the main hypha and each of the branches. As each length was isolated it was measured automatically. The image analysis software by application of a suitable algorithm measured the length of the arc (Adams and Thomas 1988). Each individual mycelial tree took approximately 1 min to characterise and measure. A photograph of the microorganism was also taken and measured using a digitising table in a method similar to Metz et al. (1981) for a direct comparison of the two methods. It was shown that the semi-automated image analysis method could replace the digitising method. It was more precise and on average gave mean lengths 6% greater than digitising because the latter used chord lengths to represent arc lengths. The semi-automatic image analysis method although it had an overwhelming advantage over digitising in time and convenience, had not reached its full potential as considerable manual intervention was still required.

Recently a very similar method to the one described above has been used to characterise the morphological parameters for early growth and branching of a *Streptomyces tendae* in a growth chamber using image analysis (Reichl et al. 1990). This method still used considerable interaction from the operator for carrying out procedures such as closing small gaps in the hyphae as the mycelia were not stained and also for the identification of the individual branches. The growth of mycelial particles was followed over several hours and it was found that after a few hours growth it was no longer possible to distinguish between all of the hyphae particularly those in the centre of the mycelial tree. The duration of the image analysis was found to depend on the complexity of the mycelial tree and the number of interactive steps needed. Analysis of simple hyphal trees took approximately 3 min to analyse and the highly complex trees formed after several hours growth took up to 15min to analyse. Although this study did not advance the use of image analysis from that already reported in 1988 (Adams and Thomas 1988), it demonstrated that the methodology could be used intricately for following the growth of individual mycelium in detail over time and also that the methodology was not limited to just one manufacturers equipment.

2.0 Introduction to Image Analysis

Image analysis is a versatile technique and has found applications in a wide range of scientific disciplines. For microscopists, who have measured samples manually for many years with the aid of tools such as eye-piece and stage graticules, image analysis will be an invaluable tool. It is an automated procedure and thus removes most of the subjectivity and operator fatigue associated with manual methods and has the ability to obtain quantitative results by application of strictly identical criteria of measurement which should be independent of the operator. Additionally the measurement of samples by image analysis should be considerably faster than by manual means and the processing power of the technique is such that it will allow the development of novel applications that were previously impossible.

Image analysis may be defined as the acquisition of an image followed by the quantification and classification of components in it. At present there is commercially available a wide range of diverse technology for image analysis as systems and software are being developed by most of the major computer manufacturers as well as many small specialised companies. Each company appears to have its own philosophy on the structure of the technology and software which reflects the fact that image analysis has only recently become of major commercial interest. The principle stages of image analysis are image capture, segmentation, object detection, measuring and analysis. These are described below along with some other features fundamental to the processes used in the software during this project. For a detailed description of image analysis and processing a wide range of specialised books have been published of which two books (Gonzales and Wintz, 1977; Joyce Loebl, 1985) give a good general guide to processing and analysis.

2.1 Image Capture and Enhancement.

Image capture involves the conversion of the image into an electronic signal suitable for digital processing and storage. There are a number of video input devices, the most common being a high quality and high resolution closed circuit T.V. camera. Other devices include S.E.M. and videotape recorders. Basically the image capturing process quantises the image in both tone and space. Spatially the image is usually divided into a square or rectangular grid of picture elements, known as pixels or pels. For the systems used in the project a format of 512 by 512 pixels is used. Each pixel is assigned a greyness or intensity level representing the tone in the locality of the pixel on the original image. Typically 64 or 256 levels of greyness are used producing a digitised image which is acceptable to the human eye. Lower numbers of grey levels tend to produce a distinctly stepped display , with obvious changes between the grey levels. Also the number of pixels determines the smoothness and resolution of the image.

Once the image is captured it is often necessary to enhance features of it to correct distortions or simply to discern any detail. This requires image processing and a large number of techniques have been developed. Some of the most useful techniques are grey level transformations where the grey level of each pixel is transformed to another value by reference to a predetermined rule independent of any of the other pixel values. Other useful techniques are grey level convolutions and filters which transform the value of a pixel by a rule which takes into account the neighbourhood of the pixel. A number of image processing techniques may be carried out on an image until it becomes useful for analysis. Once enhanced the image can then be thresholded.

2.2 Segmentation.

In order to carry out measurements it is necessary to seperate regions of interest within an image from the background. This process is known as segmentation. There are different methods of segmenting an image; the method used in the project is thresholding. A simple example of this is all tones below a certain level are treated as black i.e. of interest, and all above as white i.e. as background. Most modern I.A. systems allow two thresholds to be set allowing a slice of grey tone to be taken as of interest with the lighter and darker tones above and below the slice being treated as background. Segmentation thus creates a binary image from a multi-tonal grey image containing pixels with the value of 0 or 1. The pixels in the area of interest are then easily identified from the background as they have the value of 0 or 1 depending on the convention used.

2.3 Object Detection.

The word object is used to describe each of the individual regions of interest within the image. Object detection is a data reduction step which produces a description of each object rather than just a list of coordinates of each
pixel it encompasses.There are different means of achieving this depending usually on the design of the image analysis system and software. The two most frequently used are chord-based connectivity analysis and boundary coding. The latter is used in this
project and determines the development of software.

The algorithm used for boundary analysis is known as Freeman chain coding (Freeman 1961). The algorithm in the systems used incorporates this coding. First the system looks at each pixel in turn scanning from the bottom left hand corner of the image and working upwards row by row until an object is encountered. Once found , the search changes to a sweep around the pixel to find the next connected pixel working in a clockwise direction. Once the next pixel is

located, its neighbourhood is searched for the next pixel in the boundary. This is repeated until the system recognises that it has returned to the starting point and thus has a complete description of the boundary of the object , which is then stored. From the boundary, the region of an object can be calculated, this is the total space enclosed by and including, the boundary. This is a list of chords, which allows local image processing to be carried out over just this region. Once the objects have been detected it is then possible to carry out numerous measurements.

2.4 Measurement and Analysis.

As the pixels are square it is relatively simple to calibrate the system, for one pixel width will be the equivalent to some real distance. When using a microscope this is achieved by making measurements of a slide graticule so that a calibration factor is generated for conversion of pixels to microns. Two main levels of measurements are used: field measurements, in which the contribution of each object is not individually recorded but summed to provide a single measure for the whole image, and secondly individual object measurements. The actual measurements made are varied and depend upon the application but typical measurements for fields are counts of objects,area; and for objects: area, perimeter,diameter, length, breadth and so on.

Once quantitative measurements are made then analysis of the data must be considered. The data is generally displayed as a statistical summary by the system or stored as a data file where it is available for data processing by statistical packages.

2.5 The Measuring Frame.

In order to eliminate counting and measurement errors due to objects crossing over the edge of the image an active measuring frame with a guard region is used. The measuring frame is a precise defined area within which to measure. Each object has a unique counting point, the bottom leftmost pixel of the object. The guard region around the measuring frame is wide enough to encompass the largest size of object to be measured and the system only includes the object and its measurements in the result for that field if the unique counting point lies within the field. This is shown in Figure 6. As the unique counting point for the image analysis systems used are always below the object then only a single pixel guard region below the measuring frame is required.

2.6 The Motorised Stage and Focus.

To obtain complete coverage of a whole or part of a sample on a microscope slide an automatic stage is used. The stage has a fixed step size for movement in the X and Y directions, usually 1,5 or 20microns and its movement is controlled from the image analysis system. This enables the stage movement to be preprogrammed for the required type of coverage of the slide allowing a range of coverage from random fields to abutting frames. The number of fields to be measured is also controlled. Automatic focusing is also usually used in conjunction with the stage, and another common option is automatic lamp control.

3.0 Materials and General Methods

3.1 Materials

3.1.1 Organisms

The main microorganism used for this study was a high producing mutant of *Penicillium chrysogenum* developed by Panlabs Inc. (Fayetville, N.Y, U.S.A.). It was designated P-1 and produces Penicillin V, using phenoxyacetic acid (P.O.A.) as a precursor. Subsidiary organisms used were *Penicillium chrysogenum* Panlabs P-2, *Penicillium chrysogenum* NRRL 1951 and also a filamentous prokaryote *Streptomyces clavuligerus* ATCC 27064.

3.1.2 Chemicals

The chemicals used were general purpose reagents supplied by BDH Ltd. (Dagenham, UK), FSA Laboratory Supplies (Loughborough, UK) and Sigma (Poole, Dorset). Specialised media ingredients were supplied by Oxoid Ltd. (Basingstoke, UK).

3.1.3 Equipment

3.1.3.1 Image Analysis Systems

During the study two image analysis systems were used. Initially a Magiscan 2A (Joyce Loebl Ltd., Gateshead,U.K) with a Nikon Optiphot microscope (Nikon Ltd. U.K, Telford, U.K) attached to it was used. The second system was a Magiscan MD system (Joyce Loebl Ltd.) with a Polyvar Widefield microscope (Leica Ltd, Cambridge, U.K.) attached. Motorised stages were fitted to each optical microscope. These have precision X- and Y- drives, 20µm and 5µm steps for the respective systems, and a focus drive. Computerised microscope controllers operated the stage drives and also controlled the lamp brightness. The controllers and stages were also supplied by Joyce Loebl Ltd. and controlled by software from the same company. Both image analysis systems used square images of 512 by 512 pixels. For the digitisation of images tonally the systems used 64 intensity levels (grey levels).

A representation of the hardware incorporated in the Magiscan MD image analysis system is shown in Figure 3. It had two colour monitors, one for text displays for the controlling software and the other for the image display. A keyboard and two pointing devices :a mouse for the text screen and a light pen for the image display, were also used. A monochrome TV camera was mounted onto the microscope. The rest of the hardware consisted of the image processing unit, a system unit for a personal computer, the microscope controller and a printer. The pres-

ence of the personal computer, which carried out a limited amount of actual image analysis routines, provided a very useful and familiar interface to the image processing unit as DOS (Disc Operating System) was used as the operating system. The Magiscan MD was also provided with a specialised software for image processing and analysis consisting of Genias (General Image Analysis Software), Genial (General Image Analysis Library) and a data analysis package, Results. Genial is a library of units and modules for the features of the Magiscan MD which can be linked into Pascal programs compiled with the Microsoft Pascal Compiler (Microsoft Corporation, Redmond, USA).

The Magiscan M2A system is an earlier version of the MD system and did not have a PC incorporated into the hardware so all of the required functions are in one purpose built unit. The rest of the hardware was virtually the same as for the MD (Figure 4) except there was not a mouse and one of the monitors was monochrome. Both monitors had identical displays of the image partially overlaid with text but the colour monitor was able to display pseudo colour images. The M2A system used a UCSD operating system (University of California, San Diego, USA). A number of software libraries incorporating units and modules for image processing and analysis were supplied with the system and these were used in conjunction with a developmental software package, Bones; an in-house tool of Joyce Loebl Ltd. Applications for the project were written using this software and the UCSD Pascal Compiler (University of California, San Diego, USA).

3.1.3.2 Digitising Table

A Hewlett Packard 9874A digitiser (Hewlett Packard Ltd., Wokingham, U.K.) linked to a BBC Master Series Computer (Acorn Computers Ltd., Cambridge, U.K) was used. The system was set so that the coordinates of points covered by the cursor were taken by the digitiser with a step length of about 2mm on the drawing (equivalent to a real length of approximately 1.1μm).

3.1.3.3 Waring Blender

A Waring Blender (model 31BL44, Blender 8011) was used for chopping hyphae. The blender had two fixed speeds of rotation of the blade, high and low, which when evaluated with a tachometer were found to be 17000 and 14000rpm.

3.1.3.4 Fermenters

Several different fermenters were used for the provision of samples for the evaluation of the methodologies developed in this study, as many of the samples were taken from other research workers fermentations. The fermenters used were:

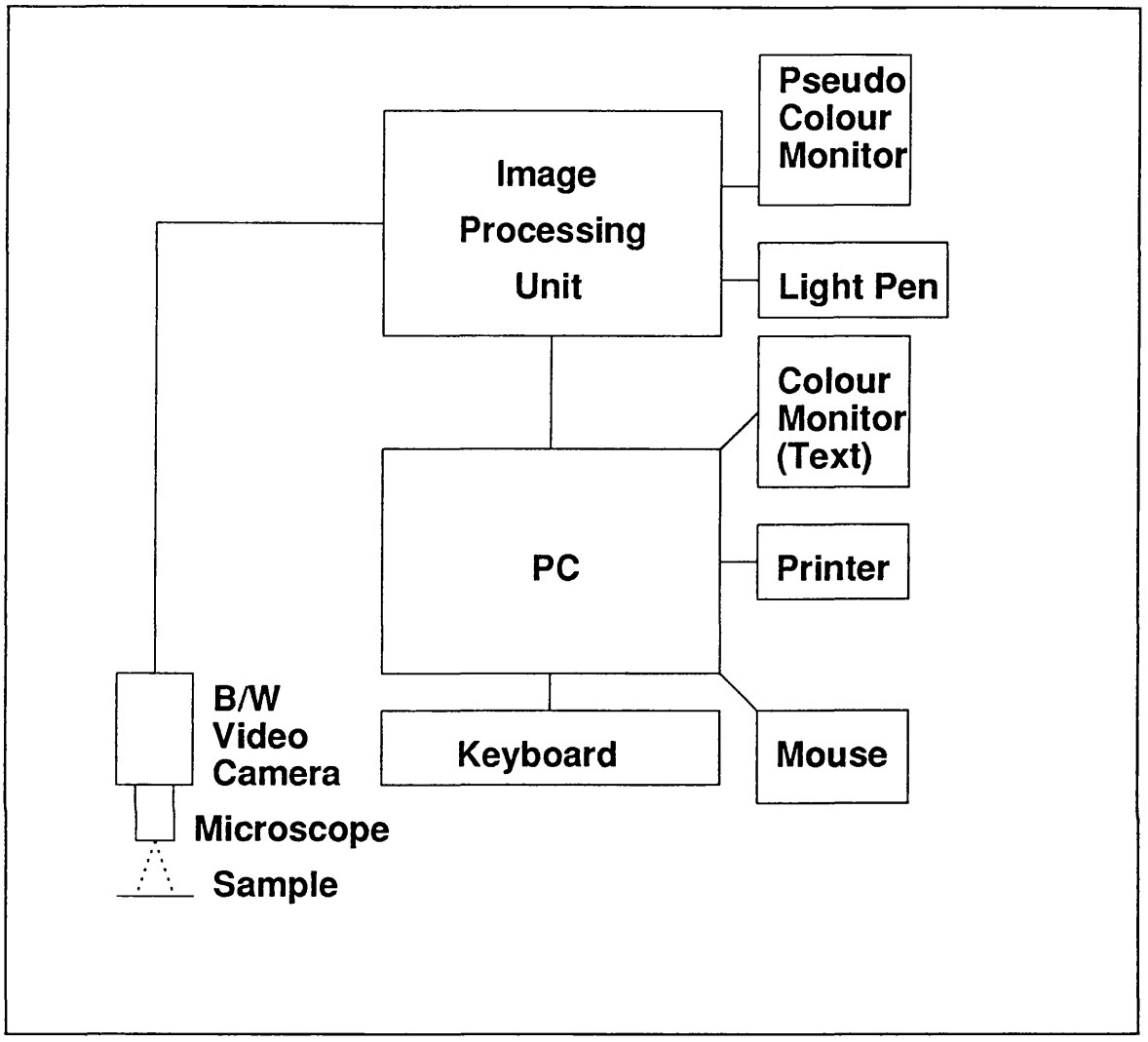

Figure 3. The hardware configuration of the Magiscan MD image analysis system

1. A 7L LH 2000 series fermenter with 3000 series instrumentation (LH Fermentation Ltd., Maidenhead, U.K). This had a 5L working volume and was baffled with 4 baffles. Three Rushton turbines were mounted on the stirrer shaft.
2. A 14L Chemap AG fermenter with a 10L baffled working volume (Chemap A.G., Mannedorf, Switzerland) and three disc turbine impellers attached to the stirrer shaft.
3. A 150L 5000 series baffled LH fermenter with 3000 series instrumentation This had a 100L working volume, with three disc turbine impellers.

3.2 Methods

3.2.1 Slide Preparation

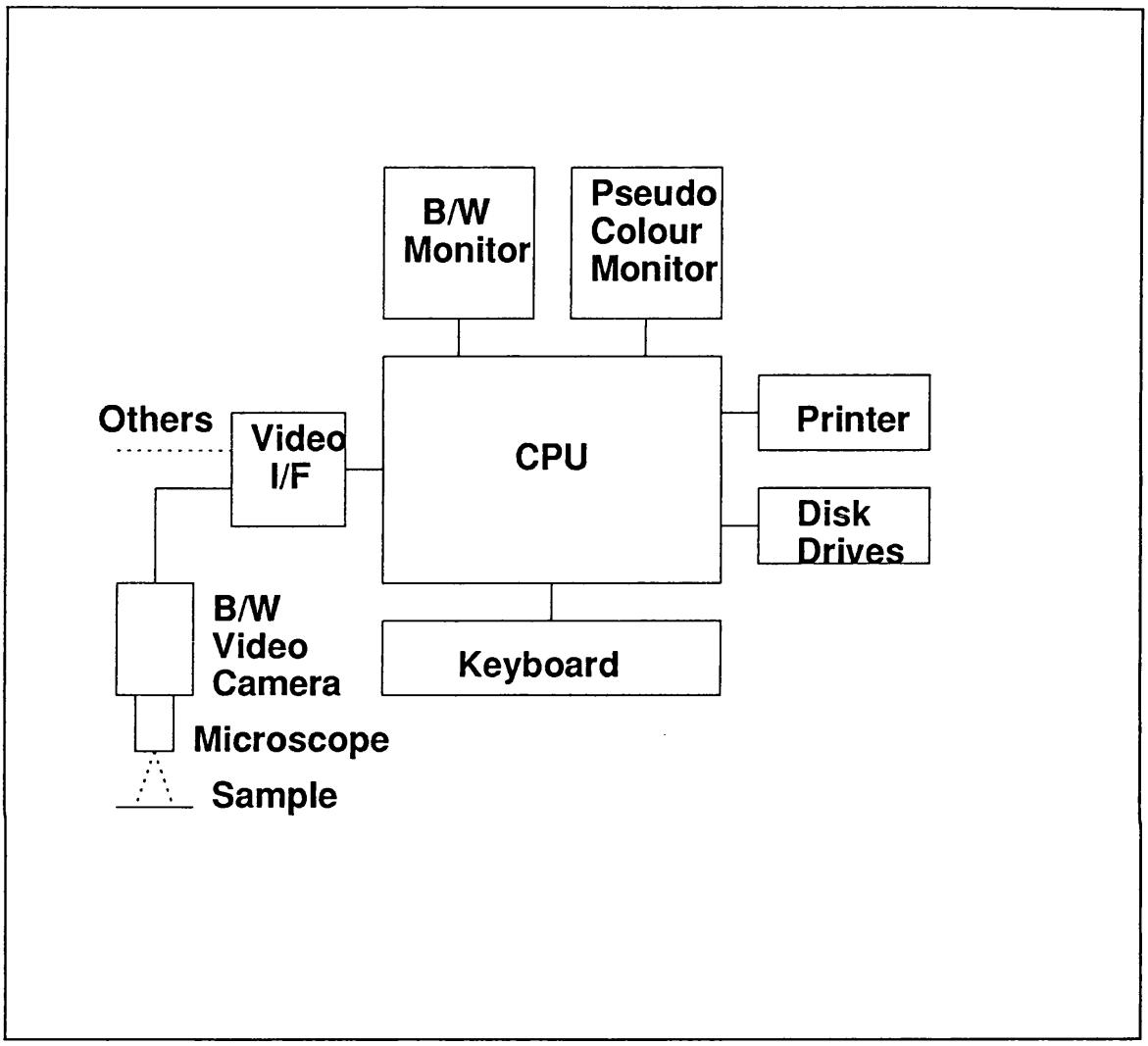

Figure 4. The hardware configuration of the Magiscan M2A image analysis system

3.2.1.1 *Streptomyces clavuligerus*

Once a sample was withdrawn from the fermenter it was diluted immediately in distilled water. For characterisation of samples across the fermentation time course, the samples were all diluted 400-fold. However for study of the effects of dilution the sample was diluted additionally to 100- and 1000-fold. A 40µL aliquot was then removed from the diluted sample and this was gently spread onto a glass microscope slide (76 by 26mm, 1.0/1.2mm thick, KTH 390, Chance Propper Ltd.,Warley, U.K.). The slide was left to dry at room temperature before staining with methylene blue. For staining the slide was immersed in methylene blue stain (0.3g methylene blue, 30ml 95% ethyl alcohol in 100ml distilled water) for approximately 1 minute, and washed with water. The slide was allowed to dry again at room temperature. This method of staining was developed to avoid potential damage by heat treatment of the microorganisms in the

sample and also it provided excellent colour enhancement of the microorganisms for image analysis.

3.2.1.2 *Penicillium chrysogenum*

Once a sample was withdrawn from the fermenter it was mixed immediately in an equal volume of fixative (Table 2)

Table 2. The fixative (Righelato et al, 1968)

Components	**(mL)**
40% (w/v) formaldehyde	13
glacial acetic acid	5
50% (v/v) ethanol in water	200

The samples were stored at 4°C until required. Before morphological measurement the samples were diluted to a degree determined by trial and error for each sample, but generally about 20-fold overall. A small amount (0.8ml) of lactophenol Tryphan Blue stain (0.25g Tryphan Blue to 100mL of lactophenol) was added to 9.2mL of the fixed and diluted sample. A drop of approximately 0.5mL was spread onto a slide and covered with a cover slip. The dilution was adjusted to separate mycelial particles on the slide until there were only a few in the field of view. The procedure for sample preparation for biomass and cell volume estimation is discussed later as this was a very important procedure in the estimation technique.

3.2.2 Photomicrography

Photomicrographs were taken of *Streptomyces clavuligerus* for analysis using the digitising table. For each sample (microscope slide) photographs of 100 microorganisms were taken at 100 times magnification. Usually there were approximately three or four microorganisms in each frame. The slide was moved essentially randomly though aggregated microorganisms were rejected. Photomicrographs of a graticule scale at 100 times magnification were also taken. For photomicrographs of *Penicillium chrysogenum*, taken to illustrate various points, the samples were prepared as for morphological characterisation.

3.2.3 Morphological Characterisation Using the Digitiser

Using a slide projector, the photomicrograph negative was projected onto paper. The outlines of distinguishable hyphae and the graticule scale were drawn on to the paper using a carbon pencil. Next each drawing was traced using the cursor of the digitiser. Coordinates of points covered by the cursor were determined by the digitiser. The coordinates were analysed by the linked computer, which calculated the distance of a straight line between the pairs of coordinates, to give a length measurement. Branch lengths were measured separately from the main hypha. Before measurement it was possible to enter on the digitiser a number to identify the microorganism, the main hypha and the branches. The linked computer merely gave a printout of the length results from which statistical analysis was carried out separately. The morphological parameters measured were those proposed by Van Suijdam and Metz (1981).

1. length of the main hypha
2. total hyphal length
3. number of tips (number of branches plus 2)
4. the hyphal growth unit

For all of the samples the means and their errors were calculated.

3.2.4 Growth of *Penicillium chrysogenum*

3.2.4.1 Spore Production and Storage of *Penicillium chrysogenum* P-1

Spores were produced by inoculating petri-dishes or medical flat bottles, containing a sporulation medium , with spores. The sporulation medium (Keshavarz et al., 1989) was as follows:-

Table 3. Sporulation medium (Keshavarz et al. 1989)	
Constituents	**(g/L)**
molasses	2.5
glycerol	7.5
Yeast extract	1.0
MgSO4.7H20	0.05
KH_2PO_4	0.06
NaCl	10.0
Peptone	5.0
$FeSO_4.7H_2O$	0.003
$CuSO_4.5H_2O$	0.001
Oxoid agar no.1	20.00

The pH of the medium was adjusted to 6.5 before sterilisation at 121°C. for 40min.

Once prepared the plates were inoculated immediately with spores and incubated for ten days at 26°C. The spores were then harvested by scratching the surface of the agar with a wire loop or sterile glass beads, and washing them off in a sterile solution containing:-

Sucrose 20% (w/v)

Tween80 0.1% (v/v)

dissolved in phosphate buffered saline (Oxoid)

The spore suspension was sonicated in an ultrasonic bath for 10 min to evenly disperse the spores. The suspension was counted in a heamocytometer, before being dispensed into sterile universal bottles and stored until required at -20°C. Master stocks were stored at -70°C. When required the spores were thawed at room temperature and shaken vigorously to redisperse the spores.

3.2.4.2 Shake Flask Fermentations

Shake flask fermentations were used to provide samples for blending and biomass. For the breakage of the samples in the Waring Blender, the original medium used by Savage and Vander Brook (1946) was used:-

Table 4. Savage and Vander Brook growth medium (1946)

Components	**(g/L)**
Lactose	20
Corn steep liquor solids	20
$MgSO_4$	0.125
KH_2PO_4	0.25
$NaNO_3$	2

This was prepared in tap water and the pH after sterilisation for 20min at 121°C was 4.5.

For the calibration of the biomass slide preparation methodology a defined growth medium was used (Deo and Gaucher, 1984):-

Table 5. Deo and Gaucher growth medium (1984)

Constituents	**(g/L)**
KH_2PO_4	3.0
Glucose	35
Ammonium lactate	9
Ammonium acetate	3.5
Ammonium ferric sulphate	0.1
Na_2SO_4	0.5
$MgSO_47H_2O$	0.25

The medium was sterilised for 18min at 121°C Two sterile trace mineral solutions were added post heat sterilisation to the medium at a concentration of 5mL/L of each. These were trace A containing 1g/L copper sulphate, 4g/L zinc sulphate and 4g/L manganese sulphate, and trace B which contained 10g/L of calcium chloride. The pH of the medium was 6.8.

The volume of each shakeflask was always 2L.
All of the shakeflasks used were filled with 10%(v/v) of media and were incubated at 26°C in an orbital shaker (model G25 Incubator shaker, New Brunswick Scientific Ltd., Watford, U.K.: 200rpm, 5cm throw). The shakeflasks were inoculated with spores of *Penicillium chrysogenum* P-1 or NRRL1951 as appropriate, to give an initial concentration of 10^6 spores/mL.

3.2.4.3 Fermentations Without Undissolved Solids

These fermentations contained media without any undissolved solids post sterilisation. For the provision of samples to test the morphological analysis software *Penicillium chrysogenum* P-1 was grown in batch culture in the 7L LH fermenter at 900rpm (tip speed 3.2m/s)and an air flow rate of 0.5vvm on the defined growth medium of Deo and Gaucher (1984, see above section). The temperature was controlled at 26°C and the pH at 6.8. Samples were taken after inoculation and at various times throughout the fermentation time course to 101.5h.

For biomass estimation the same basic medium was used but for this the production medium was used for *Penicillium chrysogenum* P-1. This medium contained only 25g/L of glucose and 0.38g/L of phenoxyacetic acid. These fermentations were carried out in the 14L Chemap fermenter at 800rpm (tip speed 3.35m/s) and an air flow rate of 0.5vvm. The pH was controlled at 6.8. Two fermentations were carried out, A at 26°C and B at 30°. The fermenters were inoculated with spores of *Penicillium chrysogenum* P-1 to an initial concentration of 10^6 spores/mL. Samples were taken after inoculation and were withdrawn at various intervals during the fermentation time course.

Samples from a 100L batch fermentation of *Penicillium chrysogenum* P-1 were provided for biomass estimation. The medium used was developed by Makagiansar (1991) and used sucrose and lactose as the carbon sources. A stirrer speed of 400rpm (tip speed 3.8m/s) and an air flow rate of 0.5vvm. The pH was controlled at 6.7 and the temperature at 26°C. The fermenter was inoculated with a 10% (v/v) 30h old mycelial inoculum. Samples were withdrawn at timed intervals for biomass estimation.

3.2.4.4 Fed-batch Fermentation

Samples from two fed-batch fermentations in the 7L fermenter *Penicillium chrysogenum* P-2 were provided for biomass estimation and morphological characterisation (Stone, 1990) The medium used was that of Mou and Cooney (1983), the air flow rate was 0.5vvm, pH was controlled at 6.5 and the temperature at 26°C. For the fermentation which provided samples for morphological characterisation the stirrer speed was variable and the glucose feed rate (of 4g/L) was exponential for 30h and was then constant. A vegetative inoculum was used to inoculate the fermenter which gave an initial biomass of concentration of 3 g dry cell wt/L. For the second fermentation, which provided samples for biomass estimation, the stirrer speed was constant at 1300rpm (tip speed 4.6m/s). During the fermentation the glucose feed rate was maintained at 7.08mL/h but the glucose feed concentration was increased after 26h of fermentation time from 485g/L to 638g/L. A vegetative inoculum was used, which gave an initial biomass concentration of 1 g dry cell weight/L in the fermenter.

The fermentation medium used for the fed-batch fermentation contained corn steep liquor solids. The amount of solids present in the medium post-sterilisation was approximately 2.5g/L.

3.2.4.5 Lactose/Pharmamedia Fermentation

This fermentation was used to test the performance of the biomass estimation methodology in the presence of large quantities of undissolved solids in the fermentation medium. A 10% (v/v) vegetative 54h old inoculum of *Penicillium chrysogenum* P-1 was used to inoculate the 7L fermenter containing the lactose/Pharmamedia medium. The seed medium was non-defined (Smith *et al*, 1990).

Table 6. Non-defined seed medium (Smith et al., 1990)

constituents	**(g/L)**
Glucose	30
Lactose	10
Corn steep liquor	30
Ammonium Sulphate	2
KH_2PO_4	0.5
$CaCO_3$	5

A spore inoculum of 1 x 10^6 was used. The seed culture was grown in shake flasks under the conditions as described for shake-flask fermentation. The 7L fermenter was used for the lactose/Pharmamedia medium fermentation. The stirrer speed was 950rpm (tip speed 3.35m/s) and an air flow rate of 0.5vvm was used. The amount of solids post sterilisation was 30g dry weight/L.

Table 7. The lactose/Pharmamedia production medium (Vardar and Lilly, 1982)

Constituents	**(g/L)**
Lactose	130
Pharmamedia	25
$CaCO_3$	10
$CaSO_4.2H_20$	5
Na_2SO_4	4
Ammonium Sulphate	5
Potassium phenoxyacetate	6
antifoam (NOPCO)	1

Potassium phenoxyacetic acid was prepared by neutralising aqueous phenoxyacetic acid with excess KOH and then adjusting the pH to 7.0 with concentrated HCl.

3.2.5 *Streptomyces clavuligerus*

Samples were provided for morphological analysis of *Streptomyces clavuligerus* ATCC 27064 grown by the method of Belmar Campero and Thomas (1988) in the 7L fermenter. The stirrer speed was 1300rpm (tip speed 4.6m/s) and the air flow rate 0.5vvm. A sample was taken 21h after inoculation with spores and then at approximately 24h intervals.

3.2.6 Conventional Dry Weight Assay

For dry weight determination 5mL of broth was filtered through a predried and preweighed glass microfibre filter (Whatman, grade GF/A, 4.7cm diameter) under vacuum. the filtered mycelia were then washed with 10mL of distilled water before oven drying at 105°C for 24h. Usually samples were taken in duplicate and the mean value was used as the measurement of dry cell weight.

3.2.7 Statistical Analysis

To compare samples to determine if morphological changes had occured the Students t-test, one-way analysis of variance (ANOVA) and the Duncan multiple range tests were used (Perry and Green, 1984; Chatfield, 1983). These three tests are based on the assumption that the distributions of the measured values are normal. However the tests can be used to compare the means when the distributions are not normal, because for large samples sizes (for example greater than 30) the means are distributed normally according to the Central Limit Theorem (Chatfield, 1983). On the figures showing morphological data the means for the sample and the 95% confidence limits for the mean are plotted. For means of large numbers of measured values the 95% confidence limits are ±2 multiplied by the standard deviation of the mean.

4.0 Morphological Characterisation

Filamentous microorganisms are commercially of great significance as they are involved in the manufacture of a large number of different products, notably antibiotics. The distinctive morphologies exhibited by these microorganisms present a number of problems in the development of a process. In submerged culture the mycelia can be divided into two types: the pelleted and the filamentous forms. The filamentous form is common in industrial fermentations. However, in this form, mycelial entanglement combined with a high concentration of biomass in the fermenter, can lead to high broth viscosities and pseudoplastic behaviour. These high viscosities give rise to serious mixing and mass transfer problems, for example, oxygen limitation and hence low specific growth rates and metabolite production. Morphology therefore influences mixing, mass and heat transfer, and as these factors also affect microbial physiology, they can influence morphology. Characterisation of morphology is therefore important in studies of filamentous fermentations and also in the operation and design of fermenters for these organisms.

Existing methodologies for the morphological characterisation of filamentous microorganisms were labour-intensive and the results tended to be operator dependent (1.5.2, Methods for Morphological Characterisation). Initially a semi-automated method of measurement using image analysis was developed (Adams and Thomas 1988), this was reviewed in 1.5.2, Methods for Morphological Characterisation. Even though the image analysis methodology proved to be superior to the digitising method, it still had considerable dependency upon the skill of the operator and used the image analyser as a sophisticated digitiser, making little use of the potential of image analysis for the development of rapid automated systems. Therefore there was a need to develop a method of characterisation that would provide reliable, precise and rapid measurements which could also be automated to eliminate operator intervention and standardise the results for easy comparison between workers in the field.

In order to achieve the aims stated above, methodologies and software were developed. Two pieces of software have been written

- Version 1, for the Magiscan 2A which was a developmental system and was used to establish the methodology.
- Version 2, which has been designed for a different system, the Magiscan MD, and is a simpler version but has different measurements incorporated.

4.1 Morphological Characterisation Version 1

This program was designed to be very flexible in order to allow methodologies for morphological characterisation to be developed. It is able to run fully automatically but the option of considerable manual intervention is available at various stages. The overall algorithm of this program is shown in Figure 5 and is described below.

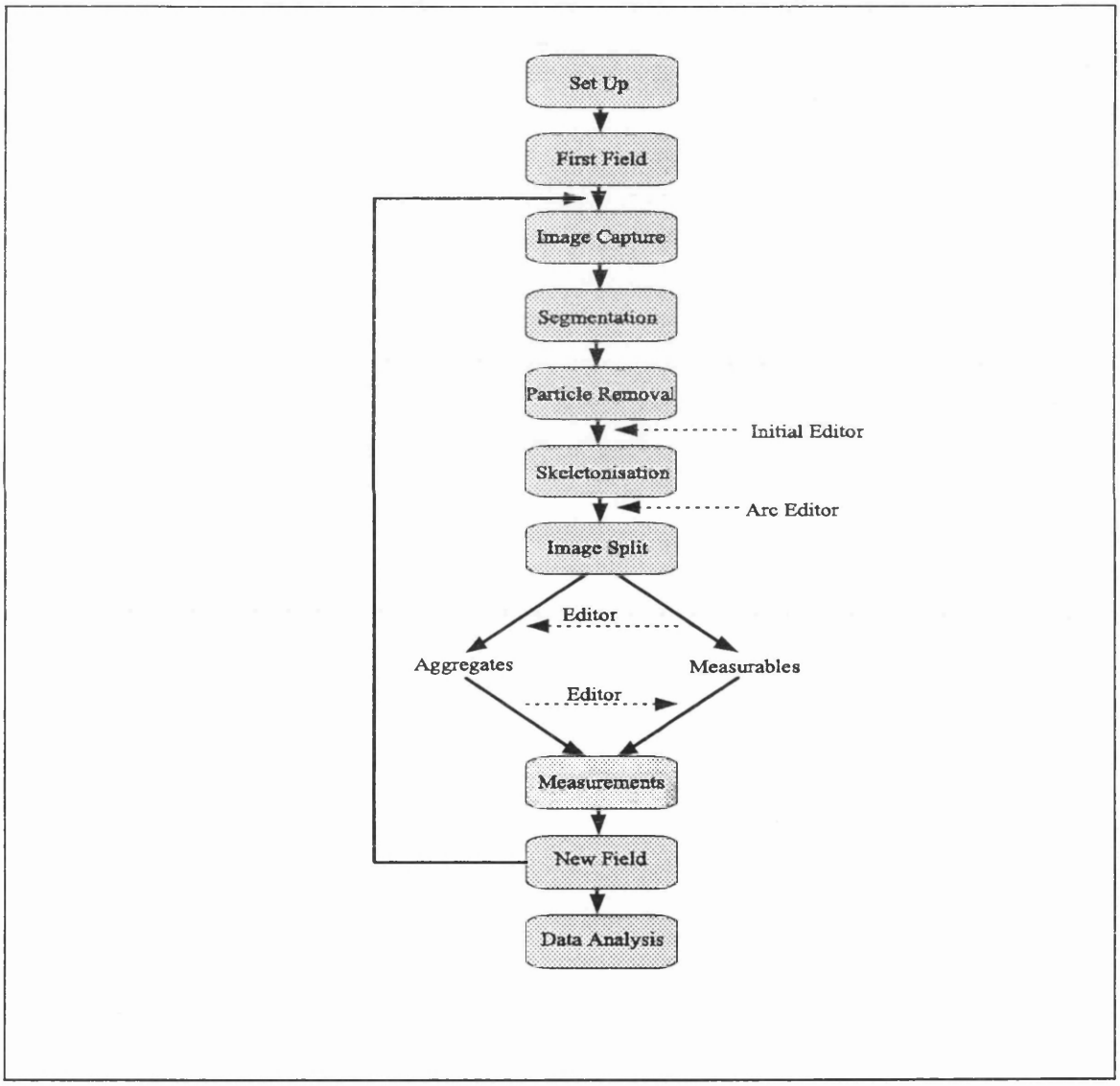

Figure 5. Algorithm of the morphological characterisation program for the M2A System

4.1.1 The Requirements of Version 1

The software is designed to run on the Joyce Loebl M2A image analysis system with the peripherals and input devices as described in 3.1.3.1, Image Analysis Systems. A general purpose image analysis developmental package was used as the framework, Bones (Joyce-Loebl).

4.1.2 Set-up

A number of parameters must be set up before each new application of the program such as for a new strain of microorganism or a major change in the undissolved solids in the medium. The first set of parameters are those involved in the creation of the "environment" in which analysis is conducted. These include calibration of the system, the size of the active measuring frame and guard region, and programming of the movement of the stage (2.0, Introduction to Image Analysis). For calibration a ruled graticule slide is placed on the microscope stage at the magnification used to characterise the microorganisms. Two points on the graticule scale, of known distance apart, are touched with a light pen so that the coordinates are recorded and a scale factor to convert pixels to microns is calculated. The microscope magnification must be selected so that the single microorganisms appear at least approximately 10mm (approximately 30 pixels) long on the image monitor (170mm by 170 mm, 512by 512pixels) and so that branches can be easily distinguished and are typically at least several millimetres (approximately 9 pixels) long. The size of clumps of microorganisms also determines the magnification as these must be of width less than one quarter of the screen in order to ensure their quantification. A measuring frame is set up with the guard region wide enough to encompass the largest clump of microorganisms present in the sample. It is possible that a sample might have very large clumps present and if the magnification were to be adjusted for the clumps the individual microorganisms may appear so small that they can not be characterised accurately. In such a case the magnification should be adjusted to characterise the single microorganisms accurately, forgoing the measurement of the percentage of clumps. The movement of the stage is also defined; this is set to cover a specific number of fields with the stage moving to abutting frames and thus giving total coverage of a region of the slide. These parameters once selected for an application are stored in a file, the "environment" file and read in at the start of each sample processing run.

A second set of parameters must also be set up before processing. These parameters include the length of noise spike removal, the presence or absence of editors and the mode of running of the program: without display for speed, with display for viewing or in demonstration mode. The noise spike removal and the use of editors is described in detail at their point of application

during processing (4.1.3, Processing). Once again when the parameters have been selected they can be stored in a file.

Once the 'environment' is set then the region of interest on the slide is selected. For this, the first field of the scan pattern is chosen and focused. Then each of the remaining corners are located automatically and focused by the user. By setting up the focal points of the extremes this enables a focus grid to be devised which can take into account any differences in depth of field across the region of interest. A suitable brightness level of the lamp for processing is determined and a typical image is captured for setting the segmentation limits. As the level of brightness directly influences the thresholding process it is essential that the light level is stable during processing, therefore the brightness is continually monitored throughout processing. If the level changes processing is halted and a warning sounds to alert the operator. Processing will only continue when the light level has been adjusted back to the correct level by the operator. A data file is created for data storage and the next phase begins.

4.1.3 Processing

Following set-up the first image is captured and thresholded to create the binary image for processing. If the display has been selected, coloured binary images are used throughout the processing phase so that an operator can instantly recognise the current stage of processing. There are three stages of processing and four of optional editing before measurement. The processing stages are the initial, arc and separation phases. The uses of the optional editors are described at their point of application.

4.1.3.1 Initial

Objects other than the microorganisms are also present in the binary image. These tend to be undissolved solids from the medium or small particles present in the liquid or even just particles of dust from the atmosphere. These particles may be distinguished from the microorganisms by their size and shape. Therefore it is necessary to carry out a series of measurements on the undesired particles and the hyphae to determine a set of criteria for the removal of undesired objects from the binary image. One parameter, the circularity proved very useful in removing the particulate material as it depends on the sphericity of the object.

$$\text{Circularity} = 4 \times \text{Pi} \times \text{area}/(\text{perimeter})^2$$

Circularity equals one for a circle and is close to zero for a long thin fibre. During the writing of the software streptomycetes (filamentous microorganisms) were determined as having a circularity value of less than 0.4 so any objects of circularity of 0.4 and greater were regarded as undesirable particles. Many clumps of organisms were also spherical so these were treated separately.

For object removal each object in the field of view is detected and first tested to see if it contains 'holes'. If the detected area, the number of pixels with a value of 1 within the boundary, is less than the area, the total number of pixels (of either value) within the boundary, of the object then the object contains at least one hole. A hole is effectively a region of background enclosed within the object. This algorithm is used throughout the software to distinguish aggregated organisms from non-aggregated organisms for loops tend to be formed when organisms are aggregated. If the object is hole free and has a circularity of 0.4 or greater then it is removed by setting its pixels to zero and effectively drawing it out of the binary image. The parameters for object removal are embedded in the software and would thus require the software to be rewritten to change them.

Upon completion of the object removal phase, the objects are sorted even further using the active measuring frame shown in Figure 6. Any objects touching the edge of the image are also removed as these span more than one image and if measured in the truncated form would bias the results. Also any object with its bottom leftmost pixel, the unique counting point, outside the measuring frame is removed from the image. An option exists for filling small holes in objects. If this option has been selected in the setup phase, it is applied to the remaining objects after object removal. Next an optional manual editor is displayed. This enables the operator to edit the binary image quite simply using a light pen and options are available for drawing, erasing, filling holes in objects, selecting and rejecting objects. The editors effectively give complete control to the operator over the objects that are to be measured. The image is then ready for the next phase of processing.

4.1.3.2 Arc

The remaining objects are skeletonised, that is the pixels medial between the edges are found, outlining skeletons for analysis. To do this a thinning routine is used. In order to obtain the skeleton the thinning routine is used cyclically to strip off one pixel widths from the object with a test for changes in the area of the objects applied at the end of each cycle. As thinning will not remove objects of one pixel width, when the area of an object does not decrease between two cycles the skeleton has been found and the cycle is halted. With the use of this thinning algorithm there is a tendency to get small side branches formed on the true axes of the object, for as soon as the routine has thinned part of the object down to one pixel it will not carry out any further processing on that part. Therefore any slight misshapenness on the side of an object will become a very small branch or noise spike, as shown in Figure 7.

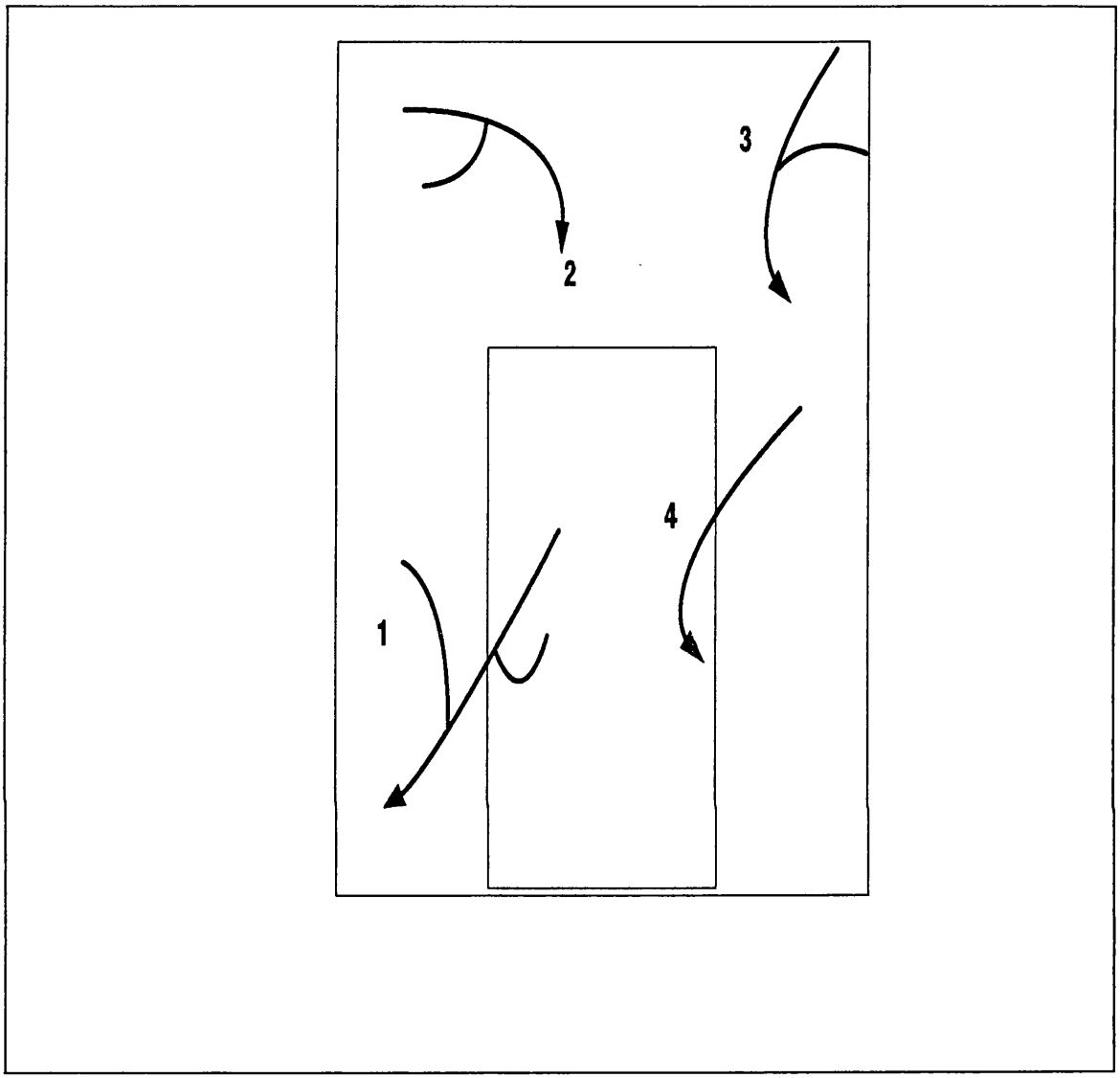

Figure 6. The active measuring frame.

1. Not measured as it is outside the frame
2. Not measured as it is outside the frame
3. Not measured as it touches the edge of the image
4. Measured

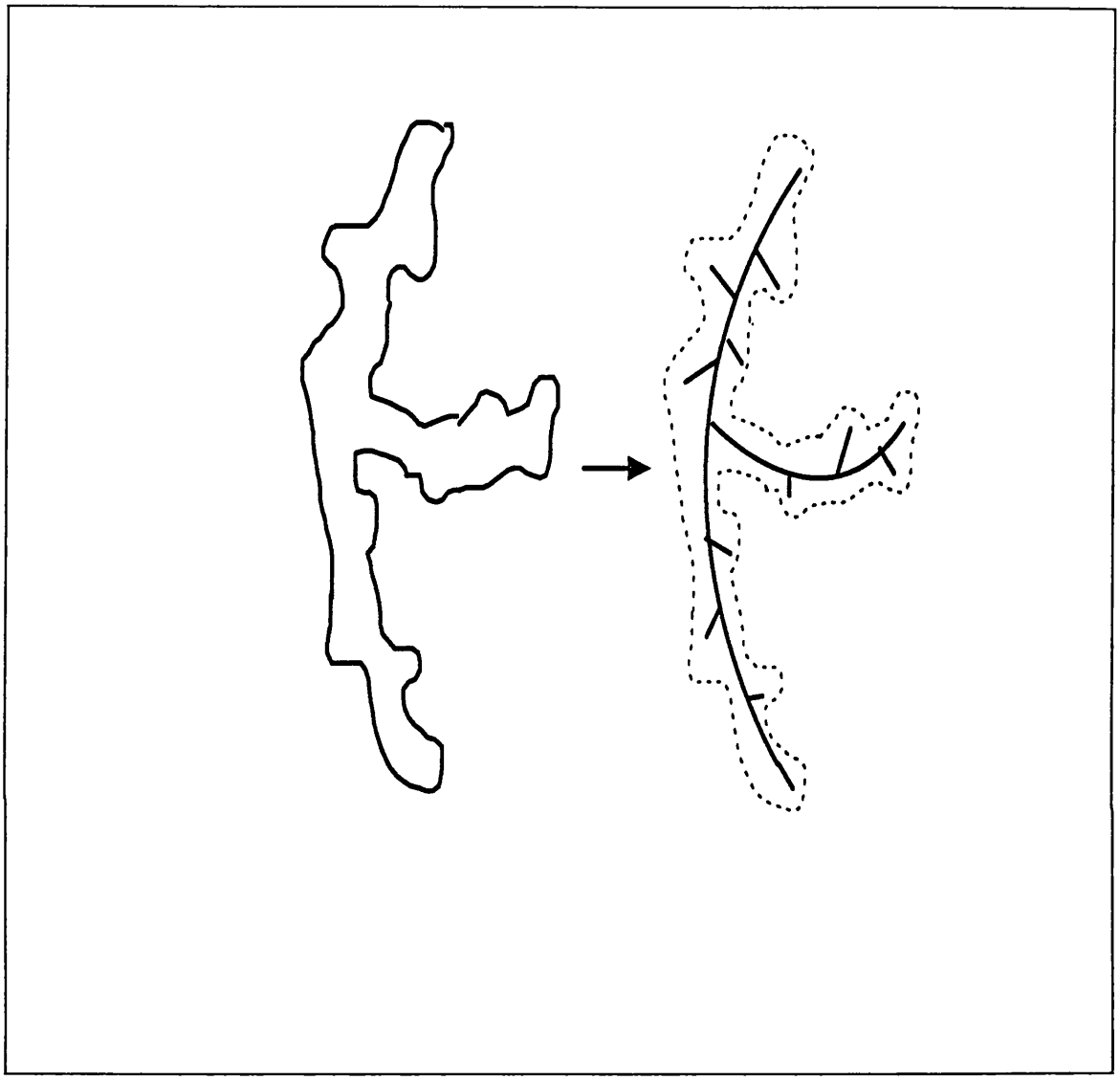

Figure 7. The generation of noise spikes by skeletonisation

Noise spikes, of lengths less than some preset number of pixels, are removed from the skeletons. The spikes are artifacts caused either by the skeletonisation process or more frequently by particulate matter touching the hyphae which is then treated as being part of the same object as far as the object detection and removal algorithm is concerned. Noise spikes are removed otherwise they would be measured as branches. A second phase of binary image cleaning is also used at this stage for the removal of very small objects. The parameters are set for the removal of objects less than 20 pixels without holes and for those with holes at less than 40 pixels. The second optional editor is also available at this stage. It might be used for editing simple crossovers of microorganisms or branches, filling small gaps in hyphae, removing artefactual branches and filling small holes.

4.1.3.3 Separation

The skeletonised objects are separated into two binary images, one containing all of the objects with holes, the clumps (Figure 8), and the other the characterisable microorganisms. During the development of the characterisation algorithms visual inspection was made of the aggregates to establish if disentanglement using software to give characterisable microorganisms was possible. However for all but the extremely simple crossovers it was not possible to trace most of the individual microorganisms in the mycelial clumps even by eye. The microorganisms are very flexible and even in simple crossovers the branches often twist around each other preventing separation. Therefore no attempt has been made to write algorithms to disassociate the aggregates into measurable mycelia. Two optional editors are available at this stage, one for each image. For the image containing clumps of organisms, the editor has all the usual options in order to enable simple changes to be made to some of the organisms such as filling holes, deleting simple crossovers or separating objects that were touching.

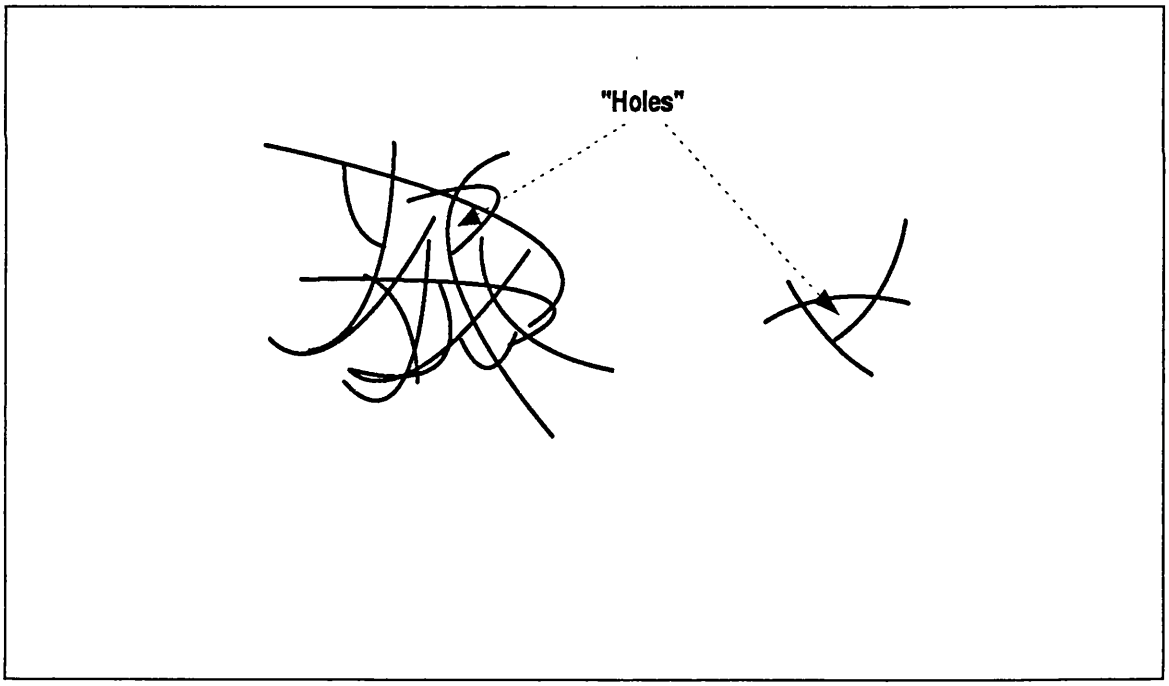

Figure 8. Objects defined as clumps due to the presence of holes

Once the operator leaves the editor, if any changes have been carried out, the objects are skeletonised again, noise spikes removed and tested for the presence of holes. If any of the objects are now without holes and therefore measurable, the system checks with the operator then proceeds to copy these objects into the characterisable binary image. The editor for the characterisable image contains very few editing options, just allowing the reclassification of

objects which are not true single microorganisms (such as two microorganisms lying across each other without forming a hole) from the characterisable image to the clumped image and the option to abort measurement of the field altogether.

4.1.4 Measurement

4.1.4.1 The Aggregates

The binary image containing the clumped or clumped microorganisms is measured first. Each clump is located, its detected area is measured and converted from pixels into microns^2 using the scale factor. The resultant value is then stored in the data file which will be described later. Once measured each object is drawn out of the image until the image is empty.

4.1.4.2 Characterisable Microorganisms

Each microorganism is detected and characterised in turn. A microorganism in processing terms can be considered as consisting of one or more arcs. An unbranched microorganism consists of one arc and branched organisms of more than one. An arc has an origin and is a series of vectors describing the directions between its constituent pixels, Figure 9.

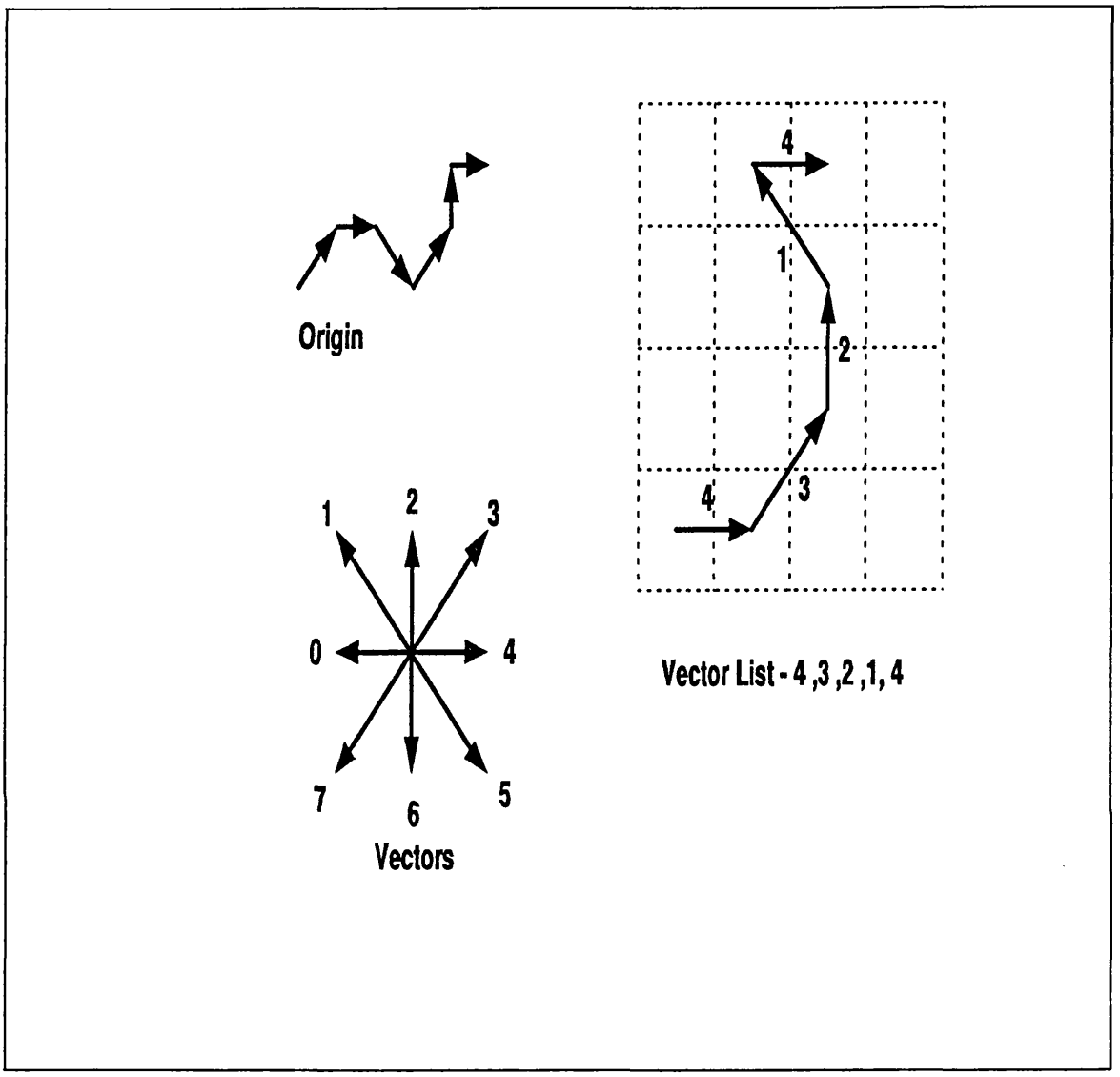

Figure 9. The structure of an arc as an origin and a series of vectors.

4.1.4.2.1 Main Hyphal Length: The main hyphal length is defined as the longest connected path through the microorganism (Figure 10).

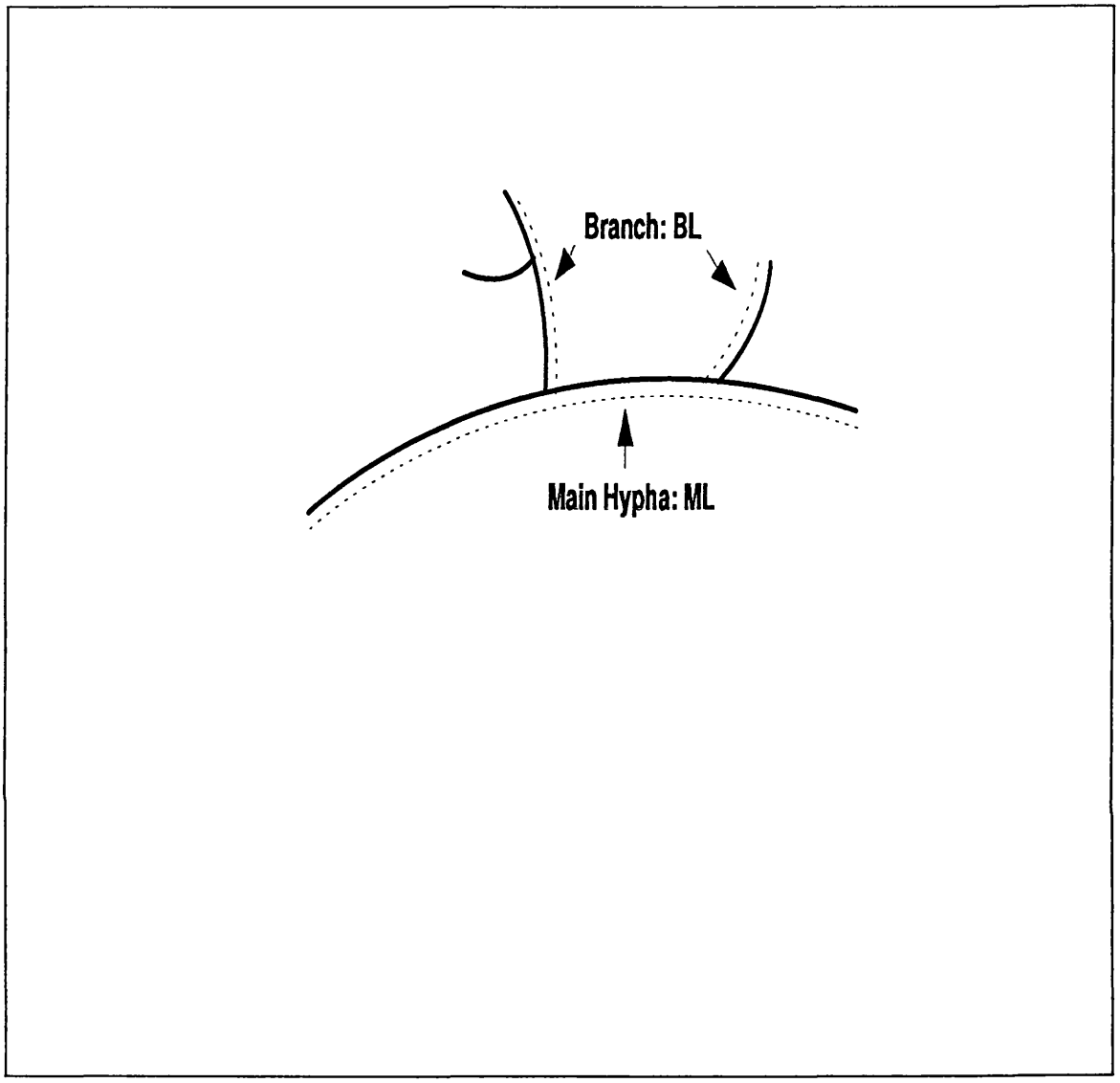

Figure 10. The main hypha and branches of a microorganism

This is found by repeatedly removing the shortest outside branches until only a single arc remains i.e. the longest path through the structure. The first step is to find the shortest branch. An arc is a group of pixels each with only two neighbours, except for the pixels at the end of the arc which can either have just one neighbour, an endpoint, or more than two, a junction, Figure 11.

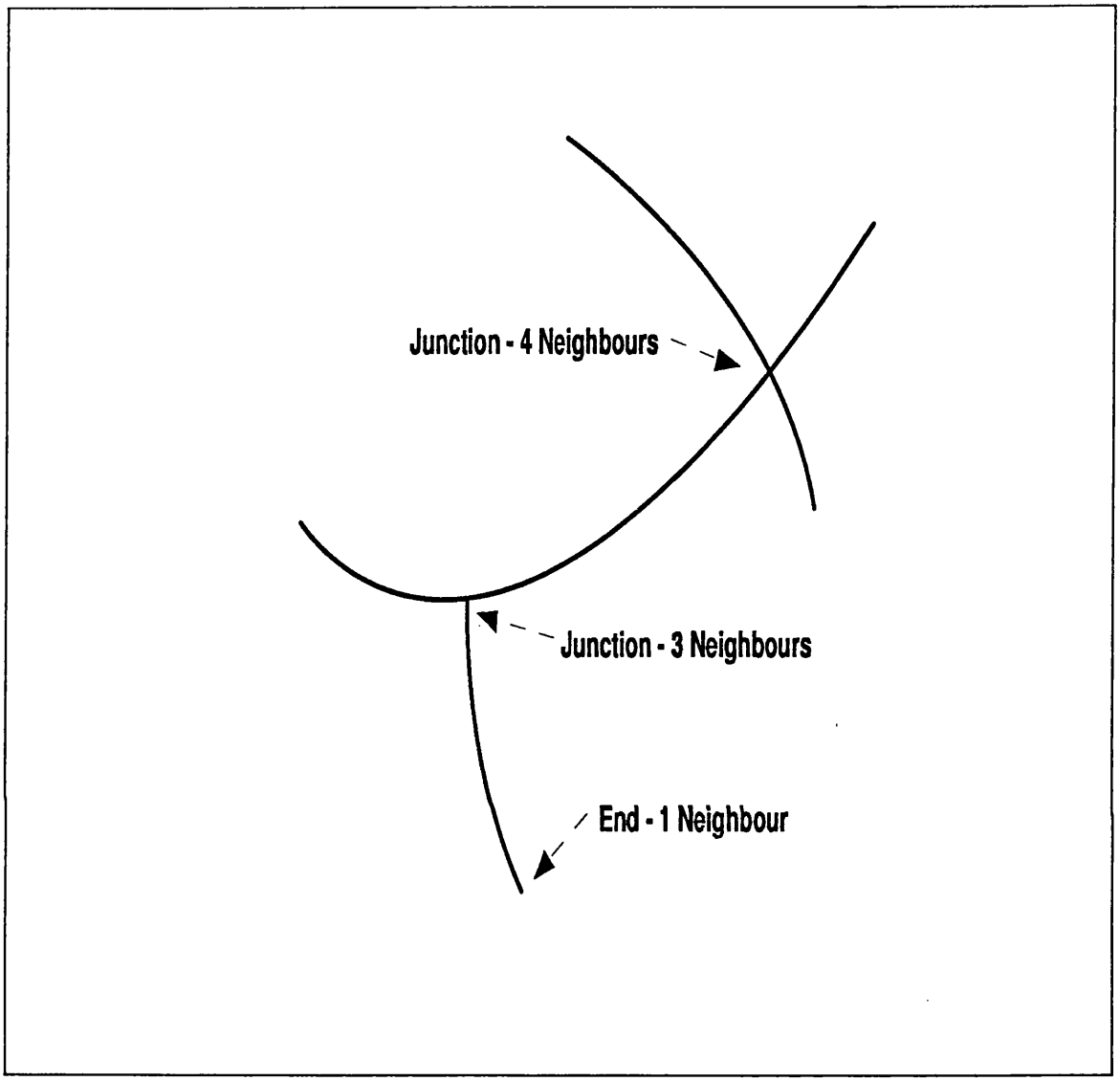

Figure 11. The possible pixel neighbourhoods in a microorganisms skeleton

It is therefore possible using these values of neighbourhood number of pixels to analyse the skeleton of a microorganism by breaking it into its constituent segments. A branch can therefore be defined as an arc with one end pixel with a neighbourhood of one and the other end a neighbourhood greater than two. Each arc in an object is located and tested in turn. If it fits the criteria for a branch then it is measured and values for its length and location are retained. Every time a branch is found to be smaller than the previous one, then the values recorded for the previous one are discarded and the new arc is recorded. This is repeated until every branch has been tested and thus the values of the shortest branch remains, the branch can then be drawn out of a second copy of the image by nibbling away its pixels until the junction is reached. The whole process is then repeated until eventually only the longest connected arc remains (Figure 12) which is then measured and drawn out of the image.

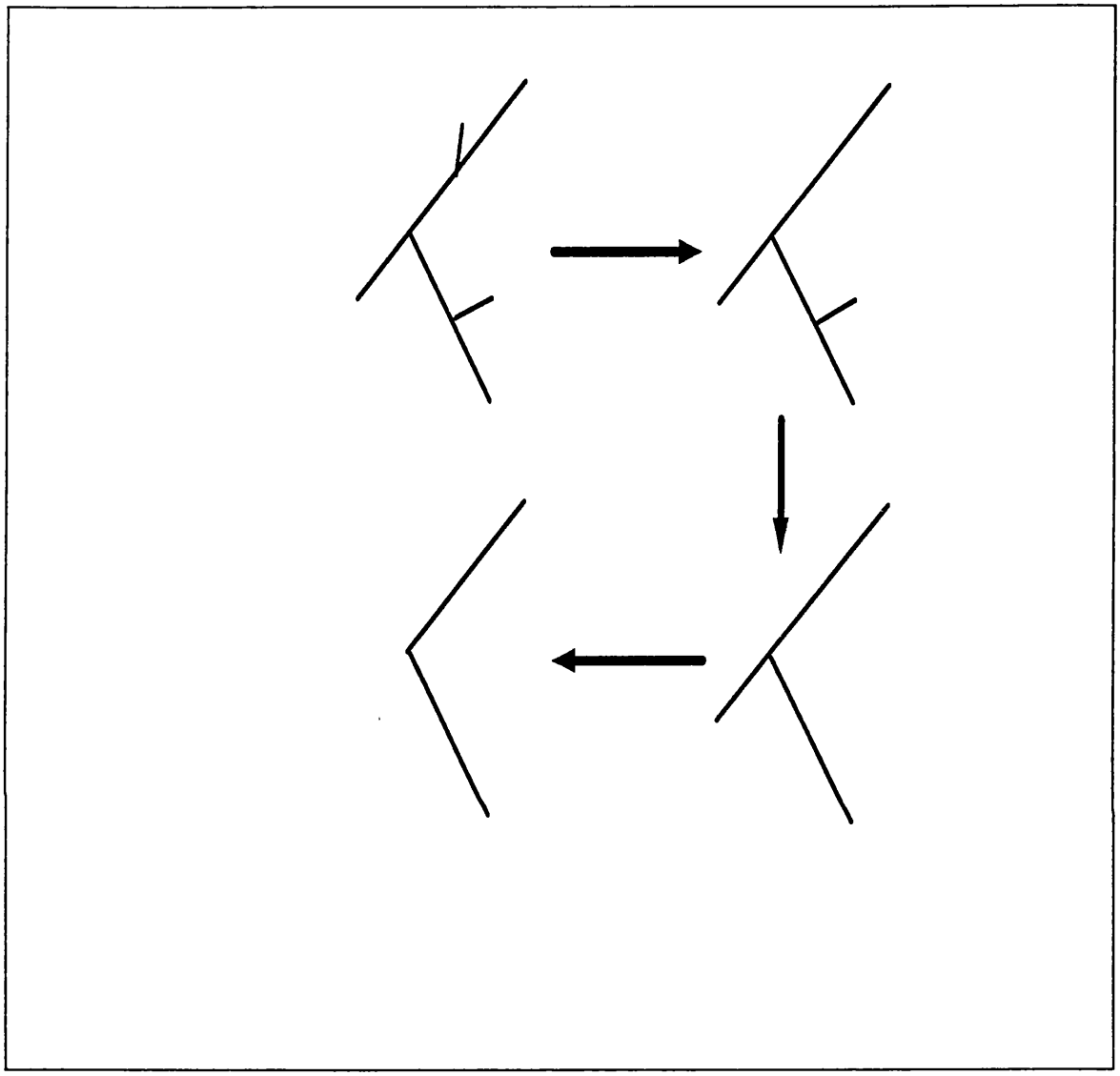

Figure 12. The steps in the determination of the main hypha

4.1.4.2.2 The Branches: Once the main hyphal length has been found the branches are analysed. Each separate branch tree is analysed in turn and its connectivity to the main hyphae is taken into account. First the longest path through the branch tree is found, measured and removed. Next the rest of the branches are measured and removed using the same recursive algorithm. This continues until all of the arcs in the object have been drawn out (Figure 13).

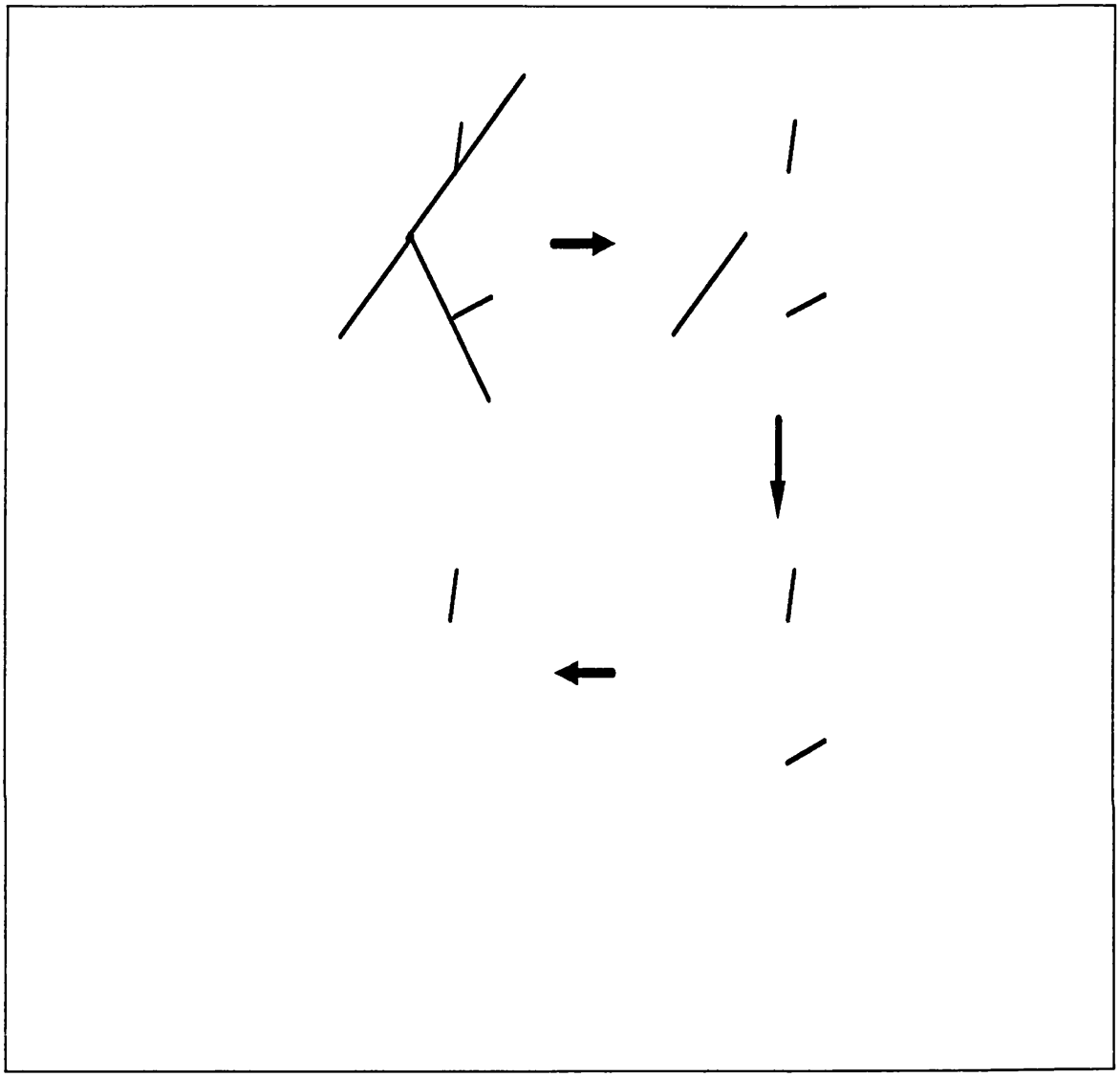

Figure 13. Sequence of operation of the hyphal characterisation algorithm

4.1.4.2.3 Analysis: A series of measurements are made on each microorganism. These were selected on the basis of the study by Van Suijdam and Metz (1981).

The number of tips is the sum of the number of branches plus two more tips to account for the main hypha,

The length of the main hypha. For length measurement the vector list of the arc is used , the number of horizontal and vertical vectors in the list are recorded and the number of diagonal vectors is recorded separately. Then for each horizontal vector the length is assigned the value of one, whereas for each diagonal vector the length is assigned the value of the square root of two. The length is calculated by summing the vector lengths and multiplying this by the calibrated scale factor for conversion into microns.

The branch length is calculated for each branch using the same algorithm as the main hyphal length.

The total hyphal length is the sum of the main hyphal length and the branch lengths for each microorganism.

The hyphal growth unit is the total hyphal length divided by the number of tips.

4.1.5 The data file

All of the measurements are recorded in a data file to enable analysis in a separate proprietary statistical package. The data are arranged in a hierarchical structure for easy access. A sample of the data file is shown in Appendix A. Each individual measurement record consists of several parts, as follows,

- a two letter identifier to describe the measurement type

Identifier	Measurement Type
ML	The main hyphal length
HL	The total hyphal length (sum of the main hyphal and branch lengths)
BL	The branch length
NT	The number of tips
TL	The total length (the pixel count)
MC	The microorganism count per field
NM	A boolean operator which distinguishes between clumps and characterisable microorganisms with the value of 1 for clumps and 0 for characterisable microorganisms
SN	The sample number to enable different samples to be recorded in the same data file

- the record level which determines location of the measurement in the hierarchy these have a value 0 to 4 giving the following structure

Record Level	Contents
0	A field summary of the total length for all objects and the sample number.
1	The field totals of the measurements for all of the measured objects.

2 The sums of the individual object measurements.

3 The main hyphal length measurement for an individual organism.

4 The individual branch measurement.

Using the sum of the clumped material and the sum of the total hyphal lengths the percentage of material present in the form of aggregates can be calculated.

4.2 Morphological Characterisation Version 2

A second version of the morphological characterisation software was written for the Magiscan MD, a later version of the Magiscan 2A hardware. The software was changed significantly for the following reasons:

1. for the different architecture of the system;
2. to incorporate the morphological characterisation software into a general purpose image analysis software package;
3. to enable calculation of hyphal diameters: and
4. to produce a more efficient version.

A flow diagram of the software is shown in Figure 14.

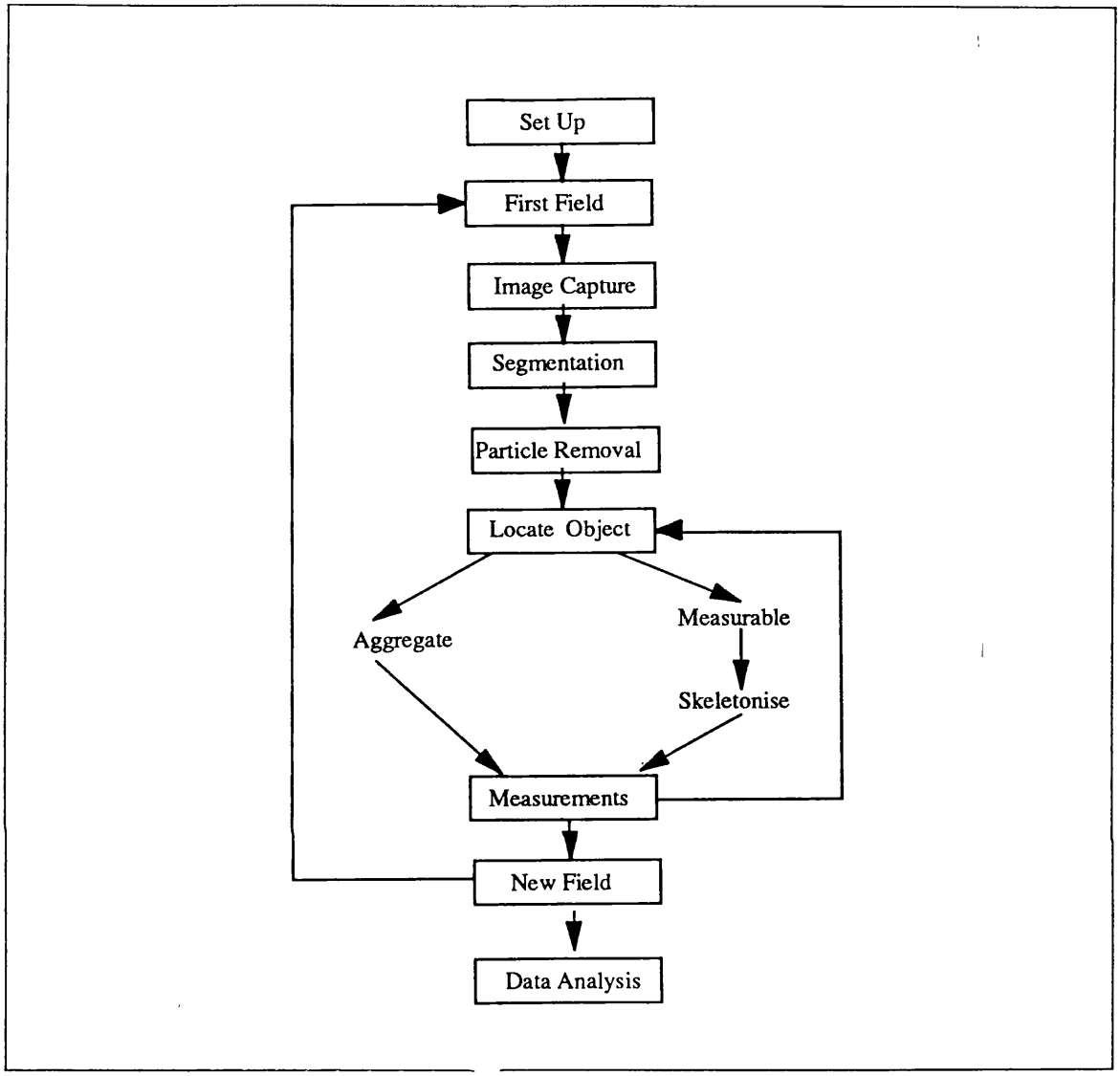

Figure 14. The algorithm for Version 2 of the morphological characterisation software

4.2.1 The Requirements of Version 2.

As mentioned above the software was written for the Magiscan MD system with the peripherals and input devices (3.1.3.1, Image Analysis Systems). A general purpose image analysis package, Genias (Joyce-Loebl), was used as part of the software.

4.2.2 Setup

As in version 1 an 'environment' is set up for each application containing the calibration, microscope scan pattern, and the measuring frame. This is then read in at the start of every processing run.

4.2.3 Processing

There are two phases of processing, the first phase is carried out using the Genias standard software package and the second phase was written to merge onto Genias.

4.2.3.1 Phase 1, binary image processing.

The Genias software package is driven by selecting options such as thresholding, and editing, from menus. The selections are then recorded in a task list which is played back automatically as many times a required. This allows a very flexible front end to the hyphal characterisation software as it is a simple matter to change parameters such as those for non-dissolved solids removal and add image processing functions, for changes in application without the requirement for programming. Once the 'environment' is read in the live grey image is captured and thresholded. Next binary image processing options are selected to delete the undesired solids. For this the desired parameters are selected, based on measurement of the particles, such as area, circularity, perimeter and so on. For example, a circularity factor of greater than 0.35 removes the debris effectively for some fermentation conditions of *Penicillium chrysogenum.* An editor with all the usual functions may also be selected from the menu for use before characterisation. Once the binary image has been cleaned of background particles and only mycelia are left the second phase of processing begins. The Genias software passes the objects one at a time into the next phase.

4.2.3.2 Phase 2, characterisation

Each object is tested to see if it is an clump or a characterisable microorganism using the same test for holes as in version 1. If the object is an clump the detected area is measured and recorded and the object is drawn out of the image and discarded. If the object is a characterisable microorganism first the detected area is measured and recorded, after which it is skeletonised and cleaned of noise spikes as in version 1. The recursive algorithm for measuring the lengths of the main hypha, branches and number of tips is applied. Once the organism has been characterised it is eliminated from the binary image and the next object is passed into the characterisation phase.

4.2.4 Measurement

All of the algorithms for measuring, except for the percentage of clumped material, are the same as the previous version. The amounts of clumped and characterisable material are measured as area and therefore this is used to calculate the percentages of each type of material. An extra measurement is also available, the hyphal diameter, this is calculated for characterisable microorganisms as the area divided by the total hyphal length.

4.2.5 The data file

All of the measurements are stored in a datafile for analysis in a statistical package. The layout of the data file is less complex than in version 1 as only the measurements that were frequently used by the operators of version 1 have been retained, therefore all of the field summaries apart from the detected area are not recorded. Once again the two letter identifiers are used to record the data points but the record levels are not required.

Identifier	Measurement type
ML	the main hyphal length
HL	the total hyphal length
BL	the branch length
NT	the number of tips
CA	the area of a clump
MA	the area of a characterisable microorganism

In addition to these measurements the Genias software also records the total area of all the measured objects in a field, the number of objects in a field and the sample number. An example of a data file is shown in Appendix B..

4.3 The Use Of Image Analysis For Morphological Measurements

To enable assessment of the performance of the software and to establish methodologies for its use, a series of experiments was performed. A filamentous prokaryote, *Streptomyces clavuligerus*, had been used in the initial application of image analysis for morphological characterisation (Adams and Thomas 1988) and therefore the experience gained through handling and measuring this microorganism had contributed significantly during the development of the software. *Streptomyces clavuligerus* was, therefore, used to compare the performance of the image analysis system against the digitiser and to establish practical methodologies for use of the image analyser.

The main aim during development of the software had been to establish a technique of measurement with a wide application, therefore measurements were conducted on two strains of *Penicillium chrysogenum*, a filamentous eukaryote, grown in different fermentation conditions.

Although the study here concerns only *Streptomyces clavuligerus* and *Penicillium chrysogenum* a number of other microorganisms have since been characterised using the methodologies described such as *Fusarium graminearium, S.griseus, S.rimosus, S.coelicolor,* and other *Penicillium chrysogenum* strains.

4.3.1 Methods

4.3.1.1 Comparison Between the Use of Digitising and Image Analysis

An isolate of *Streptomyces clavuligerus* ATCC27064 was grown in defined medium, in batch fermentation from a spore inoculum by the method of Belmar Campero and Thomas (1988). This is described in 3.2.5, *Streptomyces clavuligerus*. Samples were withdrawn from the fermenter at timed intervals and prepared for analysis using the protocol described in 3.2.1.1, *Streptomyces clavuligerus*. A comparison was made between the digitising table method, and the manual and fully automatic image analysis methods. One hundred organisms from each sample were then characterised using the digitiser method (3.2.3, Morphological Characterisation Using the Digitiser) and a manual image analysis method based on version 1 of the morphological characterisation software and employing editors at each stage. For this the microscope stage was moved manually to select fields for measurement. Once captured the image was edited using the initial editor (4.1.3.1, Initial) so that the following changes could be made: simple crossovers removed, false small branches, caused by insoluble particles in the medium touching the hypha, were erased, and also any false holes were filled. The microorganisms to be measured were then selected manually and all other objects were discarded. For both methodologies the following measurements were made for each microorganism: the total hyphal length, the main hyphal length, the branch lengths, the number of tips, the hyphal growth unit and the time taken for measurement.

As the manual method was to provide a means of direct comparison with the digitising table but used few of the capabilities of the image analysis system, fully automated image analysis was also used to measure approximately one hundred microorganisms to compare against the results for the other two methods. The fully automated system was also used in further trials to assess and develop methodologies. The fully automatic setup of version 1 of the software was used, this involved the use of the motorised stage and no intervention of manual editors. Binary images were also not displayed to speed up processing. Beside the direct comparison with the manual image analysis and the digitiser methods, a number of other experiments were conducted. One thousand organisms were characterised for each of the five samples in order to obtain distributions. The circularity parameter was set at 0.4 and the noise spike removal at 4 pixels (3.9μm). The microscope magnification was 200 times with bright field illumination.

4.3.1.2 Measurement of *Penicillium chrysogenum* broths

Penicillium chrysogenum strains P-1 and P-2 were grown as described in 3.2.4.3, Fermentations Without Undissolved Solids and 3.2.4.4, Fed-batch Fermentation respectively. Only fully automatic image analysis was used for measurement. The microscope magnification was set at 60 times. The circularity parameter of 0.4, embedded in the software, removed the background particles effectively. The parameter for removing branch artefacts was set at 3 pixels (10μm). For the time course of the P-1 fermentation approximately 200 organisms from each sample were characterised, whereas for the P-2 fermentation approximately 100 organisms
from each sample were characterised. For both time courses the time taken for characterisation, the proportion of clumps and the number of fields taken were recorded as well as the measurements taken for hyphal characterisation.

4.3.1.3 The Effect of Sample Dilution

For dilution studies, the sample of *Streptomyces clavuligerus* at 96.5h was diluted as described (3.2.1.1, *Streptomyces clavuligerus*) to 100, 400 and 1000 times and then characterised using the fully automatic image analysis method described previously (4.3.1.1, Comparison Between the Use of Digitising and Image Analysis). For *Penicillium chrysogenum* P-1, the fixed sample taken at 68h was diluted 10-, 20-,80-,160- fold (overall). A fixed *Penicillium chrysogenum* P-2 sample taken at 116h was diluted 20-,40-, 80-,160,320-,640-,1280-fold (overall). In both cases serial dilution in the fixative (3.2.1.2, *Penicillium chrysogenum*) was used.

About 100 micro-organisms were characterised at each dilution. The time taken for measurement, the proportion of material in clumps and the number of fields analysed were recorded for each case, as well as the morphological characteristics.

4.3.1.4 The Use of Noise Spike Removal

In order to study the effect of the noise spike removal parameters on the results generated by fully-automatic processing, the samples from the *Streptomyces clavuligerus* time course were run with two different settings of the parameters. One run was conducted with the parameter set to the typical size of skeletonised debris (4 pixels; 3.9μm). For the second run the parameter was set to the size of a noise spike generated during the skeletonisation process (3 pixels; 2.9μm).

4.3.1.5 The Performance of Version 2 of the Software

To assess the performance of version 2 of the software, samples from a *Penicillium chrysogenum* fermentation were measured using both image analysis systems (Magiscan MD and M2A) so that the results and time taken could be compared. The fermentation was of *Penicillium chrysogenum* P-1 grown in a defined medium (Deo and Gaucher 1984) under the same conditions as the fermentation used for the trials of version 1 (3.2.4.3, Fermentations Without Undissolved Solids). Each sample was diluted 20 fold in fixative, two slides were made from each sample which were then processed simultaneously on both image analysis systems. One hundred fields were analysed for each slide. The time taken for measurement and the morphological parameter measurements were recorded.

4.3.2 Results

4.3.2.1 Comparison Between the Methods of Characterisation

The microorganisms, streptomycetes, at 21h were typically highly branched and of the largest mean hyphal lengths for the fermentation. Fragmentation then occurred resulting in fewer branches and shorter lengths, as found in the sample at 45h. Some regrowth was then observed for the later samples at 70, 94 and 119h, though the microorganisms were still relatively short and unbranched. Typical morphologies for the 21h and 119h are shown in Figure 15.

Figure 16, Figure 17 and Figure 18 show the comparisons between the three measurement methods for the mean total hyphal length, the mean main hyphal length and the mean number of tips for each of the samples. The nature of the error shown on the mean value is described in 3.2.7, Statistical Analysis. Using the distribution free Wilcoxon-Mann-Whitney test, the differences between the three methods were tested.

Figure 15. Typical morphologies of *Streptomyces clavuligerus* samples

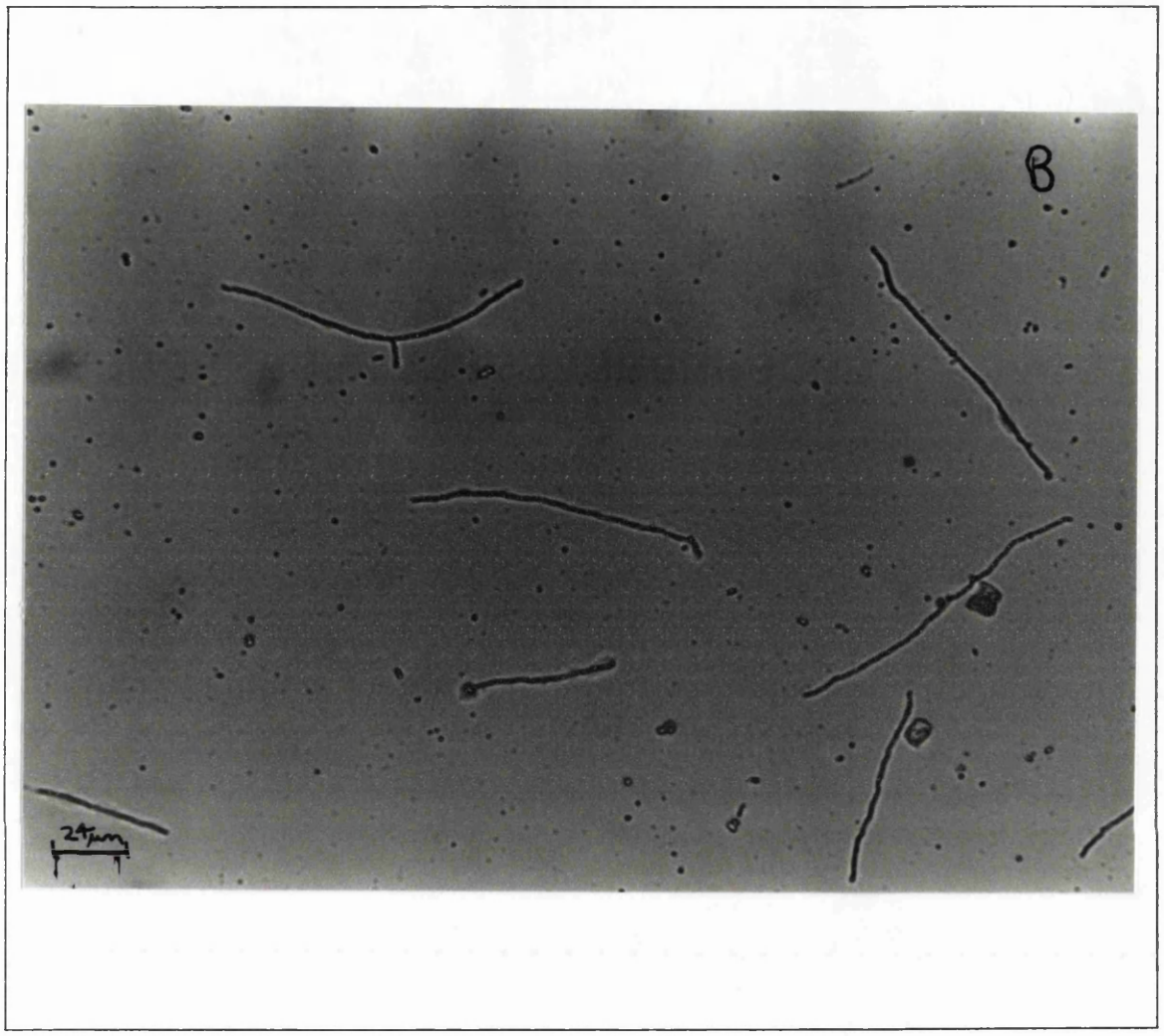

Figure 15 (Part 2 of 2). Typical morphologies of *Streptomyces clavuligerus* samples. Photograph A is from sample 1 (21h) and shows a typical clump. Photograph B is from sample 5 (119h) and shows relatively unbranched microorganisms (1cm=24µm).

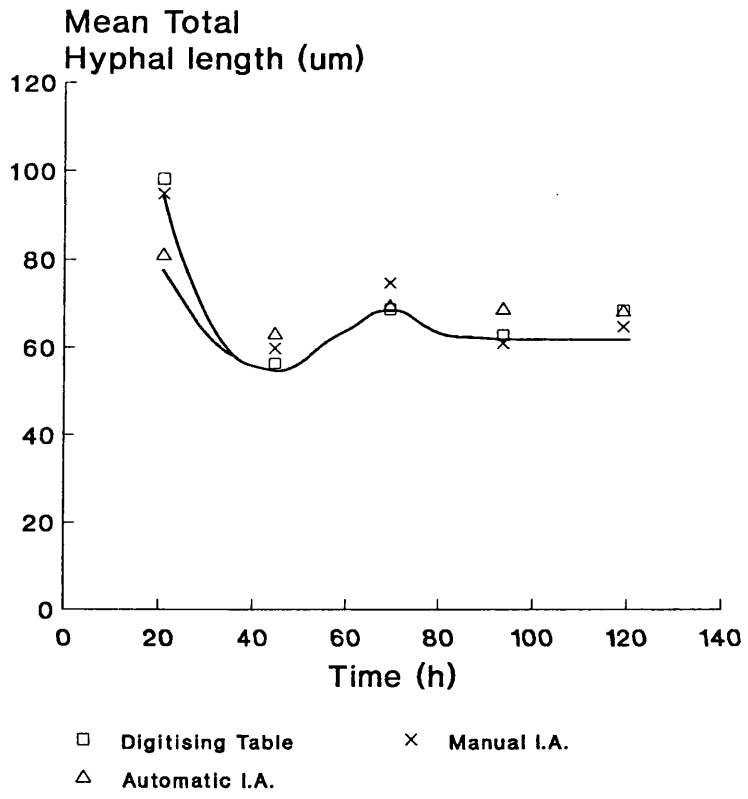

Figure 16. Time course of mean total hyphal length of *Streptomyces clavuligerus*. The mean total hyphal length measured by the three methods is shown.

Figure 17. Time course of mean main hyphal length of *Streptomyces clavuligerus*. The mean main hyphal length measured by the three methods is shown

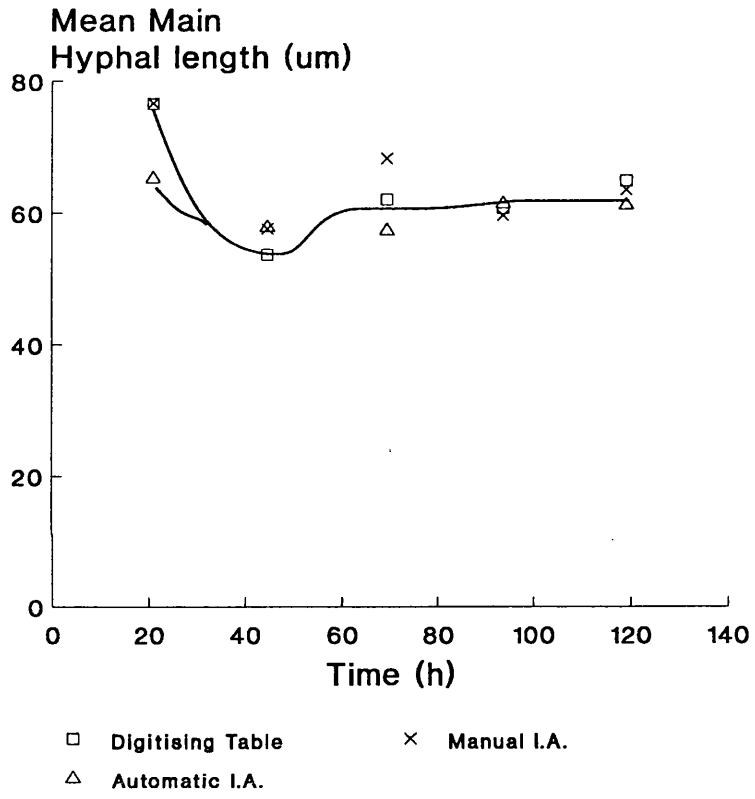

Figure 18. Time course of mean number of tips of *Streptomyces clavuligerus*. The mean number of tips measured by the three methods is shown

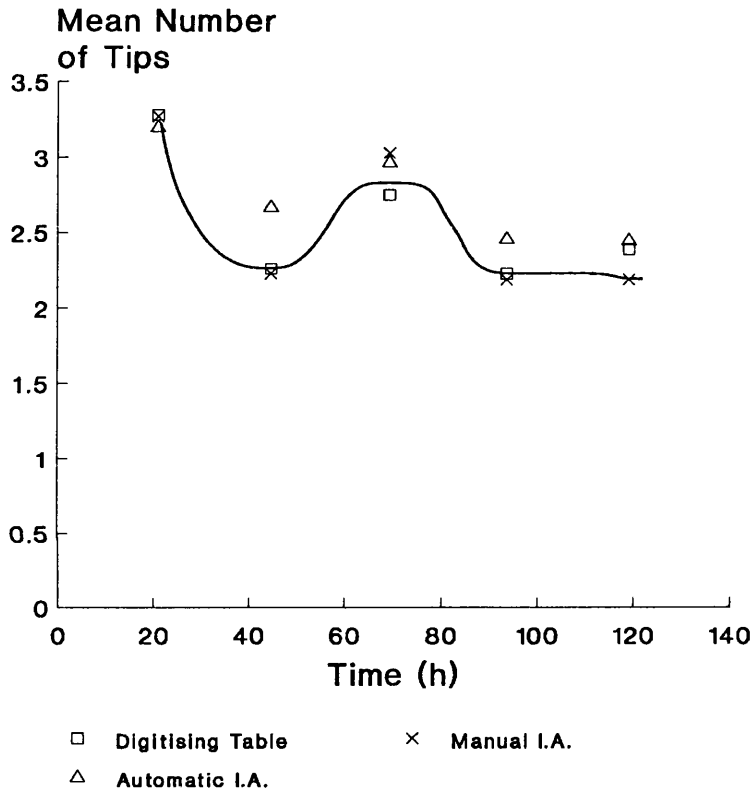

For the sample at 21h, at the 95% confidence level there were significant differences between the fully-automatic and the other two methodologies for the mean total hyphal length and the mean main hyphal length but not for the mean number of tips. For the samples from 45h there were no significant differences between the methodologies. Table 8 shows the times required for measurement of 100 microorganisms for each sample, using the 3 methodologies. The time taken for film processing was excluded from the timings of the method using the digitising table.

Table 8. Times taken to measure 100 microorganisms of *Streptomyces clavuligerus*. Each of samples 1 to 5 was measured using the different methods (the timings for the digitising method do not include film development and processing). Time taken (min)

Sample number	Fermentation time (h)	Digitising Table	Manual Image Analysis	Fully Auto-matic Image Analysis
1	21	115	45	53
2	45	80	25	20
3	70	80	17	18
4	94	70	17	17
5	119	83	21	12

Besides the morphological parameters the fully automatic method also gave an estimate of the quantity of material in the clumped or "clumped" form in each sample. These are shown in Table 9 and varied between 59 and 36%. The average time for measuring each microorganism was 0.24min. Table 10 shows the time taken to measure 1000 microorganisms for each of the samples. Figure 19 shows the distributions of total hyphal length, main hyphal length and the number of tips for the sample at 119h. For comparison Figure 20 shows the distributions for the length of the main hypha for all five samples. Using a Chi-squared test the distributions for all three measured morphological parameters were shown to be log normal with better than 90% confidence.

Table 9. Percentage of material in clumps of *Streptomyces clavuligerus* measured by fully automatic image analysis

Sample number	% of clumps
1	59
2	40
3	57
4	38
5	36

Table 10. Times taken to measure 100 and 1000 microorganisms of *Streptomyces clavuligerus*. Each of samples 1 to 5 was measured using fully automatic image analysis

Sample number	Time taken for 1000 (min)	Time taken for 100 (min)
1	230	53
2	170	20
3	115	18
4	130	17
5	90	12

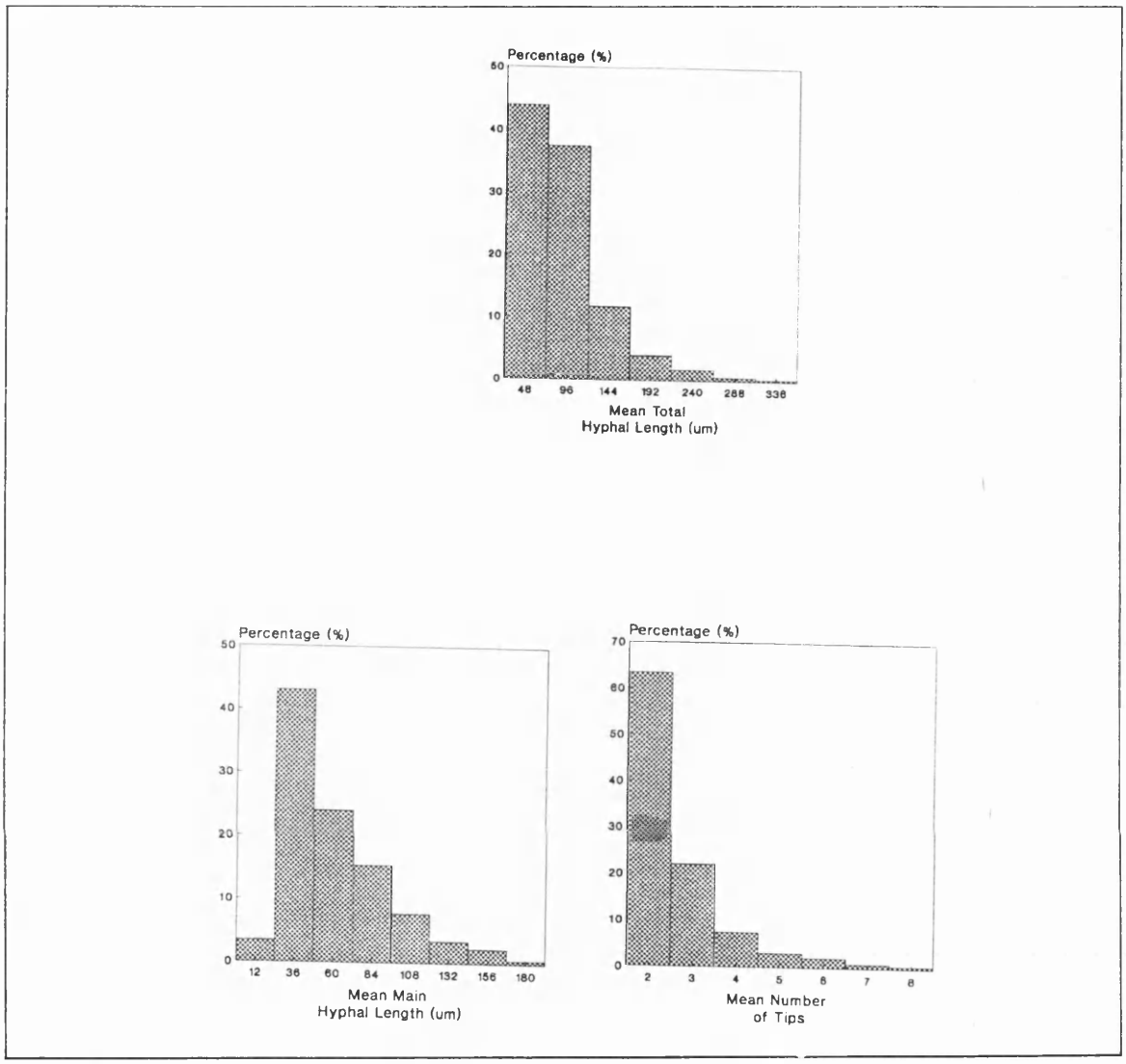

Figure 19. Distributions of the morphological parameters of *Streptomyces clavuligerus*. The distributions shown are for sample 5 (119h) and were measured using the fully automatic image analysis method.

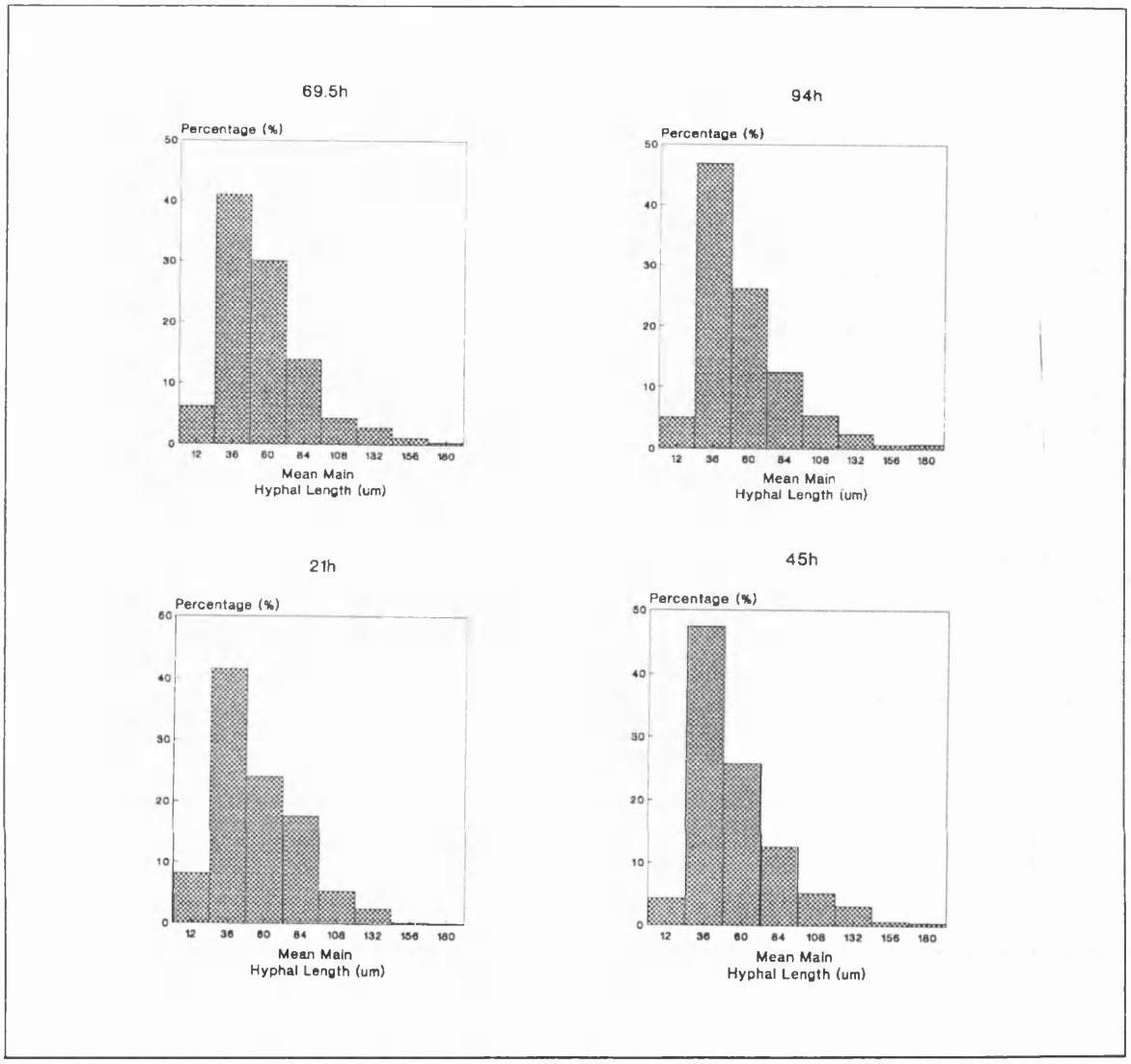

Figure 20. Distributions of main hyphal length for *Streptomyces clavuligerus*. The distributions shown are for samples 1 to 4 and were measured using fully automatic image analysis.

Figure 21 is a comparison between the results for two different settings of the noise spike parameters. This parameter determines the length of the noise spikes removed during fully-automatic image analysis. The lower curve on Figure 21 shows the parameter set to a typical debris size (4 pixels ; 3.9µm) and the second curve was set to the size of the noise spike generated during the skeletonisation process (3 pixels ; 2.9µm).

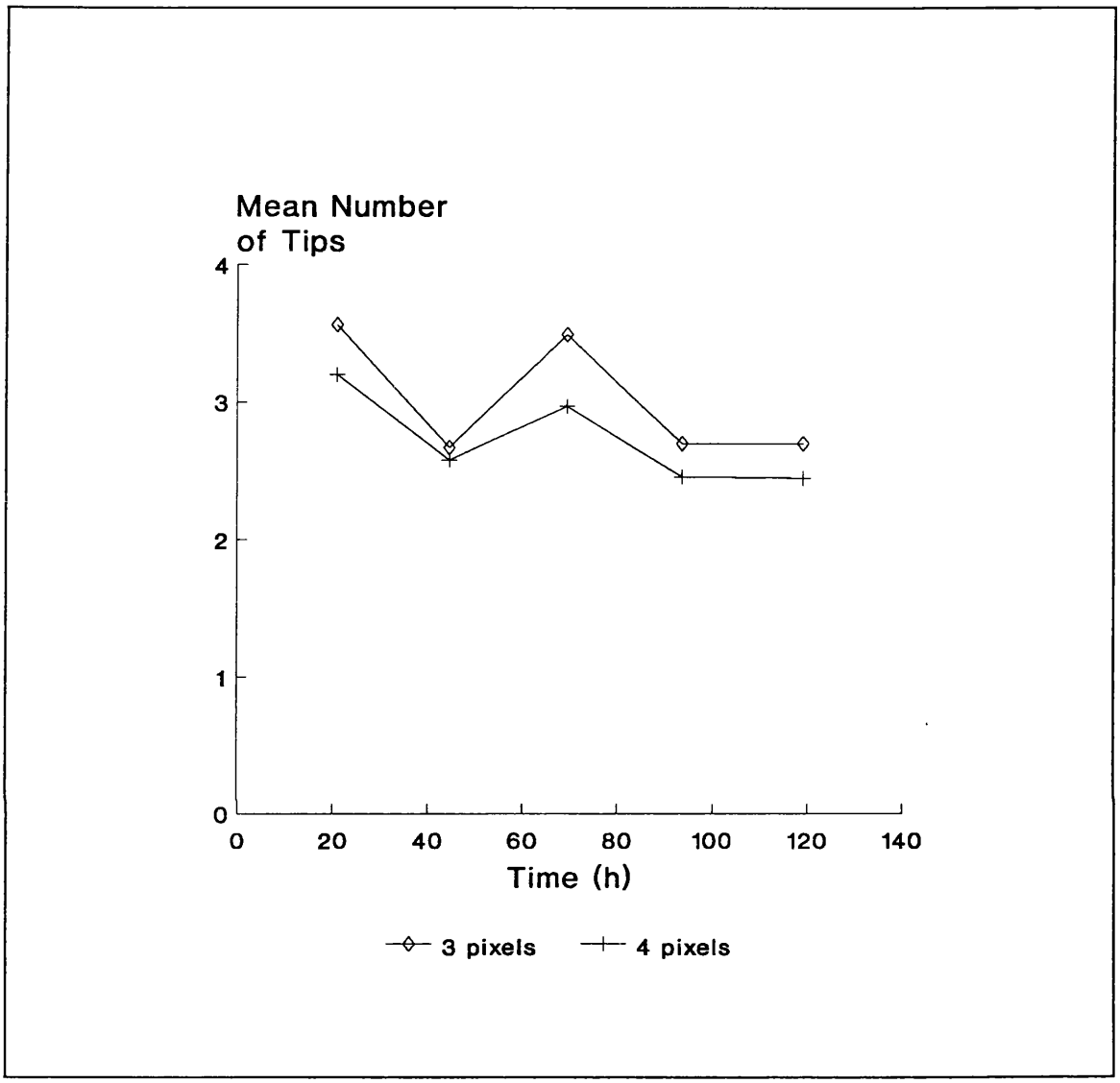

Figure 21. Comparison of measurements of the number of tips by fully automatic image analysis. The measurements were made on the samples from the *Streptomyces clavuligerus* fermentation with noise spike parameter settings of 3 pixels (2.9µm) and 4 pixels (3.9µm).

4.3.2.2 Characterisation of *Penicillium chrysogenum* Broths

Figure 22 shows a typical time course of mean total hyphal length and Figure 23 of mean main hyphal length for the *Penicillium chrysogenum* P-1 fermentation. Initially the lengths of the microorganisms increased up to 25.5h and then there was rapid fragmentation to 30h. This was followed by an apparent steady state for morphology. This was also seen in the profile for the mean number of tips (Figure 24). After 50h growth ceased as shown by the time course of the dry cell weight (Figure 23) and the cells once again underwent fragmentation but not as vigorously as in the

initial fragmentation phase. At the end of the fermentation an increase in length and the number of tips occurred, (Figure 22,Figure 23,and Figure 24) probably due to some regrowth of the remaining microorganisms as the contents of lysed cells are scavenged.

Figure 22 also shows the percentage of material in clumps. This was very high for most of the duration of the fermentation despite fragmentation of the mycelia. Because of the clumped material the time taken for measurement of each microorganism was longer than that for *Streptomyces clavuligerus* at 56h for 12 samples of approximately 200 microorganisms which is equivalent to 1.4min per microorganism.

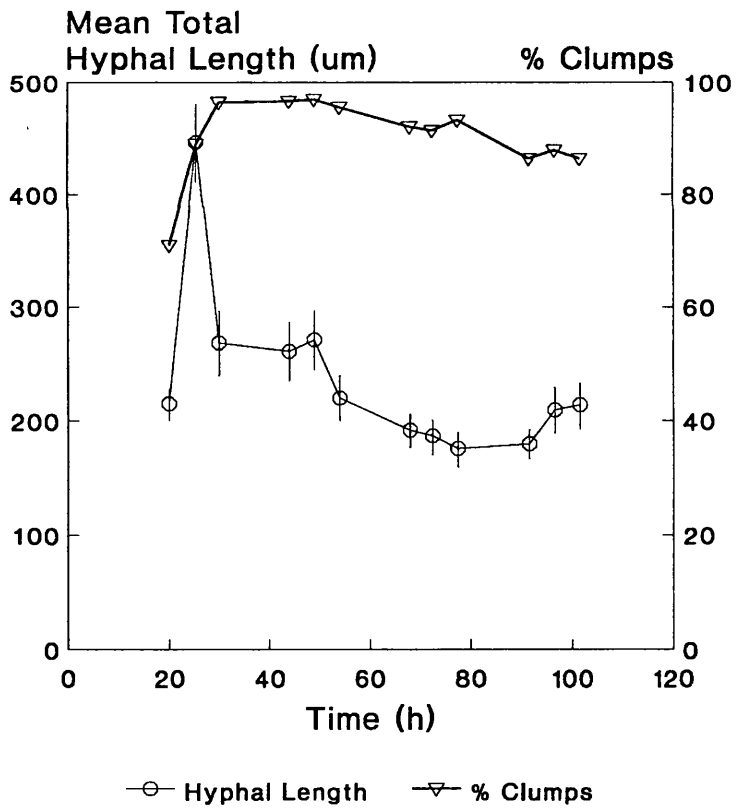

Figure 22. Time course of mean total hyphal length and clumps for *Penicillium chrysogenum* P-1. The samples were from a batch fermentation and were measured using fully automatic image analysis.

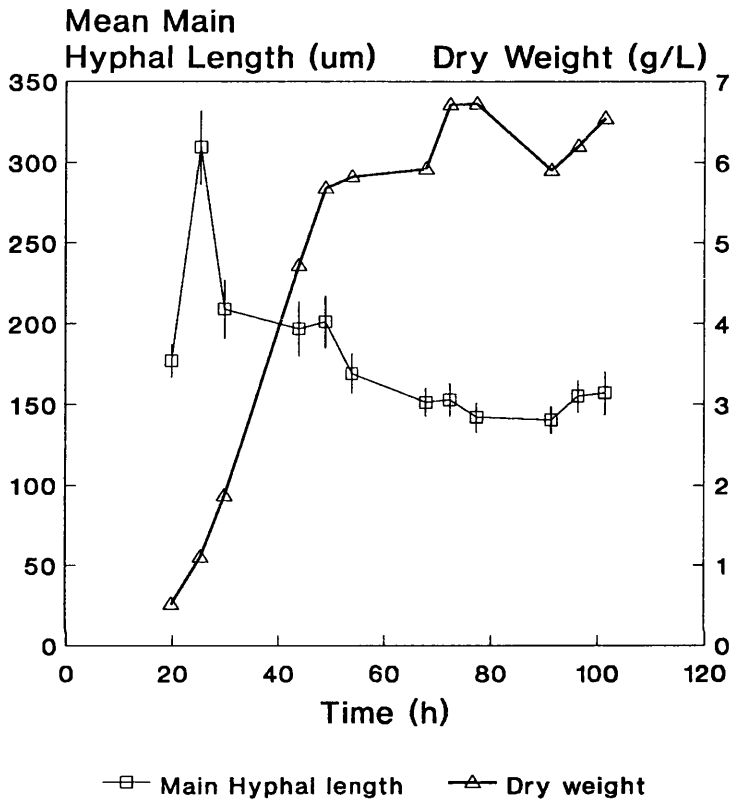

Figure 23. Time course of mean main hyphal length and biomass for *Penicillium chrysogenum* P-1. The samples were from a batch fermentation and were measured using fully automatic image analysis.

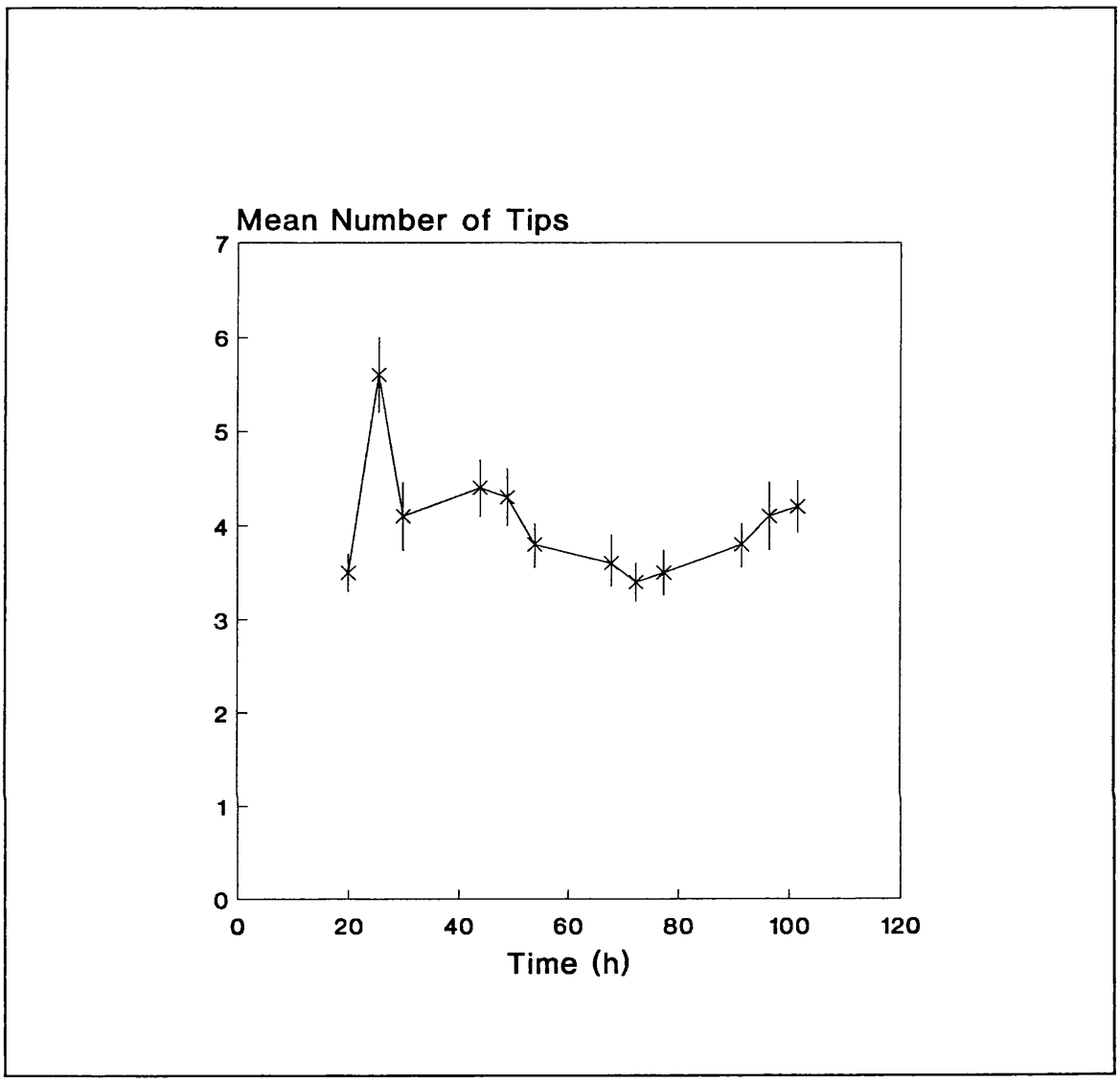

Figure 24. Time course of mean number of tips for *Penicillium chrysogenum* P-1. The samples were from a batch fermentation and were measured using fully automatic image analysis.

The time course for a *Penicillium chrysogenum* P-2 fed-batch culture is shown in Figure 25, Figure 26 and Figure 27. Initially there was a transient phase where the morphology did not show a consistent trend. Typical mycelia are shown in Figure 28. Then after 90h the lengths of the microorganisms steadily declined as growth slowed. Once again the percentage of mycelia in the form of clumps was high, Figure 25, and only a slight decrease was seen during the fermentation. The transient phase was probably due to the adaptation of the morphology of the microorganisms in the inoculum from the relatively mild shear conditions in shake flasks to a more appropriate morphology for the fermenter. The time taken for measurement for 8 samples of approximately 100 was nearly 10h which is equivalent to 0.75min per microorganism.

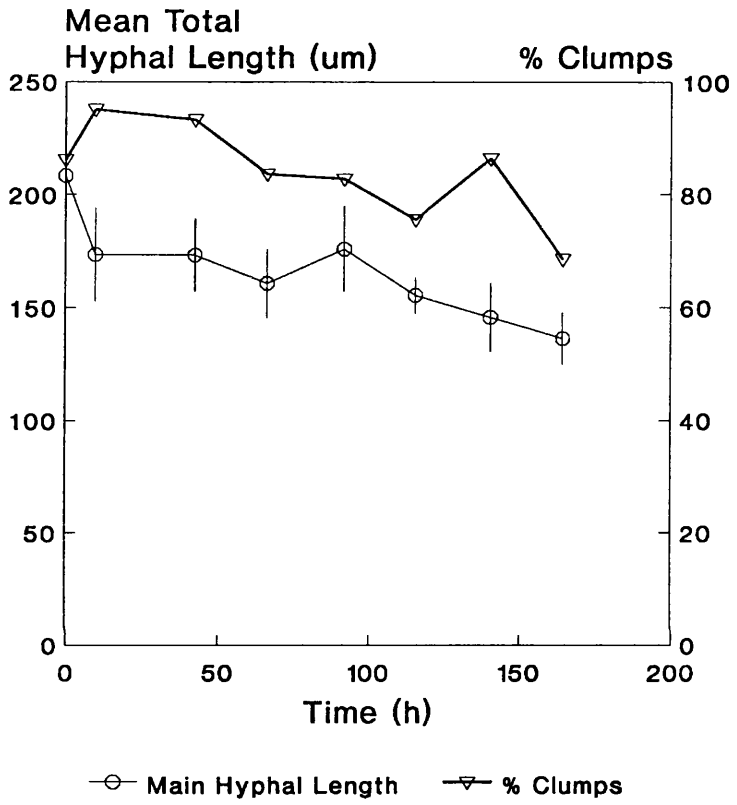

Figure 25. Time course of mean total hyphal length and clumps for *Penicillium chrysogenum* P-2. The samples were from a fed-batch fermentation and were measured using fully automatic image analysis.

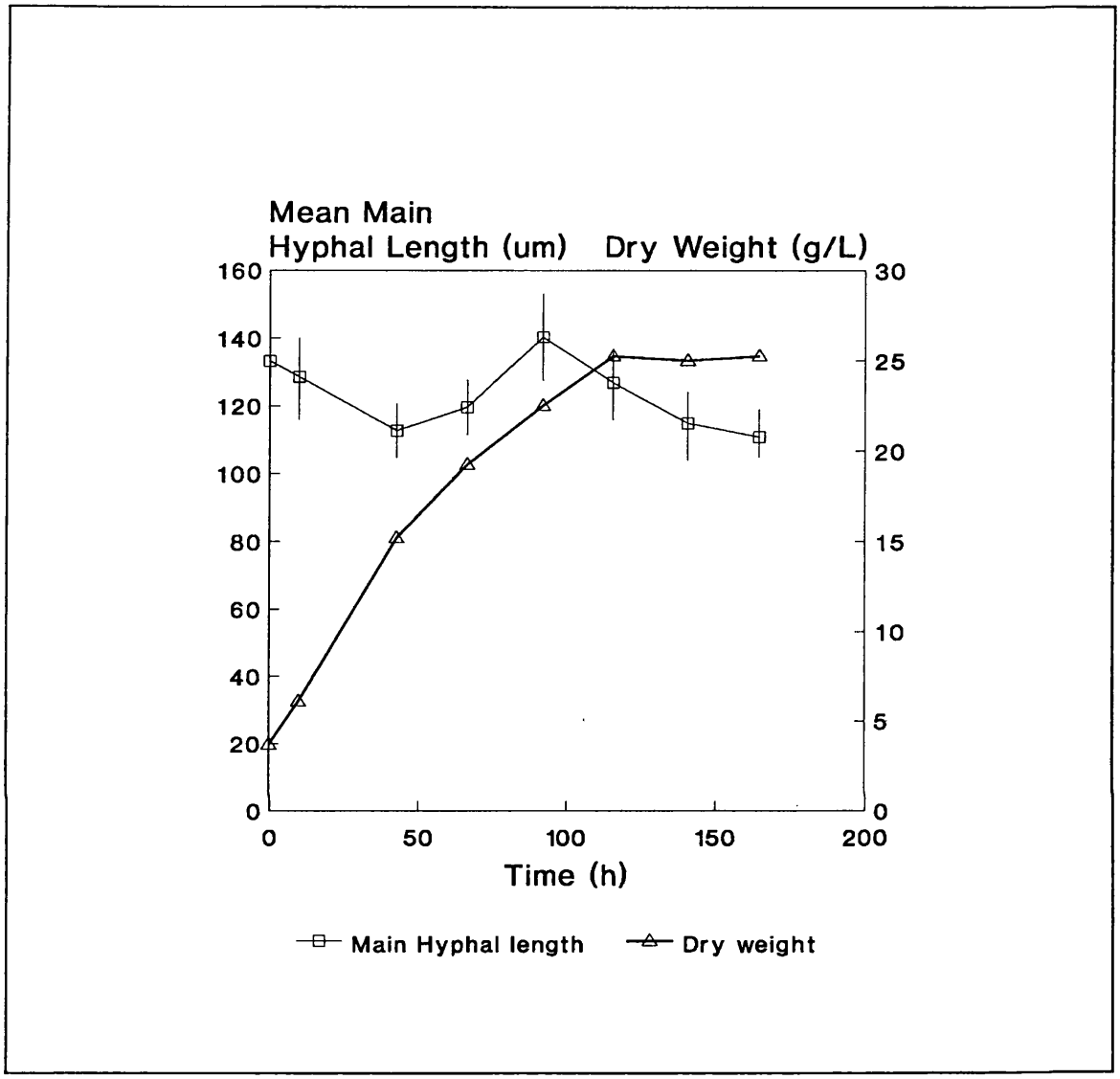

Figure 26. Time course of mean main hyphal length and biomass for *Penicillium chrysogenum* P-2. The samples were from a fed-batch fermentation and were measured using fully automatic image analysis.

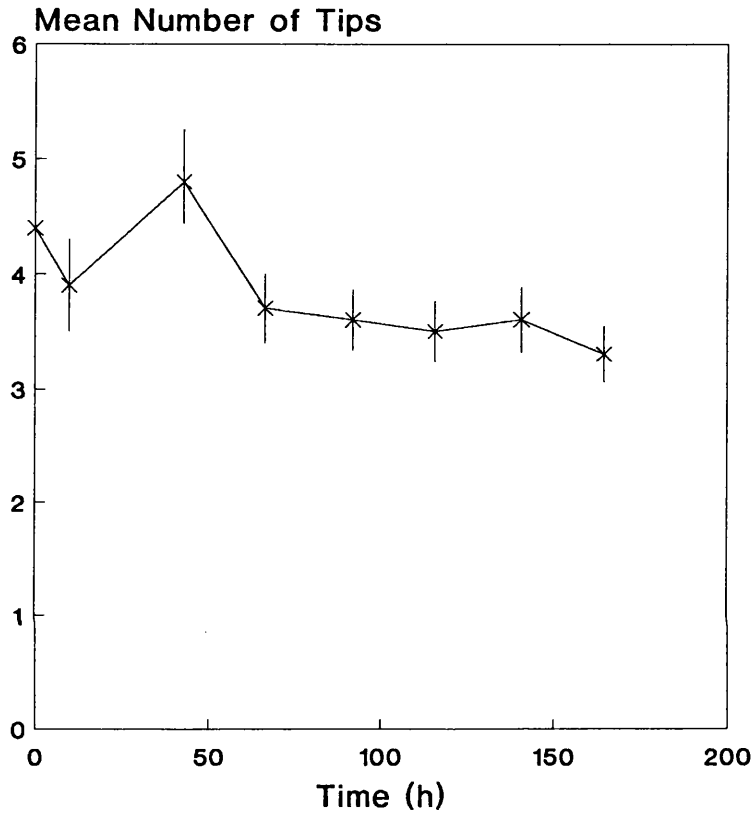

Figure 27. Time course of mean number of tips for *Penicillium chrysogenum* P-2. The samples were from a fed-batch fermentation and were measured using fully automatic image analysis.

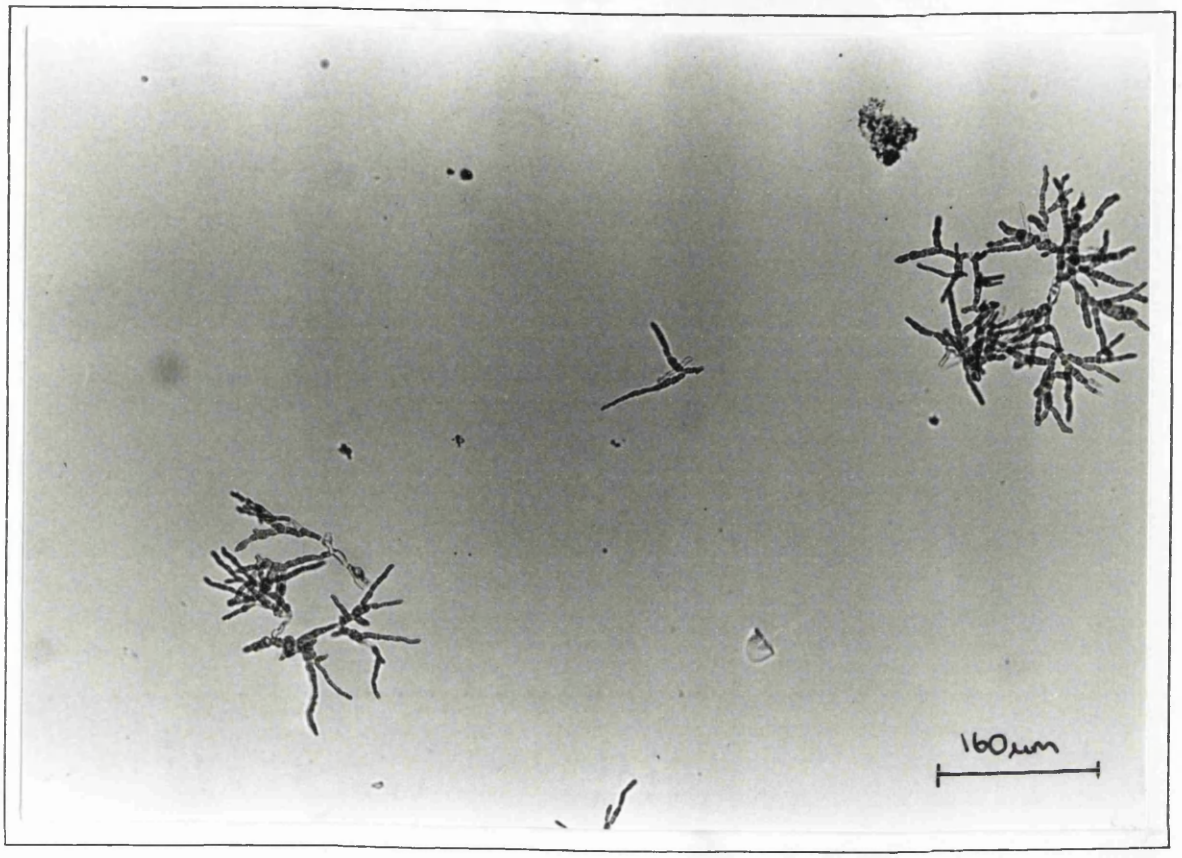

Figure 28. Typical morphologies of *Penicillium chrysogenum* P-2 (1cm=80µm).

4.3.2.3 The Effect of Dilution

Table 11, Table 12 and Table 13 show the effect of dilution on the measurement of morphological parameters on one sample for each fermentation. Except for the low dilutions where there was a high density of cells on the slides, the morphological parameters appeared to be fairly insensitive to the extent of dilution. The amount of clumped material was dilution dependent. Also shown are the number of fields analysed, the mean number of microorganisms per field and the mean time to measure one microorganism.

Table 11. Effect of dilution on various morphological and measurement parameters. Sample 3 from the *Streptomyces clavuligerus* fermentation (70h, 4g/L) was measured using fully automatic image analysis

Dilution (fold)	**100**	**400**	**1000**
Number of microorganisms measured	103	108	105
Mean main hyphal length (µm)	62.7 ±6.8	57.4 ±6.6	62.7 ±6.9
Mean total hyphal length (µm)	81 ±12	69.4 ±10	77.1 ±12
Mean number of tips	4.1 ±0.4	3.5 ±0.4	3.7 ±0.4
% clumps	69	57	31
Total measurement time (min)	17	18	7
Number of fields analysed	16	17	10
Mean number of microorganisms per field	6.4	6.4	10.5
Mean time to measure one microorganism (min)	0.17	0.17	0.07

Table 12. Effect of dilution on various morphological and measurement parameters of *Penicillium chrysogenum* P-1. The dilutions of the sample at 68h (5.9g/L) from the batch fermentation were measured using fully automatic image analysis

Dilution (fold)	**10**	**20**	**80**	**160**
Number of microorganisms measured	100	102	102	102
Mean main hyphal length (μm)	142.9 ±13	151.5 ±8.5	159.8 ±12.8	163.6 ±18.3
Mean total hyphal length (μm)	173 ±18.2	191.7 ±14.7	200.2 ±18.8	202.8 ±25.5
Mean number of tips	3.4 ±0.3	3.6 ±0.5	3.8 ±0.4	3.6 ±0.3
% clumps	76	92	87	70
Total measurement time (min)	25	30	35	75
Number of fields analysed	32	33	35	102
Mean time to measure one microorganism (min)	0.25	0.29	0.35	0.74

Table 13. Effect of dilution on various morphological and measurement parameters of *Penicillium chrysogenum* P-2. The dilutions of the sample at 116h (25.5g/L) were measured using fully automatic image analysis

Dilution (fold)	**20**	**40**	**80**	**160**	**320**	**640**	**1280**
Number of microorganisms measured	109	112	121	131	109	112	111
Mean main hyphal length (μm)	112.9 ±6.7	132.3 ±11	116.8 ±8	129.4 ±9	125.1 ±9.6	135.3 ±11.8	121.9 ±9
Mean total hyphal length (μm)	138.5 ±9.6	170.8 ±16.2	148.5 ±13.4	156.5 ±13.2	147.2 ±12.2	157.6 ±15.2	141.7 ±11
Mean number of tips	3.4 ±0.2	3.9 ±0.3	3.5 ±0.3	3.3 ±0.2	3.1 ±0.2	3.0 ±0.2	3.1 ±0.2
% clumps	91	92	88	69	64	51	66
Total measure-ment time (min)	27	53	47	48	60	96	130
Number of fields analysed	28	56	55	60	78	140	185
Mean number of microorganisms per field	3.9	2.0	2.2	1.9	1.4	0.8	0.6
Mean time to measure one microorganism (min)	0.25	0.48	0.40	0.43	0.57	0.87	1.25

4.3.2.4 The Performance of Version 2 of the Software

Figure 29, Figure 30 and Figure 31 show the mean values for total hyphal length, main hyphal length, and number of tips for the *Penicillium chrysogenum* time course. The differences between the results obtained for the two versions of the software were tested using the Students T-test. For all three morphological parameters, at the 95% confidence level, no significant differences were found between the two versions of the software. The results for the percentage of clumps are shown in Figure 32, all of the values except for sample one for version 2 were high throughout the time course. The times required for measurement of 100 fields are shown in Table 14 for each of the samples using version 1 of the software and hardware and in Table 15 for version 2. Version 2 also records the measurement for the size of clumps and the hyphal diameter these are shown in Table 16.

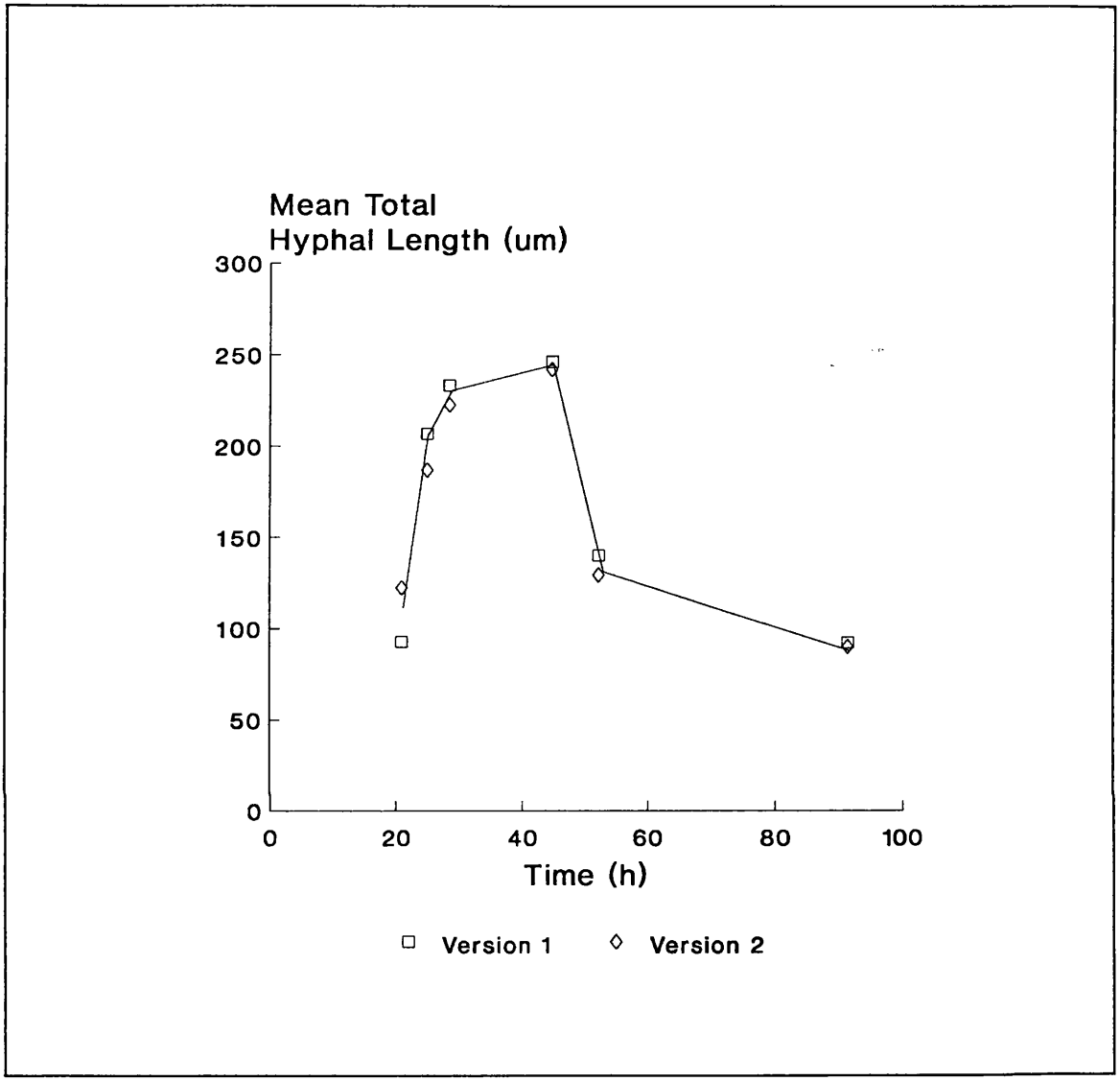

Figure 29. Time course of mean total hyphal length for *Penicillium chrysogenum* P-1. The samples were from a batch fermentation and were measured by the two versions of the software

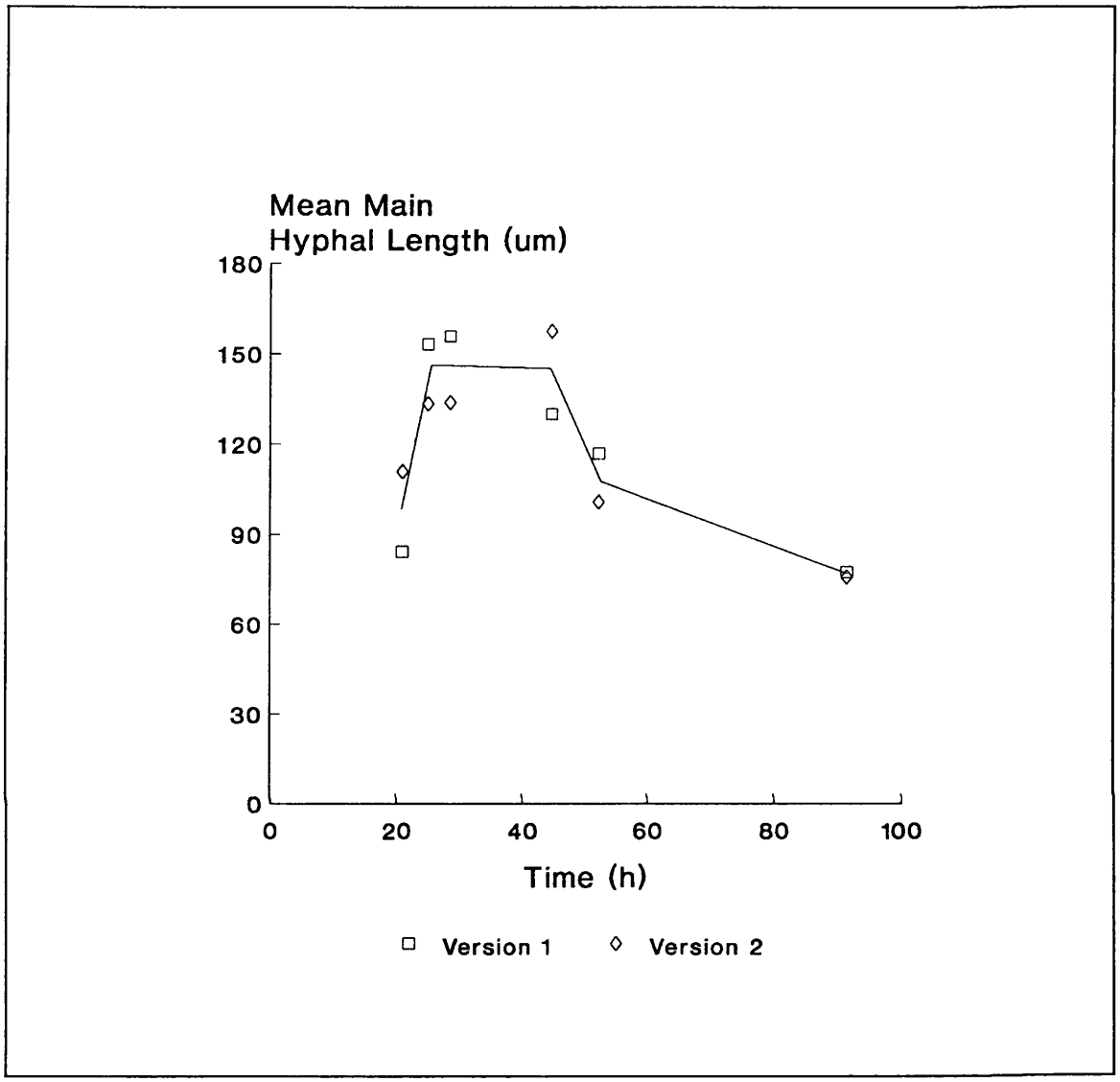

Figure 30. Time course of mean main hyphal length for *Penicillium chrysogenum* P-1. The samples were from a batch fermentation and were measured by the two versions of the software.

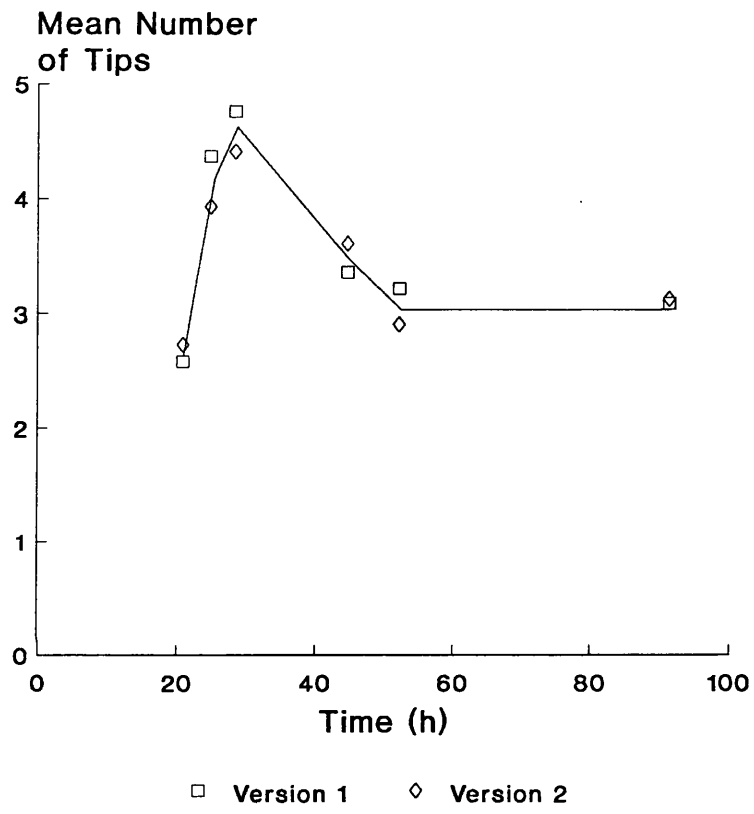

Figure 31. Time course of mean number of tips for *Penicillium chrysogenum* P-1. The samples were from a batch fermentation and were measured by the two versions of the software.

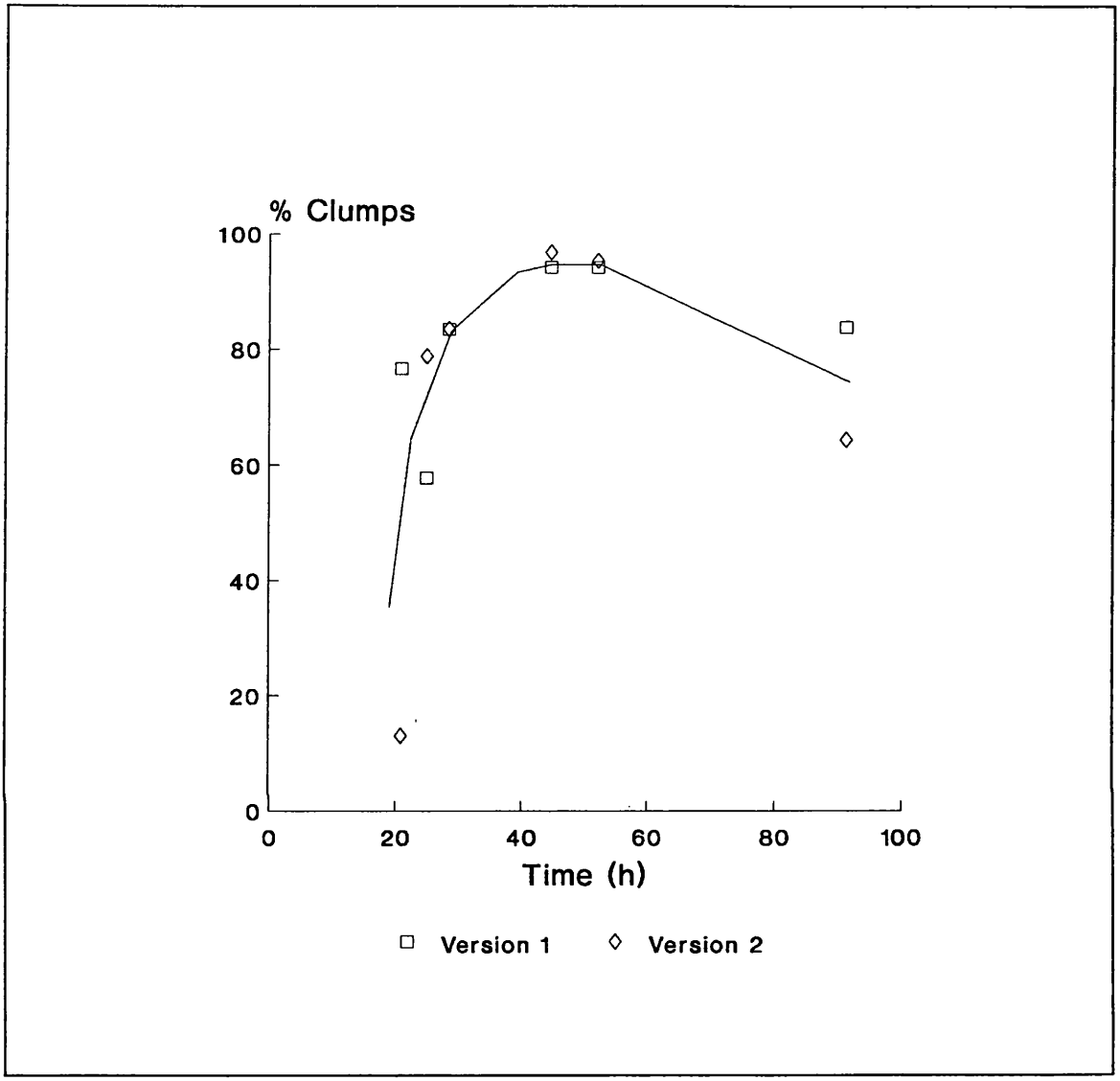

Figure 32. Time course of clumps for *Penicillium chrysogenum* P-1. The samples were from a batch fermentation and were measured by the two different versions of the software.

Table 14. Measurement times and number of microorganisms measured for 100 fields of samples of *Penicillium chrysogenum* P-1. The samples were from a fermentation time course and were measured using Version 1 of the software running fully automatically

Sample number	**1**	**2**	**3**	**4**	**5**	**6**
Number of microorganisms measured	19	27	42	11	81	390
Measurement time for 100 fields (min)	63	63	68	65	73	80
Mean measurement time per field (s)	37.8	37.8	40.8	39	43.8	48
Mean measurement time for one microorganism (s)	199	140	97.1	354.55	54	12.3

Table 15. Measurement times and the number of microorganisms measured for 100 fields of samples of *Penicillium chrysogenum* P-1. The samples were from a fermentation time course and were measured using Version 2 of the software running fully automatically

Fermentation time (h)	**1**	**2**	**3**	**4**	**5**	**6**
Number of microorganisms	11	27	37	18	108	586
Measurement time for 100 fields (min)	24	26	26	25	27	48
Measurement time per field (s)	14.4	15.6	15.6	14.7	16.2	28.8
Measurement time per microorganism (s)	130.9	57.8	42.2	81.7	15.0	4.9

Table 16. Size of clumps and hyphal diameter measured using Version 2 running fully automatically			
Sample number	**Clump area (um^2)**	**Number of clumps**	**Hyphal diameter (um)**
1	550.8	4	6.6
2	507.2	14	3.8
3	3109	47	3.4
4	12106	33	2.9
5	10568	71	2.5
6	1865	164	2.5

4.3.3 Discussion

4.3.3.1 Comparison Between the Methods of Characterisation

For the digitising and the manual image analysis methods of morphological characterisation there were no statistical differences between the mean values of the total hyphal length, the main hyphal length and the number of tips. Except for the sample at 21h, there were no significant differences between all three of the methods. The anomalous behaviour of the sample at 21h was attributed to the frequent occurrence of highly branched, relatively long microorganisms in this sample. This would result in an increased frequency of artefactual 'clumps' being formed by microorganisms touching or crossing over each other on the slide and particularly by long branches on individual microorganisms looping across each other. These clumps would not be characterised thus introducing a bias against microorganisms with long branches by the fully automatic method, giving lower mean total hyphal lengths and mean main hyphal lengths. The relatively low amount of measurable material in the sample at 21h, Table 9, also shows this clumping effect.

The image analysis methods had a considerable advantage in speed over the digitising method (Table 8) for measuring 100 characterisable microorganisms. However the fully-automatic method was only slightly faster than the manual method but it provided a measurement of the proportion of the material in clumps. The time taken by the fully-automatic method includes the extra number of fields that were processed before the 100 characterisable microorganisms had been located, as some fields did not contain characterisable microorganisms. In the manual method the stage was moved, manually, to measure only fields with characterisable

microorganisms. The measurement of clumps is useful as an indication of the likely reliability of the morphological characterisations. For larger distributions the fully-automatic method will gain over the other methods as the influence of the setting up time on the overall time taken will diminish (Table 10). For example for the sample at 119h, it took only 90min to characterise 1000 microorganisms and obtain the distribution shown in Figure 19.

The mean values for the number of tips presented in Figure 21for fully automatic image analysis were dependent on the length of noise spike removal parameter set in the program. The lower curve with the parameter set to the medial undissolved particle size (4 pixels, 3.9um) ensured few artefactual branches due to particles touching the hyphae, but resulted in some small branches actually being removed. The other curve with the length preset to that of a typical noise spike generated by skeletonisation (3 pixels, 2.9um) had a higher number of tips due to undissolved particles being interpreted as branches. Unfortunately, undissolved particles can not be distinguished easily from branches of similar size, and the number of tips is therefore not a completely reliable measurement.

The fully-automatic method is reliable and fast for relatively fragmented microorganisms and especially for the determination of distributions. For the more highly branched microorganisms the advantage of speed and the measurement of clumps must be weighed up against an apparent loss of accuracy. A further advantage of the fully automatic method though not demonstrated here would be the elimination of operator variability.

The algorithm used to select the main hypha, the longest connected path appeared to give good results. There were no differences between the main hyphae selected during the use of the digitiser and those selected by the software algorithm applied in the manual image analysis methodology. Therefore for streptomycetes which are of small diameter and are extremely flexible the use of this algorithm to replace the main hypha was a good choice, though for some fungi or for studies of detailed branching structure this may not prove to be the most useful algorithm as it does not allow the main hyphae to be distinguished from branches by considering internal cell structures such as septa. For engineering studies e.g. on broth rheology, the use of the longest connected path for flexible microorganisms would be the best measure of the "effective length" defined by Metz et al.(1981)

There were no discrepancies in the actual length measurements of the hyphae between the digitising table and the image analysis methods. In the work prior to that reported here, measurements of the main hypha by image analysis, using a proprietary arc measurement algorithm, were 6% greater than the measurements using the digitiser (Adams and Thomas 1988). The digitiser measures a series of chords lengths and the sum of the chord lengths will always be less than the true arc length, with the difference increasing with cursor step length and the

curvature of the microorganism. However for image analysis the trend is for the converse, for representation of a curve by a set of points taken from an array of discrete points, i.e. a digitised image, can result in severe over estimation of line lengths (Cornelisse and van der Berg, 1984), unless the scale of digitising is very fine. The arc measurement algorithm used in the software, the sum of the interpixel vector distances, does not include a smoothing algorithm to prevent any tendency to over estimation as the digitisation on the image analysis system is fine, an array of 512 by 512 pixels, and by increasing the level of magnification on the microscope when objects appear small (such as small fragments of hyphae), their digitisation will remain fine.

Also a second factor, skeletonisation, affects the length measurement during image analysis, for often during the skeletonisation process pixels are lost from the ends of the object. It would be possible to add algorithms both for smoothing the arcs and adding pixels back onto the ends of skeletons, but these would increase processing time and as the image analysis system and digitiser show good agreement it was decided not to alter the current algorithms.

4.3.3.2 Measurement of *Penicillium chrysogenum*

Figure 22 shows clearly that the fully automatic image analysis method can be used to characterise the morphology of a filamentous fungal fermentation and obtain reasonably precise data. The total time taken for the analysis of the time course of the *Penicillium chrysogenum* P-1 fermentation was long (56h) and this was due to two factors. The first is the number of microorganisms characterised, 200 for each of 12 samples, but by scaling up the time taken to measure the samples of *Streptomyces clavuligerus* microorganisms for

each of 5 samples took 120min in total) this would account for less than 10h of processing time: a minor effect. The major reason was that there were relatively few free microorganisms to measure as the percentage of mycelia in clumps was very high throughout the fermentation, Figure 22. Even with this time that is required for measurement, using image analysis would be the only practical way to carry out routine analysis and certainly the only method which enables the amount of material in clumps to be assessed. The degree of clumping in both of the *Penicillium chrysogenum* fermentations provided a very stringent test of the capabilities of the image analysis system.

The studies on the fed-batch fermentation of *Penicillium chrysogenum* P-2 (Figure 25) show that the image analysis method is also applicable to another strain grown in different conditions and at a higher biomass. This fermentation contained undissolved media particles in the broth which did not prevent characterisation.

4.3.3.3 The Effect of Dilution

Increasing dilution of the samples, except for low dilutions, had little effect on the morphological parameters when measured by fully-automatic image analysis. At low dilutions microorganisms tended to lie touching and crossing over one another. This would lead to a bias in the results against long microorganisms if "clumps" were formed or alternatively if 'holes' were not formed, particularly in the case of shorter organisms touching, then this would lead to falsely high values for the morphological parameters especially for the total and main hyphal lengths. From Table 11, Table 12 and Table 13 it can be seen that as long as low dilutions are avoided then the dilution does not affect the measurements for the morphological parameters.

The level of dilution used does have an affect on the amount of time taken for measurement (Table 11, Table 12 and Table 13). The time taken for measurement depends on the number of fields that must be analysed before the desired number of microorganisms have been measured. The number of fields required is dependent upon the number of free microorganisms, non-aggregated, in each field which would be reduced by excessive dilution thus increasing analysis times. From Table 12 and Table 13, it can also be seen that the relatively high amount of clumps present in the *Penicillium chrysogenum* samples mean that there are few free microorganisms per field available to be measured so analysis is slow, whereas for *Streptomyces clavuligerus* there is less clumping, giving more organisms for characterisation and thus decreasing the measurement time. At approximately equal biomass concentrations for *Penicillium chrysogenum* on the slides (e.g. 1/160 for P-1 and 1/640 for P-2) analysis times were similar as there were similar numbers of free microorganisms per field (Table 12 and Table 13).

It might be presumed that in a filamentous fermentation that some mycelia are in permanent clumps which would only disaggregate if the microorganisms within them were disrupted. These clumps would be likely to affect the mass transfer and broth rheology so it would be useful to be able to quantify the proportion of these clumps in the biomass in the fermenter. A second form of non-permanent clumps would also probably exist and these loose agglomerations would be likely to disassociate easily, say when passing through the impeller regions of a stirred tank vessel. One of the aims of the dilution study was to establish a method for the quantification of permanent aggregates in a filamentous fermentation.

The .*Penicillium chrysogenum* fermentations both contained a high proportion of mycelial clumps in particular the *Penicillium chrysogenum* P-2 fermentation with its relatively high biomass. Table 12 and Table 13 indicate that there may be an irreducible proportion of clumps in these fermentations, although the measure of clumps was rather scattered. The scatter was due partly to the uneven spread of material on the slide as the mycelial aggregates tend to lie

in the region they are placed on the slide, and also the because there is not necessarily a simple correlation between the pixel count of the skeletonised clumps and the biomass in the clumps. The quantification of the clumps would tend to be an underestimation of the material present as it would not be able to take into account changes in thickness and crossovers.

For the *Streptomyces clavuligerus* fermentation (Table 11) the situation appears to be different for the percentage of clumps declined with dilution. This was due to the loose nature of the clumps which disaggregated with dilution. There may indeed have been an irreducible proportion of permanent clumps in this fermentation but the dilutions required to measure this would have resulted in unacceptably long times for the other morphological parameters.

The proportion of material in clumps is potentially a useful extra measurement obtained by fully-automatic image analysis, but it may not be a reliable indication of the permanent clumps in the fermenter unless long analysis times are acceptable.

4.3.3.4 Performance of Version 2

Statistical analysis showed that there were no significant differences in the mean values for total hyphal length, main hyphal length and the number of tips between the two versions of the software running on different hardware. As the algorithms used for characterisation and analysis of the morphological parameters are identical this result was anticipated. However for the percentage of the material in clumps different measurement algorithms are used for the two versions of the software with version 1 measuring the skeletons of the clumps and version 2 measuring the area of the unskeletonised clumps. For all of the samples except for the first and last sample the percentage of clumps were similar (Figure 32). For the last sample, version 2 characterised more organisms (586) than version 1 (390) so the measurements were probably taken in a less clumped part of the slide. For the first sample the percentage of clumps recorded by version 2 was 13% and by version 1 76.7%. This again is probably a reflection of uneven dispersion of material across the slide for the 13% is due to the measurement of only 4 clumps by version 2.

In addition to the morphological parameters of total hyphal length, main hyphal length and the number of tips, version 2 also measures the size and number of clumps and enables the hyphal diameter to be measured which are valuable additions to the data collected. Also version 2 produced a decrease in processing time of a factor of about 2.3 times against fully automatic processing on Version 1, which is a significant increase in speed. This increase in speed is a significant step towards the processing speed that would be required for on-line control and this was achieved without using an advancement in computer hardware technology such as parallel processors or transputers, with systems such as these it may be possible to increase speed by

a factor of 10 allowing the information collected to be used to change the fermentation conditions.

4.4 Summary

From the studies of the performance of the image analysis methodologies it has been shown that good sample preparation is essential for the efficient running of the characterisation software. The recommendations for sample preparation are as follows

- The sample must appear as two dimensional as possible when observed under a microscope. It should therefore either be dried down onto the slides as was used here for streptomycetes or alternatively when a wet mount is necessary, such as for *Penicillium chrysogenum*, the depth of liquid under the cover slip should be minimised.
- The microorganisms should be diluted to minimise the number touching each other and thus reducing the number of crossovers.
- The number of characterisable microorganisms per field directly influences the time required for processing so it is desirable to keep this as high as is reasonably possible. Usually it is necessary to reach a compromise between the requirements for reduced processing time and that for reduced crossovers.
- Colour enhancement of the microorganisms with a suitable stain is required.

Image analysis can be used for the rapid, and in most cases, accurate characterisation of the morphology of filamentous microorganisms. This novel method of measurement should allow the routine study of morphological development during filamentous fermentations. The fully automatic image analysis method reported here not only measures the usual morphological parameters but also the proportion of material in aggregates, which may be related to the permanent aggregates in a fermenter and is certainly an excellent indicator of the validity of the morphological measurements on a slide. The speed of measurement using the image analysis system also enables greater number of microorganisms to be measured which when one considers the large variances on the mean values of morphological parameters (Van Suijdam and Metz, 1981) then measurement of large populations would be required to detect small changes in the morphology of the microorganisms.

The partial optimisation of the software when it was transferred to a second image analysis system gave a considerable increase in the speed of performance between the two versions of the software, although most of the hardware is actually the same in both systems. If the software and hardware were both to be improved by using one of the new generation of image

processing systems that are now available then a considerable gain in speed could well be obtained, which could permit the use of image analysis as an additional process control tool for those cases in which morphological development is vital to the productivity of the fermentation.

5.0 The Estimation of Cell Volume and Biomass

The aim of this study was to establish a methodology for the measurement of biomass and cell volume for fermentations of filamentous fungi using image analysis. The methodology has been established using *Penicillium chrysogenum* grown under different fermentation conditions and in different media. In particular one of the overwhelming reasons for the development of the methodology was to enable the measurement of the cell volume and biomass of the microorganisms in the presence of considerable quantities of undissolved solids in the medium which has not been achieved by previous methodologies (1.5, Evaluation of Mycelial Growth). The establishment of the technique involved three main areas of work, firstly sample preparation, then the devising of the image analysis techniques and finally the use of these for measurement of cell volume and biomass.

5.1 Sample Preparation

5.1.1 Reducing Aggregates in the Sample

The morphological characterisation of *Penicillium chrysogenum* showed that throughout the fermentation a large proportion of the cells were present as aggregates (Figure 22). For a quantitative measurement of the mycelial material present in a volume of fermentation broth, the presence of the aggregates poses the following potential problems:-

1. Inaccuracies in pipetting small volumes of diluted broth. In a small volume of diluted sample, such as a microlitre, the presence of large aggregates would result in heterogeneity in the dispersion of material.

2. The presence of crossovers of mycelia would result in inaccuracy in the two dimensional measurement of surface area as hyphae lying underneath other hyphae would not be detected and measured. Also the presence of crossovers would cause changes in depth of the mycelia on the slide which could cause problems with focusing the microorganisms for analysis.

Several approaches were considered in an attempt to reduce aggregation in the fermentation samples:.

1. Dilution. However this effects the time required for processing. Also a point would be reached where dilution would not affect the clump size any further (4.3.3.3, The Effect of Dilution).

2. Surface active agent addition to fermentation broth samples. This is unlikely to have a significant effect on the size of clumps and previous studies to obtain filamentous mycelia have used these agents during the growth phase often to cause the cells to grow in a non-pelleted form (for example Elmayeri *et al.* 197 3). Establishing a system which required the addition of agents to the fermentation would not be acceptable just to obtain a measure of biomass as it would potentially have adverse effects on metabolite production, increase production costs and affect fermentation conditions such as mass transfer and dissolved gas concentrations.

3. Mechanical breakage. There are studies in the literature that have used a Waring Blender to break aggregates and pellets to provide hyphal fragments for use as an inoculum for fermentation (Savage and Van der Brook 1946, Murase and Kendrick 1986). The studies have shown that the fragments remain viable and thus the breakage of cells was limited.

From the options available the use of a Waring Blender for mechanical breakage of microorganisms based on the results of previous studies was selected and tested for sample preparation for biomass estimation.

5.1.1.1 Method

Two strains of *Penicillium chrysogenum* NRRL1951 and P-1 were used in this study. The first is one of the original strains on which the effect of high speed blending on *Penicillium chrysogenum* was assessed (Savage and Van der Brook 1946). Both organisms were grown in a corn steep liquor medium. The medium and growth conditions are described in 3.2.4.2, Shake Flask Fermentations. Each shake flask contained 300mL of media and duplicate flasks were used for each strain. After 72h of growth, following inoculation, individual samples of 120ml were removed from each shakeflask for blending in a Waring Blender (3.1.3.3, Waring Blender). The effect of blending mycelia was assessed at two different speed settings of high and low which when measured using a tachometer were evaluated as 17000rpm and 14000rpm. Each sample was blended for a set time (0, 0.5, 1, 2, 3, 4, 5 or 10 min) at either high or low speed. Once blended the sample was removed from the blender and left for 5min to allow any foam to subside and was then gently shaken before the withdrawal of two 5mL samples for dry weight measurement.

Samples for morphological analysis were also removed from the blended sample. For this 5mL of sample were mixed with an equal volume of fixative (3.2.1.2, *Penicillium chrysogenum*). Before analysis the samples were diluted further in the fixative using a constant dilution for all of the samples for each strain, 1 in 4 for NRRL 1951, and 1 in 16 for P-1. These were stained with lactophenol tryphan blue and prepared for analysis as described in 3.2.1.2, *Penicillium chrysogenum*.

Version 2 of the morphological characterisation software was used for analysis. A semi-automatic methodology was selected which consisted of automatic stage movement but the microorganisms were selected manually by touching them with a light-pen on the screen. This methodology was chosen to ensure that all blended fragments were measured as many would be very small and not appear as typical fungal morphologies so they would not necessarily be selected with fully-automatic measurement. For analysis a magnification of 100 times was used for the measurement of P-1 samples and of 125 times for the NRRL1951 strain. For each sample 40 fields of view were analysed and the results were recorded in a data file.

5.1.1.2 Results

The morphologies of the two different strains after growth were different. *Penicillium chrysogenum* NRRL1951 had grown as pellets whereas the culture of P-1 was filamentous. With duration of blending the dry weight of the samples decreased rapidly until it reached a final value which was no longer affected by further blending (Figure 34 and Figure 33). The speed of blending only affected the length of blending time required to reach a final dry weight concentration. The actual drop in dry weight varied between the different strains. Strain NRRL1951 lost 90% of its initial biomass in just 30s of high speed blending whereas the P-1 strain in the same medium lost only 16% for the same blending conditions.

The actual size of the individual clumps also decreased with duration of blending until a minimum clump size was obtained which was not affected by further blending (Figure 36 and Figure 35). After only 30s of blending the reduction in the size of aggregates was considerable, with the pellets in strain NRRL1951 breaking down into aggregates and P-1 showing a 58% reduction in aggregate size at high speed. The percentage of clumps, the ratio of aggregated hyphae to total hyphae, for the samples is shown in Figure 37 and Figure 38. For strain NRRL1951 after the pellets had been broken down, a further maximum reduction in percentage of clumps of only 15% was achieved. Strain P-1 in solids medium showed a maximum decrease in aggregate size of approximately 45%.

The effects of blending on total hyphal length for P-1 and NRRL1951 are shown in Figure 37 and Figure 38 for high speed. A decrease in mean total hyphal length occurred with length of time of blending for P-1 and also the standard deviation of the means decreased indicating that the homogeneity of the sample improved with time. A similar effect on the standard deviation of the means was also found for the NRRL1951 samples. The mean total hyphal length of the samples of NRRL1951 also decreased with time of blending its hyphal lengths fell from 92.6μm to 51.2μm over the blending period and were considerably smaller than the P-1 mean total hyphal lengths which ranged from 138μm to 70μm.

The mean number of tips for P-1 and NRRL1951 are shown in Figure 35 and Figure 36 for high speed blending. The P-1 strain showed very little change in the number of tips whereas the number of tips decreased after the initial breakdown of pellets to a mean of 4 tips per organism which had a high error of ±0.75 tips, then this decreased after one minute of blending to approximately a mean of 3 tips per organism though the error on the mean decreased to between 0.3 and 0.11 for the samples. The effects of blending on the fungal hyphae are shown in Figure 39 and Figure 40 when observed under light microscopy.

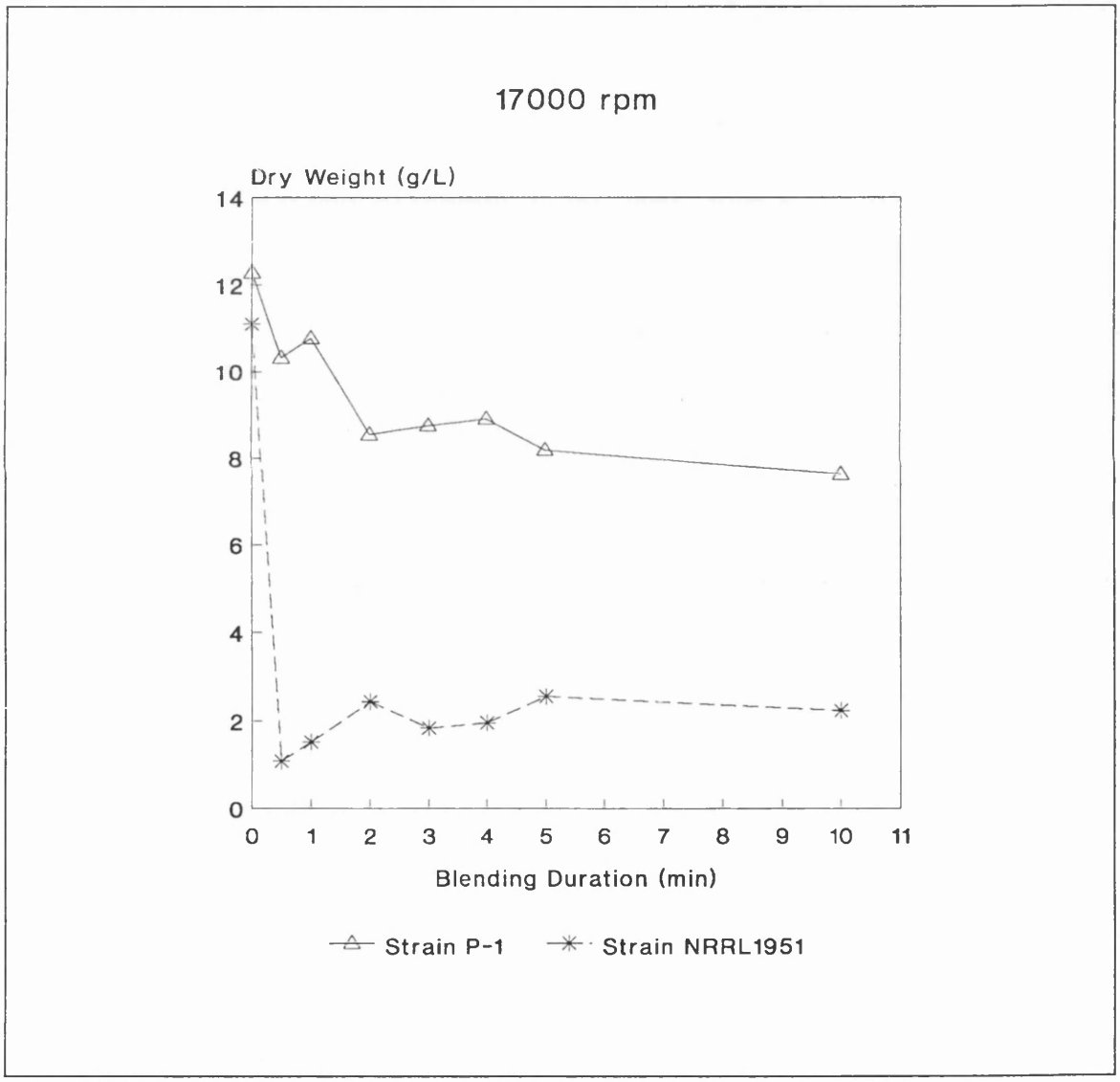

Figure 33. The effect of high speed blending on dry weight. The is shown for samples of *Penicillium chrysogenum* P-1 and NRRL1951.

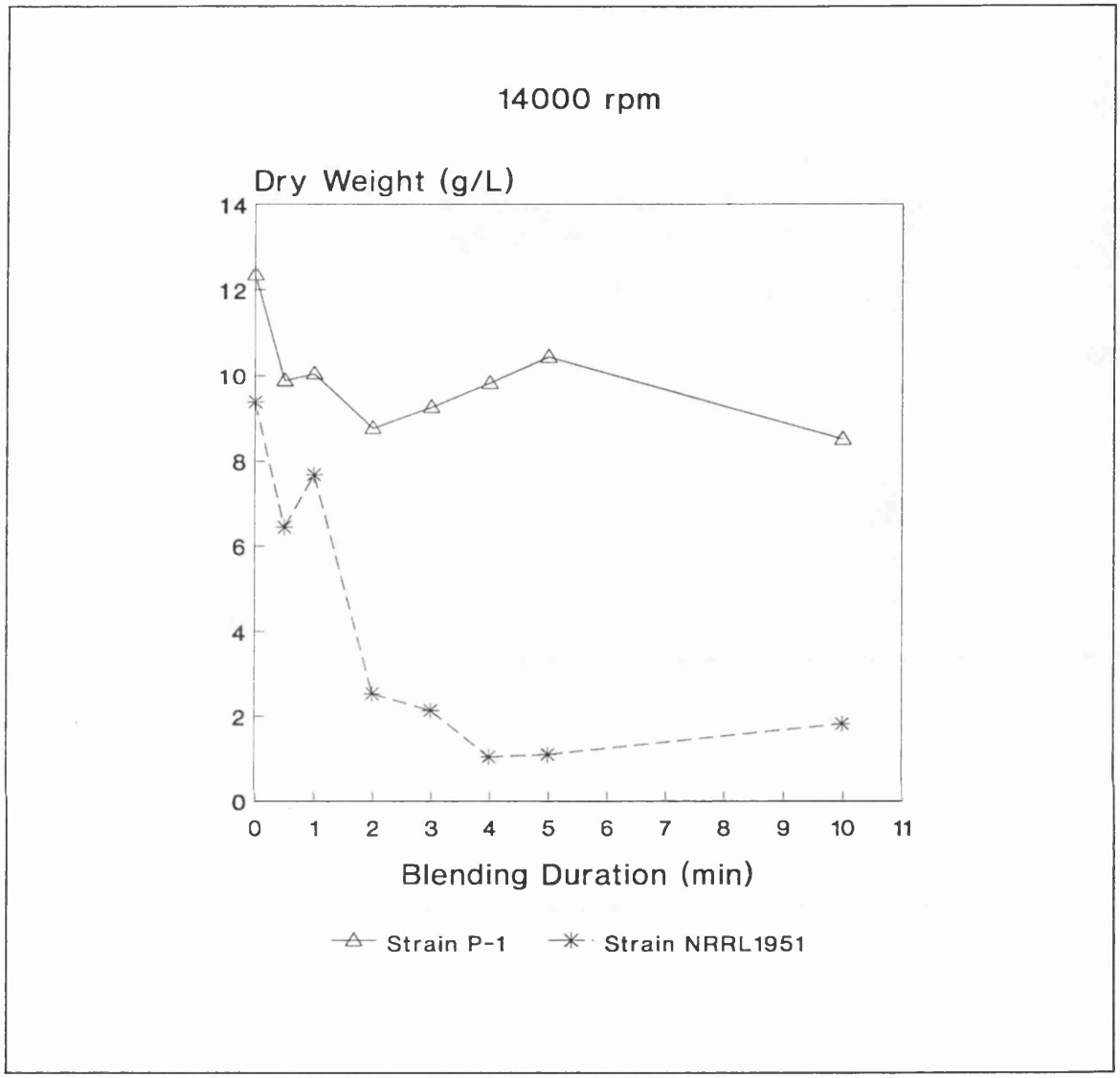

Figure 34. The effect of low speed blending on dry weight. The effect is shown for samples of *Penicillium chrysogenum* P-1 and NRRL1951.

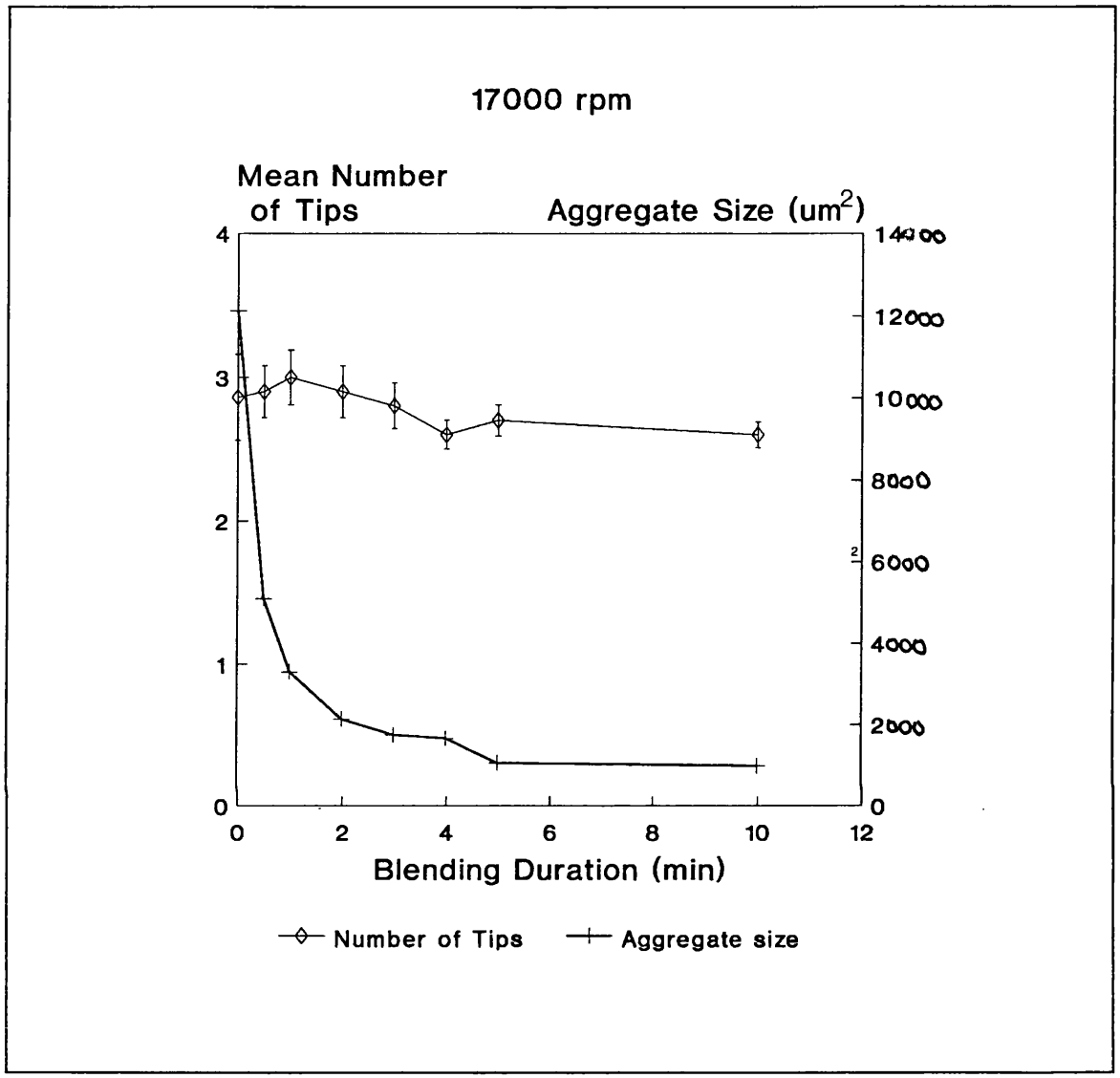

Figure 35. The effect of blending on the morphological parameters of *Penicillium chrysogenum* P-1

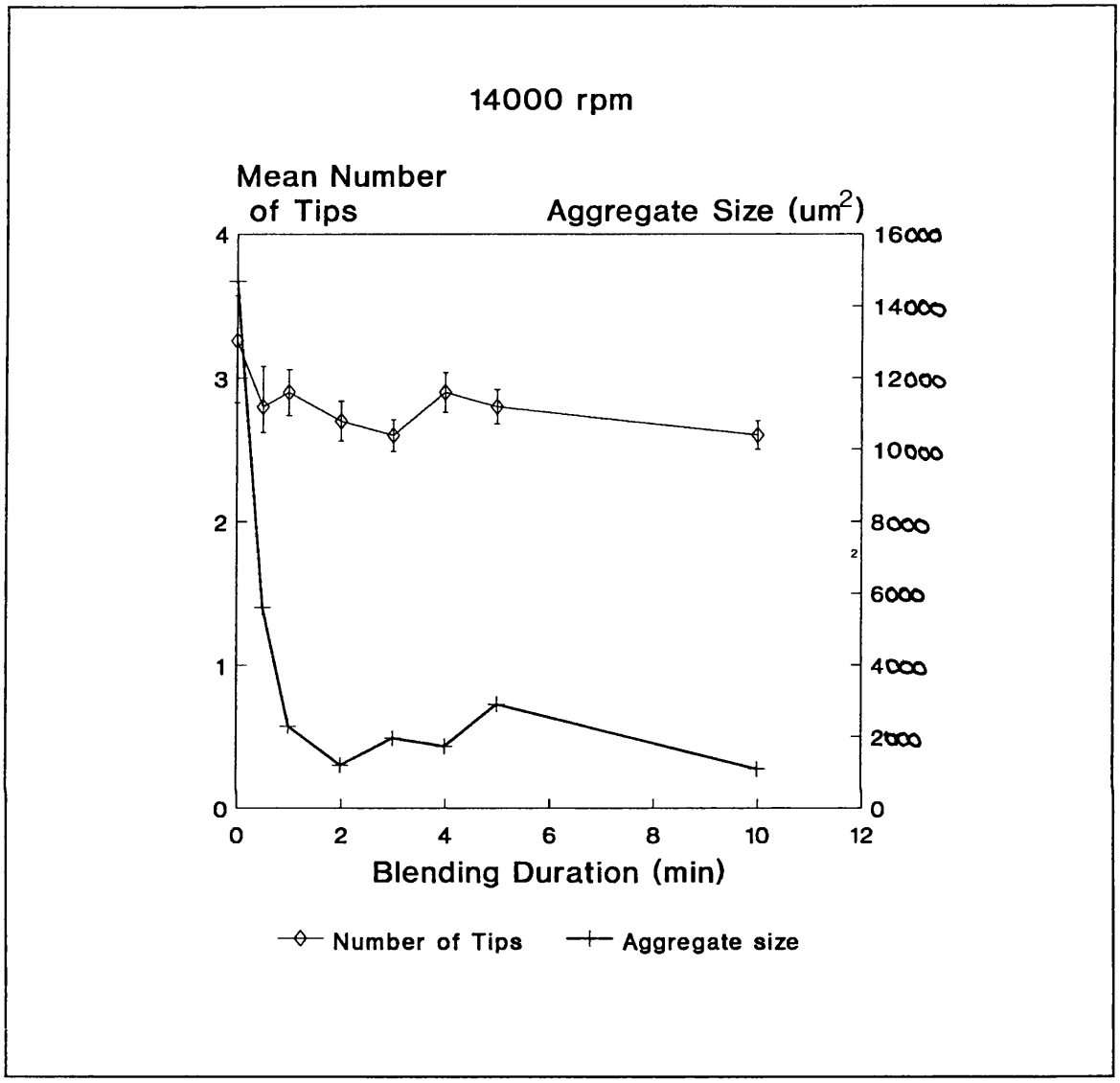

Figure 35 (Part 2 of 2). The effect of blending on the morphological parameters of *Penicillium chrysogenum* P-1. The effect of blending at high and low speed on the mean number of tips and size of clumps is shown.

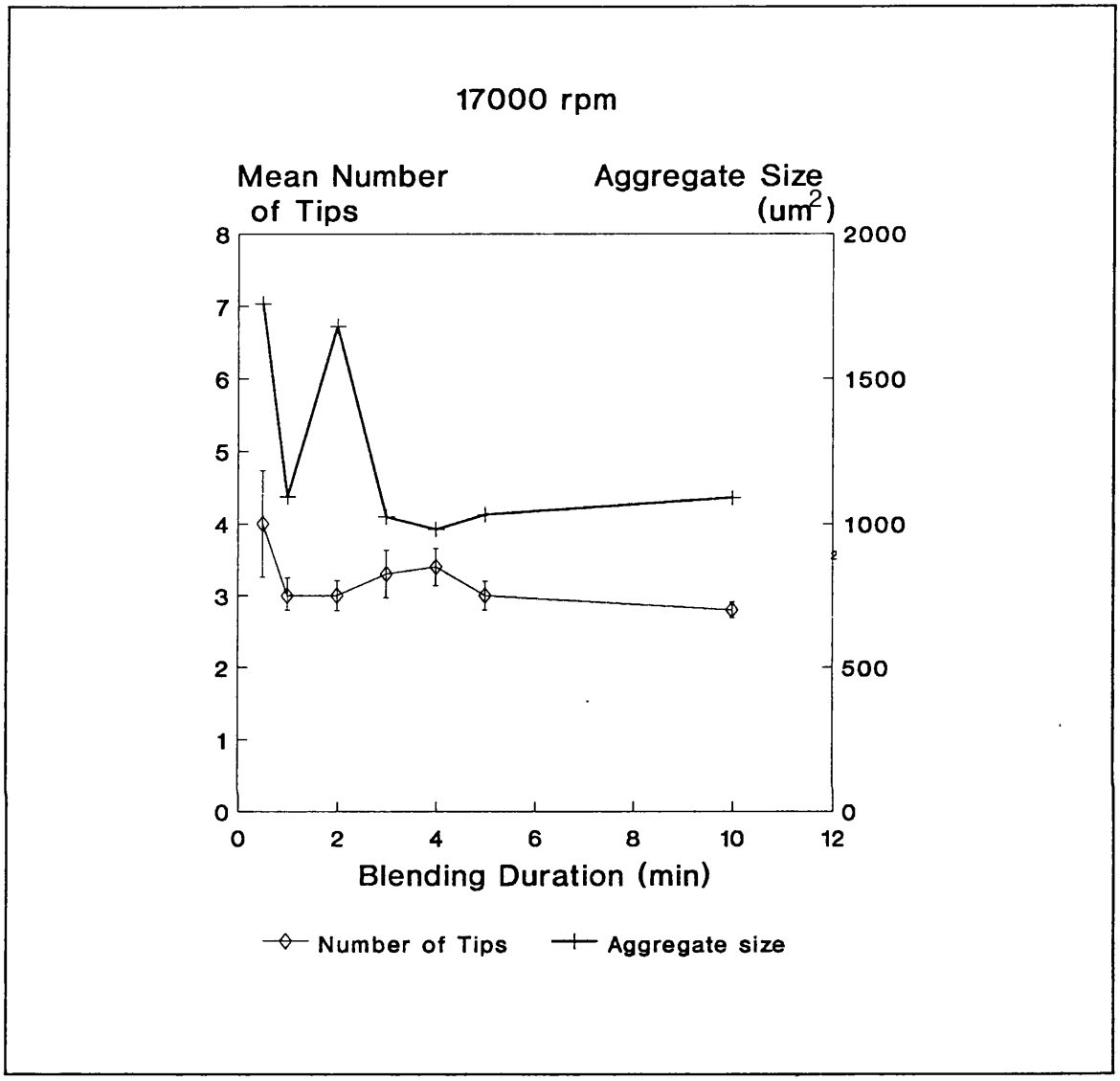

Figure 36. The effect of blending on the morphological parameters of *Penicillium chrysogenum* NRRL1951

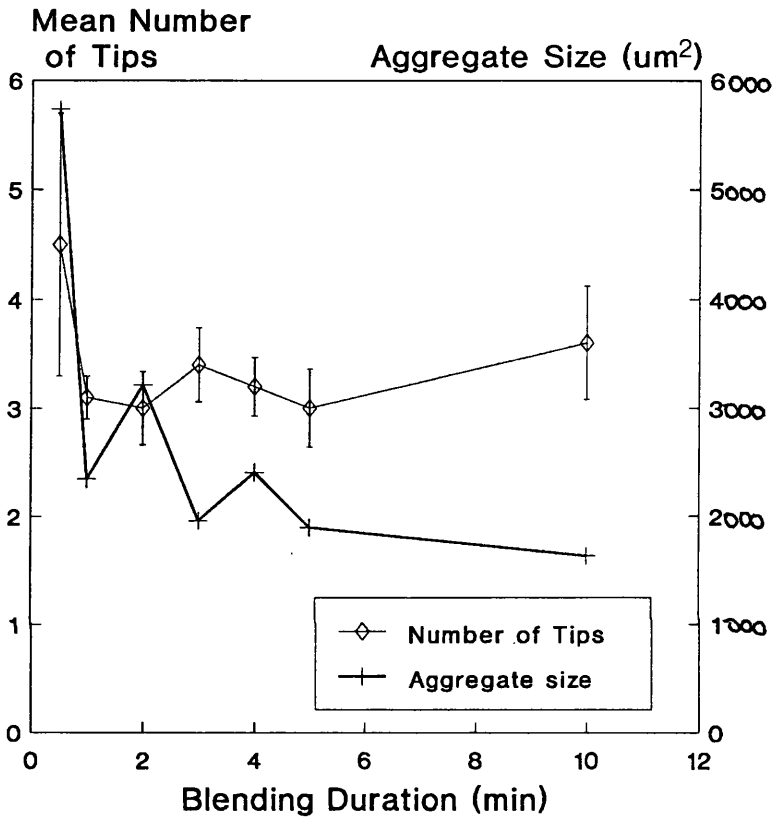

Figure 36 (Part 2 of 2). The effect of blending on the morphological parameters of *Penicillium chrysogenum* NRRL1951. The effect of blending at high and low speeds on the mean number of tips and size of clumps is shown.

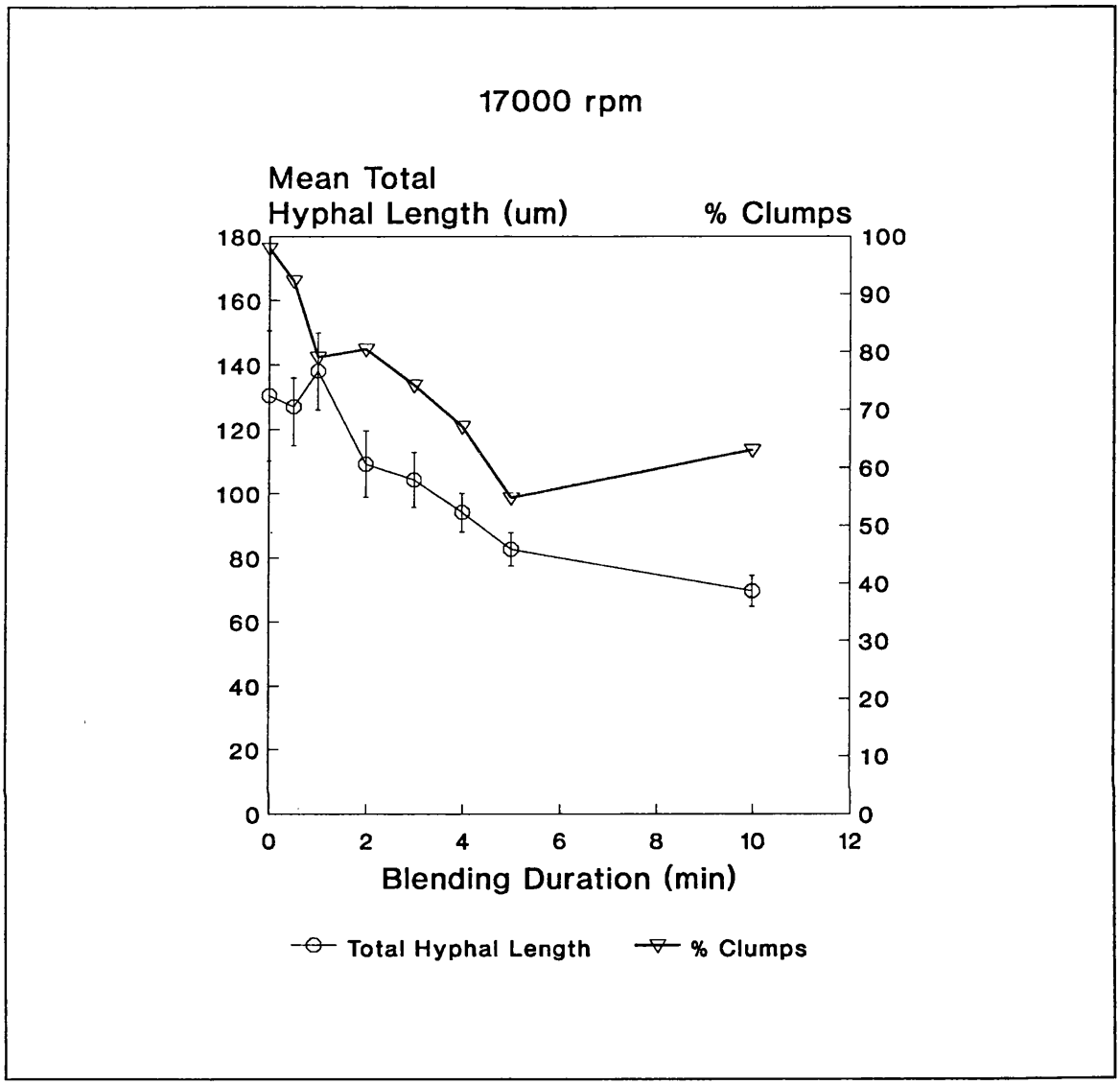

Figure 37. The effect of blending on the morphological parameters of *Penicillium chrysogenum* P-1

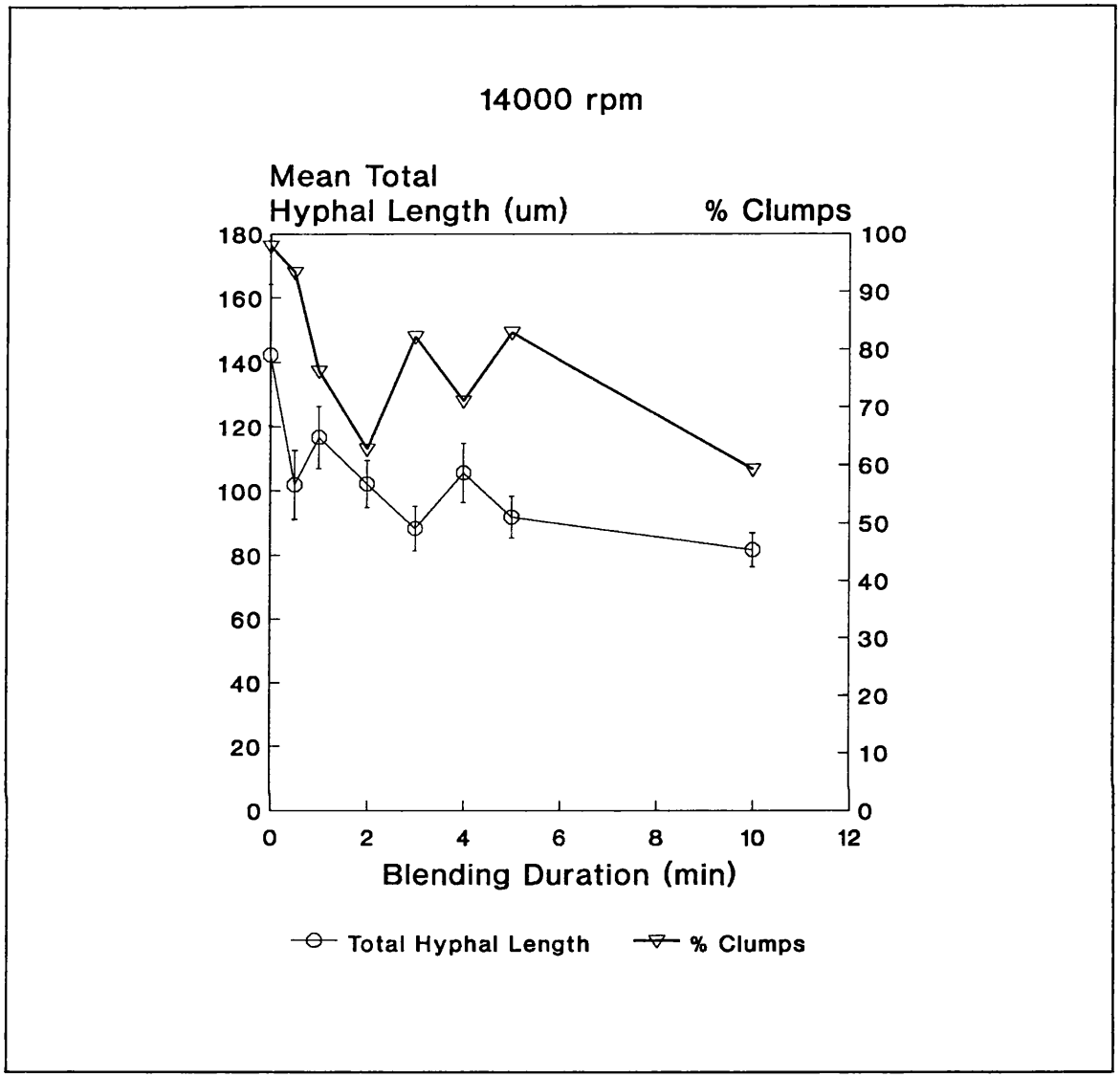

Figure 37 (Part 2 of 2). The effect of blending on the morphological parameters of *Penicillium chrysogenum* P-1. The effect of high and low speed blending on the mean total hyphal length and percent clumps is shown.

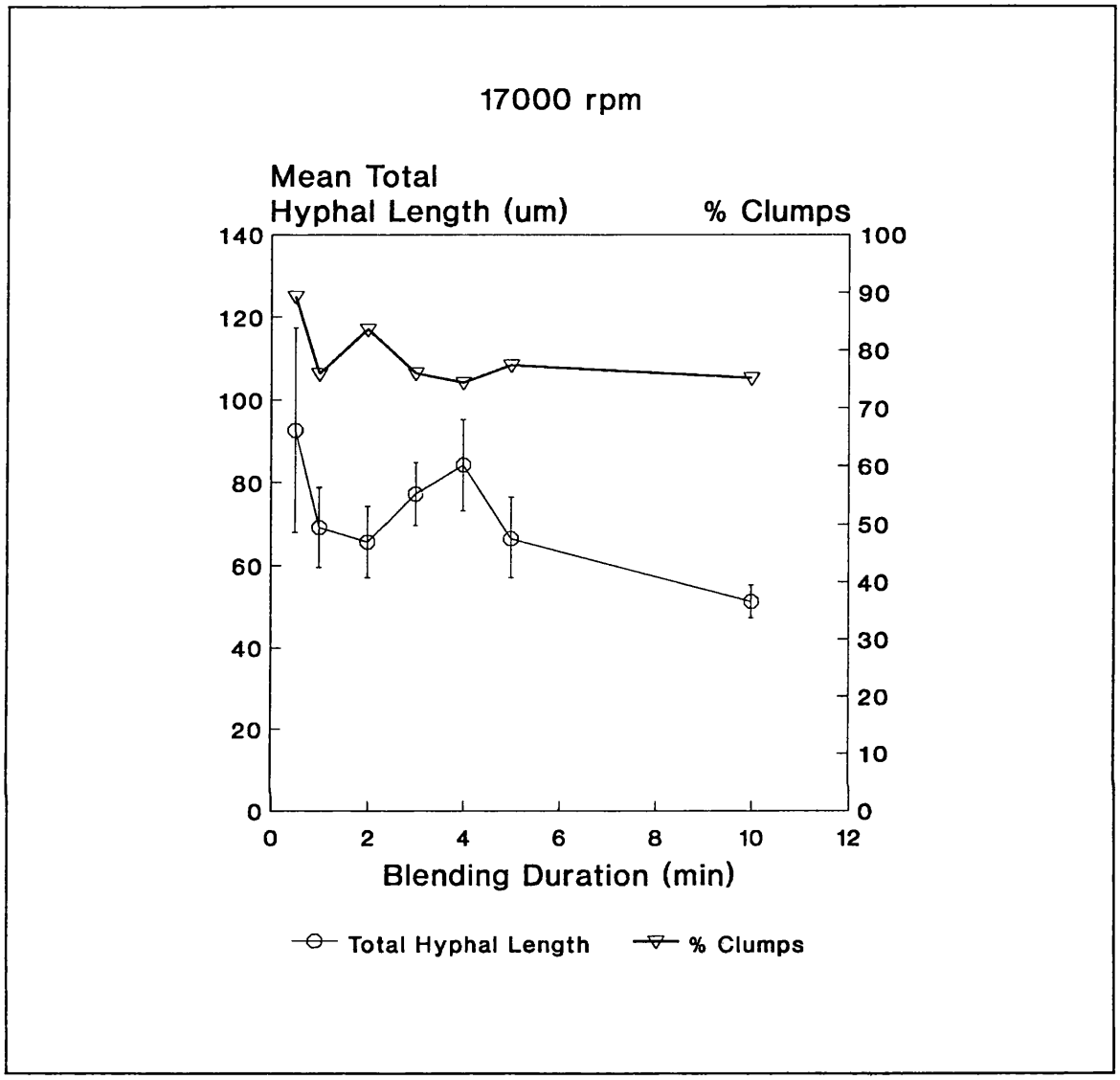

Figure 38. The effect of blending on the morphological parameters of *Penicillium chrysogenum* NRRL1951

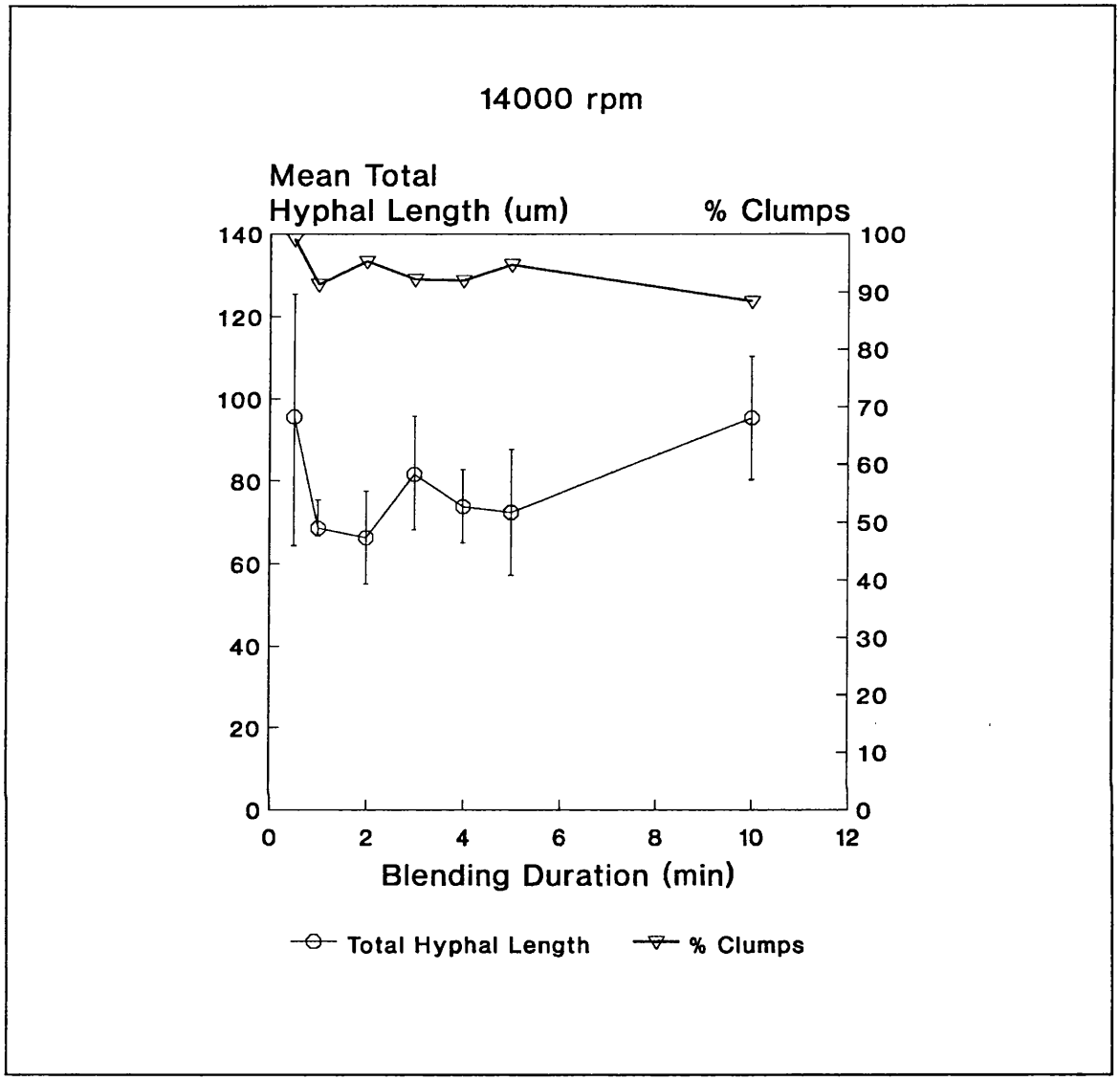

Figure 38 (Part 2 of 2). The effect of blending on the morphological parameters of *Penicillium chrysogenum* NRRL1951. The effect of blending at high and low speed on the mean total hyphal length and percent clumps is shown.

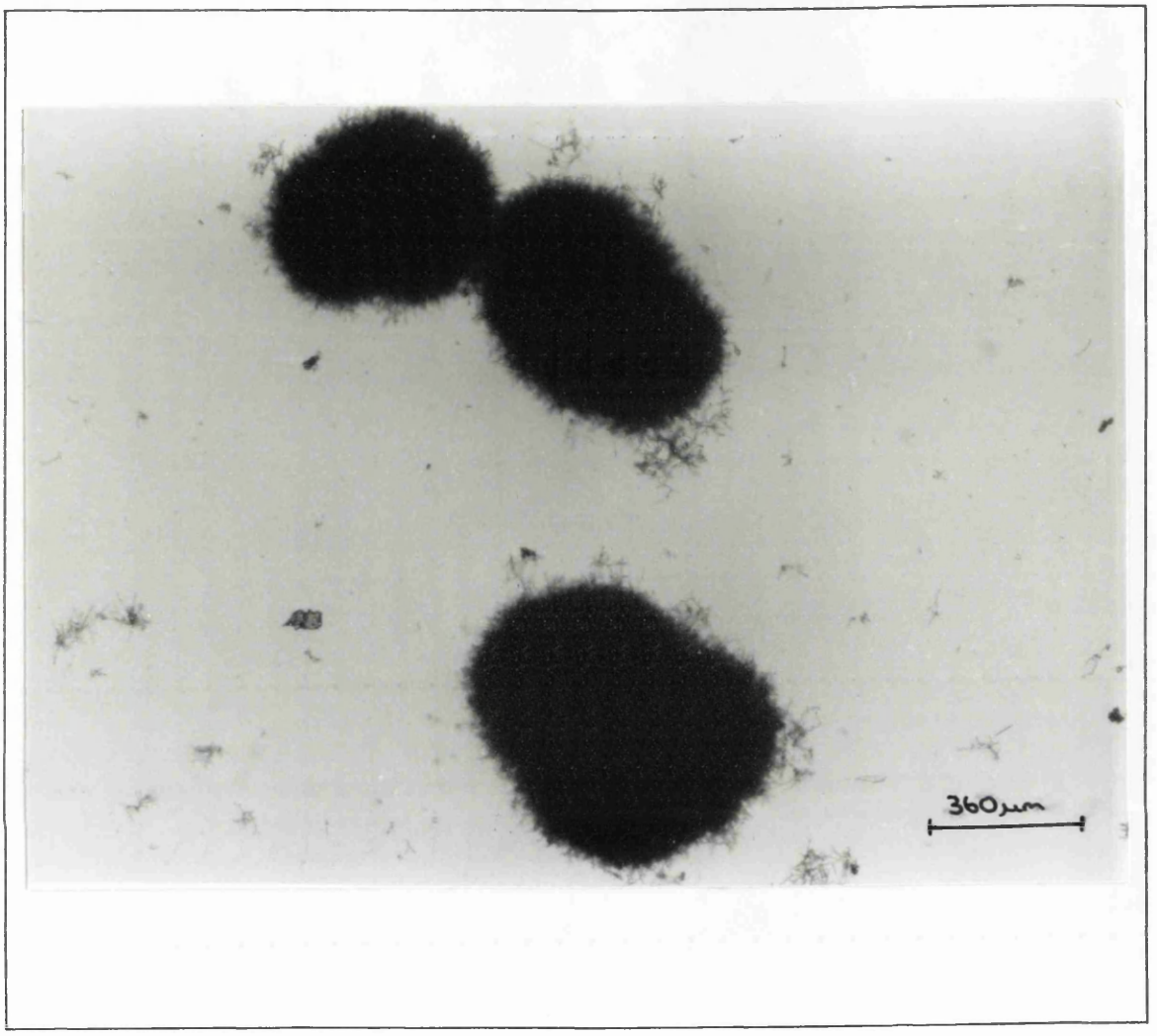

Figure 39. Typical hyphal fragments of *Penicillium chrysogenum* NRRL1951

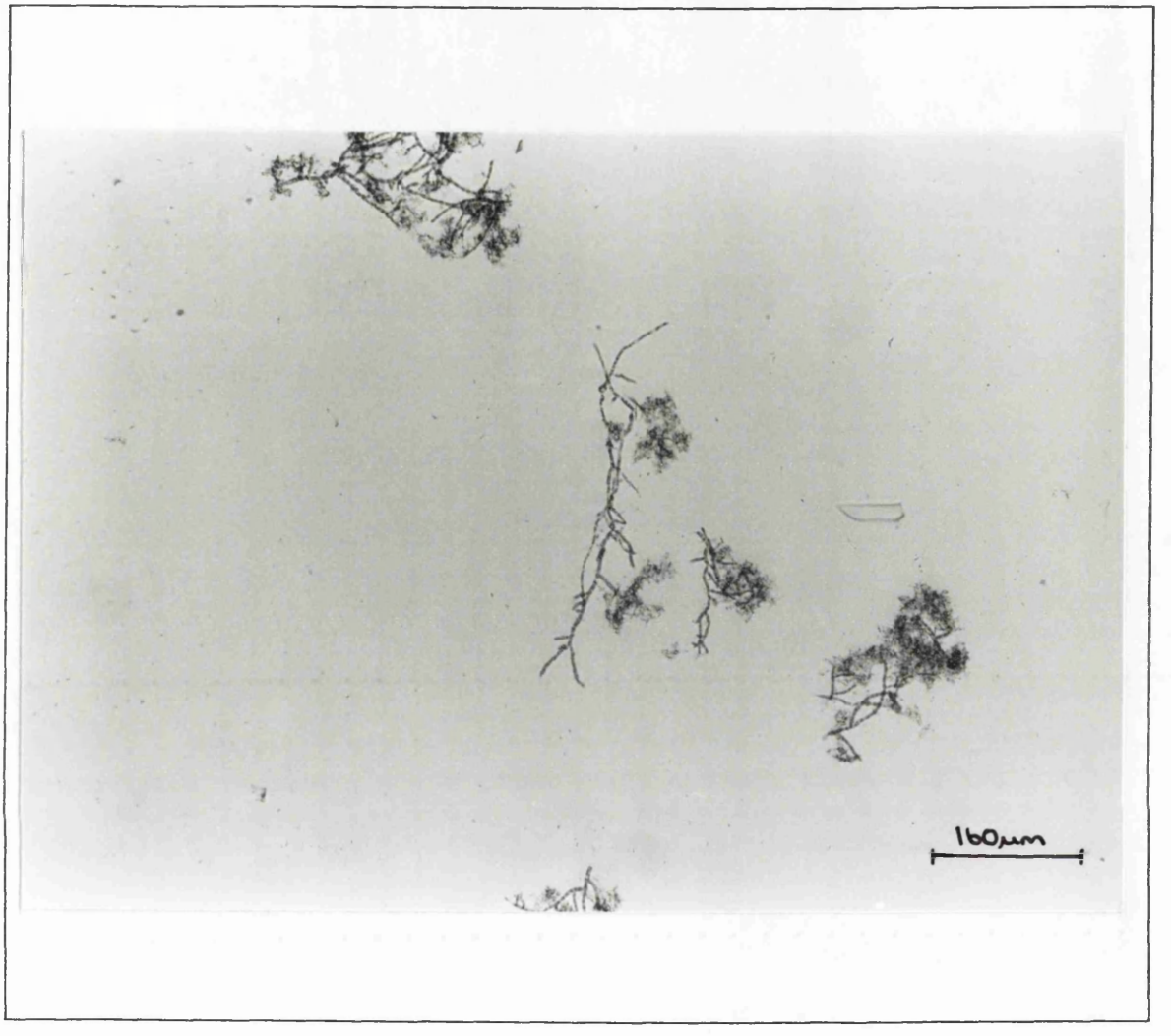

Figure 39 (Part 2 of 2). Typical hyphal fragments of *Penicillium chrysogenum* NRRL1951. The fragments were generated by blending at high speed. Photograph (a) shows the mycelia before blending (1cm=180µm), and (b) shows the mycelia after blending for 1 min at high speed (1cm=80µm)

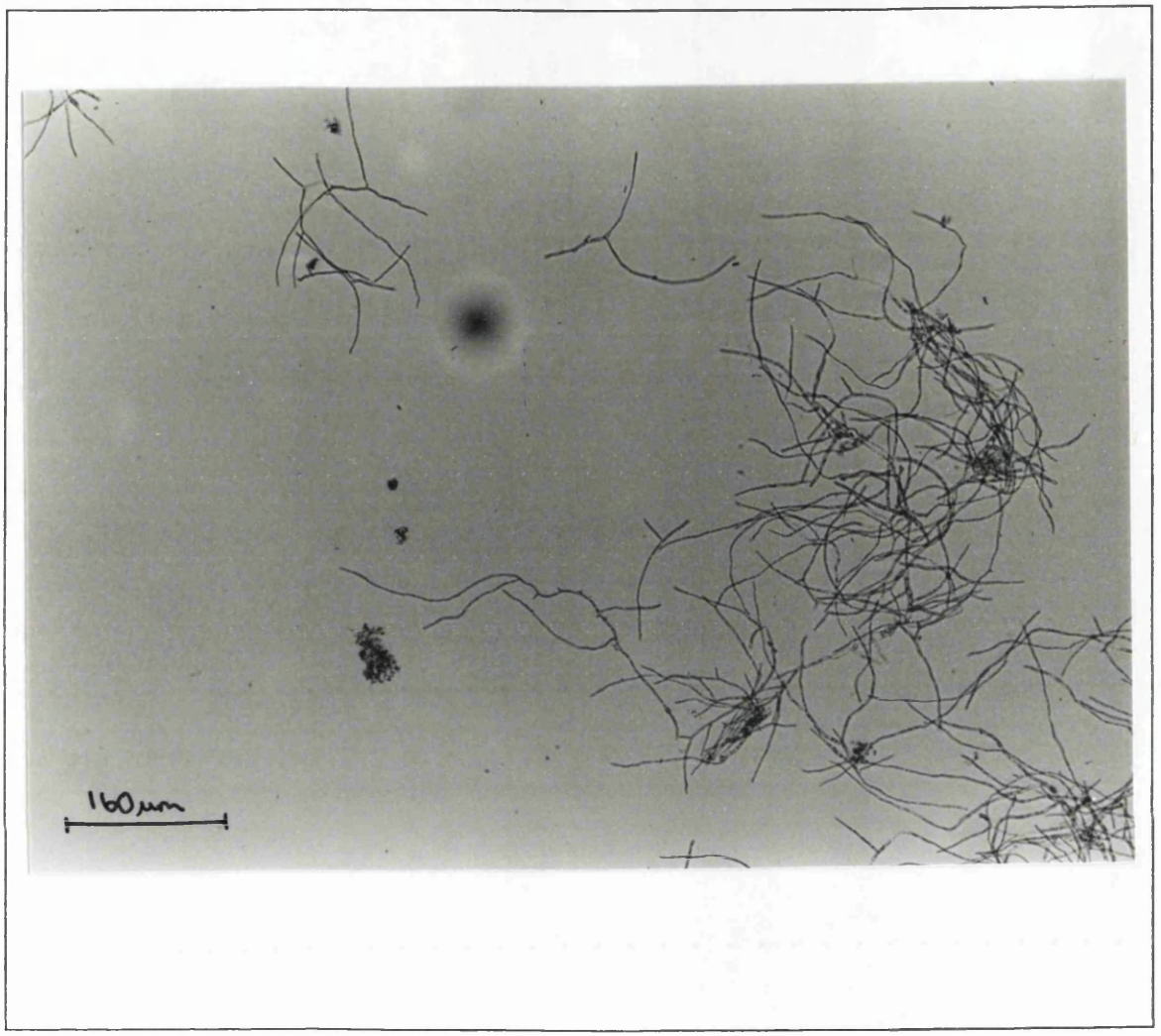

Figure 40. Typical hyphal fragments of *Penicillium chrysogenum* P-1

Figure 40 (Part 2 of 2). Typical hyphal fragments of *Penicillium chrysogenum* P-1. The fragments were generated by blending at high speed. Photograph (a) shows the unblended mycelia, and (b) the mycelia after blending for 1min at high speed. (1cm=80µm)

5.1.1.3 Discussion

The results clearly showed that blending hyphae in a high speed blender reduced the size of both strains, P-1 and NRRL1951, of *Penicillium chrysogenum* mycelial aggregates in samples of broth after only short periods of blending. These findings were in agreement with previous studies on the use of high speed blending on filamentous fungi (Savage and Van der Brook, 1946, Murase and Kendrick, 1986). For both strains, for each treatment some very small hyphal fragments were produced and as the duration of chopping increased the homogeneity of the fragments improved, as shown by the errors on the hyphal parameters (Figure 37 and Figure 38). The percentage of clumps for *Penicillium chrysogenum* NRRL1951 showed hardly any reduction with increased time of blending after the initial breakdown of the pellets. For this

strain it seemed that further blending after one minute produced only very small changes. For *Penicillium chrysogenum* P-1 though increasing duration of blending produced decreases in the size of hyphal fragments and the percentage of clumps decreased as hyphal fragments were chopped off

The results showed that blending for any length of time produced a decrease in dry weight which must be due to considerable damage occurring to the hyphae during blending. For NRRL1951 Savage and Van der Brook (1946) reported that when pellets were chopped in a Waring Blender, continuously for 2min at 10,000rpm, hyphal fragments were obtained of 1-10 cells, with a mean of 4 cells per fragment. Using microscopical observation they reported that fragmentation occurred primarily at the septa and only in approximately 20% of the fragments breakage occurred due to fracture of the cell wall. Therefore if one hundred hyphal fragments are considered then these would consist of 400 intact cells and 40 fractured cells due to loss of cytoplasm which is equivalent to a loss of 9% of the starting cells. Using a graticule on the microscope and rough estimation by eye, typical cells were found to be approximately 15μm long and therefore 4 cells would be 60μm long.

When the dry weight values obtained from this study are considered NRRL1951 lost 90% of its initial dry weight after 30s of high speed blending and 31% at low speed which is not consistent with the earlier study by Savage and Van der Brook (1946). One reason for this inconsistency could be the differences in the speed of blending used, although the actual size of hyphal fragments produced did seem to be at least 4 cells long. Also the earlier study did not measure the dry weight of the samples after blending because the purpose of the original experiment was to obtain fragments for use as a seed inoculum for fermentation so it is possible that similar effects could have occurred especially if considerable damage had occurred to the cell walls breaking them into small fragments that were not observed under the microscope. *Penicillium chrysogenum* P-1 showed a greater resistance to the blending than the NRRL1951 strain with only 16% and 20% losses at high and low speed at 30s. This result was not surprising as P-1 is a more recent strain developed for industrial purposes and thus would have been optimised to be able to grow in fermenters under high rates of shear, unlike NRRL1951 which is an early undeveloped strain. Additionally the strains had different gross morphologies in the shakeflask, NRRL1951 was pelleted and P-1 filamentous, therefore the effect of blending on the microorganisms would probably be different. The differences between the filamentous and pelleted morphologies are described in 1.0, Introduction

The aim of this study was to ascertain whether the use of blending would be a good means of breaking up aggregates into fragments to overcome sample preparation problems for biomass estimation. As there are considerable decreases in the dry weight measurements for the samples after blending this method would not be suitable for sample preparation as part of the

biomass estimation. Even if a particular duration of blending resulted in a fixed proportional loss of material for a sample the method would still not be suitable as other factors such as changes in dry weight, age of the cells and morphology would all affect the result of blending.

5.1.2 Slide Preparation

The first step in slide preparation is the dilution of the fermentation sample in fixative to get a less viscous more evenly dispersed sample for pipetting and analysis. As the aggregates in the mycelial sample could not be eliminated a method of obtaining an accurate fixed volume for analysis had to be designed around the problems caused by the presence of the aggregates. The main problem caused by the presence of aggregates is that when a small volume of material is dropped onto a surface the large mycelial particles tend to remain where they have fallen whereas the liquid fraction is able to flow. Commercially available counting chambers, such as haemocytometers, depend upon the sample being uniformly dispersed and capillary action to fill the chamber to the correct depth, ruling out their use with aggregated mycelial samples. A second standard method of particle counting using microscopic techniques is to use proportional counts with internal standards. For this the cells are counted in a specific and reproducible volume whose actual size is unknown but which includes a counting standard such as a known concentration of latex particles (Mallette 1969). With this technique it is then possible to count the cells and the counter particles in a few fields or in an area of the slide and calculate the volume measured from the standard particle count and the concentration of cells. For mycelial samples the use of such a system would pose two problems, the first is that as the suspending fluid and the mycelia disperse differently then it would be necessary to measure the whole volume used which removes one of the advantages of using this technique Secondly there would be inaccuracies in enumerating the number of particles using automated image analysis techniques as they would touch or become entrapped in the mycelial networks and the particles themselves may not uniformly disperse but cluster. This would lead to counting errors leading to inaccurate quantification of the volume and as the total volume would have to be measured anyway then the advantages of using the particles would be lost.

Rather than design a specialised chamber for biomass estimation which would have involved complex manufacture and probably considerable changes made to it as the biomass methodology was developed a simple approach was taken. A glass coverslip of 18mm by 18mm was used to provide a fixed area for analysis and then a fixed volume was pipetted onto a glass microscope slide. The volume chosen was 4µL so that the depth of liquid under the coverslip was 12.3µm and the field of view appeared two dimensional under the microscope. This depth is greater than the diameter of typical hyphae and thus allows for crossovers so that the liquid touched the two glass surfaces at all points.

To make a slide for measurement the fixed volume of 4μL was pipetted onto a clean glass slide and a coverslip was gently laid over the sample. The liquid in the sample then flowed to the edges of the coverslip (smaller volumes than 4μL would not flow to the edges of the coverslip). To prevent evaporation of the liquid from the slide the edges of the coverslip were sealed using ordinary commercial nail polish. To determine whether or not this method of slide preparation filled the requirements for volume and biomass estimation the methodology was tested.

5.1.2.1 Slide Preparation Errors

5.1.2.1.1 Method: To determine the errors of slide preparation two samples were removed from a shakeflask fermentation, as described in 3.2.4.2, Shake Flask Fermentations, at 30.5h and 90h after inoculation with spores. Ten replicated dilutions to ten fold of each sample in fixative were made. A slide was made for each of these and the quantity of mycelial material present was measured for each slide. In addition, for the sample at 90h, 10 slides were made and measured from one of the repeated dilutions.

For quantification of the material present the Magiscan MD image analysis system, running the Genias software, was used (3.1.3.1, Image Analysis Systems). The image processing used was identical to the first part of version 2 of the morphological characterisation software except that immediately after particle removal a measure of the detected area in the binary image was made and recorded (Figure 14). The environment file was calibrated for the microscope set at 100X magnification, the measuring frame was adjusted to encompass all of the image, and the scan pattern was adjusted to measure the whole of the coverslip area. The microscope illumination was set manually at the beginning of each set of 10 slides and this value was maintained during processing of the each set of samples. The morphology of the diluted samples at 90h and 30.5h was also characterised using version 2 of the software running fully automatically.

5.1.2.1.2 Results: The detected areas measured for the amount of material present on each slide for the repeated slide preparations and the slides of the repeated dilutions are shown in Table 17. Statistical analysis, using one way analysis of variance at the 95% confidence level, showed that there were no significant differences in the distribution of material on the slide for the repeated dilutions and slide preparations. The F_{crit} value (for 10 degrees of freedom and a sample size of 2550) at the 95% confidence level was 1.88 and the values for the repeated dilutions for $F_{(10,2540)}$ were 0.36 and 0.5 for the repeated dilutions of the samples at 30.5h and 90h respectively, and for the repeated slide preparations 1.4. For the sample at 90h the % error of pipetting material onto the slide, at the 95% confidence level, was 8.3% and for the dilutions was 7.3%. For the young cells (30.5h) the error of dilution was 4%. The percentage of material in the form of aggregates was 76% for the sample at 30.5h and 96% for the sample at 90h.

Table 17. Total detected area of mycelial material for repeated slide preparation and repeated dilutions.		
10 dilutions at 30.5h (μm^2)	**10 dilutions at 90h (μm^2)**	**10 slides at 90h (μm^2)**
$4.41x10^5$	$1.41x10^6$	$2.75x10^6$
$4.27x10^5$	$1.77x10^6$	$3.05x10^6$
$4.52x10^5$	$1.60x10^6$	$2.69x10^6$
$4.68x10^5$	$1.73x10^6$	$3.26x10^6$
$5.04x10^5$	$1.60x10^6$	$2.63x10^6$
$4.97x10^5$	$1.86x10^6$	$3.20x10^6$
$4.64x10^5$	$2.00x10^6$	$2.75x10^6$
$5.01x10^5$	$1.78x10^6$	$2.65x10^6$
$4.55x10^5$	$2.08x10^6$	$3.07x10^6$
$4.23x10^5$	$1.55x10^6$	$2.57x10^6$

5.1.2.1.3 Discussion: The repeated dilutions and slide preparations showed that the major error in the sample preparation was due to the placement of the 4µL sample onto the slide. The dilution error was masked by the error of pipetting onto the slide. The pipetting device used, a Gilson Pipetman™ P20 pipetter, would have contributed ±2% error for repeated dispensing of the volume used, according to the manufacturers reference data. The sample at 90h showed a larger error than the one at 30.5h due to the different morphologies of the samples. The mycelia at 90h showed a considerable degree of entanglement and clumping whereas at 30.5h the mycelia consisted of mainly loose individual organisms. Therefore the material in the diluted sample at 30.5h was more evenly dispersed than that of the sample at 90h which accounts for the different errors for pipetting a small volume (4µL) of each sample. The dry cell weight of the sample at 30.5h was 2.19g/L and at 90h it was 4.56g/L.

Notably the total values for the 10 repeated slide preparations at 90h are higher than those for the the repeated dilutions for the same sample even though they were taken from one of the dilutions. This is due to the manual setting of the lamp. The lamp is adjusted using a knob until a needle reaches a point on a scale. This adjustment is obviously not accurate enough so for the estimation of biomass the light level must be set and controlled precisely.

As there were no significant differences between the repeated slide preparations and dilutions then this methodology for sample preparation is suitable for use for biomass estimation. The error on the biomass estimations due to sample preparation using image analysis was therefore assumed to be approximately ±8.4%.

5.2 Estimation of Hyphal Volume and Biomass

An indirect method of measurement of cell volume and biomass has been established by Nestaas and Wang (1981) for *Penicillium chrysogenum* grown in a medium containing few solids. Nestaas and Wang (1981) developed a "Filtration Probe" and through a theoretical analysis of the filtration behaviour of the mycelia were able to estimate mycelial cell volume. Also from the filter cake volume the total cell mass could be estimated. The "Filtration Probe" is reviewed in 1.5.1.4, Wet Weight and Cell Volume. However the "Filtration Probe" does not provide a direct measurement of cell volume and morphology. Therefore a methodology using image analysis has been devised for the direct quantification of mycelial differentiation and measurement of cell volume. This results additionally in an estimate of biomass in the fermentation.

Nestaas and Wang (1983) assumed two cell types were present during the penicillin fermentation:-

1. the "healthy" cells completely filled with cytoplasm,
2. the degenerated cells from which the cytoplasm had been lost.

However, when samples of *Penicillium chrysogenum* are observed using light micros copy the cells are seen to be undergoing a gradual process of degeneration as increasing vacuolisation is observed within the hyphae until eventually the cells consist of empty cell walls. The growth and structure of hyphae is reviewed in 1.2, Fungal Growth Therefore it was decided to take the intermediate stages into account by using image analysis techniques to pick out the large vacuoles in the cells, so two regions of hyphae are defined to describe the growth of mycelia during fermentation.

1. The cytoplasmic region, which contains all of the "healthy" cells and the partially "healthy" cells (partially degenerated) but large vacuoles are excluded from this region.
2. The degenerated region, which contains all of the cells without cytoplasm and the large vacuoles.

The hyphal regions are shown in Figure 41.

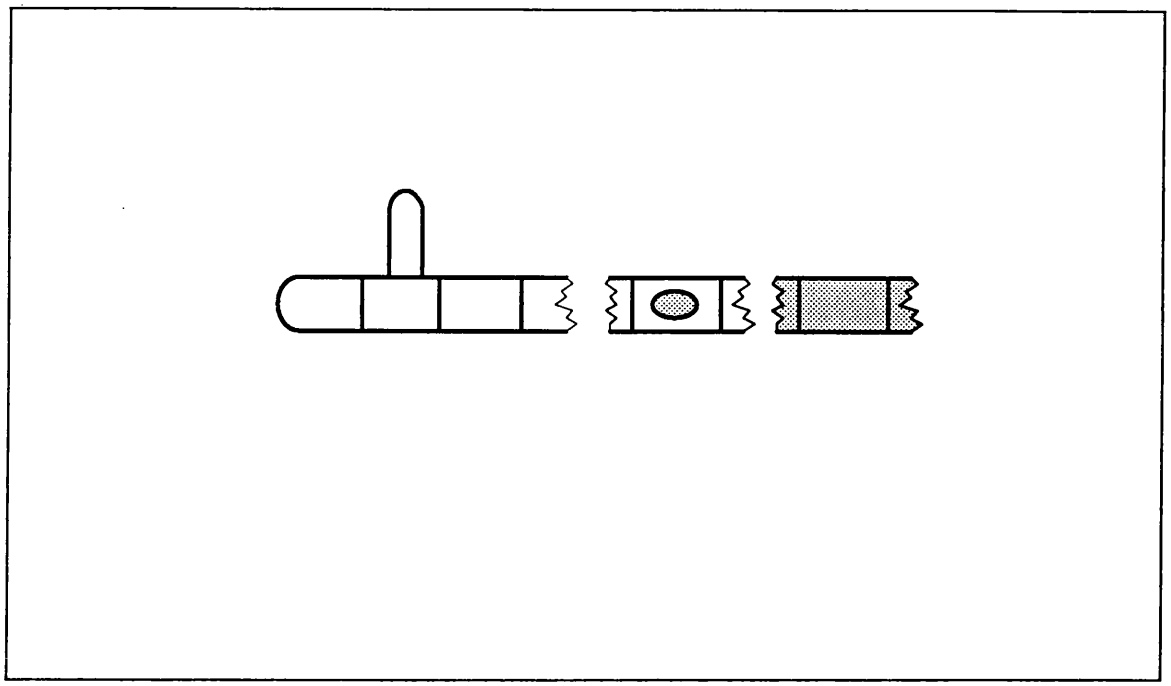

Figure 41. The regions of hyphal differentiation during the penicillin fermentation.. The shaded areas comprise the degenerated regions and the unshaded the cytoplasmic regions.

5.2.1 Methods

The software for the measurement of the hyphal regions consists of a series of task lists created in and running under the Genias (Joyce Loebl) general purpose developmental software (3.1.3.1, Image Analysis Systems). By using the task lists it was possible to make changes to the image processing techniques used by the selection of suitable algorithms from the available menus and incorporate these into the task lists without considerable software programming effort. For all of the methods the Magiscan MD image analysis system was used with the microscope and automatic stage described in 3.1.3.1, Image Analysis Systems.

5.2.1.1 Measurement of Hyphal Regions

5.2.1.1.1 Setup: The microscope was set for brightfield illumination and the magnification was set at 100 times. The system was calibrated to convert pixels to microns as described in the setup for version 1 of the morphological characterisation software (4.1.2, Set-up). The measuring frame was set to encompass the whole of the image and the movement of the stage was defined to move to abutting frames and the number of fields to be measured was specified so that the whole of the coverslip area was analysed. Also automatic light control was set which allowed the user to set a value for the light level which was maintained by the software throughout a measurement run. The lamp is controlled by use of a scale ranging from 0 (dark) to 60 (bright), the operator incrementally adjusts the lamp level until it reaches the required

value. The process of adjustment is not straightforward as the lamp level tends to under and over shoot the desired value and will often decrease by a level during processing. Throughout this study the lamp level was at 49 ±2 at the start of each processing run. As the level of brightness directly influences the thresholding it is essential that it is stable during processing. The settings were then stored in an "environment" file which was used for all measurements of the hyphal regions. The file was read at the start of each analysis run.

Once the environment file was read then the field of view at the first corner of the coverslip was located and focused, the light level was selected, then the field at each corner of the coverslip was focused by the operator and the light level was checked. A focus grid was determined automatically to take into account any differences across the region of the coverslip. Also a data file for the measurements was set up. Then the processing phase started.

5.2.1.1.2 Processing: Following set up the first grey image was digitised. Shading correction was then applied. When an image is generated by a TV camera viewing an illuminated scene there is generally an effect known as shading present. This causes the system to record different grey levels at different positions in the image even though the object being viewed is of uniform brightness. On the image analysis system used in this study any shading present was due to uneven illumination across the microscope fields. Shading correction was used to eliminate shading from the image. First an image of an empty field using a clean glass slide was captured and stored. The grey values of this image were then analysed by the system and the range of intensity variation of the shade image is obtained. This was used to appropriately scale the pixel intensities of the image of the sample. For example if a shade image had a highest pixel intensity of twice the lowest then the pixels of the image to be corrected would be multiplied by numbers varying between 1 and 2 in order to correct the shading. The same corrected image was used for all of the samples as the microscope was not adjusted during this study. Once shading correction was completed the image of the sample was captured, i.e. frozen for further processing.

The captured image was thresholded to create a binary image. For measurement of the total area the captured image was thresholded so that all of the fungal material was included in the binary image whereas for the measurement of the cytoplasmic region the threshold level excluded large vacuoles and lysed regions from the binary image. For this system the threshold was set at 0 to 54 for the total region and at 0 to 49 for the cytoplasmic region. However these values are system specific and would not necessarily even apply to another Magiscan MD system. The threshold values would also be dependent on the nature of the biomass used, such as the species of the fungus.

Once thresholded the binary image contained particles other than the microorganisms due to undissolved media ingredients or particles in the suspending liquid. For fermentations using defined media or low concentrations of corn steep liquor then a simple circularity parameter was used to eliminate the particles (4.1.3.1, Initial). This was set for removal of particles of a circularity greater than 0.35 as in version 2 of the morphological characterisation software. However during the establishment of the biomass estimation a lactose/Pharmamedia fermentation was also used which contained 30g/L of undissolved solids after sterilisation when analysed for dry weight using filtration. In the samples from this fermentation medium particles often became entrapped in the mycelia aggregates and additional processing was required to eliminate these.

For this, after the image was captured it was thresholded to detect the very dark regions within the media particles by setting a threshold to select grey levels 0 to 26. Crossovers in the mycelial network also often appeared dark and had grey values within this range therefore it was necessary to eliminate these by removing any objects of less than 25 pixels which was smaller than the dark regions in the media solids. Then the binary image was dilated by the addition of pixels to the objects in the binary image. This process enlarged the dark regions within the medium particles to encompass the whole of the particles. For this on the first pass every pixel that had the initial value of one is replaced by a 3 by 3 pixel cross and on the second pass every pixel is replaced by a 3 by 3 pixel solid box. This enlarged the thresholded dark regions to the size of the whole solids particles. However some pieces of mycelia were still present in the binary image of the solids so these were measured in a typical image and it was determined that the sizes of the thresholded mycelial fell into two categories:-

1. area between 290 to 800 pixels and circularity 0.2 to 0.8
2. area between 200 to 400 pixels and circularity 0.75 to 1.0.

So these values were used to eliminate the unwanted mycelial particles from the image. The binary image containing the solids particles from the mycelial network was stored in the image memory.

The captured image was thresholded for the total or cytoplasmic hyphal regions and the particle elimination parameter of all objects greater than a circularity than 0.35 was applied. The image also included some large particles without dark regions which were removed using area greater than 1000 pixels and circularity greater than 0.2. The stored binary image containing the particles from the mycelial networks was then subtracted from this binary image to eliminate all of the media particles. Once the images were cleaned of undesired media particles then the measurement phase started. Flow diagrams of the algorithm used for analysis of the samples are shown in Figure 42 and Figure 43. Figure 42 shows the overall structure for both applications, with and without considerable quantities of undissolved media solids. However the processing phase changes depending on the application and the different phases are shown in

Figure 43. For the media without undissolved solids just Phase 1 is inserted into the processing phase. For the lactose/Pharmamedia fermentation first Phase 2 was carried out, then Phase 1 and finally Phase 3 during each processing run.

5.2.1.1.3 Measurement: The detected area of the remaining objects, the hyphae, in the binary image was measured. For this all of the pixels remaining switched on in the binary image were summed and the scale factor was applied to convert them into square microns. The value for each field was recorded in the data file. Once the pixels were summed the microscope stage moved to the next field and processing commenced again. This was repeated until each field had been measured and thus the whole of the coverslip region. Using the statistical package, Results, the sum of all of the field areas was found.

5.2.1.2 Hyphal Diameter Measurement

The average hyphal diameter was measured manually by touching two opposite points on the hyphal wall in a captured image using a light pen. The microscope magnification was set at 400 times and the hyphae were selected randomly. The inter-point distance was then calculated by the software and stored in a data file for later analysis. The process was repeated at least 100 times using new positions on the same and on different hyphae.

5.2.1.3 Volume Estimation

If a hypha is regarded as a solid cylinder then the volume of the hypha can be expressed as:-
Volume=(Π x hyphal diameter x Area)x 0.25

The volume was calculated for the total hyphae and the cytoplasmic regions. The degenerated region was calculated as the difference between them. The sample dilution factor was then taken into account and the results converted into cm^3 of cell volume per L of fermentation broth.

5.2.1.4 Biomass Estimation

Once the volumes of the regions had been measured then it was possible to convert these into dry weight estimations. The values of hyphal densities (g dry weight/cm^3 of cell volume) for *Penicillium chrysogenum* are available in the literature. For cytoplasmic regions it is 0.35g/cm^3 and for the degenerated regions 0.18g/cm^3 (Nestaas and Wang 1983). Therefore the volumes can be converted to biomass using the formula in Figure 44

Dry Weight (g/L) = (volume of cytoplasmic region (cm^3/L) x 0.35(g/cm^3))
+ (volume of degenerated region (cm^3/L) x 0.18(g/cm^3))

Figure 44. Dry Weight Calculation

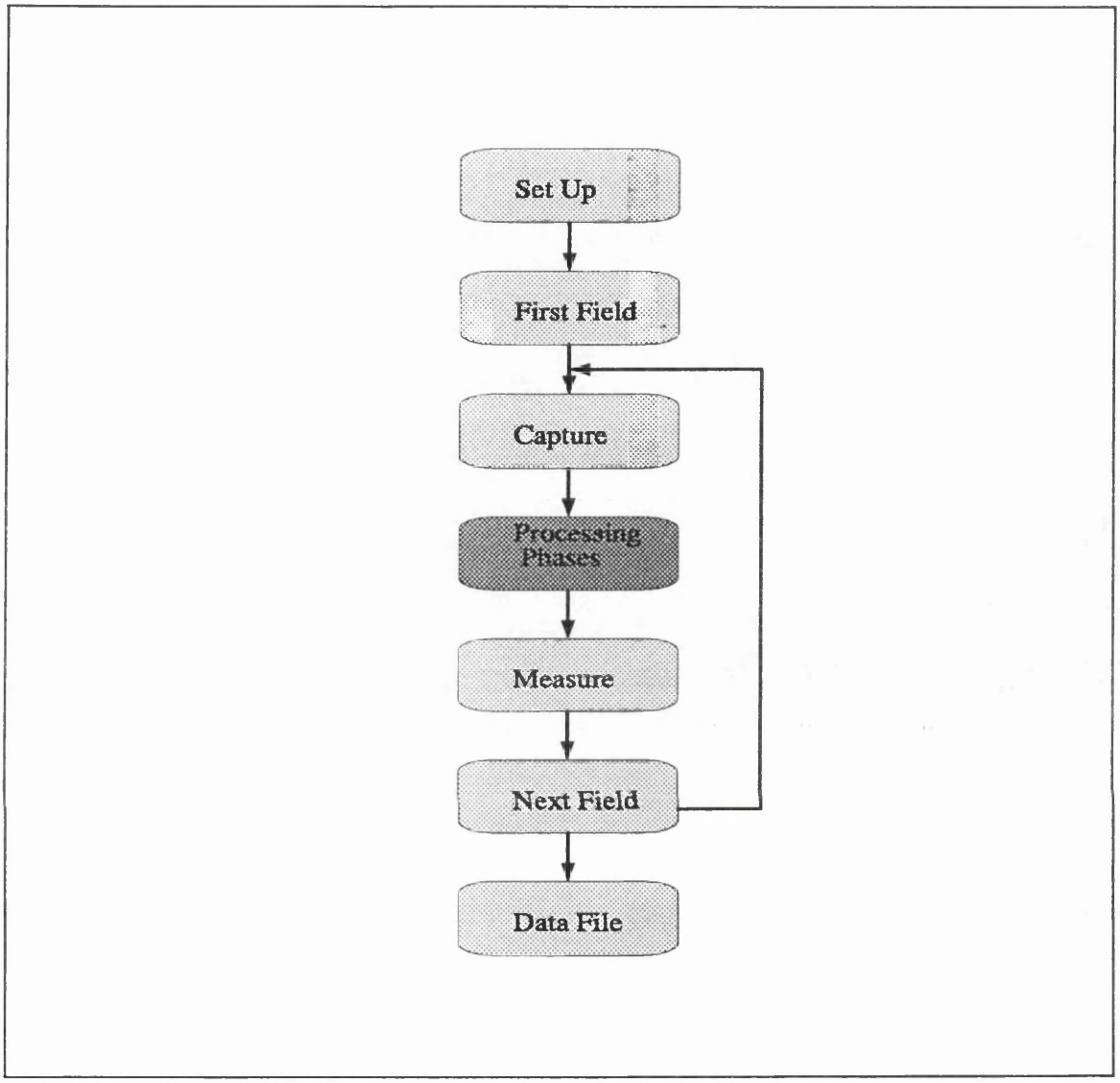

Figure 42. The overall algorithm of the biomass estimation software

5.2.1.5 Hyphal Density

The mean hyphal density for each sample was calculated as the ratio of biomass estimated from image analysis and total cell volume.

5.2.1.6 Fermentation

Penicillium chrysogenum P-1 was grown as a batch culture using defined media and a Lactose/Pharmamedia production medium as described in 3.2.4.5, Lactose/Pharmamedia Fermentation. Two fermentations were carried out using defined medium (with glucose as a carbon source) in a 5L fermenter, fermentation A at 26°C and the other, fermentation B, at 30°C, to get different growth profiles. A third fermentation in a different defined medium (with

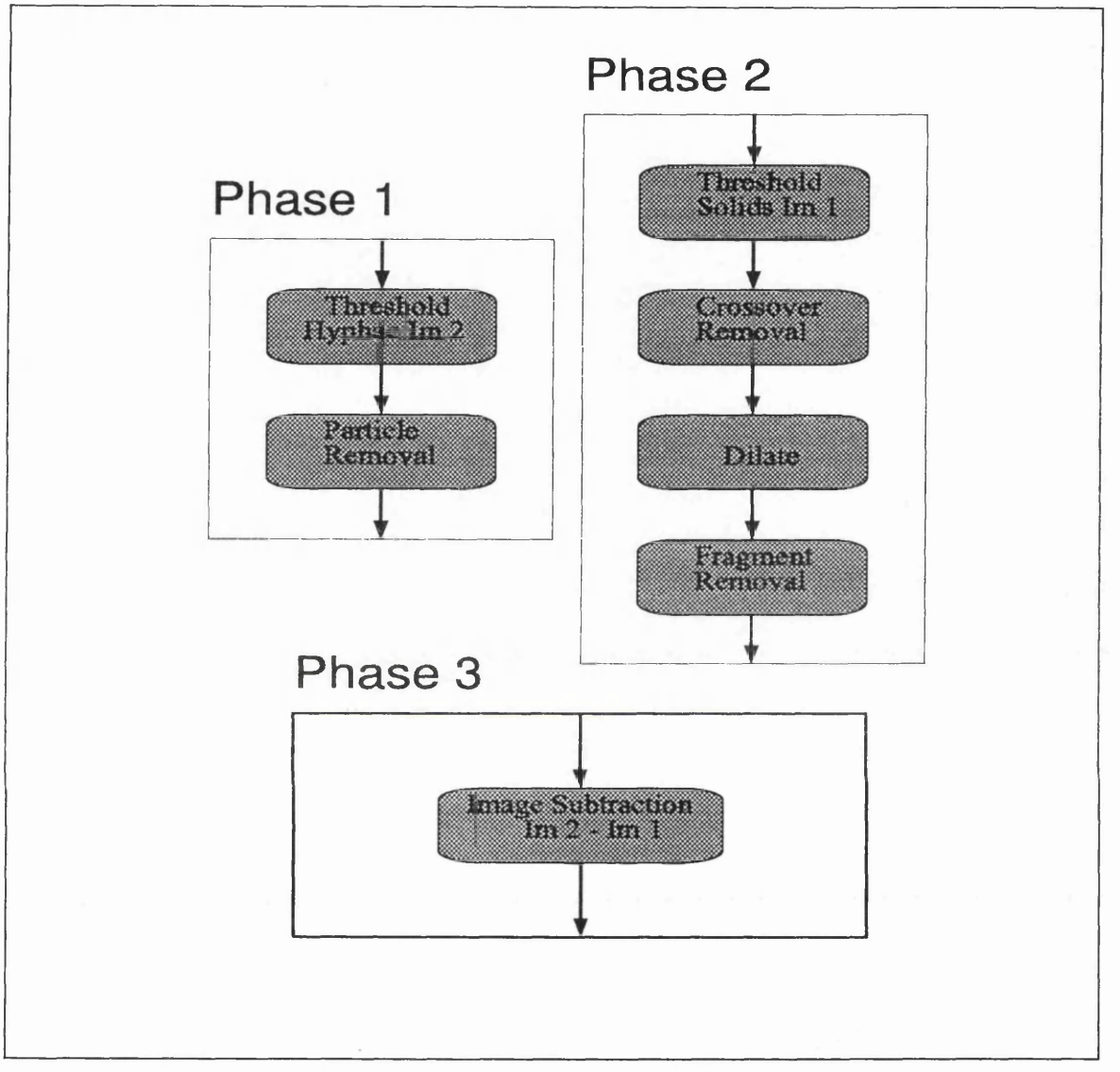

Figure 43. The processing phases of the biomass estimation software

sucrose and lactose) was carried out in a 100L fermenter (3.2.4.3, Fermentations Without Undissolved Solids). The lactose/Pharmamedia production medium contained 30g/L of undissolved solids post-sterilisation, measured using the filtered dry weight technique (3.2.6, Conventional Dry Weight Assay). *Penicillium chrysogenum* P-2 was grown in fed-batch culture (3.2.4.4, Fed-batch Fermentation). This medium contained 2.5g/L of undissolved solids post-sterilisation. Samples were removed from the fermenters at timed intervals for biomass estimation using the image analysis method described above and conventional filtered dry weight.

5.2.1.7 Sample Preparation

Samples from the fermentation were mixed immediately with an equal volume of fixative. The fixed sample was further diluted with fixative to 10 fold or in the presence of solids to 20 fold. A duplicate set of samples was obtained from the defined medium fermentation. These were combined with a pre-inoculation sample of lactose/Pharmamedia medium and diluted to give a final concentration of undissolved solids equivalent to that of a 20 fold dilution of samples taken directly from the lactose/Pharmamedia fermentation. During this process the defined media samples were diluted 20 fold. A slide was then prepared as described previously (5.1.2, Slide Preparation).

5.2.1.8 Morphological Characterisation

The morphology of all of the samples was characterised using Version 2 of the software (4.2, Morphological Characterisation Version 2). This was set for fully-automatic measurement. Approximately 100 microorganisms were measured for each sample.

5.2.2 Results

Figure 45 shows the relationship between the dry cell weight estimated by image analysis and measured by conventional filtration for the pooled samples of all the fermentations except for the lactose/Pharmamedia fermentation. The relationship shown is the line of best fit through the data which has a slope of 1.01 and the intercept is at 0.08. The data has a correlation coefficient of 0.99 at the 95% confidence level.

The time course of biomass measured by the filtration method and estimated by image analysis for fermentation A in the defined medium at 26°C is shown in Figure 46. Figure 47 shows the time courses of the biomass for each of the hyphal regions, total, cytoplasmic and degenerated, estimated by image analysis. The cell volumes of each of the regions are shown in Figure 48. The dry weight profiles (Figure 47) show that after germination rapid growth occurred until 52h. During this growth phase the biomass of the cytoplasmic region was slightly less than that for the total hyphae as some vacuolisation tends to always be present although the biomass of the degenerated region was very low (0.26g/L maximum). After 52h the total biomass decreased due to the onset of lysis and death of the cells. During this phase the biomass of the cytoplasmic region decreased rapidly as the contents of the cells were lost, so the cytoplasmic curve diverged from the total biomass curve. As the contents of the cells in the cytoplasmic region are lost then empty cells are formed which is shown by the increase in the biomass of the degenerated region. The cell volumes of the regions (Figure 48) show similar trends to the dry weight profiles, however unlike the total biomass the total cell volume does not decrease at the onset of cell lysis and death as the hyphal walls stay intact as the cells are broken down.

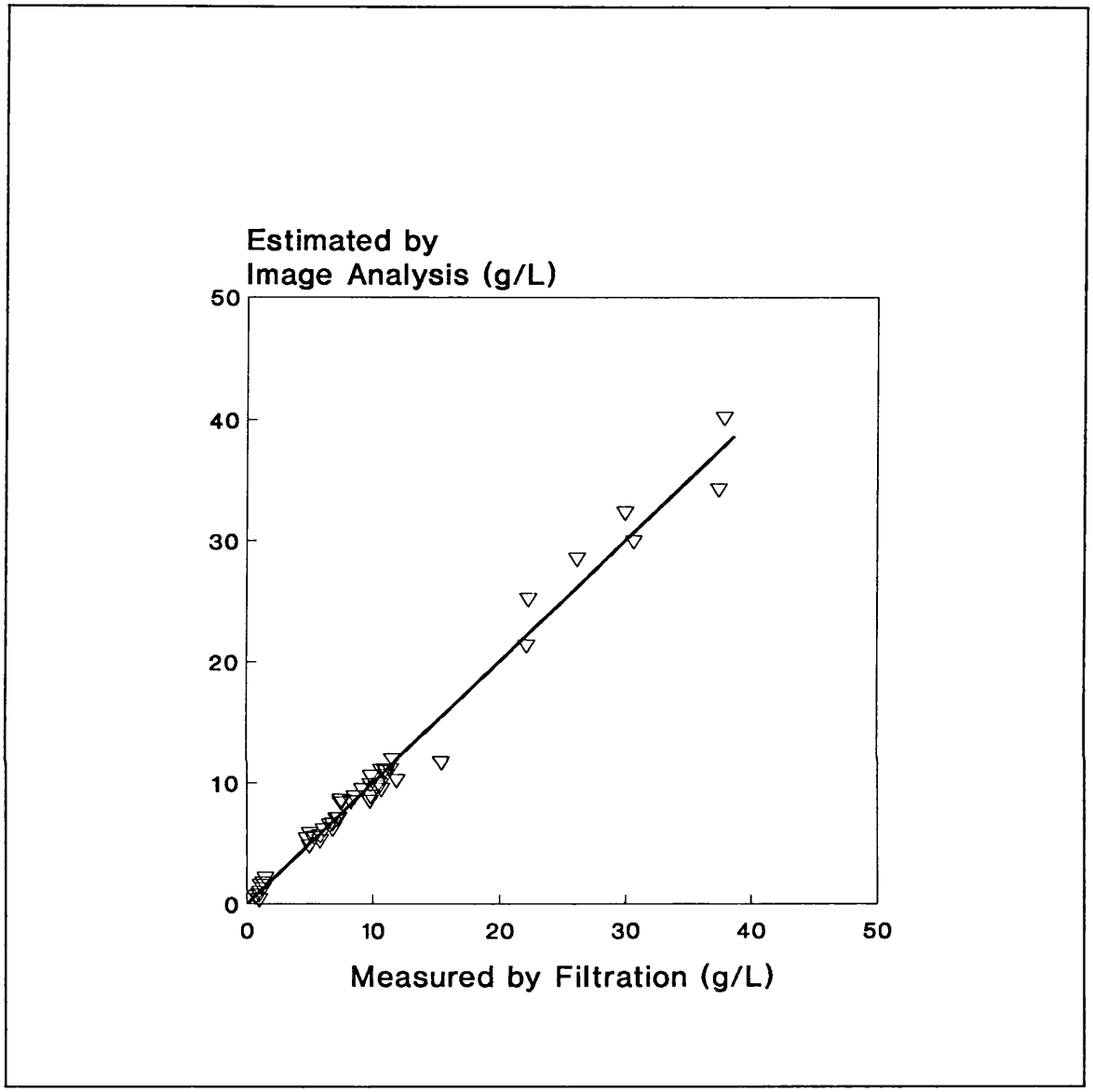

Figure 45. The relationship between the methods for dry cell weight. The dry cell weight estimated by image analysis and measured by filtration is shown.

The calculated hyphal density is also shown in Figure 48 and decreases steadily during the fermentation as the volume of the degenerated region increases. The mean hyphal diameters for fermentation A are shown in Table 18.

The means for total hyphal length and percentage of clumps for the time course of fermentation A are shown in Figure 49. The other morphological parameters, the mean number of tips, the mean main hyphal length and the mean hyphal growth unit, are shown in Table 18. The mean total hyphal and main hyphal lengths increased during the growth phase until 45h after which fragmentation occurred resulting in the decrease of the mean lengths and number of tips of the

mycelial particles. The occurrence of fragmentation coincided with the onset of vacuolisation and lysis (Figure 47).

Table 18. The morphological parameters for the time course of fermentation A.

Time (h)	Mean Hyphal Diameter (μm)	Mean Main Hyphal Length (μm)	Mean Hyphal Growth Unit	Mean Number of Tips
25.0	4.8	105.9 ± 15.3	45.8 ± 5.7	2.9 ± 0.3
28.5	4.5	148.1 ± 20.0	45.8 ± 6.4	3.5 ± 0.4
44.8	5.0	203.6 ± 35.4	59.5 ± 12.7	3.5 ± 0.5
52.3	4.6	96.0 ± 7.1	43.1 ± 4.1	2.7 ± 0.2
76.3	4.3	80.4 ± 5.1	29.7 ± 1.1	2.6 ± 0.1
93.3	3.5	79.9 ± 4.4	28.1 ± 0.7	2.6 ± 0.1

In the second fermentation, B at 30°C, a different time course of biomass with slower growth was obtained (Figure 50) when measured by filtration and estimated by image analysis. Figure 50 also shows the dry weight profile obtained when lactose/Pharmamedia medium (to a final concentration of 30g dry weight/L of solids) was added to samples from fermentation B. The biomass measurements obtained using image analysis were unaffected by the presence of non-dissolved medium solids. Figure 51 shows the dry weight profiles for the hyphal regions and Figure 52 shows the cell volumes for the regions, for fermentation B. This fermentation was stopped before the onset of cell death. The profiles show that growth occurred throughout the time course with the occurrence of some vacuolisation during growth. The total and cytoplasmic cell volumes were equivalent until 47h after which they diverged due to the onset of vacuolisation which increased rapidly from 2.26cm^3/L at 46h to 9.48cm^3/L. The amount of vacuolisation as shown by the degenerated cell volume and biomass did not increase further after approximately 51h. The average hyphal density is also shown for fermentation B (Figure 52), initially this as at 0.35g/cm^3 but, as the profiles of volume diverged, it fell to 0.31g/$cm^3$for the remainder of the fermentation. The measurements of the mean hyphal diameters for fermentation B are shown in Table 19. The measurements of the morphological parameters for the time course of fermentation B are shown in Figure 53 and Table 19. Once again the occurrence of fragmentation coincided with the onset of vacuolisation and lysis of the cells after 47h.

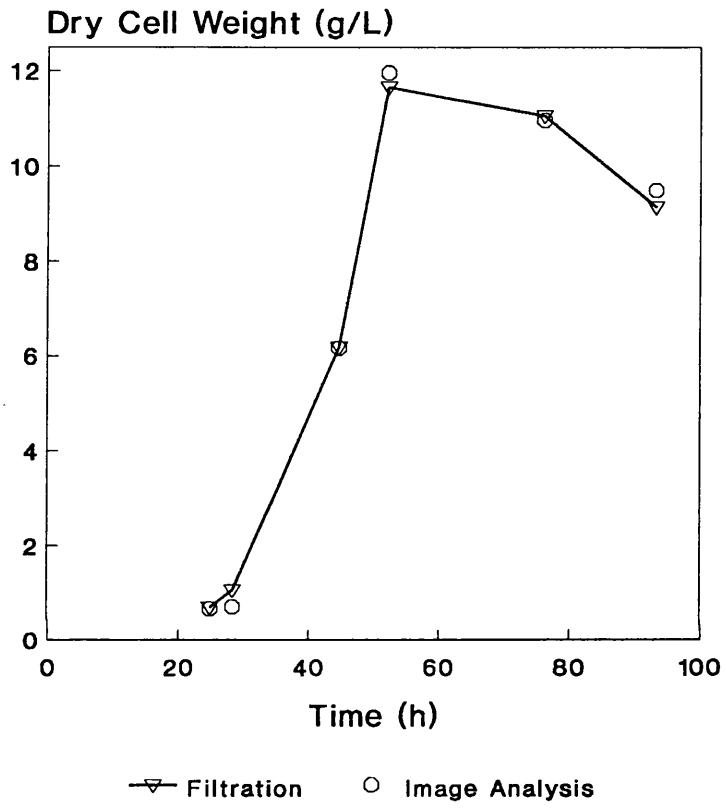

Figure 46. Time course of biomass for fermentation A. The biomass estimated by image analysis and measured by filtration is shown.

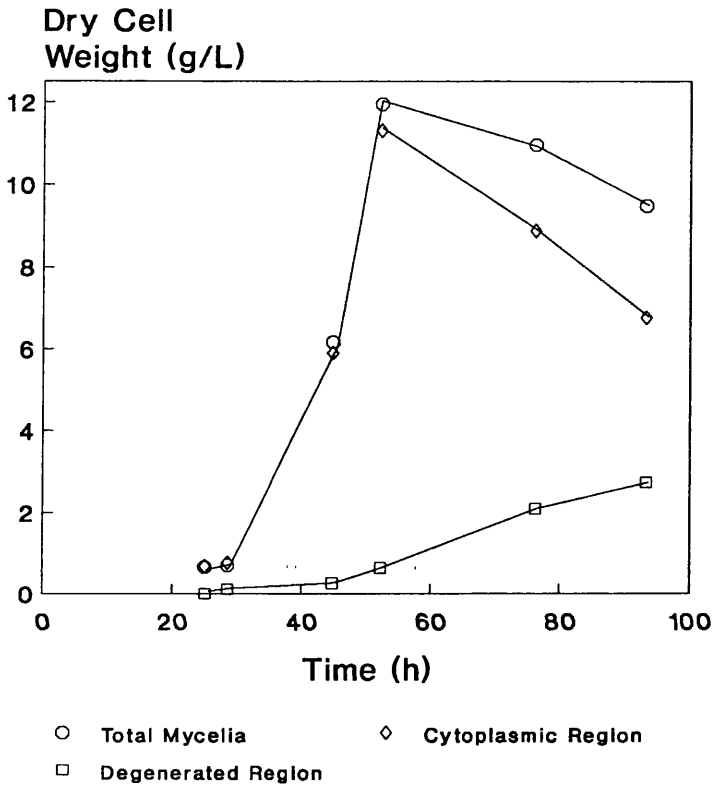

Figure 47. The biomass of the hyphal regions for fermentation A. The biomass estimated by image analysis for the total, cytoplasmic and degenerated regions is shown .

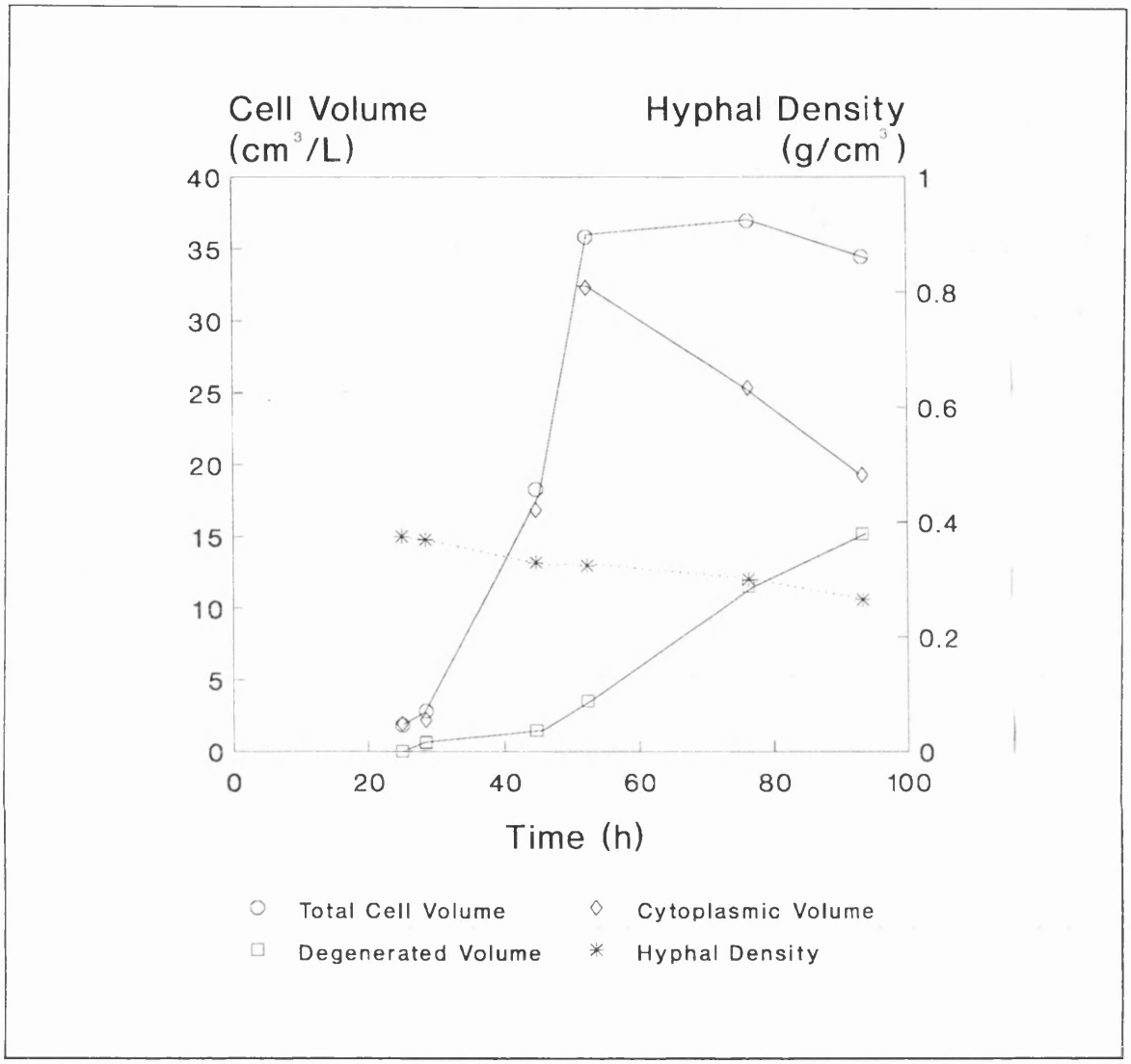

Figure 48. The cell volumes of the hyphal regions for fermentation A. The volumes of each of the hyphal regions measured by image analysis are shown.

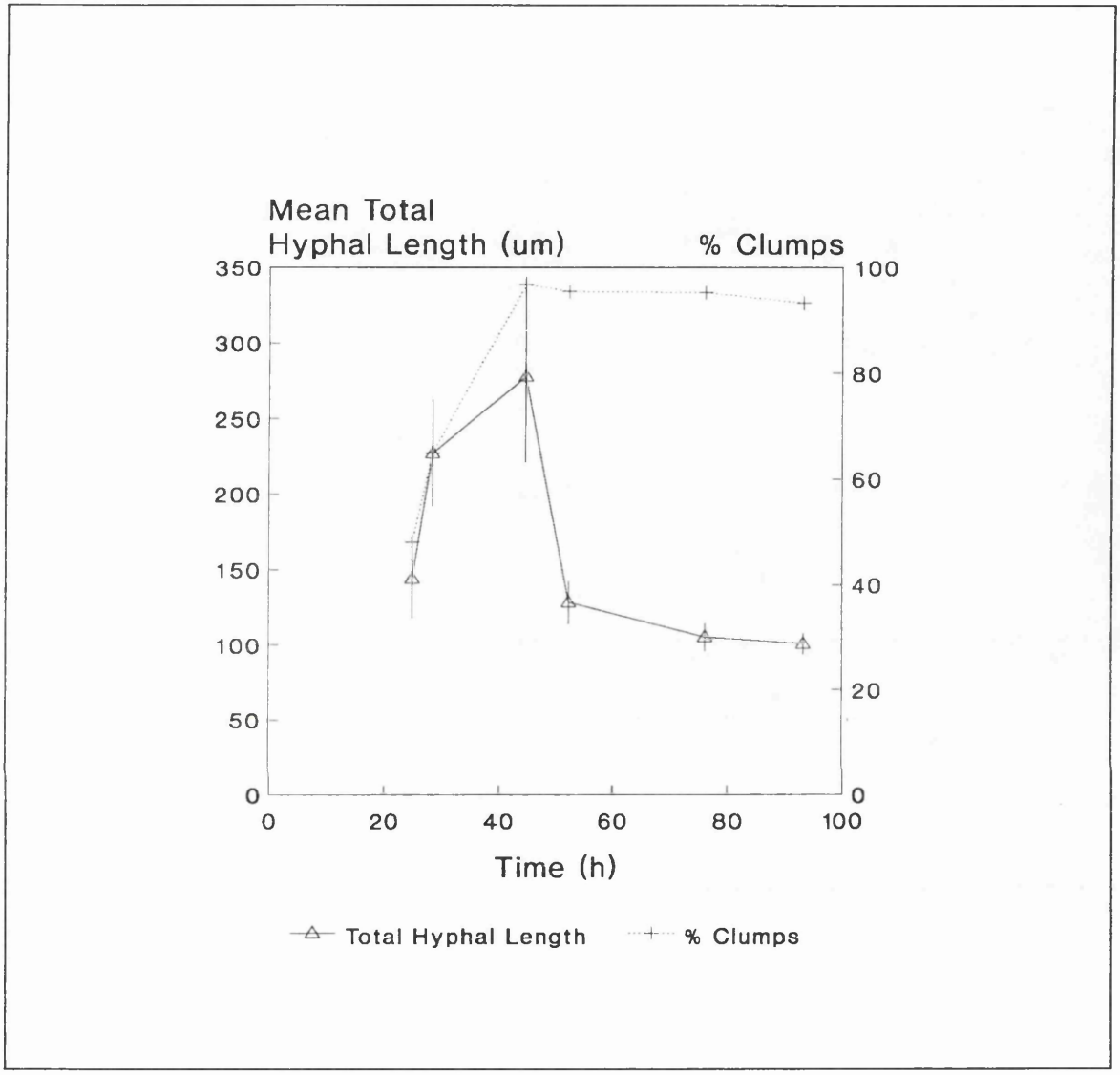

Figure 49. The mean total hyphal length and number of tips for fermentation A.

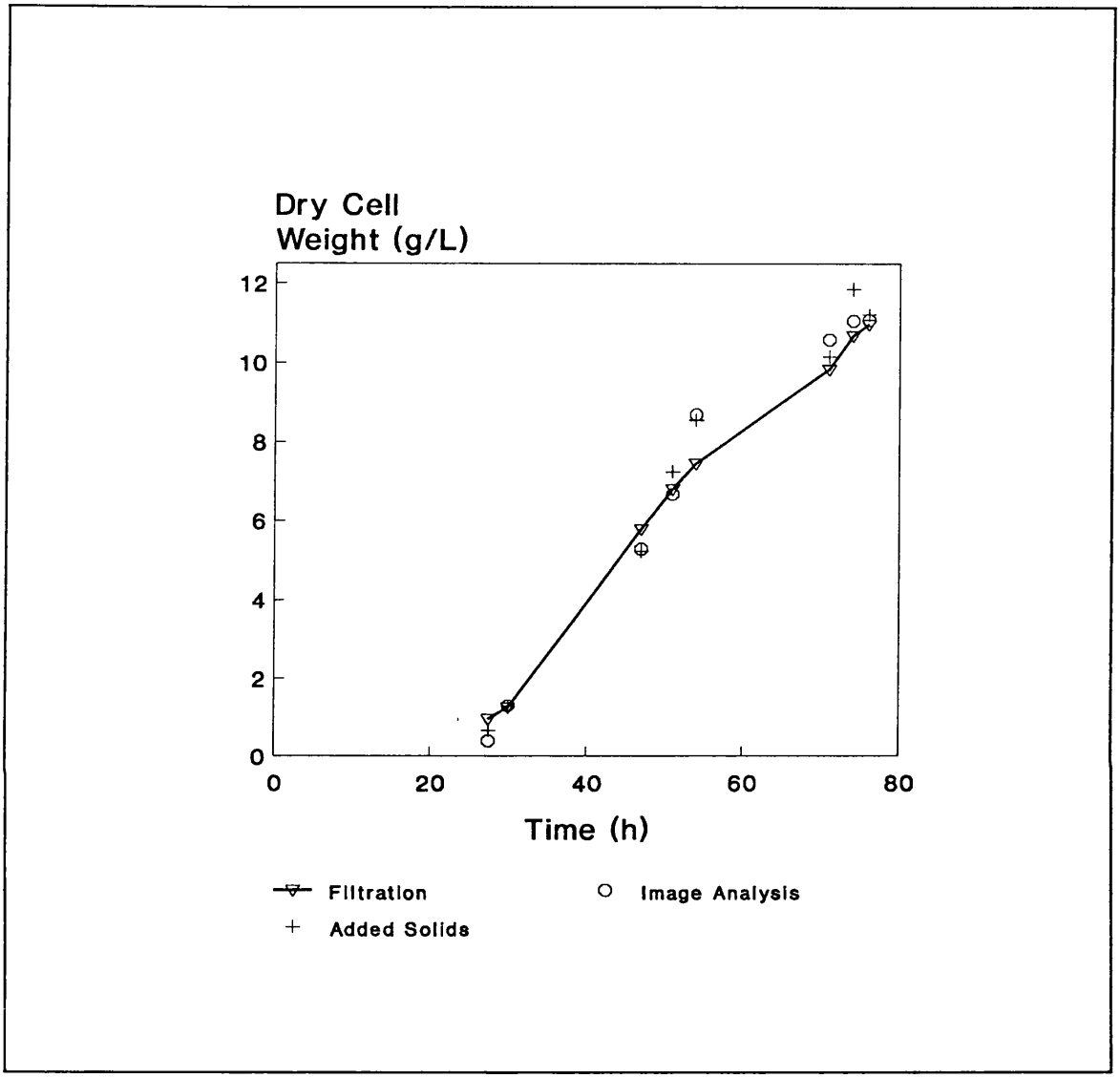

Figure 50. Time course of biomass for fermentation B. The biomass measured by filtration and estimated by image analysis is shown.

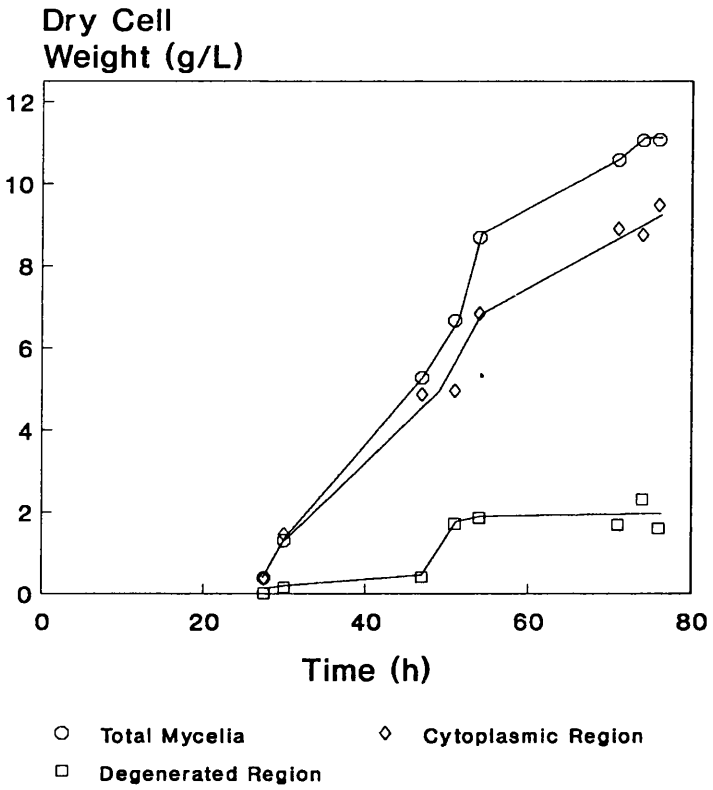

Figure 51. The biomass of the hyphal regions for fermentation B. The biomass of the hyphal regions estimated by image analysis is shown.

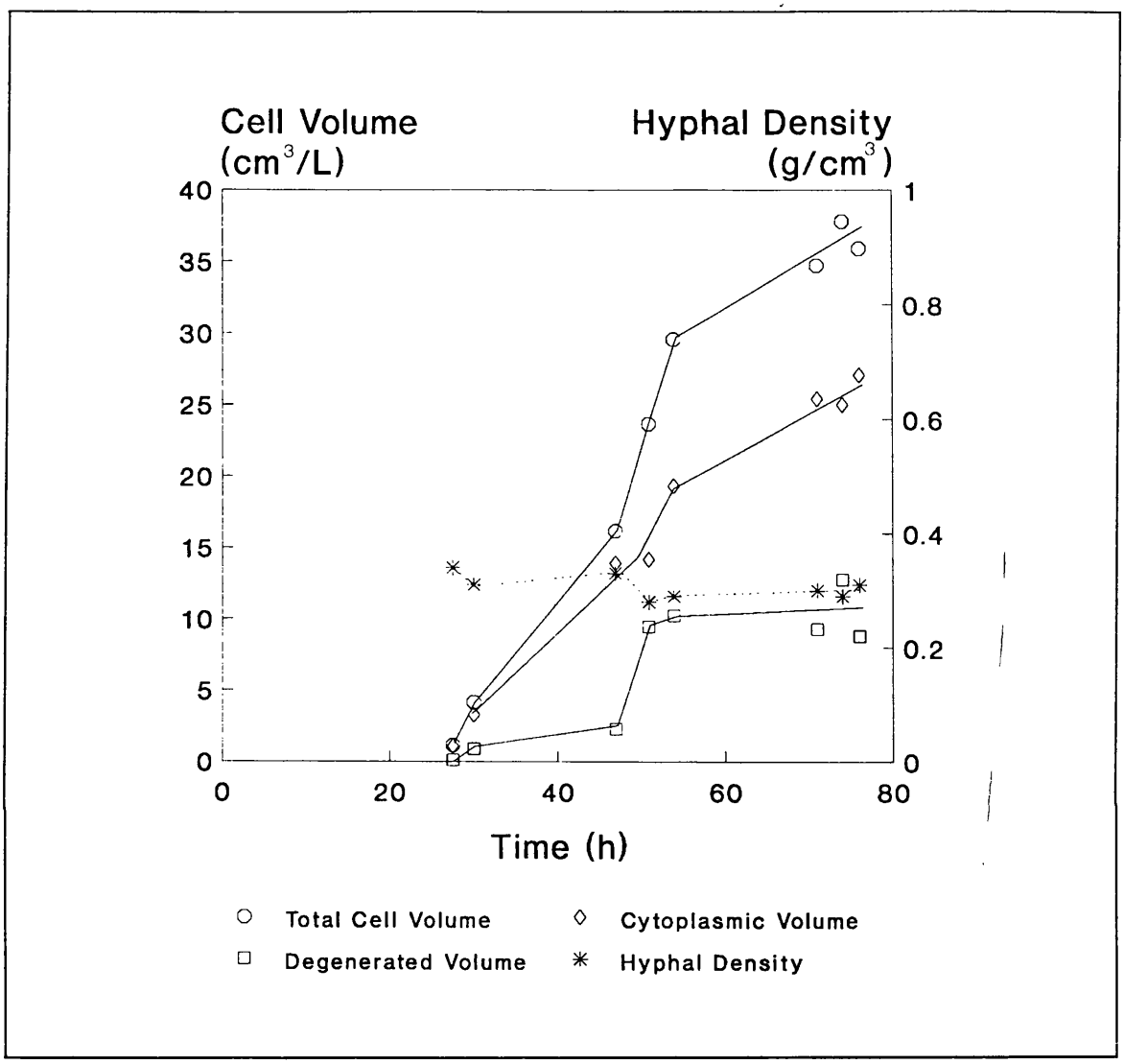

Figure 52. The cell volumes of the hyphal regions for fermentation B. The cell volumes and the hyphal density measured by image analysis are shown

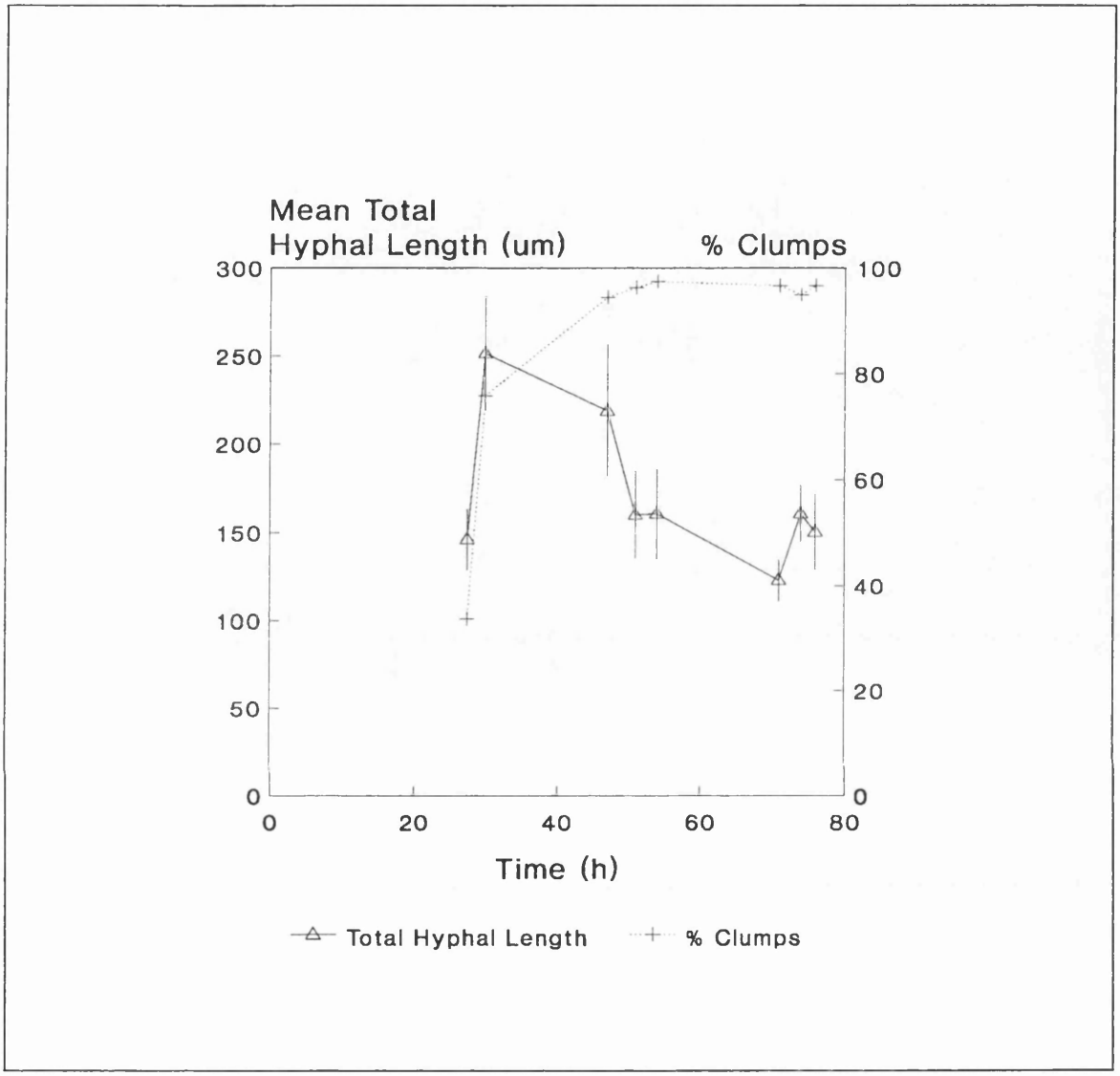

Figure 53. The mean total hyphal length and number of tips for fermentation B.

Table 19. The morphological parameters for fermentation B				
Time (h)	**Mean Hyphal Diameter (μm)**	**Mean Main Hyphal Length (μm)**	**Mean Hyphal Growth Unit**	**Mean Number of Tips**
27.5	4.4	104.3 ± 10	28.9 ± 2.9	3.1 ± 0.2
30	4.7	140.3 ± 14.4	55.6 ± 4.6	4.2 ± 0.4
47	5.2	147.2 ± 21.1	58.4 ± 6.2	3.3 ± 0.3
51	5.2	122.6 ± 15.2	49.8 ± 4.6	2.8 ± 0.2
54	4.8	115.4 ± 14.6	49.2 ± 4.8	2.9 ± 0.2
71	4.4	90.9 ± 6.7	41.2 ± 2.1	2.8 ± 0.1
74	4.3	110.9 ± 8.8	46.6 ± 2.4	3.1 ± 0.2
76	4.5	108.4 ± 12.8	44.5 ± 3.2	3.0 ± 0.3

Figure 54 shows the time course of biomass for the 100L fermentation in defined medium measured by filtration and estimated by image analysis. The profiles of biomass and cell volumes for the hyphal regions are shown in Figure 55 and Figure 56. Until 22h the growth was rapid and the total and cytoplasmic biomass and cell volume profiles were very similar although the values of the cytoplasmic regions were lower than those for the total cell volume. This was due to the use of a mycelial inoculum so vacuoles were present at inoculation as shown by the degenerated cell volume and dry weight. The amount of vacuolisation did not increase during this period of rapid growth. Between 22h and 46h the biomass decreased (Figure 55). This was due to a decrease in the volume of the cytoplasmic region giving a corresponding increase in the degenerated region, so vacuolisation was occurring (Figure 56). After 46h the biomass increased during the time course as did the volume and dry weights of all of the regions. Notably by 125h approximately 50% of the volume of the total cells had degenerated. The mean hyphal density for the time course is also shown in Figure 56. The hyphal density increased until 22h after which it decreased over the time course. The mean hyphal diameters for the 100L fermentation are shown in Table 20. The measurements of the morphological parameters are shown in Figure 57 and Table 20. Hyphal fragmentation occurred after 22h at the time of the decrease in biomass with the degeneration of the cytoplasmic region.

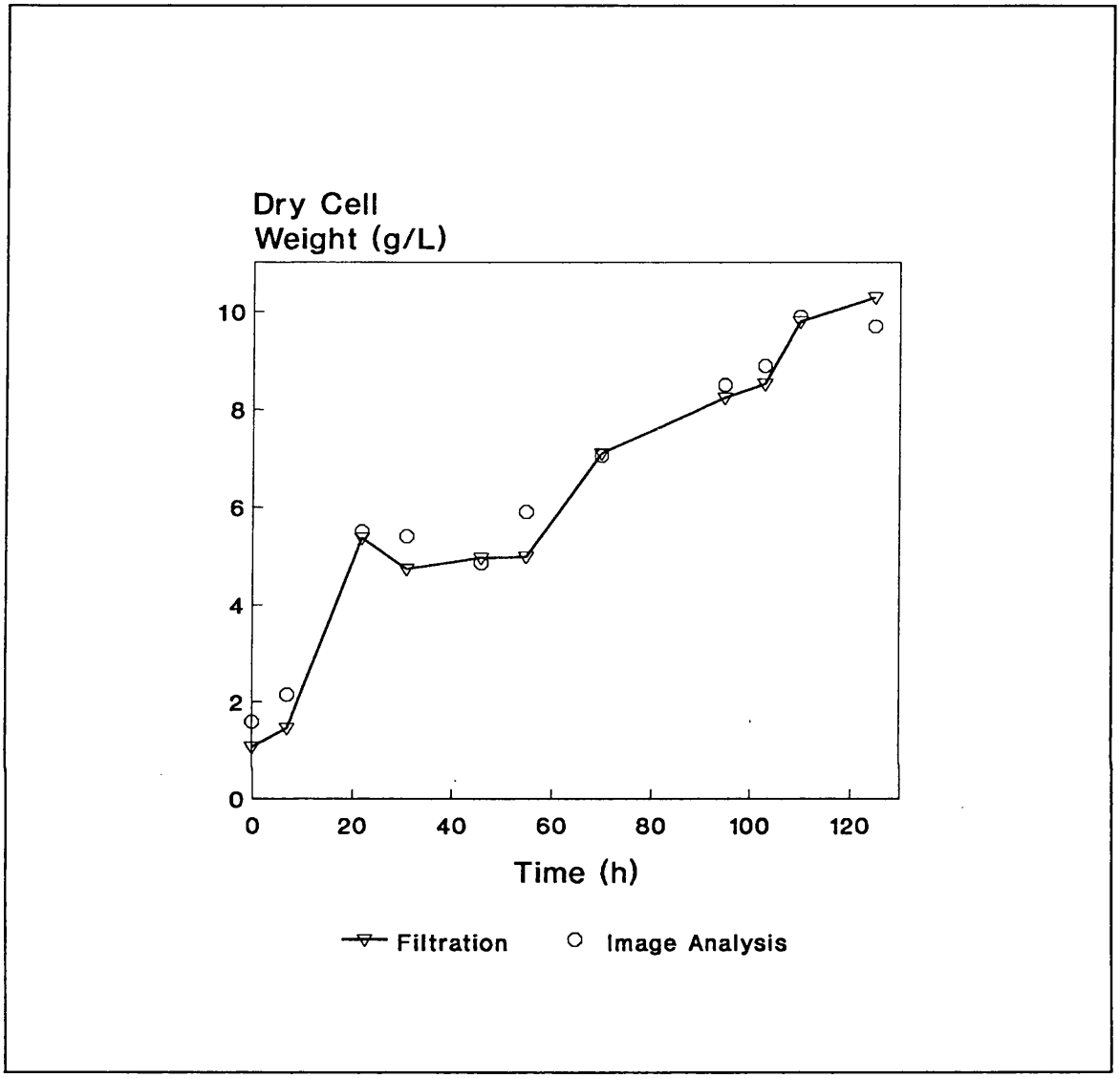

Figure 54. Time course of dry weight for the 100L fermentation. The dry weight was measured by filtration and estimated by image analysis.

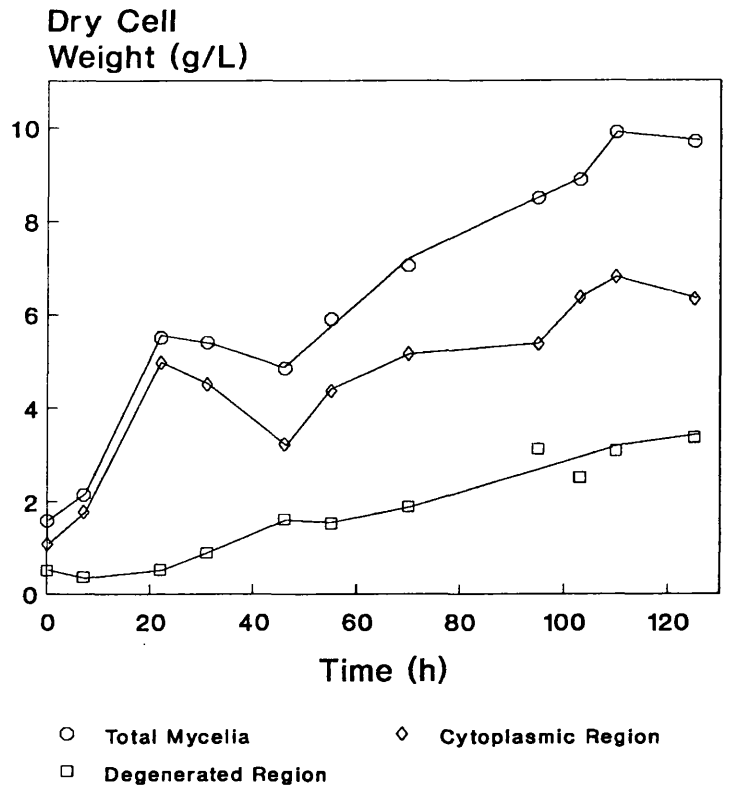

Figure 55. The biomass of hyphal regions for the 100L fermentation. The biomass of each of the hyphal regions estimated by image analysis is shown.

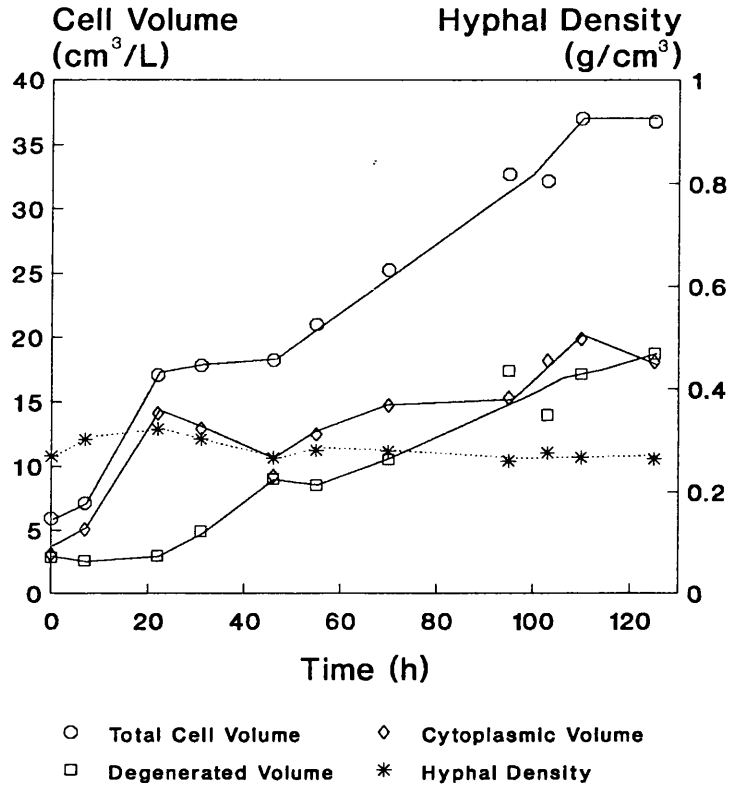

Figure 56. The cell volumes of the hyphal regions for the 100L fermentation. The cell volumes of each of the hyphal regions and the hyphal density measured by image analysis are shown.

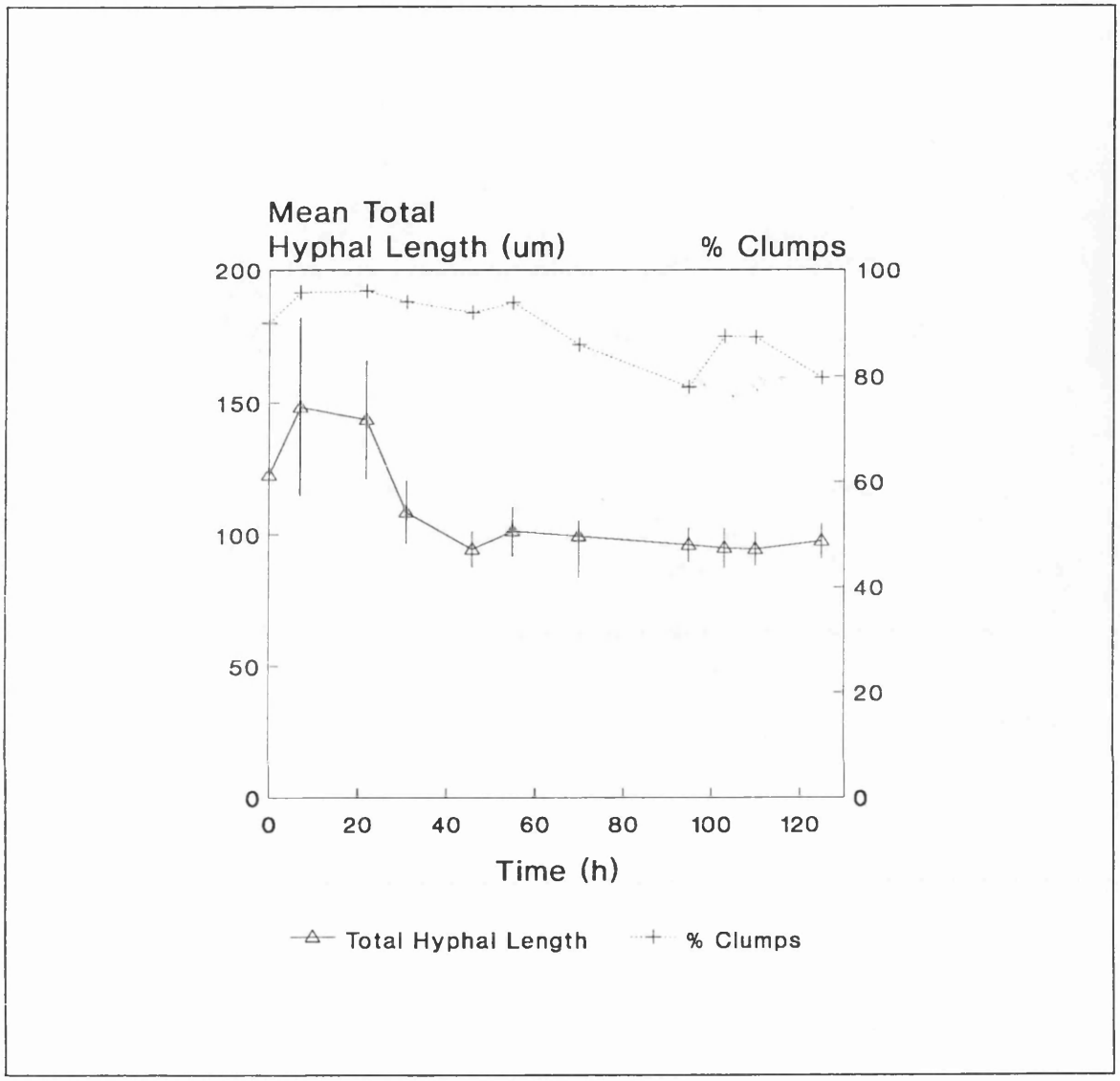

Figure 57. The mean total hyphal length and number of tips for the 100L fermentation

Table 20. Morphological parameters for the 100L fermentation.

Time (h)	Mean Hyphal Diameter (μm)	Mean Main Hyphal Length (μm)	Hyphal Growth Unit	Mean Number of Tips
0	4.8	76.3 ± 14.0	32.4 ± 3.1	3.3 ± 0.6
7	4.7	105.6 ± 17.2	40.7 ± 4.5	3.3 ± 0.5
22	4.3	120.2 ± 16.8	48.1 ± 5.8	2.9 ± 0.2
31	4.3	91.0 ± 8.1	38.5 ± 2.3	2.7 ± 0.2
46	4.4	75.2 ± 4.4	32.6 ± 1.5	2.8 ± 0.1
55	4.3	79.2 ± 6.1	34.0 ± 1.8	2.8 ± 0.2
70	4.6	75.3 ± 4.9	32.7 ± 1.5	2.9 ± 0.1
95	4.8	72.5 ± 3.8	30.0 ± 1.1	3.0 ± 0.1
103	4.3	76.0 ± 4.9	32.1 ± 1.5	2.9 ± 0.2
110	4.5	71.2 ± 3.9	30.0 ± 1.2	3.0 ± 0.1
125	4.3	76.6 ± 4.1	32.3 ± 1.3	2.9 ± 0.1

The biomass time course for the fed-batch fermentation with strain P-2 is shown in Figure 58, confirming with a different strain that the profiles of the image analysis estimate and the measured dry weight are closely matched. The dry weights of the hyphal regions are shown in Figure 59 and the cell volumes in Figure 60. The total hyphal volume and biomass increased steadily throughout the time course. The volume of the cytoplasmic region though increased rapidly until towards 64h where the rate of increase decreased due to vacuolisation as is shown by the rapid increase in the volume of the degenerated region. The mycelial inoculum was vacuolised at inoculation and the level of vacuolisation changed little until 64h when it started to increase rapidly. The morphological parameters for the fed batch fermentation are shown in Figure 61 and Table 21. From these it can be seen that hyphal fragmentation occurred between 40h and 64h as the mean lengths and number of tips of the mycelial particles fell. An increase in vacuolisation of the hyphae did occur during fragmentation as the as the biomass of the degenerated region increased from 1.75g/L to 2.91g/L and the rate of formation of degenerated region appeared to change during this period (Figure 59). The hyphal density is also shown in Figure 60. It showed some increase until 64h after which it decreased as the volume

of the degenerated region increased. The mean hyphal diameters for the *Penicillium chrysogenum* P-2 fermentation are shown in Table 21.

Table 21. The morphological parameters of the fed-batch fermentation.

Time (h)	Mean Hyphal Diameter (μm)	Mean Main Hyphal Length (μm)	Mean Hyphal Growth Unit	Mean Number of Tips
16.3	6.3	70.9 ± 15.3	28.9 ± 4.7	3.6 ± 0.5
21.4	6.8	77.3 ± 14.3	31.6 ± 4.6	4.0 ± 0.7
25.1	6.3	70.3 ± 12.1	26.2 ± 1.7	4.8 ± 0.7
39.8	6.3	108.5 ± 6.2	34.4 ± 1.3	4.2 ± 0.5
64.3	6.1	60.7 ± 5.7	22.6 ± 1.6	3.8 ± 0.4
70.3	5.5	56.5 ± 4.7	23.5 ± 1.6	3.3 ± 0.3
94.3	5.4	65.8 ± 4.4	25.5 ± 1.3	3.6 ± 0.2
112.7	5.2	59.8 ± 4.2	24.9 ± 1.2	3.3 ± 0.2
117.5	5.2	60.1 ± 3.7	24.5 ± 1.0	3.4 ± 0.2
161.6	5.4	59.4 ± 5.3	23.3 ± 12.0	3.5 ± 0.2
165.5	5.3	60.3 ± 4.4	24.1 ± 1.5	3.6 ± 0.2

The biomass time course of the lactose/Pharmamedia fermentation, measured by filtration and image analysis is shown in Figure 62. Until 65h the undissolved medium solids masked the mycelial growth in the measurements by filtration, then the dry weight increased until 90h after which it decreased rapidly. Figure 63 shows clearly that even at 118h a large quantity of medium solids was still present in the fermentation broth. The biomass estimated for the hyphal regions is shown in Figure 64 and the cell volumes in Figure 65. The cytoplasmic and total cell volumes increased until 97h after which the total volume levelled but the cytoplasmic volume decreased rapidly with the onset of lysis. This was reflected by the volume of the degenerated region which increased rapidly. Some vacuolisation was present after inoculation as a mycelial inoculum was used but this changed little until 24.5h after which the volume of the degenerated region increased to 18.83cm^3. During the remainder of this fermentation the quantity of the degenerated region was high, often at 40 to 50% of the total volume present. The

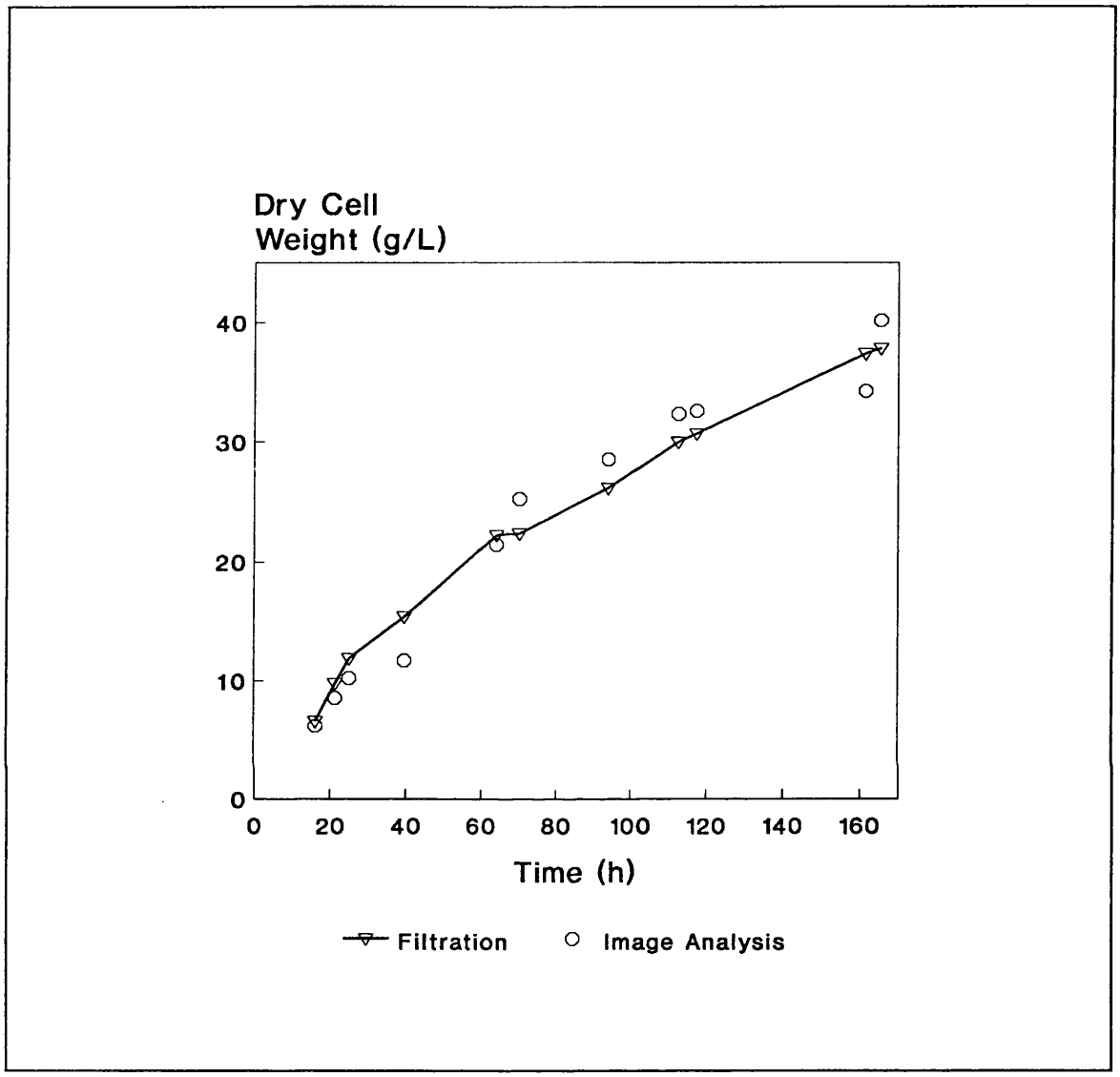

Figure 58. Time course of biomass for the fed-batch fermentation. The dry cell weight measured by filtration and estimated by image analysis is shown.

morphological parameters for the fermentation are shown in Figure 66 and in Table 22. From these it can be seen that fragmentation occurred after 24.5h as there is a decrease in the values of the mean hyphal lengths and number of tips. The hyphal density is also shown in Figure 65, this showed a slight increase to 24.5h and then decreased gently to 97h after which it fell rapidly as the cytoplasmic region lysed. the mean hyphal diameters for the lactose/Pharmamedia fermentations are shown in Table 22.

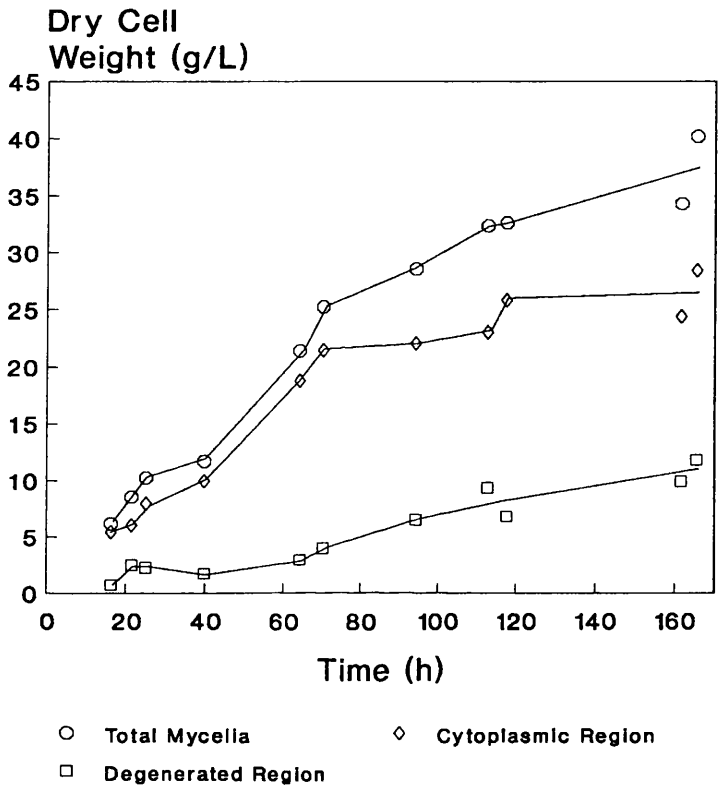

Figure 59. The biomass of the hyphal regions of the fed-batch fermentation estimated by image analysis

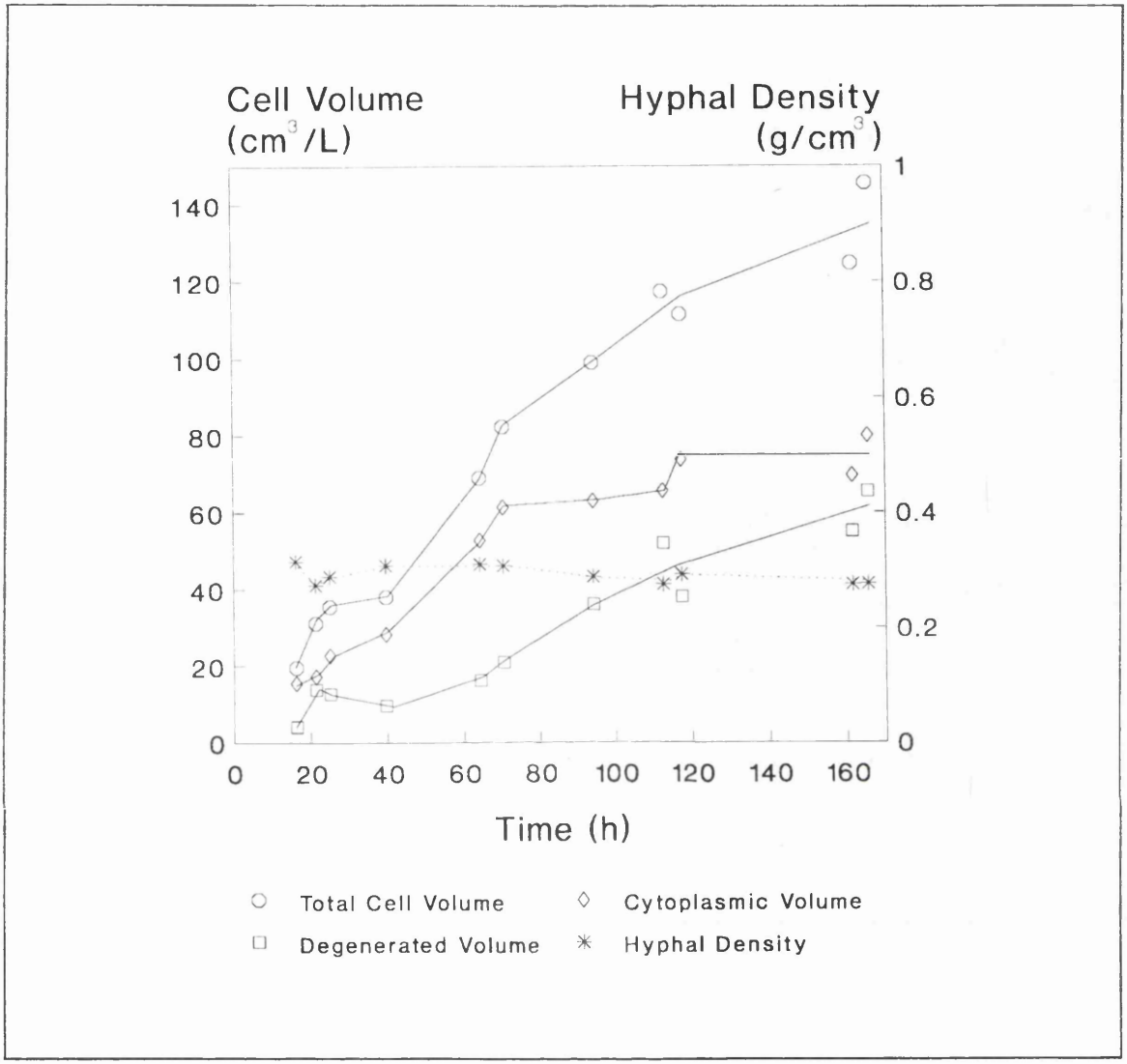

Figure 60. The cell volumes of the hyphal regions of the fed-batch fermentation. The cell volumes and hyphal density measured by image analysis are shown.

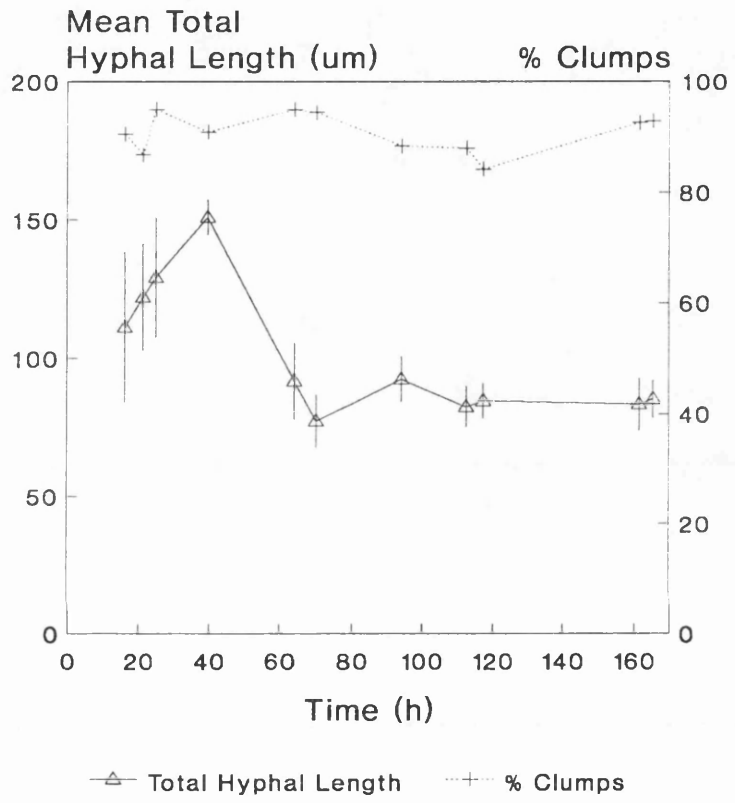

Figure 61. Mean total hyphal length and number of tips for the fed-batch fermentation

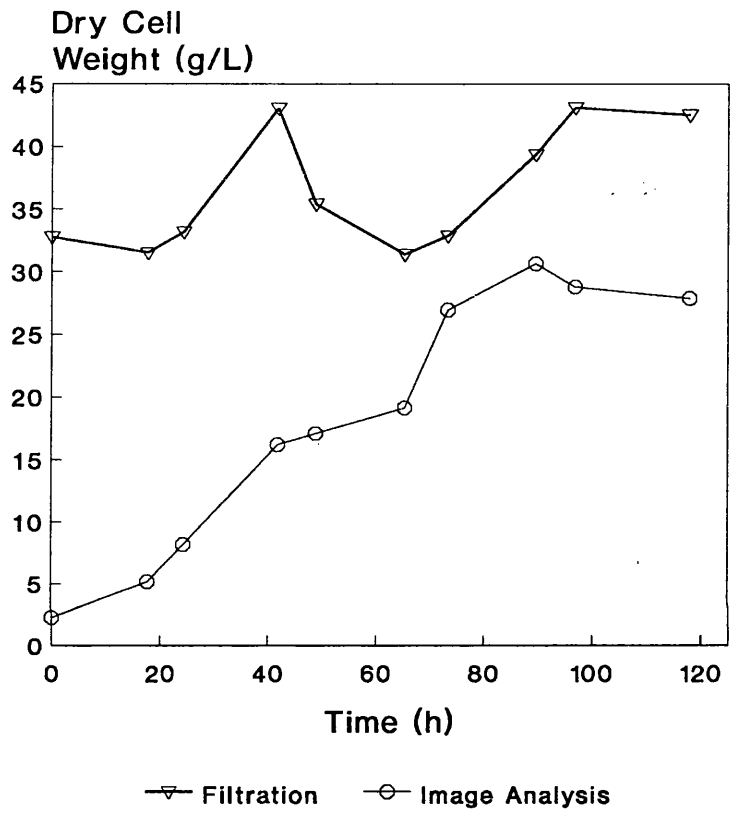

Figure 62. Time course of biomass for the lactose/Pharmamedia fermentation. The dry cell weight measured by filtration and estimated by image analysis is shown.

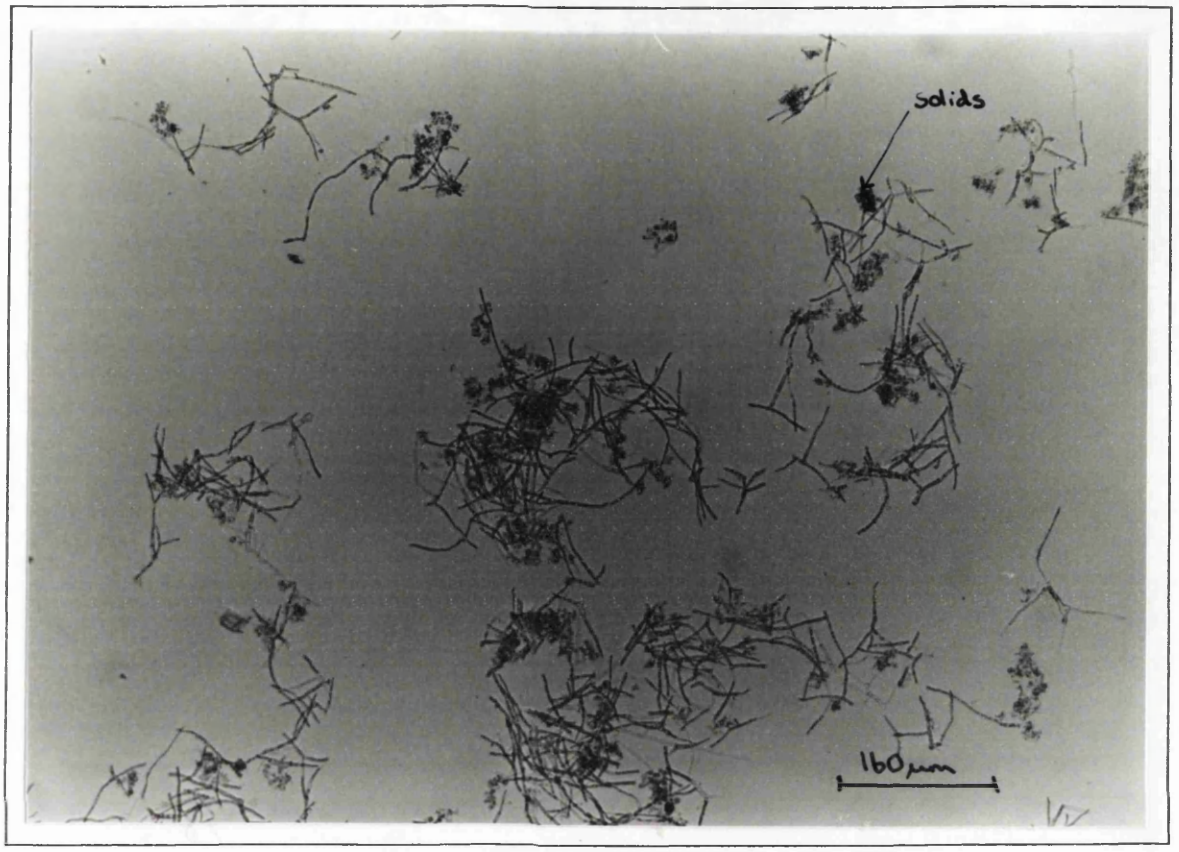

Figure 63. Mycelia at 118h from the lactose/Phairmamedia fermentation. The photograph shows the presence of undissolved solids in the sample.

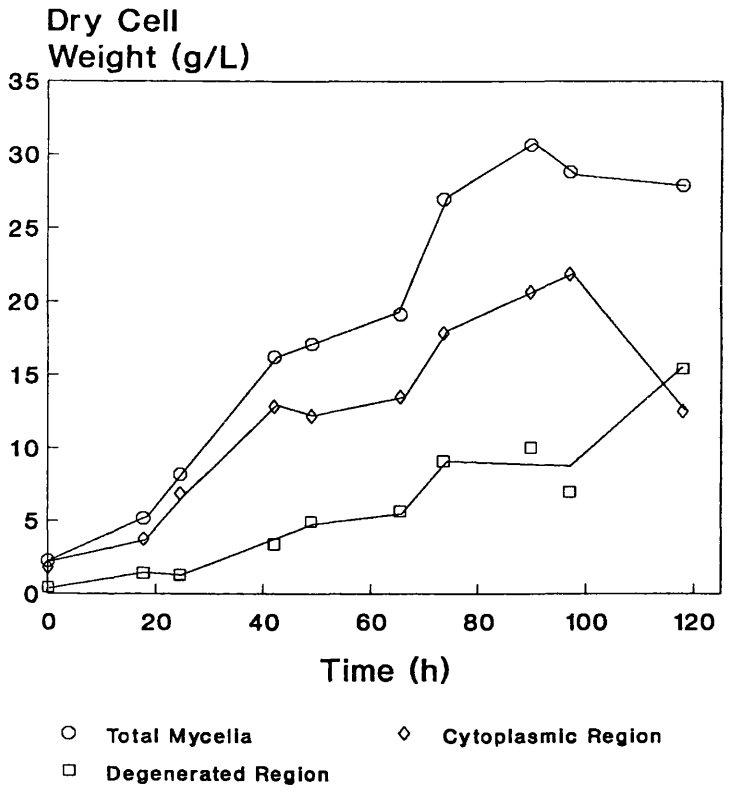

Figure 64. Biomass of the hyphal regions of the lactose/Pharmamedia fermentation. The biomass of each of the hyphal regions measured by image analysis is shown

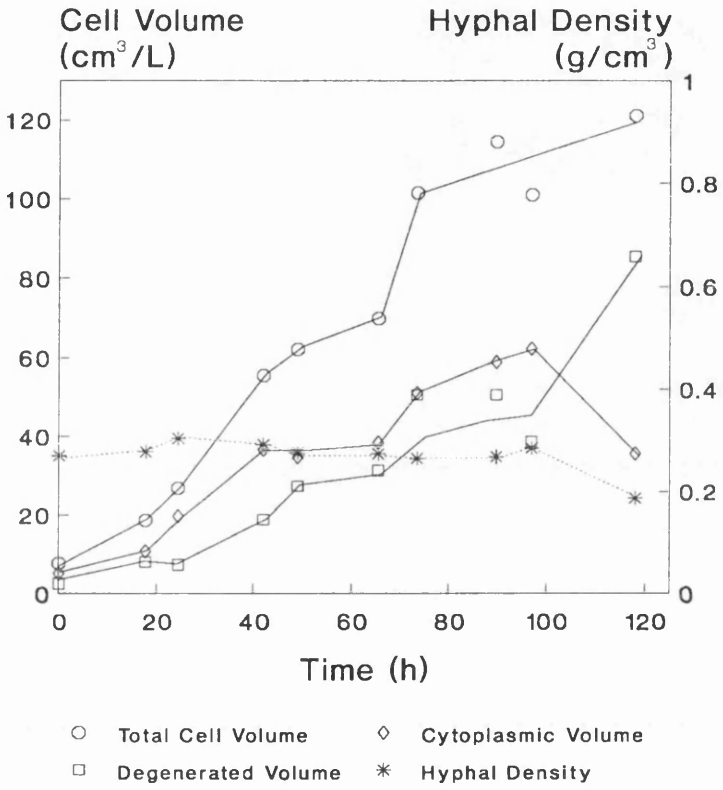

Figure 65. Cell volumes of the hyphal regions for the lactose/Pharmamedia fermentation. The cell volumes and hyphal density measured by image analysis are shown.

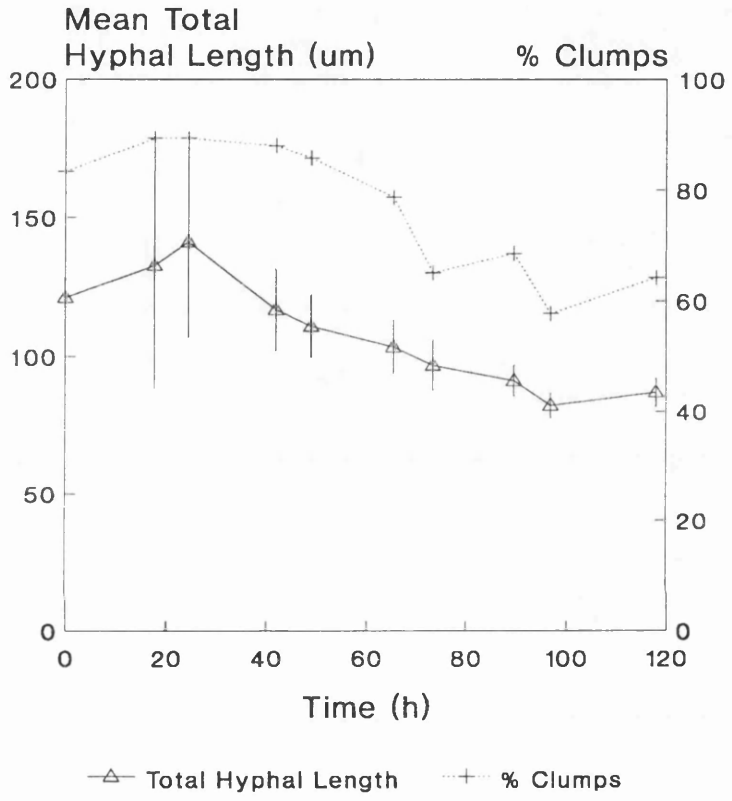

Figure 66. The mean total hyphal length and number of tips for the lactose/Pharmamedia fermentation.

Table 22. The morphological parameters for the lactose/Pharmamedia fermentation.				
Time (h)	**Mean Hyphal Diameter (μm)**	**Mean Main Hyphal Length (μm)**	**Mean Hyphal Growth Unit**	**Mean Number of Tips**
0.0	4.8	83.6 ± 12.1	33.7 ± 4.1	3.8 ± 0.3
17.8	4.5	97.5 ± 29.4	35.2 ± 7.5	3.4 ± 0.6
24.5	5.0	98.1 ± 22.3	38.2 ± 6.3	3.7 ± 0.5
42	4.6	90.4 ± 8.6	37.5 ± 2.6	3.0 ± 0.3
49	4.0	88.8 ± 7.6	36.6 ± 2.3	2.8 ± 0.2
65.5	4.0	80.3 ± 6.4	33.8 ± 1.9	2.9 ± 0.2
73.5	3.5	74.6 ± 4.9	31.2 ± 1.4	2.9 ± 0.2
89.8	4.1	70.0 ± 3.5	29.4 ± 1.1	3.0 ± 0.1
97	4.0	62.0 ± 2.6	27.1 ± 4.0	2.9 ± 0.1
118	3.3	65.9 ± 3.0	28.1 ± 0.9	3.0 ± 0.1

5.2.3 Discussion

Figure 45 shows the good agreement between the dry cell weight estimated by image analysis and the measured dry weight using the conventional filtration method. However there is some scatter from the line of best fit which is due to various sources of errors on the biomass determinations for both methodologies. A major error in the image analysis method was due to the placement of material onto the slide which was approximately ±8.4% (5.1.2, Slide Preparation). Another error was due to fluctuations in the light level which occasionally changed during processing. Also the initial step of diluting a sample, just taken from the fermenter, into fixative would also produce an error on the final biomass estimation particularly when the biomass was high and the broth was difficult to pipette accurately. This source of error and other errors, such as those from sampling the fermenter, would be also be common to the conventional filtration method of measuring biomass. These common sources of errors have not been calibrated.

The conventional biomass technique is prone to additional error as it also involves washing the sample and the weighing of the filters. The error of the conventional dry weight methodology has been calibrated for a *Penicillium chrysogenum* P-2 fermentation with biomass from 1 to 35g/L (K.Stone, 1990).The error of measurement at the 95% confidence limits was ±12 to 2% respectively with the error being greatest at the lower dry weights. The errors on the values measured using image analysis are similar to those obtained by the conventional method. However from the sample preparation errors, it appears that the error is influenced by the morphology and the biomass, with the lowest error on low biomass and evenly dispersed samples which is the opposite to the conventional dry weight technique where low biomass produced the greatest errors. Notably for the fed-batch fermentation of P-2 measured by image analysis the percentage difference between the conventional and image analysis measurement techniques for the samples between 30 and 40g/L were between 6 and 8.4% so the image analysis technique did not become less accurate with increasing biomass and was within the slide preparation error (8.4%) for a sample of 4.56g/L.

In the analysis of fermentation A (Figure 47) the capability of the image analysis method was shown as it was able to follow the culture through the growth phase and into the phase of lysis and death of the cells after 65h, measuring the biomass accurately through both phases. The measurements of the volumes of the cytoplasmic and degenerated regions in particular showed the onset of lysis as the cytoplasmic volume which had closely matched the total volume diverged from it and was matched by a corresponding increase in the volume of the degenerated region (Figure 48).

The results from the 100L fermentation also demonstrate the potential of this technique for the study of fermentation, for at 22h there is a decrease in the total biomass of the cells (Figure 55). This could be due to a physiological event such as during diauxic growth as the cells switch from sucrose utilisation to lactose and the image analysis technique is sensitive enough to detect the occurrence of a change in the state of the microorganisms. In Figure 56 during this event, the drop in total biomass can be seen to be due to vacuolisation and lysis of the "healthy" cells as the volume of the cytoplasmic region rapidly declines. The total cell volume remains constant so there is not breakdown of the hyphal walls and the drop in cytoplasmic volume produces a corresponding increase in the volume of the degenerated region.

The fed-batch fermentation initially contained a small amount of undissolved solids in the medium but there is no evidence of their presence in the dry cell weight profiles (Figure 58). Therefore considering that the first sample was at 16.25h after inoculation it is likely that the solids had been broken down and were only present, if at all, in insignificant quantities. *Penicillium chrysogenum* P-2 was used for the fed-batch fermentation and the image analysis

methodology was able to estimate the cell volume and biomass for this strain successfully without any changes to the technique even though P-2 is different in morphology to P-1.

The image analysis technique estimated a growth curve for the biomass during a lactose/Pharmamedia fermentation (Figure 62). Comparison of the two profiles on Figure 62 show there was a significant quantity of solids present throughout the fermentation. Initially the effect of the breakdown of the solids by metabolism on the dry weight values must be compensated for by the increasing mycelial biomass though still over a base line of solids. The difference between the two biomass profiles indicated that the remaining solids concentration at this stage was up to 15g/L, microscopical observation confirmed the presence of undissolved solids at the end of the fermentation (Figure 63).

The measurements of hyphal volumes followed the hyphal growth during the lactose/Pharmamedia fermentation (Figure 65). The inoculum was mycelial therefore some vacuolisation had already occurred as shown by the presence of 0.5g/L of degenerated cell regions at inoculation (Figure 64). The amount of the degenerated region continued to increase steadily throughout the fermentation causing the divergence of the profiles of the total and cytoplasmic cell regions. When cell death and lysis started after 97h the volume of the cytoplasmic region decreased rapidly with a corresponding increase in the degenerated region (Figure 65). However the total volume of hyphae present remained constant as the cell walls do not tend to degrade or breakup easily due to the chitin network present in the walls. These events are also indicated by the hyphal density which decreased at the onset of cell death and lysis. The measurement by the technique of mycelia in the high undissolved solids concentrations during the lactose/Pharmamedia fermentation showed the effectiveness of measurement using image analysis. The methodology was able to avoid satisfactorily measurement of the solids particles to give a direct measurement of the volume of the hyphal regions (Figure 65).

The consideration of the hypha as a solid cylinder of diameter equal to the mean hyphal diameter of the sample for the estimation of cell volume appears to be accurate enough for comparison with conventional filtered dry weight measurements. It appears to be necessary to measure the mean hyphal diameter for all of the samples in a time course of each fermentation, rather than using a fixed value which was the approach taken by Nestaas and Wang (1983) for the estimation of hyphal cell volumes, for during some of the fermentations the values of the means appeared not to be constant. For example in the fed batch fermentation the mean hyphal diameter declined over the time course (Table 21) and this trend also appeared in the lactose/Pharmamedia fermentation (Table 22). As the hyphal diameter appeared to be changing during the fermentation it would be worth developing an accurate automated algorithm

to enable study of the diameter such as using the mean value for each mycelial particle or perhaps even the diameters of the individual regions.

For all of the fermentations except for the fed-batch fermentation which was not so clear, there appeared to be a relationship between the divergence of the cytoplasmic region from the total hyphal region and the beginning of the fragmentation of the hypha as the two events coincided. This will require further studies to confirm this but as there appeared to be a link for several very different fermentations it is likely that a relationship between the two events exists.

During all of the fermentations the percentage of clumps was usually high at greater than 80%. The area measurement of the hyphae using image analysis does not allow for crossovers so that any material lying underneath other hyphae is not measured. This had been anticipated to cause problems in the measurement of biomass and cell volumes using image analysis as the presence of clumps was expected to cause the methodology to underestimate quantity of mycelia. However the image analysis method was in good agreement with the conventional methodology so the area measurement used is accurate enough for the level of precision required for estimation of dry weight.

During this study the image analysis methodology was used to estimate biomass in fermentation samples ranging from 0.68 to 38g/L before dilution. If dilution is taken into account the minimum cell concentration used was 0.034g/L and there would theoretically be no upper limit of resolution as the sample could simply be diluted. This demonstrates the versatility of the image analysis technique. The performance of the image analysis technique was not affected by the presence of up to 30g/L of undissolved solids in the medium (Figure 50). The methodology also provides measurements of the total, cytoplasmic and degenerated cell volumes, and the biomass of each of these regions which will allow a greater understanding of physiological changes during the fermentation. Using the profiles obtained for each of the regions it would be possible to calculate the rates of change of the regions. The proportions of the regions and their rates of change may be related to the rate of product formation and other metabolic parameters such as maintenance coefficients. Studies of fermentation using these measurements will allow a greater understanding of physiological changes during fermentation and also aid the modelling of systems using parameters such as the maintenance energy as the proportion of biomass that is active is quantified.

For this study the software has not been optimised so the time taken for processing is quite considerable at approximately seven hours for the samples from the lactose/Pharmamedia fermentation and four hours for each of the samples from the other media. This is due to the time required to measure the whole of the coverslip area, 225 fields for each hyphal region, as each field requires up to a minute in processing time using the present hardware. The magni-

fication used for quantification of the mycelia was set at the lowest possible while still enabling the hyphal regions to be determined. An increase in the magnification would give better resolution of the hyphal regions, in particular the vacuoles, which should result in more accurate measurement of the hyphal volumes and biomass but with the present hardware this would have resulted in considerably longer processing times which would not have been practical. It should be noted that small vacuoles will be of relative unimportance. A vacuole of one tenth of the linear dimension of a large vacuole will only be one thousandth of the volume (for the same shape). Large vacuoles will therefore dominate the volume fraction of vacuoles in the hyphae. With faster image analysis equipment this versatile technique would have the potential to be used for rapid direct measurement of hyphal volumes and rapid estimation of biomass for industrial fermentations with high concentrations of non-dissolved solids. With the addition of automated sampling and an automatic hyphal diameter measurement algorithm it would be possible to use this technique on-line. In its present form the image analysis technique is a valuable research tool for the measurement of biomass and the estimation of cell volume for *Penicillium chrysogenum* and it should be possible to adapt the principles established in this study to measure other filamentous microorganisms in a variety of different media.

6.0 Conclusions and Future Work

Image analysis is a versatile and powerful technique. It can be used for rapid and in most cases accurate characterisation of filamentous microorganisms. The gross morphological characterisation method reported here not only measures the usual morphological parameters but also the proportion of the material in clumps, which might be related to permanent aggregates in a fermenter.

The image analysis methodology for the estimation of the cell volume and biomass of the hyphal regions in filamentous fungi, is a very powerful technique for quantification and characterisation of fungi. This methodology enables measurement of the physiological state of the microorganism by measurement of the active and degenerated cell mass. Also the biomass and volumes of the hyphal regions may be quantified in the presence of solids.

Using all of the characterisation methods to study fermentations will facilitate engineering studies on filamentous microorganisms and will aid elucidation of their growth and product formation.

The image analysis methodologies determined in this project are novel and exciting and have created a means to carry out a wide range of studies on filamentous microorganisms in the future without further development of the measurements. However, it should be possible to extend the use of this powerful tool to automate the methods and increase the speed of measurement: use a higher magnification of the cells (with staining techniques) for more detailed analysis of the hyphal structures; and extend the measurement of cell volume and biomass to actinomycetes.

7.0 REFERENCES

Adams, H.L. and Thomas, C.R. (1988) Biotech. Bioeng., **32** 707-712.

Agar, D.W. (1985) Comprehensive Biotechnology **4**, Ed. Robinson and Howell, Permagon Press. 305-327.

Allan, EJ., Prosser, J.I. (1985) J. Gen. Microbiol, **131** 2521-2532.

Archer, D.B. (1977) Biochem. J. **164** 653-658.

Aronson, J.M, Cooper, B.A. and Fuller, M.S.(1967) Science N.Y. **155** 332- 335.

Bartnicki-Garcia, S (1968) Ann. Rev. Microbiol. **22** 87-108.

Bartnicki-Garcia, S (1973) Symp. Soc. Gen. Microbiol. **23** 245-267.

Bartnicki-Garcia, S., Bracker, C.E. and Ruiz-Herrera, J. (1978) Exp. Mycol. **2** 173-192.

Belmar-Campero, M.T. and Thomas, C.R. (1988) 2nd Int. Conference on Bioreactor Fluid Dynamics. ed. R. King, Elsevier Applied Science Publishers, paper E2.

Blake-Coleman, B.C., Clarke, D.J., Calder, M.R., Moody, S.C. (1986) Biotech. Bioeng. **28** 1241-1249.

Braun, S., and Vecht-Lifschitz, S. (1991) Tibtech **9** 63-68.

Burnett, J.H. (1979)Fungal Walls and Hyphal Growth,ed.J.H. Burnett and A.P.J. Trinci, Cambridge University Press, 1-25.

Butler, M and Harris, C.G.M. (1949) J. Gen. Microbiol. **3** vi.

Calam, C.T. (1969) Methods in Microbiology **1** 567-592

Caldwell, I.Y. and Trinci, A.P.J. (1973) Arch. Mikrobiol. **88** 1-10.

Carter, B.L.A. and Bull A.T. (1971) J. Gen. Microbiol. **65** 265-273.

Chatfield, C. (1983) Statistics for Technology, 3rd edition, Chatman and Hall.

Clarke, D.J., Blake-Coleman, B.C, Carr, R.J.G., Calder, M.R., Atkinson,T. (1986) Trends in Biotech. July 173-178.

Clarke D.J., Calder, M.R., Carr, R.J.G., Blake-Coleman, B.C., Moody, S.C. and Collinge, T.A.C. (1985) Biosensors **1** 213-320.

Cochet N., Tyagi R.D., Ghose T.K., Lebeault J.M. (1984) Biotechnol. Lett. **6** 155-160.

Conway, E.J. and Downey, M. (1950) Biochem. J. **47** 347-355.

Collinge, A.J. and Markham, P. (1985) Exp. Mycol. **9** 80-85.

Deo, Y.M. and Gaucher, G.M. (1984) Biotech. Bioeng. **26** 285-295.

Dion, W.M., Carilli, A., Sermonti, G., Chain, E.B. (1954) Rend. Instituto Superiore di Sanita, **17** 187-205.

Dion, W.M., Kaushal, R. (1954) Sel. Sci. Papers of Instituto Superiore di Sanita, **2** 357-369.

Doskocil, J., Sikyta, B., Kasparova, J., Doskocilova, D., Zajicek, J., (1958) J. Gen. Microbiol. **18** 302-314.

Duckworth, R.B. and Harris G.C.M. (1949) Trans. Br. Mycol. Soc. **32** 224-235.

Elmayeri, h., Scharer, J.M., Moo-Young, M. (1973) Biotech. Bioeng. **15** 845-849.

Endo, H., Sode, K., Ogura, K., Karube, I., (1989) J. Biotechnol. **12** 307-316.

Forage, R.G., Harrison, D.E.F., Pitt D.E. (1985) Comprehensive Biotechnology **1**, ed. A.T. Bull and H. Dalton, Permagon Press, 251-280.

Fencl, Z. (1970) Biotech. Bioeng. **12** 845-847.

Fencl, Z. (1978) The Filamentous Fungi, **3** ed. J.E. Smith and D.R. Berry, Edward Arnold, 389-405.

Frame, K.F., Hu W-S. (1990) Biotech. Bioeng. **36** 191-197.

Freeman, H., (1961) IRE Trans Electronic Computers EC10 Pt2.

Girbardt (1955) Flora **142** 540-563.

Gonzales, R., Wintz, P., (1977) Digital Image Processing, Addison Wesley.

Gooday, G.W. (1971) J. Gen. Microbiol. **67** 125-133.

Gooday, G.W. and Trinci, A.P.J. (1980) The Eukaryotic Microbial Cell, ed. G.W. Gooday, D. Lloyd, A.P.J. Trinci, Cambridge University Press. 207-251.

Graafsmans, W.D.J. (1973) Arch. Microbiol. **91** 67-76.

Green (1969) Ann. Rev. Plant Physiol. **20** 365-394.

Grove, S.N. (1978) The Filamentous Fungi, **3**, ed J.E. Smith and D.R.Berry, Edward Arnold, 28-50.

Grove, S.N and Bracker, C.T (1970) J. Bacteriol. **104** 989-1004.

Gull, K. (1978) The Filamentous Fungi, ed. J.E.Smith and D.R.Berry. **3** Edward Arnold, 78-93.

Harris, C.M., Kell, D.B. (1985) Biosensors **1** 17-84.

Harris, C.M., Todd, R.W., Bungard, S.J., Lovitt, R.W., Morris, J.G., Kell, D.B. (1987) Enz. Microbiol. Technol. **9** 181-186.

Harrison, D., Chance, B. (1970) Appl. Microbiol. **19** 446.450.

Hendy, N.A., Gray, P.P. (1979) Biotechnol. Bioeng. **21** 153-156.

Herbert, D., Phillips, P.J., Strange, R.E. (1971) Methods of Micro. **56** 244.

Hiraoka, M., Kazushi, T., Baba, K., Nogita, S., Mori, S. (1986) U.S. Patent 4,564,444. Jan 14 1986.

Ho, C.S., Smith, M.D. (1986a) J. Gen. Microbiol. **132** 3479-3484.

Ho, C.S., Smith, M.D. (1986b) Biotech. Bioeng. **28** 668-677.

Hockenhull D.J.D. (1963) Biochemistry of Industrial Microorganisms, ed. C. Rainbow and A.H. Rose, Academic Press, 227.

Howard, R.J. (1981) J. Cell. Sci. **48** 89-103.

Howard, R.J. and Aist J.R (1980) J. Cell. Biol. **87** 55-64.

Hunsley, D., Burnett J.H (1970) J. Gen Microbiol **62** 203-218.

Hysert, D.N., Dovecses, F., Morrison, N.M. (1976) J. Am. Soc. Biochem. Chem. **34** 145-150.

Ishimori, Y., Karube, I., Suzuki, S. (1981) Appl. Environ. Microbiol. **42**(4) 632-637.

Issac, S., Ryder, N.S., Peabody, J.F. (1978) J. Gen. Microbiol. **105** 45-50.

Joyce Loebl (1985) Image Analysis: Principles and Practices, Joyce Loebl, U.K.

Ju, L-K, Ho, C.S (1988) Biotech. Bioeng. **32** 95-99.

Kalakoutskii, L.V., Agre, N.S. (1976) Bacteriological Reviews, **40**(2) 469-524.

Katz, D., Goldstein, D., Rosenberger, R.F. (1972) J. Bacteriol. **109** 1097-1100.

Katz, D., Rosenberger, R.F. (1971) J. Bacteriol. **108** 184-190.

Kell, D.B., Markx, G.H., Davey, C.L., Todd, R.W. (1990) Trends in Analytical Chemistry, **9**(6) 190.

Keshavarz, T., Walker, E., Eglin, R., Lilley, G., Holt, G., Bull, A.T., Lilly, M.D.L. (1989) **30** (1989) Appl. Microbiol. Biotechnol. **30** 487-491.

Kilburn, D.G., Fitzpatrick, P., Blake-Coleman, B.C., Griffiths, J.B. (1989) Biotech. Bioeng. **33** 1379-1384.

Koch, A.L. (1982) J. Gen. Microbiol. **128** 947-951.

Konig, B., Seewald, C.H., Schugerl, K., (1981) Eur. J. Appl. Microbiol. Biotechnol. **12** 205-211.

Makagiansar, H.Y. (1990) Personal Communication.

Metz, B. (1976) From Pulp to Pellet, Ph.D thesis, Technical Uni. Delft.

Metz, B., De Bruijn, E.W., van Suijdam, J.C. (1981) Biotech. Bioeng. **23** 149-162.

Miles, E.A., Trinci, A.P.J (1983) Trans. Br. Mycol. Soc. **81** 193-208.

Mou D-G. and Cooney C.L. (1976) Biotech. Bioeng. **18** 1371-1392.

Mou D-G. and Cooney C.L. (1983) Biotech. Bioeng. **25** 257-269.

Murase, G., Kendrick, B., (1986) Biotechnol. Lett. **8** 25-30.

Nestaas, E., Wang, D.I.C. (1981) Biotech. Bioeng. **23** 2803-13.

Nestaas, E. Wang, D.I.C., Suzuki, H., Evans, L.B. (1981) Biotech. Bioeng. **23** 2815-24.

Nestaas, E., Wang D.I.C. (1983) Biotech. Bioeng. **25** 781-796.

'O' Toole, D.K. (1983) Appl. Env. Microbiol. **46** 506-8.

Oliver, S.G., Trinci, A.P.J. (1985) Comprehensive Biotechnology, **1**, ed. A.T. Bull and H. Dalton, 159-188.

Perry, R.H., Green, D. (1985) Perry's Chemical Engineering Handbook, 6th edition, McGraw Hill Book Co.

Phillips, J.A. (1990) Computer Control of Fermentation Processes, ed. D.R. Ormstead,, CRC Press, 15-72.

Pirt, S.J., Callow, D.S. (1959) Nature **184** 307-310.

Pitt, D.E., Bull, A.T. (1982) Trans. Br. Mycol. Soc., **78** 97-104.

Prosser, J.I., Tough, A.J. (1991) Critical Reviews in Biotechnol. **10** (4), 253-271.

Reichl, U., Buschulte, T.K., Gilles, E.D. (1990) J. Microscopy **158** 55-62.

Reuss, M. (1990) Computer Control of fermentation Processes, ed. D.R. Ormstead,, CRC Press, 307-324.

Riesenberg, D., Bergter, F. (1979) Zeitschrift fur Allgemeine Mikrobiologie, **19**(6) 415-430.

Riesenberg, D., Erdmann, A.,Bergter, F. (1979) Zeitschrift fur Allgemeine Mikrobiologie, **120**(1) 24-30.

Ride, J.P., Drysdale, R.B. (1972) Phys. Plant. Path. **2** 7-15.

Righelato R.C., Trinci A.P.J., Pirt S.J. and Peat A. (1968) J. Gen. Microbiol. **50** 399-412.

Robertson, N.F. (1965) Trans. Br. Mycol. Soc. **78** 353-355.

Robinson, P.M., Smith, J.M. (1976) Trans. Br. Mycol. Soc., **66** 413-420.

Robinson, P.M., Smith, J.M. (1979) Trans. Br. Mycol. Soc., **72** 39-47

Rosenberger, R.F., Kessel, M. (1967) J. Bacteriol. **94** 1464-9.

Rosenberger, R.F., Kessel, M. (1968) J.Bacteriol. **96** 1208-13.

Saunders, P.T., Trinci, A.P.J. (1979) J. Gen. Microbiol. **110** 469-473.
Savage, G.M., and Vander Brook, M.J. (1946) Bacteriol. 52, 385-391.
Scheper, Th. (1985) Dissertation, Univ. Hanover.

Scheper, Th., Lorenz, Th., Schmidt, W., Schugerl, K. (1986) J. Biotechnol. **3** 231-238.

Schuhmann, E., Bergter, F. (1976) Z. Allg. Mikrobiol., **16** 201-215.

Smith, J. (1985) PhD thesis, Univ. London, U.K.

Smith J.E. (1975) The Filamentous Fungi, **1**, ed.J.E. Smith and D.R.Berry, 1-15.

Smith, M.D., Ho, C.S. (1985) J. Biotechnol. **2**(6), 347-363.

Smith, J., Lilly, M.D.L., Fox, R.I. (1990) Biotech. Bioeng. **35** 1011-1023.

Smith, M.A.L., Spomer, L.A. (1987) In Vitro Cellular and Developmental Biology **23** 67-74.

Singer, S.J and Nicolson, G.L (1972) Science **175** 723-731.

Steele, G.W., Trinci, A.P.J. (1975a) J. Gen. Microbiol. **91** 362-368.

Steele, G.W., Trinci, A.P.J. (1975b) New Phytol. **75**, 583-587.

Steele, G.W., Trinci, A.P.J. (1977) Arch. Microbiol. **113** 43-8.

Stone, K. (1990) Personal Communication.

Strehler, B.L., McElroy, W.D. (1957) Methods of Enzymology **3** 871.

Thomas, D.C., Chittur, V.K., Cagney, J.W., Lim, H.C. (1985) Biotech. Bioeng. **27** 729-742.

Trinci A.P.J. (1970) Arch. Mikrobiol.**73** 353-367.

Trinci A.P.J. (1974) J. Gen. Microbiol. **81** 225-236.

Trinci A.P.J. (1978) The Filamentous Fungi. **3**, ed. J.E.Smith and D.R. Berry. N.York. Wiley, 132-163.

Trinci, A.P.J (1979) Fungal Walls and Hyphal Growth. Ch15 Ed J.H.Burnett and A.P.J.Trinci, Cambridge University Press.

Trinci, A.P.J. Collinge, A.J. (1973) Arch Mikrobiol **91** 355-364.

Trinci, A.P.J., Righelato, R.C. (1970) J. Gen. Microbiol. **60** 239-40.

Trinci, A.P.J., Saunders, P.T. (1977) J. Gen. Microbiol **103** 243-248.

Ujcova, E., Fencl, Z., Musilkova, M., Seichart, L., (1980) Biotech. Bioeng. **22** 237-251.

Van Suijdam, J.C., Metz, B. (1981) Biotech. Bioeng. **23** 111-148.

Vardar, F., Lilly, M.D.L. (1982) Europ. J. Appl. Microbiol. Biotechnol. **14** 203-211.

Villanueva, J.R. (1966) The Fungi **2** Ed. G.C, Ainsworth and A.S.Sussman, New York Academic Press, 2-62.

Wessels, J.G.H., Sietsma, J.H. (1981) Cell Walls, ed. D.G. Robinson and H. Quader, Wissenschaftliche Verlagsgesellschaft, Stuttgart. 135-142.

Zabriski, D.W., Humphrey, A. (1978) Appl. Env. Microbiol. **35** 337-349.

Zetalki K., Vas, K. (1971) J. Gen. Microbiol, **65** 265-273.

7.1 Publications and Conferences

H.L.Adams and C.R.Thomas, Biotechnology and Bioengineering, Vol 32, 707-712 (1981) "The Use of Image Analysis for Morphological Measurements on Filamentous Microorganisms".

H.L.Packer, M.T.Belmar Campero and C.R.Thomas., Fourth International Congress on Computer Applications in Fermentation Technology: Modelling and Control of Biotechnical Processes, September 1988, 23-26."Morphological Measurements on Filamentous Microorganisms by Image Analysis".

H.L.Packer and C.R.Thomas, Biotechnology and Bioengineering, Vol 35, 870-881 (1990) "Morphological Measurements on Filamentous Microorganisms by Fully Automatic Image Analysis".

C.R.Thomas and H.L.Packer, Report of the Symposium of the Computer Users Group of the Society of General Microbiology, Applications of Image Analysis in Microbiology (Part 2), Jan 1990 meeting, Binary, Vol 2, 47-54 (1990). "Morphological and Structural Measurements in Filamentous Microorganisms".

UK Patent Application for the method of measuring biomass filed 21stMarch 1991. "Improvements in, or relating to, volume measurements of microbial organisms".

H.L.Packer, E.Keshavarz-Moore, M.D.Lilly and C.R.Thomas, submitted for publication (March 1991) "The Estimation of Cell Volume and Biomass of *Penicillium chrysogenum* using Image Analysis".

Appendix A. A Typical Data File From Version 1

Joyce-Loebl Magiscan 2 program : RESULTS Date : 4-Jun-91

Sample identifier : UCLHYPHA   File name : $S:HYTS70.DATA   Data file author :
Reference number : 0   File date : 4-Jun-91

MEASUREMENTS/EXPRESSION REPORT   Page: 1

Object	Level	Ref	BL	HL	MC	ML	NM	NT	SN	TL
1	0								1.00000	6.69953E3
2	1	1					1.00000			5.40295E3
3	2	1.1					1.00000			1.34324E3
4	2	1.2					1.00000			2.50313E2
5	2	1.3					1.00000			3.32310E3
6	2	1.4					1.00000			4.43302E2
7	1	2			4.00000	1.04194E3	2.00000	2.00000E1		1.29653E3
8	2	2.1		7.12640E2			0.00000	1.00000E1		5.56625E2
9	3	2.1.1				4.57857E2				
10	4	2.1.1.1	9.79418E1				0.00000			
11	4	2.1.1.2	1.13799E1				0.00000			
12	4	2.1.1.3	1.60935E1				0.00000			
13	4	2.1.1.4	2.00872E1				0.00000			
14	4	2.1.1.5	8.04677				0.00000			
15	4	2.1.1.6	2.69014E1				0.00000			
16	4	2.1.1.7	6.02324E1				0.00000			
17	4	2.1.1.8	1.13799E1				0.00000			
18	2	2.2		1.24942E2			0.00000	2.00000		1.16656E2
19	3	2.2.1				1.24942E2				
20	2	2.3		3.43723E2			0.00000	5.00000		2.76647E2
21	3	2.3.1				1.92787E2				
22	4	2.3.1.1	6.96599E1				0.00000			
23	4	2.3.1.2	6.65633E1				0.00000			
24	4	2.3.1.3	1.47130E1				0.00000			
25	2	2.4		3.75674E2			0.00000	5.00000		3.06645E2
26	3	2.4.1				2.66352E2				
27	4	2.4.1.1	2.27597E1				0.00000			
28	4	2.4.1.2	2.88540E1				0.00000			
29	4	2.4.1.3	5.77800E1				0.00000			
30	0								1.00000	7.99944E2
31	1	1					1.00000			7.99944E2
32	2	1.1					1.00000			1.59989E2
33	2	1.2					1.00000			6.39955E2
34	1	2			0.00000	0.00000	2.00000	0.00000		0.00000
35	0								1.00000	2.39983E3
36	1	1					1.00000			2.21984E3
37	2	1.1					1.00000			1.23658E3
38	2	1.2					1.00000			3.83386E2
39	2	1.3					1.00000			5.99953E2
40	1	2			1.00000	1.07941E2	0.00000	6.00000		1.79987E2
41	2	2.1		1.98980E2			0.00000	6.00000		1.79987E2
42	3	2.1.1				1.07941E2				
43	4	2.1.1.1	8.04677				0.00000			
44	4	2.1.1.2	1.13799E1				0.00000			
45	4	2.1.1.3	2.47123E1				0.00000			
46	4	2.1.1.4	4.69000E1				0.00000			
47	0								1.00000	1.51969E3
48	1	1					1.00000			1.07659E3
49	2	1.1					1.00000			1.07659E3
50	1	2			2.00000	3.58200E2	0.00000	1.10000E1		4.43302E2

Appendix B. A Typical Data File From Version 2

```
Joyce-Loebl                    RESULTS                    Magiscan

Sample identifier : RESULTS              File name : test1.DAT
Data file author  : NO NAME              File date : 5-Jun-91
Reference number  :      0               Comment   :

                    MEASUREMENTS/EXPRESSION REPORT

Object          1          2          3          4          5
Level           0          1          1          1          1
Ref             1        1.1        1.2        1.3        1.4
    ------------------------------------------------------------------------
  FI:                      5          5          5          5
  SN:  1.000000E+00
  FA:              3.652330E+05                        3.652330E+05
  FD:              3.912058E+03                        7.996817E+02
  FO:              2.000000E+00                        1.000000E+00
  CN:              1.000000E+00  1.000000E+00  1.000000E+00  1.000000E+00
  NL:                        0.000000E+00  0.000000E+00
  MA:                                8.389898E+02
  CA:                      1.245890E+03
  ML:                                2.950915E+02
  HL:                                3.994134E+02
  NT:                                5.000000E+00
  BL:                                3.595488E+01

Object          6
Level           1
Ref           1.5
    --------------
  FI:           6
  SN:
  FA:
  FD:
  FO:
  CN:  1.000000E+00
  NL:  0.000000E+00
  MA:
  CA:  1.366023E+03
  ML:
  HL:
  NT:
  BL:
```

Figure 68. Part of a typical data file generated by Version 2 of the morphological characterisation software

Appendix C. An Executable Task List

```
{ Task list for GENIAS 3 }
MAIN MENU
Capture
CAPTURE                    IMAGE CAPTURE AND SHADE CORRECTION
Correct shading
Change name
shaddy
CAPTURE
Quit & photo
MAIN MENU
Threshold
THRESHOLD
Manual
0          {SLICE : LOW }     THRESHOLDING TO GET BINARY IMAGE
54         {SLICE : HIGH }    OF TOTAL MYCELIA
THRESHOLD
Quit
MAIN MENU
Binary ops
BINARY OPS
Object-based ops
OBJECT-BASED OPS
Delete objects             BACKGROUND PARTICLE REMOVAL
DELETE OBJECTS
Circularity
3.50000E-01 { Minimum?  }
1.00000E+07 { Maximum?  }
Inclusive
DELETE OBJECTS
Quit
OBJECT-BASED OPS
Quit
BINARY OPS
Quit
MAIN MENU
Measure
FIELD MEASUREMENTS              MEASUREMENT OF DETECTED AREA
Quit, to measure           OF MYCELIA
MAIN MENU
Quit
Yes
END
```

Figure 69. An executable task List to measure the area of the total mycelia present in one image.. This is for a medium without undissolved solids. The text on the right, in the upper case characters, indicates the processing phase.

Appendix D. An Executable Task List

```
{ Task list for GENIAS 3 }
MAIN MENU
Capture
CAPTURE
Correct shading                    IMAGE CAPTURE AND SHADE CORRECTION
Change name
shaddy
CAPTURE
Quit & photo
MAIN MENU
Threshold
THRESHOLD
Manual
0          {SLICE : LOW }
49         {SLICE : HIGH }
THRESHOLD                            THRESHOLDING FOR BINARY IMAGE OF
Quit                               NON-DEGENERATED MYCELIA
MAIN MENU                            (CYTOPLASMIC REGION)
Binary ops
BINARY OPS
Object-based ops
OBJECT-BASED OPS
Delete objects
DELETE OBJECTS
Circularity
3.50000E-01 { Minimum? }           BACKGROUND PARTICLE REMOVAL
1.00000E+06 { Maximum? }
Inclusive
DELETE OBJECTS
Quit
OBJECT-BASED OPS
Quit
BINARY OPS
Quit
MAIN MENU
Measure
FIELD MEASUREMENTS                      MEASUREMENT OF AREA OF MYCELIA
Quit, to measure
MAIN MENU
Quit
Yes
END
```

Figure 70. The task list that was used to measure the cytoplasmic region of the mycelia for a medium which did not contain non-dissolved solids. The characters in upper case on the right indicate the stages of processing.

Appendix E. An Executable Task List

```
{ Task list for GENIAS 3 }
MAIN MENU
Capture
CAPTURE
Correct shading                IMAGE CAPTURE AND SHADE CORRECTION
Change name
shaddy
CAPTURE
Quit & photo
MAIN MENU
Threshold
THRESHOLD
Manual
0          {SLICE : LOW }      THRESHOLDING FOR DARK REGIONS
26         {SLICE : HIGH }     INSIDE THE SOLIDS PARTICLES
THRESHOLD
Quit
MAIN MENU
Binary ops
BINARY OPS
Object-based ops
OBJECT-BASED OPS
Delete objects
DELETE OBJECTS
Area                           REMOVAL OF SMALL PARTICLES
0.00000E+00 { Minimum? }
2.50000E+01 { Maximum? }
Inclusive
DELETE OBJECTS
Quit
OBJECT-BASED OPS
Erase 1-pixel objects
OBJECT-BASED OPS
Quit
BINARY OPS
Image-based ops                DILATION OF REMAINING OBJECTS
IMAGE-BASED OPS                  (NON-DISSOLVED SOLIDS)
Dilate
2          { BINARY OPS:How many passes? }
```

Figure 71. Task list for the measurement of the area of total mycelia in a field

```
IMAGE-BASED OPS
Quit
BINARY OPS
Object-based ops
OBJECT-BASED OPS
Delete objects                REMOVAL OF ANY THRESHOLDED MYCELIA
DELETE OBJECTS
Area
2.90000E+02 { Minimum? }
8.00000E+02 { Maximum? }
Inclusive
DELETE OBJECTS
Circularity
2.00000E-01 { Minimum? }
8.00000E-01 { Maximum? }
Inclusive
DELETE OBJECTS
Quit
OBJECT-BASED OPS
Delete objects
DELETE OBJECTS
Circularity
7.50000E-01 { Minimum? }
1.00000E+00 { Maximum? }
Inclusive
DELETE OBJECTS
Area
2.00000E+02 { Minimum? }
4.00000E+02 { Maximum? }
Inclusive
DELETE OBJECTS
Quit
OBJECT-BASED OPS
Quit
BINARY OPS
Store image                   STORAGE OF BINARY IMAGE OF SOLIDS
BINARY OPS
Quit
MAIN MENU
Threshold
```

Figure 71 (Part 2 of 2). Task list for the measurement of the area of total mycelia in a field

```
THRESHOLD
Manual
0          {SLICE : LOW }     THRESHOLDING FOR TOTAL AREA
54         {SLICE : HIGH }    OF MYCELIA
THRESHOLD
Quit
MAIN MENU
Binary ops
BINARY OPS
Object-based ops
OBJECT-BASED OPS
Delete objects
DELETE OBJECTS                REMOVAL OF SIMPLE BACKGROUND PARTICLES
Circularity
3.50000E-01 { Minimum? }
1.00000E+07 { Maximum? }
Inclusive
DELETE OBJECTS
Quit
OBJECT-BASED OPS
Delete objects
DELETE OBJECTS
Area
1.00000E+03 { Minimum? }
1.00000E+10 { Maximum? }
Inclusive
DELETE OBJECTS
Circularity
2.00000E-01 { Minimum? }
1.00000E+06 { Maximum? }
Inclusive
DELETE OBJECTS
Quit
OBJECT-BASED OPS
Quit
BINARY OPS
Quit
MAIN MENU
Binary ops
BINARY OPS
```

Figure 71 (Part 3 of 3). Task list for the measurement of the area of total mycelia in a field

```
Arithmetic                      SUBTRACTION OF IMAGE CONTAINING SOLIDS
BOOLEAN OPS                         FROM IMAGE OF TOTAL MYCELIA
Subtract
BOOLEAN OPS
Quit
BINARY OPS
Object-based ops
OBJECT-BASED OPS
Delete objects
DELETE OBJECTS
Circularity
3.50000E-01 { Minimum? }        FURTHER REMOVAL OF BACKGROUND
1.00000E+06 { Maximum? }         PARTICLES
Inclusive
DELETE OBJECTS
Quit
OBJECT-BASED OPS
Quit
BINARY OPS
Quit
MAIN MENU
Measure
FIELD MEASUREMENTS                  AREA MEASUREMENT OF TOTAL MYCELIA
Quit, to measure
MAIN MENU
Quit
Yes
END
```

Figure 71 (Part 4 of 4). Task list for the measurement of the area of total mycelia in a field. This is for the fermentation medium (lactose/Pharmamedia) containing large quantities of non-dissolved solids (30 g dry weight/L post heat sterilisation).

Appendix F. An Executable Task List

```
{ Task list for GENIAS 3 }
MAIN MENU
Capture
CAPTURE
Correct shading              IMAGE CAPTURE AND SHADE CORRECTION
Change name
shaddy
CAPTURE
Quit & photo
MAIN MENU
Threshold
THRESHOLD
Manual
0          {SLICE : LOW }    THRESHOLDING FOR DARK REGIONS
26         {SLICE : HIGH }   INSIDE THE SOLIDS PARTICLES
THRESHOLD
Quit
MAIN MENU
Binary ops
BINARY OPS
Object-based ops
OBJECT-BASED OPS
Delete objects
DELETE OBJECTS
Area                         REMOVAL OF SMALL PARTICLES
0.00000E+00 { Minimum? }
2.50000E+01 { Maximum? }
Inclusive
DELETE OBJECTS
Quit
OBJECT-BASED OPS
Erase 1-pixel objects
OBJECT-BASED OPS
Quit
BINARY OPS
Image-based ops              DILATION OF REMAINING OBJECTS
IMAGE-BASED OPS                 (NON-DISSOLVED SOLIDS)
Dilate
2          { BINARY OPS:How many passes? }
IMAGE-BASED OPS
```

Figure 72. Task list used for the measurement of the area of the non-degenerated mycelia (the cytoplasmic region) in a field.

```
Quit
BINARY OPS
Object-based ops
OBJECT-BASED OPS
Delete objects                REMOVAL OF ANY THRESHOLDED MYCELIA
DELETE OBJECTS
Area
2.90000E+02 { Minimum? }
8.00000E+02 { Maximum? }
Inclusive
DELETE OBJECTS
Circularity
2.00000E-01 { Minimum? }
8.00000E-01 { Maximum? }
Inclusive
DELETE OBJECTS
Quit
OBJECT-BASED OPS
Delete objects
DELETE OBJECTS
Circularity
7.50000E-01 { Minimum? }
1.00000E+00 { Maximum? }
Inclusive
DELETE OBJECTS
Area
2.00000E+02 { Minimum? }
4.00000E+02 { Maximum? }
Inclusive
DELETE OBJECTS
Quit
OBJECT-BASED OPS
Quit
BINARY OPS
Store image                   STORAGE OF BINARY IMAGE OF SOLIDS
BINARY OPS
Quit
MAIN MENU
Threshold
THRESHOLD
```

Figure 72 (Part 2 of 2). Task list used for the measurement of the area of the non-degenerated mycelia (the cytoplasmic region) in a field.

```
Manual
0          {SLICE : LOW }     THRESHOLDING FOR NON-DEGENERATED AREA
49         {SLICE : HIGH }    OF MYCELIA (THE CYTOPLASMIC REGION)
THRESHOLD
Quit
MAIN MENU
Binary ops
BINARY OPS
Object-based ops
OBJECT-BASED OPS
Delete objects
DELETE OBJECTS                REMOVAL OF SIMPLE BACKGROUND PARTICLES
Circularity
3.50000E-01 { Minimum? }
1.00000E+07 { Maximum? }
Inclusive
DELETE OBJECTS
Quit
OBJECT-BASED OPS
Delete objects
DELETE OBJECTS
Area
1.00000E+03 { Minimum? }
1.00000E+10 { Maximum? }
Inclusive
DELETE OBJECTS
Circularity
2.00000E-01 { Minimum? }
1.00000E+06 { Maximum? }
Inclusive
DELETE OBJECTS
Quit
OBJECT-BASED OPS
Quit
BINARY OPS
Quit
MAIN MENU
Binary ops
BINARY OPS
Arithmetic                    SUBTRACTION OF IMAGE CONTAINING SOLIDS
BOOLEAN OPS                       FROM IMAGE OF TOTAL MYCELIA
Subtract
```

Figure 72 (Part 3 of 3). Task list used for the measurement of the area of the non-degenerated mycelia (the cytoplasmic region) in a field.

```
BOOLEAN OPS
Quit
BINARY OPS
Object-based ops
OBJECT-BASED OPS
Delete objects
DELETE OBJECTS
Circularity
3.50000E-01 { Minimum? }        FURTHER REMOVAL OF BACKGROUND
1.00000E+06 { Maximum? }         PARTICLES
Inclusive
DELETE OBJECTS
Quit
OBJECT-BASED OPS
Quit
BINARY OPS
Quit
MAIN MENU
Measure
FIELD MEASUREMENTS              AREA MEASUREMENT OF TOTAL MYCELIA
Quit, to measure
MAIN MENU
Quit
Yes
END
```

Figure 72 (Part 4 of 4). Task list used for the measurement of the area of the non-degenerated mycelia (the cytoplasmic region) in a field.. This is for the fermentation medium (lactose/Pharmamedia) containing large quantities of non-dissolved solids (30 g dry weight/L post heat sterilisation). The upper case characters on the right indicate the processing phase.